

University of Southampton Research Repository ePrints Soton

Copyright © and Moral Rights for this thesis are retained by the author and/or other copyright owners. A copy can be downloaded for personal non-commercial research or study, without prior permission or charge. This thesis cannot be reproduced or quoted extensively from without first obtaining permission in writing from the copyright holder/s. The content must not be changed in any way or sold commercially in any format or medium without the formal permission of the copyright holders.

When referring to this work, full bibliographic details including the author, title, awarding institution and date of the thesis must be given e.g.

AUTHOR (year of submission) "Full thesis title", University of Southampton, name of the University School or Department, PhD Thesis, pagination

FACULTY OF NATURAL AND ENVIRONMENTAL SCIENCES

Centre for Biological Sciences

Control of translation initiation and neuronal subcellular localisation of
mRNAs by G-quadruplex structures

by

James Philip Robertson Schofield

Thesis for the degree of Doctor of Philosophy

2015

ABSTRACT

FACULTY OF NATURAL AND ENVIRONMENTAL SCIENCES

CENTRE FOR BIOLOGICAL SCIENCES

Doctor of Philosophy

Control of translation initiation and neuronal subcellular localisation of mRNAs by G-quadruplex structures

by James Philip Robertson Schofield

The translation of mRNA is a key regulatory step in control of gene expression. The primary sequence of an mRNA determines much of the regulation of translation, including the location of translation initiation. The efficiency of translation initiation is determined by the initiation codon and its context. Translation initiation occurs at the canonical initiation codon, AUG, or a less efficient near canonical non-AUG alternative initiation codon (AIC). The secondary structure of an mRNA impacts its translation, principally by inhibiting binding and/or migration of ribosomal subunits. Hairpins form by hydrogen bonding between Watson-Crick complementary base-pairs. Guanine-rich nucleotide sequences form planar tetrads via hydrogen bonds and stack as stable G-quadruplex structures. Much has been reported on the impact of hairpins in regulating translation and G-quadruplex structures are emerging as an important factor in the regulation of translation of some mRNAs.

Two-pore potassium leak (K_{2P}) channels set and maintain the resting membrane potential of cells, so precise regulation of K_{2P} protein expression in cells is critical to cell behaviour and survival. The 5' untranslated regions (5' UTR) of K_{2P} channels are poorly annotated in databases. This thesis details investigations of 5' UTR primary sequence and secondary structure effects on the expression of K_{2P} leak channels. We characterised an extension to the annotated 5' UTR sequence of Task3 by 5'RACE. The extension is characterised by a 5' terminal (GGN) repeat which we show forms a G-quadruplex structure and inhibits translation of Task 3. G-quadruplex formation was measured by circular dichroism and increased fluorescence of Mesoporphyrin IX dihydrochloride. RT-PCR of Task3-FLAG mRNA relative to β -actin mRNA in polysome fractions of transfected HeLa cells suggests the inhibition of Task3 protein synthesis results from an inhibition of translation initiation due to the 5'-terminal G-quadruplex. Results suggest the inhibition of Task3 protein synthesis can be modulated by RNA-binding proteins. hnRNPA2 is shown to relieve translational inhibition, and the DEAH/RHA RNA helicases, DHX29, DHX30 and DHX36 differentially regulate translation from Task3 mRNA dependent on the presence of the 5' terminal G-quadruplex. We also investigate the use of small ligands TMPyP4 and Hippuristanol in modulating expression of Task3 in a G-quadruplex-dependent manner.

Task3 is expressed in neuronal cells and is predicted to be able to exert control over local membrane potential. The local translation of mRNAs has been demonstrated in a variety of cells. In neurons, local translation of some mRNAs at synapses have been shown in plastic changes. G-quadruplex structures have been shown to affect mRNA subcellular targeting and direct protein synthesis at the synapse. We describe detection of Task3-GFP mRNA by Fluorescence In Situ Hybridisation (FISH) in transfected primary cortical neurons. It was found for the first time that the 5'-terminal G-quadruplex in Task3 mRNA appears to mediate localisation of Task3-GFP mRNA to discrete neurite particles. The roles of G-quadruplex-interacting RNA binding proteins (RBPs), hnRNP A2 and Pur α , in the trafficking of Task3 mRNA was investigated, however, the mechanism of neurite delivery of Task3

mRNA requires further research. Dysregulation of this mechanism would cause perturbations to individual synapse excitability and therefore contribute to neuronal behaviour.

FXR2 is a paralog of the neuronal translation regulator RBP, Fragile X Mental Retardation Protein (FMRP). Ribosome profiling of mouse embryonic stem cells identified Fxr2 to be subject to alternative upstream translation initiation. Results here demonstrate the production of different N-terminal length isoforms of Fxr2 from alternative translation initiation, primarily from GUG codon, -219 from the annotated AUG initiation codon. Investigation of the 5' UTR of Fxr2 revealed a high concentration of guanine residues. We show evidence supporting G-quadruplex structures within its 5'UTR. This is the first report of potential G-quadruplex mediated control of AIC usage in an mRNA.

Contents

| | |
|--|-------------|
| Declaration of authorship | xi |
| Acknowledgements | xii |
| Abbreviations | xiii |
| List of figures | xiv |
| List of Tables | xvii |
| Chapter One | 1 |
| Introduction | 1 |
| 1.1 Regulation of translation initiation | 1 |
| 1.1.1 mRNA primary sequence determines initiation codon usage | 5 |
| 1.1.2 Leaky scanning creates diverse translation products | 8 |
| 1.2 mRNA secondary structures regulate initiation codon usage | 12 |
| 1.2.1 Hairpins impact translational mechanisms | 12 |
| 1.2.2 G-quadruplexes impact translational mechanisms..... | 14 |
| 1.3 RNA-binding proteins and the 5' UTRs of mRNAs | 21 |
| 1.3.1 RNA Helicases resolve secondary structure | 21 |
| 1.4 Modulating RNA G-quadruplex effects with small-molecules | 27 |
| 1.5 Subcellular localisation of mRNA | 28 |
| 1.5.1 mRNA structural motifs determine mRNA targeting | 32 |
| 1.6 FMRP is a G-quadruplex binding RBP and its mRNA contains G-quadruplexes | 33 |
| 1.7 Local translation affects synaptic plasticity | 35 |
| 1.7.1 G-quadruplex mediated delivery of mRNA to synaptic spines for controlled local protein synthesis..... | 40 |
| 1.7.2 G-quadruplex expansion diseases deregulate processing of G-quadruplex mRNA..... | 47 |
| 1.8 Two-pore potassium leak channels | 47 |
| 1.8.1 Potassium leak channels set the baseline membrane potential of neurons | 48 |
| 1.9 Regulated expression of K_{2p} channel proteins | 52 |

| | |
|--|-----------|
| 1.10 Alternative translation initiation in K_{2P} channel, Trek1 | 54 |
| 1.11 Bioinformatic screen of mRNAs identified an evolutionarily conserved sequence in the 5' UTR of K_{2P} channel, Traak | 55 |
| 1.12 Alternative translation initiation in Fxr2 | 56 |
| 1.13 Aims | 59 |
| Chapter Two | 60 |
| Materials and Methods | 60 |
| Chapter 2: Materials and Methods | 60 |
| 2.1 Measurement of RNA/DNA concentration..... | 60 |
| 2.2 PCR techniques..... | 60 |
| 2.2.1 Slowdown PCR | 61 |
| 2.2.2 PCR primers..... | 62 |
| 2.3 Cloning into pcDNA3.1 CMV 3XFLAG expression plasmids..... | 66 |
| 2.3.1 Restriction Digest..... | 66 |
| 2.3.2 Ligation..... | 67 |
| 2.3.3 Clean-up of DNA..... | 67 |
| 2.3.4 Transformation of competent cells | 67 |
| 2.4 Cloning into Promega pGEM-T Easy..... | 68 |
| 2.4.1 Plasmid DNA isolation..... | 69 |
| 2.5 RNA purification from cell lysate | 69 |
| 2.6 Reverse Transcription of total RNA to yield cDNA | 70 |
| 2.6.1 Reverse Transcription of total RNA with Maxima H Thermostable Reverse Transcriptase..... | 70 |
| 2.6.2 Rapid amplification of 5' complementary DNA ends..... | 71 |
| 2.7 Cell culture | 73 |
| 2.8 Transient transfection..... | 73 |
| 2.9 Primary Neuronal Cell Culture..... | 73 |
| 2.10 Transient Transfection of primary cortical neurons | 74 |

| | |
|--|-----------|
| 2.11 Polysome Fractionation | 74 |
| 2.11.1 Cell lysis | 74 |
| 2.11.2 Polysome Gradients | 75 |
| 2.11.3 Fraction Collection | 75 |
| 2.11.4 RNA Extraction | 76 |
| 2.12 <i>In vitro</i> Transcription for <i>in vitro</i> translation | 77 |
| 2.13 <i>In vitro</i> Transcription for RNA structure analysis | 78 |
| 2.14 <i>In vitro</i> Translation..... | 78 |
| 2.15 Mesoporphyrin IX dihydrochloride fluorescence | 80 |
| 2.16 Circular Dichroism..... | 80 |
| 2.17 Treatment of transfected cells with TMPyP4..... | 81 |
| 2.18 [³⁵S]-methionine incorporation assay..... | 81 |
| 2.19 Cell lysis and immunoblot analyses..... | 82 |
| 2.19.1 Standardisation of protein concentration..... | 83 |
| 2.19.2 SDS-PAGE of protein samples..... | 84 |
| 2.19.2 Visualisation of bound secondary antibodies | 85 |
| 2.20 qPCR of FLAG RNA in transfected cell lysate..... | 85 |
| 2.21 Immunofluorescence microscopy | 87 |
| 2.23 Measurements of mRNA particle distribution in neurons | 87 |
| 2.24 Site directed mutagenesis | 88 |
| Chapter Three | 91 |
| Results..... | 91 |
| 3.1.1 Bioinformatic screen of mRNAs identified an evolutionarily conserved sequence in the 5' UTR of K _{2p} channel, Traak | 91 |
| 3.2 Results | 92 |
| 3.2.1 Traak was cloned from human brain cDNA into a C-terminal FLAG-fusion expression vector | 93 |
| 3.2.2 Investigation of the use of upstream alternative initiation codons in translation of Traak | 95 |

| | |
|---|------------|
| 3.3 Analysis of putative alternative upstream translation initiation codons in other K_{2P} channel mRNAs | 97 |
| 3.3.1 Acid-sensitive Two Pore Potassium Leak Channels, Task 1 and Task 3 | 97 |
| 3.4.1 Prediction of alternative initiation codons in extended 5' UTR of Task3 .. | 101 |
| 3.4.2 Attempts to quantify relative abundance of Task3 extended 5' UTR by qPCR | 101 |
| 3.4.3 Attempts to identify the use of alternative initiation codons in Task 3 | 104 |
| 3.5 Discussion | 106 |
| 3.5.2 5' RACE revealed a 5' terminal GGN repeat in Task3 mRNA | 106 |
| 3.5.3 Conclusions | 107 |
| Chapter Four | 108 |
| Results | 108 |
| The 5'-terminal (GGN)₁₃ repeat in Task3 mRNA forms a G-quadruplex structure and inhibits translation initiation | 108 |
| 4.1 Introduction | 108 |
| 4.2 Results | 109 |
| 4.2.1 The 5'-terminal (GGN) ₁₃ of Task3 mRNA is predicted to form G-quadruplexes | 109 |
| 4.2.2 Creation of expression vectors to examine properties of the 5' UTR..... | 112 |
| 4.2.3 Task3 translation is inhibited due to the 5'-terminal GGN repeat | 114 |
| 4.2.4 Construction of a Task3-FLAG plasmid with functioning T7 promoter..... | 117 |
| 4.2.5 Fluorescence increase of NMM with (GGN) ₁₃ RNA indicated G-quadruplex structure..... | 121 |
| 4.2.6 Circular Dichroism (CD) studies confirmed G-quadruplex structure of (GGN) ₁₃ RNA | 124 |
| 4.2.7 Investigating potassium dependence on <i>in vitro</i> translation of Task3 mRNA | 126 |

| | |
|--|------------|
| 4.2.9 RT-PCR of FLAG mRNA relative to β -actin mRNA in polysome fractions of transfected HeLa cells suggests an inhibition of translation initiation due to 5'-terminal G-quadruplex | 128 |
| 4.2.10 hnRNPA2 relieved repression of translation of transfected WT Task3..... | 130 |
| 4.2.11 RNA Helicases, DHX29, DHX30, and DHX36 were cloned from human brain cDNA..... | 132 |
| 4.2.12 DHX helicases differentially change expression of transfected WT Task3 compared to Complementary GQ Task3 | 133 |
| 4.2.13 Investigation of the effects of Hippuristanol, an eIF4A inhibitor, on expression of transfected WT Task3 compared to Complementary GQ Task3 | 135 |
| 4.2.14 Investigation of the effects of TMPyP4, a G-quadruplex-targetting ligand, on expression of transfected WT Task3 compared to Complementary GQ Task3 | 137 |
| 4.2.15 TMPyP4 was shown to unfold (GGN) ₁₃ G-quadruplex | 139 |
| 4.2.16 100 μ M TMPyP4 partially relieved repression of translation of transfected WT Task3 | 140 |
| 4.3 Discussion | 142 |
| 4.3.1 The 5'-terminal (GGN) ₁₃ of Task3 mRNA forms a G-Quadruplex which inhibits translation initiation | 142 |
| 4.3.2 Specific G-quadruplex-targeting RBPs can modulate translational control of Task3..... | 144 |
| 4.3.3 TMPyP4 unfolded Task3 5'-terminal G-quadruplex and relieved translational repression | 145 |
| 4.3.4 Conclusions..... | 146 |
| Chapter Five..... | 147 |
| Results..... | 147 |
| The 5'-terminal G-quadruplex in Task3 mRNA potentially mediates local translation in neurons..... | 147 |
| 5.1 Introduction | 147 |
| 5.2 Results | 148 |

| | |
|---|------------|
| 5.2.1 The 5'-terminal G-quadruplex does not affect subcellular localisation of Task3 protein in transfected HeLa cells | 148 |
| 5.2.2 Creation of Task3-GFP expression vectors..... | 150 |
| 5.2.3 Design of Stellaris probes for FISH of Task3-GFP mRNA..... | 154 |
| 5.2.5The 5'-terminal G-quadruplex in Task3 mRNA mediates localisation of mRNA to neurite particles in transfected primary neurons | 159 |
| 5.2.6 Task3-GFP expression vectors were mutated to Task3-BFP for RBP co-localisation experiments | 164 |
| 5.2.7 hnRNPA2 expression does not alter Task3-BFP mRNA localisation in transfected HeLa cells..... | 167 |
| 5.2.8 V5-Pur- α has a similar subcellular expression pattern as mRNA of transfected Task3-BFP in HeLa cells..... | 170 |
| 5.2.9 Co-transfection of neurons with RBPs and Task3-BFP were unsuccessful | 173 |
| 5.3 Discussion | 174 |
| 5.3.1 Conclusions | 175 |
| Chapter Six | 177 |
| Results..... | 177 |
| G-quadruplex mediated alternative translation initiation generates N-terminally diverse FXR2 proteins | 177 |
| 6.1 Introduction | 177 |
| 6.2 Results | 179 |
| 6.2.1 Fxr2-FLAG expression vectors were cloned from human brain cDNA..... | 180 |
| 6.2.2 Western blot of transfected HeLa cells lysate suggests Fxr2 is predominantly translated from -219 GUG..... | 183 |
| 6.2.2 The -219 GUG initiates translation of Fxr2 in the absence of other initiation codons..... | 186 |

| | |
|---|------------|
| 6.2.3 There are multiple putative G-quadruplex-forming sequences in the 5' UTR of Fxr2 mRNA..... | 188 |
| 6.2.4 Creation of purified RNA of the wild-type Fxr2 5' UTR | 190 |
| 6.2.5 CD spectroscopy showed G-quadruplex structures in the 5' UTR of Fxr2 mRNA, destabilised by TMPyP4 | 191 |
| 6.2.6 TMPyP4 and Hippuristanol modulate expression of extended and normal length Fxr2p..... | 192 |
| 6.2.7 Co-transfection of Fxr2p with FLAG-tagged DHX expression constructs modulated expression of extended and normal length Fxr2p..... | 194 |
| 6.2.8 Investigating subcellular localisation of Fxr2 protein isoforms..... | 196 |
| 6.3 Discussion | 199 |
| 6.3.1 Conclusions..... | 200 |
| Chapter Seven..... | 202 |
| Final Discussion..... | 202 |
| 7.1 5' UTR sequences can regulate expression of K_{2p} leak channels | 204 |
| 7.2 A 5'-terminal G-quadruplex modulates translation of Task3..... | 205 |
| 7.3 Neurite localisation of Task3 mRNA is determined by a 5' terminal G-quadruplex ... | 207 |
| 7.4 G-quadruplex mediated translation initiation from upstream AICs generates N-terminally extended FXR2 protein | 207 |
| 7.5 Suggestions for continued research | 208 |
| Chapter Eight | 210 |
| References | 210 |
| Chapter Nine..... | 223 |
| Supplementary Figures..... | 223 |

Declaration of authorship

I, James Philip Robertson Schofield, declare that the thesis entitled "Control of translation initiation and neuronal subcellular localisation of mRNAs by G-quadruplex structures " and the work presented in the thesis are both my own, and have been generated by me as the result of my own original research. I confirm that:

this work was done wholly or mainly while in candidature for a research degree at this University;

where any part of this thesis has previously been submitted for a degree or any other qualification at this University or any other institution, this has been clearly stated;

where I have consulted the published work of others, this is always clearly attributed;

where I have quoted from the work of others, the source is always given. With the exception of such quotations, this thesis is entirely my own work;

I have acknowledged all main sources of help;

where the thesis is based on work done by myself jointly with others, I have made

clear exactly what was done by others and what I have contributed myself;

none of this work has been published before submission,

Signed:

Date:.....

Acknowledgements

I dedicate this work to my wife, Anneka; and children, William and Charlie for their patience, encouragement, discussion and inspiration. It is also dedicated to Stephanie Minhinnick, responsible for much of who I am, and ultimately why I love scientific research. I thank Dorothy Kerridge for nurturing my love of science. I thank my parents, Philip and Jane, for their love & support. I also thank Anneka's parents for their love and support during my study.

I am extremely grateful to the Kerkut Trust for giving me the opportunity to do this study and the support to attend conferences and present my work around the world, which I believe has greatly helped shape my thoughts. I am also grateful for receiving the Richard Newitt Bursary.

I have learnt an enormous amount during my time in the Coldwell lab, and am grateful for the excellent environment provided by the leadership and members of the lab, from Dr Coldwell, Dr Joanne Cowan, Dr Alison Yeomans, Lisa Perry, Helen Knight and many undergraduate project students. I would especially like to thank my primary supervisor, Dr Mark Coldwell for his enthusiastic support toward my development as a scientist as well as encouragement and advice on planning, carrying out and analysing experiments. I am grateful to Dr Joanne Cowan for extensive advice, training and discussion during my research. I am also very grateful for the guidance and support offered by my co-supervisor, Dr Ita O' Kelly.

I have had a great deal of support from within the department. The mouse neuronal work was made possible with the help of very generous experts within IFLS at Southampton. Dr Joanne Bailey, Dr Katrin Deinhardt, Dr Justin Kenney, Maja Genheden and Dr Tracey Newman. I am grateful to Dr Andy Van Hateren for enabling the measurement of fluorescence change of NMM binding by RNA G-quadruplexes. I am also grateful to Dr Neville Wright and Dr David Rusling for helping with experimental design and measurement of CD spectra. I am very grateful to Dr Mark Willett, Experimental Officer for The Imaging and Microscopy Centre (IMC), for help with experimental design of fluorescence microscopy studies, especially FISH of mRNA. I thank Professor Vincent O'Connor for his honest advice. I also thank Dr. Peter Todd for plasmids generously gifted to our lab and valuable discussions regarding GGN repeat biology.



The Gerald Kerkut
Charitable Trust



Abbreviations

| | |
|-----------------|---|
| AD | Alzheimer's disease |
| ADAM10 | Anti-amyloidogenic α -secretase disintegrin and metalloproteinase 10 |
| A β | β -peptide |
| BFP | blue fluorescent protein |
| BSA | bovine serum albumin |
| CD | Circular Dichroism |
| CDS | coding sequence |
| cLTP | chemically induced long-term potentiation |
| DAPI | 4'6-Diamidino-2-phenylindole |
| <i>dhfr</i> | dihydrofolate reductase |
| DHX | DEAD-box helicase proteins |
| DMEM | Dulbecco's Modified Eagle Medium |
| DTT | Dithiothreitol |
| eIF | eukaryotic Initiation Factor |
| eORF | extended open reading frame |
| ExTATIC' | EXtensions and Truncations from Alternative Translation Initiation Codons |
| FISH | Fluorescence In Situ Hybridisation |
| FITC | fluorescein isothiocyanate |
| FMRP | Fragile X Mental Retardation Protein |
| FXS | fragile X syndrome |
| FXTAS | fragile X-associated tremor ataxia syndrome |
| GFP | green fluorescent protein |
| GRS1 | glycyl-tRNA synthetase |
| hnRNPs | heterogeneous nuclear ribonucleoproteins |
| hVEGF | human vascular endothelial growth factor |
| IRES | Internal Ribosome Entry Sites |
| K _{2P} | Two-pore potassium leak channels K _{2P} |
| KH | K-homology |
| mRNA | messenger RNA |
| mRNPs | messenger ribonucleoprotein |
| NGS | Normal Goat Serum |
| NMM | Mesoporphyrin IX dihydrochloride |
| NTPase | nucleoside triphosphatase |
| PABP | PolyA Binding Protein |
| PBS | Phosphate-buffered saline |
| qPCR | Quantitative PCR |
| RACE | rapid amplification of cDNA ends |
| RBP | RNA-binding proteins |
| RRM | RNA recognition motif |
| RT-PCR | Real Time PCR |
| TMPyP4 | tetra-(N-methyl-4-pyridyl)porphyrin |
| uORF | Upstream open reading frames |
| UTR | untranslated region |

List of figures

| | |
|---|-----|
| Figure 1.1 Translation mechanism | 4 |
| Figure 1.2 Leaky scanning creates diverse translation products..... | 11 |
| Figure 1.3 5' UTR RNA hairpins inhibit ribosome scanning | 13 |
| Figure 1.4 G-quadruplex structures..... | 17 |
| Figure 1.5 5' UTR G-quadruplexes inhibit ribosome scanning | 19 |
| Figure 1.6 (CGG) ₃₃ RNA forms a G-quadruplex..... | 20 |
| Figure 1.7 Known protein interactors of DHX29 from BioGrid | 24 |
| Figure 1.8 Known protein interactors of DHX30 from BioGrid | 25 |
| Figure 1.9 Known protein interactors of DHX36 from BioGrid | 26 |
| Figure 1.10 Subcellular targeting of mRNA..... | 31 |
| Figure 1.11 Synaptic plasticity..... | 36 |
| Figure 1.12 CamkII positive feedback loops in activated dendritic spines | 38 |
| Figure 1.13 The regulation of local translation of mRNAs at active synapses | 43 |
| Figure 1.14 mRNA transport and translational control in dendrites..... | 46 |
| Figure 1.15 K _{2P} channels | 50 |
| Figure 1.16 K _{2P} channel subfamily classifications..... | 51 |
| Figure 1.17 Subcellular protein trafficking | 53 |
| Figure 1.18 Conserved 5' UTR in Traak..... | 58 |
| Figure 2.1 5' RACE PCR using SMARTer RACE. | 72 |
| Figure 2.2 Site directed mutagenesis | 89 |
| Figure 3.1 Conserved 5' UTR in Traak between H. sapiens & P. troglodytes | 95 |
| Figure 3.2 Alternative initiation codons in Traak identified by ExTATIC macro | 95 |
| Figure 3.3 Diagram of pcDNA3.1 3F plasmid | 94 |
| Figure 3.4 Traak expression in HeLa cells..... | 96 |
| Figure 3.5 Task1 and Task3 proteins structure..... | 98 |
| Figure 3.6 Task 3 nested RACE products | 99 |
| Figure 3.7 ClustalW alignment of 5' UTR sequence found by 5' RACE..... | 100 |
| Figure 3.9 PCR of Task3 mRNA variants using qPCR primers | 105 |
| Figure 3.10 Task3 expression in transfected HeLa cells | 108 |
| Figure 4.1 QGRS Mapper was used to analyse the 5'UTR of Task3 mRNA | 111 |
| Figure 4.2 FLAG-tagged expression vectors were created for Task3 | 113 |
| Figure 4.3 Task3 GQ mutant expression in transfected HeLa cells | 116 |
| Figure 4.4 T7 promoter sequence cloned into pcDNA 3.1 3F Task3 | 118 |
| Figure 4.5 Linearized pcDNA3.1 3F Task3 for in vitro transcription..... | 120 |

| | |
|--|-----|
| Figure 4.6 NMM increases in fluorescence on binding G-quadruplexes..... | 121 |
| Figure 4.7 NMM increases fluorescence when bound to (GGN) ₁₃ .RNA | 123 |
| Figure 4.8 CD measurement of G-quadruplex structure in 5' UTR of Task3 mRNA .. | 125 |
| Figure 4.9 Test of KCl concentration on Task3 expression <i>in vitro</i> | 127 |
| Figure 4.10 Polysome fractions of transfected HeLa cells suggests an inhibition of translation initiation due to 5'-terminal G-quadruplex | 129 |
| Figure 4.11 hnRNPA2 relieved repression of translation of transfected WT Task3 .. | 131 |
| Figure 4.12 DHX helicases differentially change expression of transfected WT Task3 compared to Complementary GQ Task3 | 134 |
| Figure 4.13 Hippuristanol treatment of Task3-transfected HeLa cells..... | 136 |
| Figure 4.14 TMPyP4 decreases overall translation rates | 138 |
| Figure 4.15 TMPyP4 was shown to unfold (GGN) ₁₃ G-quadruplex..... | 139 |
| Figure 4.16 TMPyP4 relieves translational inhibition by (GGN) ₁₃ G-quadruplex | 141 |
| Figure 5.1 Task3-FLAG expression in HeLa cells | 149 |
| Figure 5.2 Creating Task3-GFP | 151 |
| Figure 5.3 Creating Task3-GFP, cloning | 152 |
| Figure 5.4 Task3-GFP expression in HeLa cells | 153 |
| Figure 5.5 Stellaris FISH technique | 154 |
| Figure 5.6 Principles of Stellaris FISH of Task3 GFP | 156 |
| Figure 5.7 Distribution of Task3-GFP mRNA in HeLa cells | 158 |
| Figure 5.8 Distribution of WT GQ Task3-GFP mRNA in cortical neurons | 160 |
| Figure 5.9 Measurement of WT GQ Task3-GFP mRNA distribution..... | 161 |
| Figure 5.10 Distribution of comp. GQ Task3-GFP mRNA in cortical neurons..... | 162 |
| Figure 5.11 Measurement of comp. GQ Task3-GFP mRNA distribution | 163 |
| Figure 5.12 Mutation of Task3-GFP to Task3-BFP | 165 |
| Figure 5.13 HeLa cells were transfected with Task3-BFP | 166 |
| Figure 5.14 Interaction of hnRNP A2 with Task3 mRNA..... | 168 |
| Figure 5.15 Measurement of hnRNP A2 and Task3-BFP mRNA localisation | 169 |
| Figure 5.16 The interaction of Pur- α with Task3 mRNAs | 171 |
| Figure 5.17 Measurement of Pur- α and Task3-BFP mRNA localisation | 172 |
| Figure 6.1 AICs in the 5' UTR of Fxr2 mRNA | 180 |
| Figure 6.2 Fxr2-FLAG expression vectors were cloned from human brain cDNA | 182 |
| Figure 6.3 Testing expression from AICs in the 5' UTR of Fxr2 mRNA..... | 184 |
| Figure 6.4 Mutation of AICs in the 5' UTR of Fxr2 mRNA..... | 185 |
| Figure 6.5 -219 GUG initiates translation of Fxr2 | 187 |

Figure 6.6 QGRS Mapper was used to analyse the 5'UTR of Fxr2 mRNA.....189

Figure 6.7 Linearized pcDNA3.1 3F Fxr2 plasmid for *in vitro* transcription.....190

Figure 6.8 G-quadruplexes in Fxr2 5' UTR measured by CD.....191

Figure 6.9 Hippuristanol treatment of Fxr2 transfected HeLa cells193

Figure 6.10 HeLa cells cotransfected with Fxr2 and DHX helicases195

Figure 6.11 Fxr2 expression in transfected HeLa cells197

Figure 6.12 Fxr2 expression in transfected cortical neurons198

Figure S1 Creating Task3-GFP, cloning part 1.....224

Figure S2 Creating Task3-GFP, cloning part 2.....225

Figure S3 Creating Task3-GFP, cloning part 3.....226

Figure S4 Creating Task3-GFP, cloning part 4.....227

List of Tables

| | |
|--|-----|
| Table 1. 1 Summary of evidence for control of translation in Eukaryotes at initiation and elongation stages of the translation process..... | 2 |
| Table 1. 2 Conserved contexts of AUG translation initiation codons..... | 6 |
| Table 1. 3 Relative efficiency of non-AUG initiation codons in synthesising full-length DHFR in rabbit reticulocyte lysate..... | 7 |
| Table 1. 4 Examples of mRNA subcellular localisation studies and their importance in determining cell behaviour | 30 |
| Table 1. 5 Synthesis of proteins during LTP..... | 39 |
| Table 2.1 Primers used for cloning, mutagenesis and qPCR. | 62 |
| Table 2.2 & 2.3 The composition of qPCR reaction reactions using SYBR [®] Select Master Mix and cycle conditions using Eco qPCR System..... | 86 |
| Table 2.4 of primary antibodies used in western blot and immunohistochemistry analyses..... | 90 |
| Table 3.1 qPCR primers were designed to the task 3 mRNA..... | 102 |

Chapter One

Introduction

1.1 Regulation of translation initiation

Control of gene expression is complex and critical to normal cellular behaviour.

Dysregulation of gene expression is a major cause of disease. Approximately 1.5% of the human genome codes for protein, whilst much of the rest is thought to regulate the expression of those genes. The cell's dynamic proteome is determined by regulation of gene expression. The uncoupling of translation from transcription in Eukaryotes allows multiple levels of control. Transcription, mRNA stability, translational efficiency and subcellular localisation can all be modulated to finely tune gene expression.

Eukaryotic translation of mRNAs requires initiation, elongation and termination. The majority of described regulated protein synthesis occurs at the initiation stage. However, there is growing evidence of regulation of translation at the elongation stage (Table 1.1). Translation initiation is the assembly on an mRNA of an elongation-competent 80S ribosome (Fig. 1.1). This occurs by the joining of 40S and 60S ribosomal subunits (Jackson, Hellen & Pestova, 2010).

| Stage of translation | Evidence of control |
|-----------------------------|--|
| Initiation | <p>The most complex stage of translation (Review by McCarthy <i>et al.</i>, 1998). Most translation is cap-dependent; where the binding of the 40S ribosomal subunit to the 5' end of mRNAs is dependent on binding of multiple initiation factors.</p> <p>Phosphorylation of eIF2 inhibits global translation initiation by inhibition of eIF2B (Sudhakar <i>et al.</i>, 2000).</p> <p>eIF2 kinases act in response to stress stimuli (review by Wek, Jiang & Anthony, 2006)</p> <p>eIF1 maintains specificity of initiation at AUG codons; mutations of eIF1 increase initiation at near-cognate start codons (Cheung <i>et al.</i>, 2007)</p> <p>eIF1 promotes scanning when the P-site is occupied by a non-AUG codon by promoting the open conformation of the mRNA binding cleft of the 40S ribosomal subunit (Passmore <i>et al.</i>, 2007)</p> <p>The C-terminal region of eIF1A promotes scanning at non-AUG codons, whilst the N-terminal arrests scanning and promotes the release of eIF1 at AUG codons (Fekete <i>et al.</i>, 2007)</p> |
| Elongation | <p>Insulin causes increased protein synthesis by derestricting elongation. Elongation factor 2 (eEF2) mediates the translocation step of elongation (Redpath <i>et al.</i>, 1996). eEF2 is inactivated by phosphorylation at Thr56 (review by Proud, 2000). Insulin, in an mTOR-dependent mechanism, causes eEF2k dephosphorylation & activation of eEF2 (Wang <i>et al.</i>, 2000).</p> <p>Fragile X Syndrome is a result of an expanded 5' UTR CGG repeat of the Fmrp gene. Fragile X mental retardation protein (FMRP) is essential for normal translation of mRNAs at synapses in neurons. Phosphorylated FMRP associates causes actively translating ribosomes to stall on mRNAs (review by Richter, Bassell and Klann, 2015).</p> |

Table 1.1 Summary of evidence for control of translation in Eukaryotes at initiation and elongation stages of the translation process.

Most mRNAs are translated in a cap-dependent fashion. A post-termination (recycled) 40S subunit binds eIF1, eIF1A, eIF3, eIF5 and the eIF2 ternary complex; eIF2-GTP-Met-tRNA^{Met}_i to form a 43S pre-initiation complex. The eIF4F complex binds to the 7-methyl guanosine 5' terminal cap of mRNA, via cap-binding factor eIF4E (Fig. 1.1A) (Pestova *et al.*, 1996, Sonenberg 2008). The eIF4F complex is also comprised of the RNA helicase, eIF4A and the scaffold protein, eIF4G. The binding of eIF4F to mRNA is stabilised by association of scaffold protein eIF4G with 3' PolyA Binding Protein (PABP) (Fig. 1.1B) and results in pseudo-circularization of mRNA (Derry *et al.*, 2006; Wilkie, Dickson and Gray, 2003). eIF4F-bound mRNA and eIF3 cooperatively recruit the 43S pre-initiation complex (Fig. 1.1c). The 43S pre-initiation complex then scans the mRNA 5' untranslated region (5' UTR) 5' – 3' until initiation codon recognition and assembly of the 48S complex (Fig. 1.1D). eIF5 and eIF5B allow the attachment of the 60S subunit, by hydrolysing eIF2-GTP and displacement of eIF1 and eIF3 (Fig. 1.1E) (Pestova *et al.*, 2007). eIF5B is hydrolysed, yielding a translation-elongation competent 80S complex (Fig. 1.1F).

The primary structure of mRNA determines protein synthesis. The initiation codon is typically an AUG in a favourable context; a purine at -3 and a guanine at +4. However, the 80S ribosome can assemble, and initiate translation at a non-AUG. Translation initiation from non-AUGs is poorly annotated in online databases and is a source of increased proteome diversity (Wan & Qian, 2014). However, it is not just primary nucleotide sequence which affects translation of mRNA molecules. Secondary structure of the mRNA can greatly impact protein synthesis. Internal Ribosome Entry Sites (IRESs) are well described in viruses, and increasingly well documented in eukaryotic genes, direct translation initiation, independent of a 5' cap. Other structures within the 5' UTR typically inhibit translation initiation by inhibiting the 43S pre-initiation complex scanning.

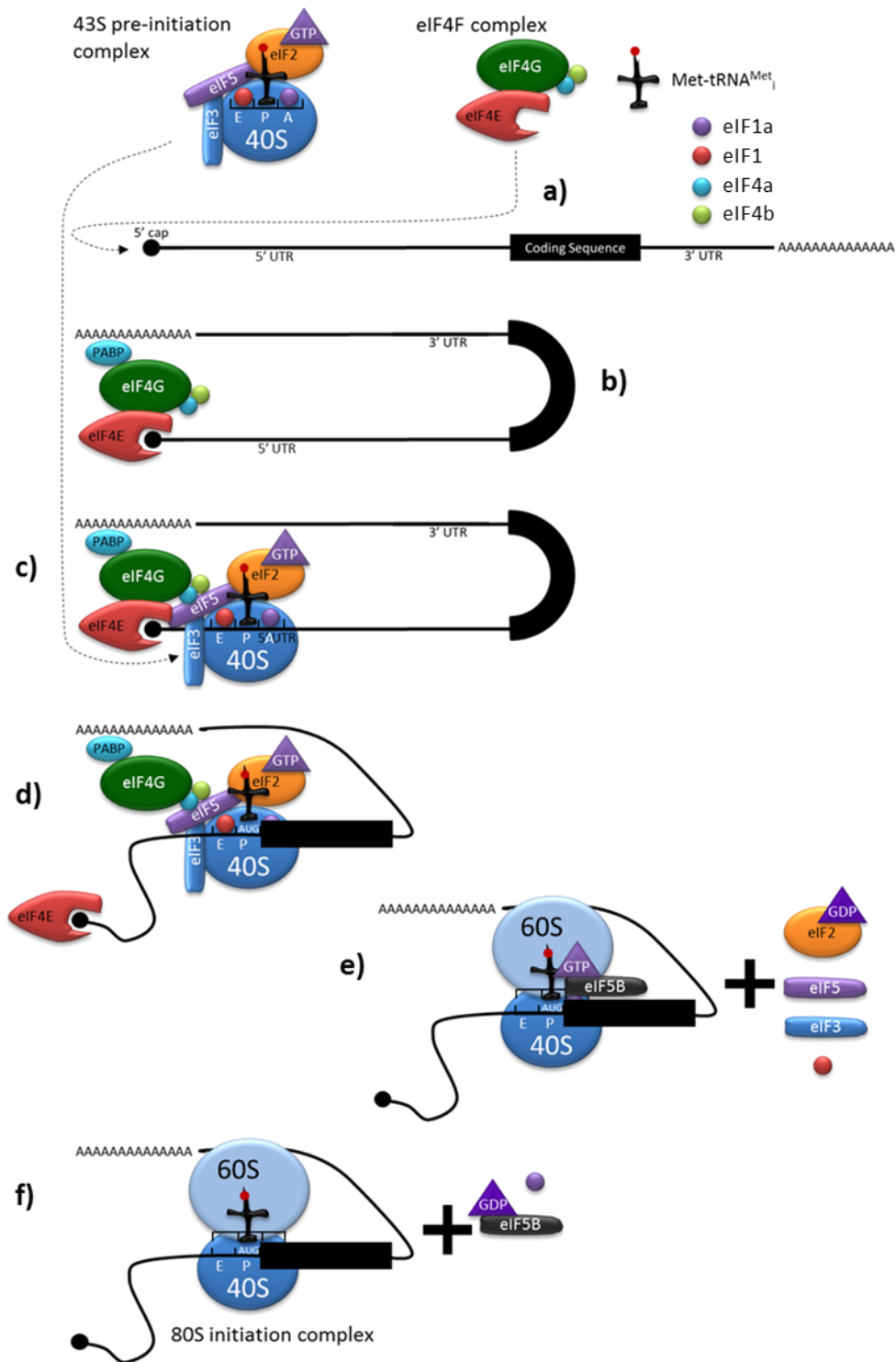


Figure 1.1 Translation initiation is dependent on sequential processing by ribosomal subunits and eukaryotic initiation factors. **A)** eIF4F complex binds 5' methylated Guanine CAP of mature mRNA. **B)** RNA circularises through eIF4G-PABP binding. **C)** 48S preinitiation complex assembly on mRNA. **D)** 5' to 3' scanning of the mRNA. **E)** hydrolysis of eIF2 and dissociation of eIF5, eIF3. **F)** Recognition of the AUG start codon causes hydrolysis of eIF5B and translation by the 80S initiation complex.

1.1.1 mRNA primary sequence determines initiation codon usage

Marilyn Kozak (1986a) described a consensus sequence that enhanced translation in vertebrates, ACCAUGG. This was expanded following further studies by Kozak (1987a & 1987b) to GCCGCC(A/G)CCAUGG. Only 0.2% of vertebrate genes possess this exact sequence (Nakagawa *et al.*, 2008), so it is more appropriately referred to as a 'conserved context'. This conserved context varies between Eukaryotes (Table 1.2). Nakagawa *et al.* (2007) found a sequence almost identical to Kozak's, as the conserved context in human genes, GCCGCC(A/G)(C/A)CAUGGCG, as well as a strong bias for GCG at the second codon. The context of an initiation codon has a massive impact on the strength/efficiency of initiating translation. A poor context means initiation from a codon is greatly decreased. Whilst a good/strong context means an improvement in the rate at which translation is initiated from that site.

Studies by Peabody (1987 & 1989) showed translation initiation from non-AUG codons. They mutated the mouse dihydrofolate reductase (*dhfr*) annotated initiation codon, AUG, to ACG, GUG, UUG, CUG, AGG, AAG, AUA, AUC, and AUU. These codons differ from AUG by only one nucleotide, and are referred to as near-cognate initiation codons. Dihydrofolate reductase was synthesised by mutant sequences (except AGG and AAG) with an SP6 promoter using in vitro transcription/translation. This was also demonstrated in cultured monkey cells. Peabody also showed initiation of translation from non-AUGs maintained the use of Methionine-tRNA at the start of peptide synthesis; radio-labelled tRNA^{Met}_i was incorporated into proteins initiated from non-AUGs (Table 1.3).

| Eukaryotic species/kingdom | Conserved initiation context | Reference |
|--|-------------------------------------|----------------------------|
| Vertebrates | GCCGCC(A/G)CCAUGG | Cavener and Ray, 1991 |
| <i>Drosophila</i> | ACAACCAAAAUGGC | Cavener and Ray, 1991 |
| Other invertebrates | UAAAT(A/C)AACAU(A/G)C | Cavener and Ray, 1991 |
| <i>Saccharomyces cerevisiae</i> | AAAAAAAAAUGTC | Cavener and Ray, 1991 |
| Monocots | GCGGC(A/C)(A/G)(A/C)CAUGGCG | (Joshi <i>et al.</i> 1997) |
| Dicots | AAAAAAA(A/C)AAUGGCU | (Joshi <i>et al.</i> 1997) |

Table 1. 2 Conserved contexts of AUG translation initiation codons.

| Mutated initiation codon | % total synthesis of full-length DHFR |
|---------------------------------|--|
| AUG (wild type) | 100 |
| ACG | 84 |
| CUG | 82 |
| AUU | 67 |
| AUA | 59 |
| AUC | 47 |
| GUG | 36 |
| AGG | 17 |
| AAG | 14 |

Table 1.3 Relative efficiency of non-AUG initiation codons in synthesising full-length DHFR in rabbit reticulocyte lysate. (Adapted from Peabody 1989).

1.1.2 Leaky scanning creates diverse translation products

Translation typically occurs via the scanning model for translational initiation (Kozak, 1989). The 40S ribosomal subunit binds the 5' CAP of an mRNA, forming a 48S preinitiation complex which scans the 5' UTR until it encounters an AUG initiation codon in a strong context (Kozak consensus sequence), whereupon, the 60S subunit joins, forming the elongation competent 80S ribosome. When the scanning 48S preinitiation ribosome does not initiate protein synthesis at an AUG in a strong context, the scanning will continue downstream within the mRNA and may initiate translation at a downstream initiation codon. This is termed leaky scanning, and leads to the generation of diverse proteins translated from the same mRNA.

The position of translation initiation codons within an mRNA significantly affects peptide synthesis (Fig. 1.2). An alternative initiation codon upstream of the annotated initiation codon for the coding sequence (CDS) gives rise to upstream open reading frames (uORF); distinct or overlapping with the CDS. Alternatively, if an alternative initiation codon lies upstream and in-frame of the annotated CDS initiation codon, an extended open reading frame (eORF) is created. Such instances give rise to N-terminally extended proteins. Alternative translation initiation downstream and in-frame of the annotated CDS initiation codon leads to N-terminally truncated open reading frames (tORF).

It was shown by Kozak (1984) that an AUG in a weak context does not always initiate translation initiation by a scanning ribosome. An AUG codon inserted in an expression plasmid upstream and out of frame with the coding sequence for preproinsulin inhibited synthesis of proinsulin. The reduced translation was modulated by changes to the nucleotide sequence context of the upstream AUG.

There is increasing evidence of significant functional consequences of alternative translation initiation. Figure 1.2 illustrates different types of alternative translation initiation and the resulting peptides produced. A) The canonical process of translation initiation is depicted. B) Translation initiation due to the 48S ribosome encountering an upstream initiation codon. The canonical coding sequence may also be translated from the canonical initiation codon, if there is an intervening stop codon. It was demonstrated by Kozak (1984) that a ribosome can reinitiate translation, where translation of a uORF terminates before the start of the coding

sequence. Where there was a short uORF upstream of the coding sequence, proinsulin was synthesised. Upon mutation of the uORF stop codon, no proinsulin was made. This confirmed that the proinsulin made from an expression plasmid with a uORF terminating before the coding sequence was not made due to leaky scanning. It was made due to the ribosome reinitiating following translation of the uORF.

Eukaryotic initiation factor-2 (eIF2) availability determines ribosome competency to initiate, or reinitiate translation. Translation of mRNA is modulated by phosphorylation of eukaryotic initiation factor-2 (eIF2) in response to cell stress. The mRNA of activating transcription factor 4 (ATF4) is regulated as a stress response via two AICs within the 5' UTR of the mRNA, generating two uORFs (Vattem & Wek, 2004). ATF4 mediates expression of genes involved in remediation of cellular stress/damage. The most upstream uORF (uORF1) is illustrated in Fig.1.2 B, it is just three amino acids in length and enhances ribosome scanning and reinitiation at downstream ORFs. The second uORF (uORF2) is like that shown in Fig.1.2 C, and is inhibitory to translation of the canonical CDS. In unstressed cells, scanning ribosomes initiate translation of uORF1, and abundant eIF2-GTP allows rapid reinitiation of translation at uORF2, repressing translation of the annotated CDS. In stressed cells, eIF2 is phosphorylated, so translation initiation is inhibited. Once translation is initiated at uORF1 in ATF4, there is a delay in the ribosome becoming initiation capable again, so decrease probability of initiating translation at uORF2, and instead, allowing increased translation of the annotated CDS. The enhanced expression of ATF4 protein in response to cell stress causes gene expression directed to relieving cell stress.

The use of alternative translation initiation codons can be modulated by RNA binding proteins (RBPs). The CCAAT/enhancer binding protein β (C/EBP β) protein is a transcription factor for immune response genes. The translation from alternative AUG translation initiation codons within C/EBP β mRNA generates different isoforms of the protein, LAP1, LAP2, and LIP (Baldwin, Timchenko and Zahnow, 2004). The longer, LAP, isoforms are generated due to translation initiation at an in-frame uORF, this type of regulation is shown in Fig.1.2 D. The truncated LIP isoform is translated from an alternative AUG initiation codon within the canonical coding sequence, downstream of the canonical AUG translation initiation codon, this type of regulation is shown in Fig.1.2 E. The truncated, LIP, isoform predisposes to tumorigenesis and its

expression is modulated by CUG repeat binding protein (CUGBP1). Epidermal growth factor receptor (EGFR) signalling causes activation (phosphorylation) of CUGBP1 which enhances binding of CUGBP1 with C/EBP β mRNA 5' UTR and eIF2 α , causing increased recruitment of ribosomes for translation of the LIP isoform (Timchenko, Wang and Timchenko, 2005).

The eukaryotic initiation factor 4G (eIF4G) is central to assembly of the 48S preinitiation complex. Leaky scanning of eIF4G1 mRNAs generate multiple isoforms through translation initiation at internal downstream AUG initiation codons (Bradley, Padovan & Thompson; 2002). Different isoforms of eIF4GII have also been shown to be generated from multiple different promoters, alternative splicing and leaky scanning and translation from downstream AIC, CUG (Coldwell *et al.*, 2012).

In the case of *Saccharomyces cerevisiae* glycyl-tRNA synthetase (*GRS1*), leaky scanning of the mRNA allows translation of two protein isoforms. *GRS1* is needed for cytoplasmic and mitochondrial glycyl-tRNA synthase. Translation initiation from position 1, AUG of the coding sequence generates a cytoplasmic protein. Translation from the -69 upstream UUG initiation codon results in a protein with a full N-terminal mitochondrial targeting sequence (Chan & Wang, 2004). The majority of *GRS1* protein synthesis occurs from the AUG at +1. Only a small fraction of the scanning ribosomes recognise and initiate translation from the non-AUG initiation codon at -69.

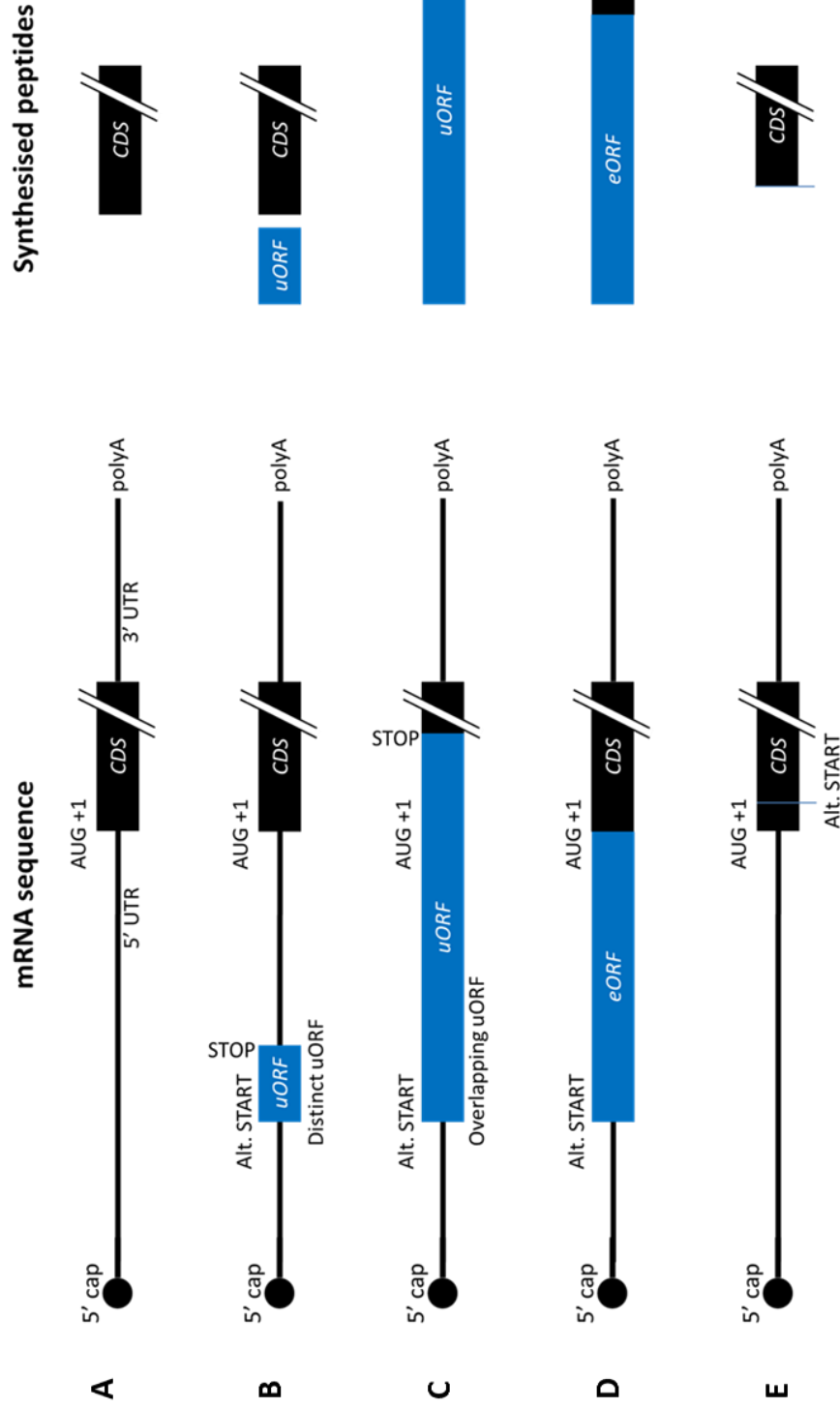


Figure 1.2 Leaky scanning creates diverse translation products. **A)** In the absence of alternative initiation codons, a ribosome initiating translation only at the annotated initiation codon. **B)** If a 48S pre-initiation ribosome encounters an alternative START codon upstream of the annotated AUG, translation will be initiated here. If there is a STOP codon before the annotated AUG, the CDS will also be translated. **C)** If there is no STOP codon upstream of the annotated AUG, and the upstream alternative initiation codon is out of frame with the CDS, then an overlapping uORF will be translated, and no CDS peptide will be produced. **D)** If there is no STOP codon upstream of the annotated AUG, and the upstream alternative initiation codon is in frame with the CDS, then an extended ORF will be translated. **E)** When the annotated AUG is in a weak context, only a portion of 48S preinitiation complexes will initiate translation at this point. Ribosomes will continue scanning until they encounter an alternative initiation codon; if this is in frame with the CDS, then a truncated ORF will be translated.

1.2 mRNA secondary structures regulate initiation codon usage

1.2.1 Hairpins impact translational mechanisms

Secondary structures within mRNA 5' UTRs typically inhibit translation initiation by disrupting eIF4E binding at the 5' cap or retarding ribosome scanning by the 43S pre-initiation complex (Gray & Hentze, 1994). It has been demonstrated that hairpin structures in the 5' UTR of an mRNA can inhibit protein synthesis by as much as 90%. The mechanism was shown as an inhibition of 43S ribosome scanning, as inhibition of translation was seen regardless of the distance from the 5' cap or the initiator AUG (Kozak, 1986). If an AUG in a strong context was part of a hairpin structure, no change in protein synthesis was seen.

In a study by Kozak (1989) into the effect of initiation codon context on translation initiation in *in vitro* assays, an unexpected increase in initiation was seen when a hairpin structure was immediately downstream of the initiation codon. It was suggested that the hairpin caused the ribosome to stall over the initiation codon, increasing the probability of recruiting the 60S ribosomal subunit and initiating peptide synthesis (Fig. 1.3).

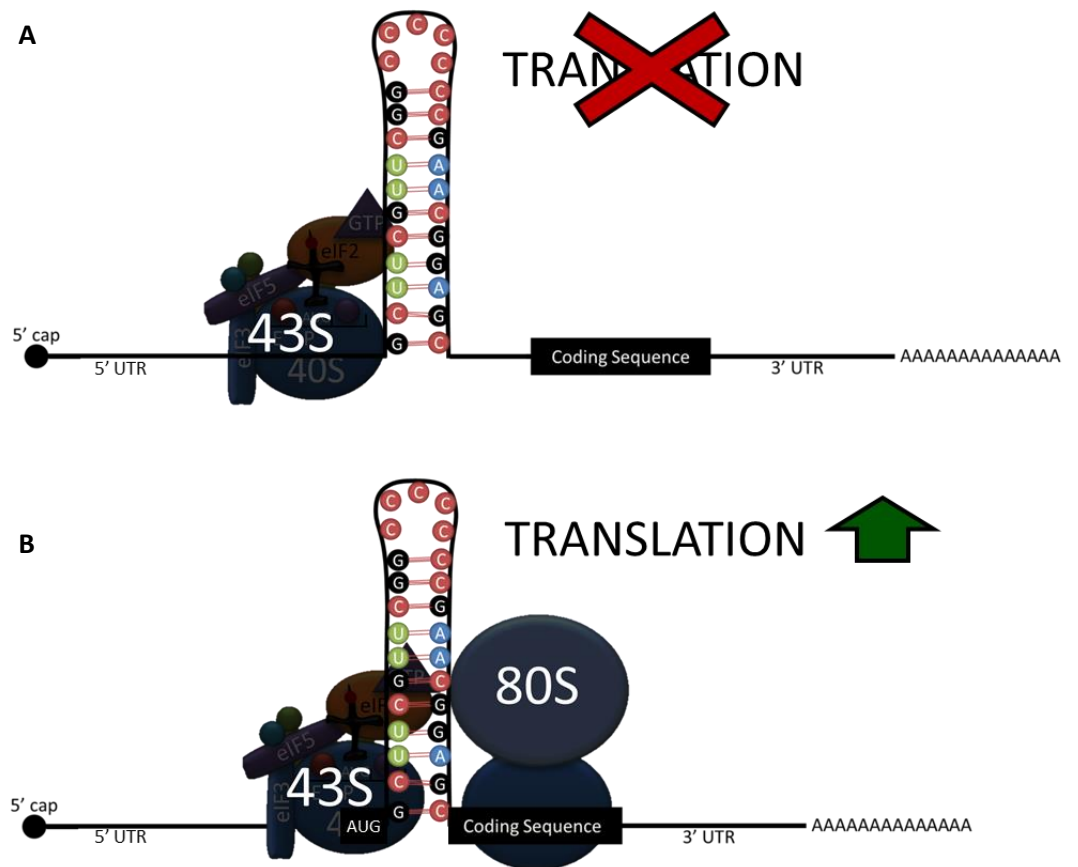


Figure 1.3 5' UTR RNA hairpins inhibit ribosome scanning and therefore inhibit translation from downstream initiation codons A) Stable hairpins can cause pausing of the scanning ribosome over proximal upstream initiation codons, increasing the probability of translation initiation B).

1.2.2 G-quadruplexes impact translational mechanisms

RNA hairpins form with hydrogen bonding between Watson-Crick complementary base-pairs. GU base pairs are also common in and between RNA molecules (Varani & McClain, 2000). Guanine-rich nucleotide sequences form stable G-quadruplex structures. Guanine nucleotides adopt a planar tetrad via hydrogen bonds; each guanine nucleotide donates and accepts two electrons (Fig. 1.4A). These tetrads stack, promoted by monovalent cations, particularly K^+ , to form increasingly stable G-quadruplexes (Fig. 1.4B, Joachimi *et al.*, 2009).

The C2' hydroxyl groups of ribose in RNA forms additional intramolecular hydrogen bonds, yielding more stable G-quadruplexes than in DNA (Bugaut & Balasubramanian, 2012). DNA quadruplexes have been shown to exist as parallel or antiparallel structures. RNA G-quadruplexes have been shown to predominately form parallel quadruplexes due to alterations in the phosphate backbone resulting from the orientation of the C2' hydroxyl groups of ribose in RNA (Collie *et al.*, 2010).

The structure of RNA G-quadruplexes relative to DNA quadruplexes is primarily determined by the ribose sugar and uracil residues. The 2' hydroxyl group of the ribose sugar allows more extensive intramolecular binding which increases stability of the structure. DNA G-Quadruplexes form both parallel and anti-parallel conformations, however, RNA G-quadruplexes are only able to form parallel conformations (Pandey, Agarwala and Maiti; 2013). The 2' hydroxyl group bonds act to restrain the G-quadruplex from forming syn-conformation, thus preventing antiparallel folding (Joachimi, Benz and Hartig; 2009). The strands are oriented in the same direction in the parallel conformation of RNA G-quadruplexes, with propeller loops (the twisting of the loops resembles the shape of propeller blades) connecting the top of one strand to the bottom of another (Fig. 1.4). Many studies have demonstrated increased stability of both RNA and DNA G-quadruplexes due to shorter loop length. The nucleotide composition of loops is significant to stability of quadruplexes too. The presence of uracil in place of thymine in loops increases stability of the quadruplex (Olsen, Lee & Marky; 2008).

Pandey, Agarwala and Maiti (2013) investigated the factors affecting the stability of RNA G-quadruplexes. Both naturally occurring UTR G-quadruplex sequences and synthesised RNA oligonucleotides were subjected to UV melting experiments to

assess thermal stability of the G-quadruplexes relative to their loop length and composition in physiological potassium concentrations. They found that the stability of G2 RNA quadruplexes (GGN) is inversely proportional to loop length. This holds true down to a single base as the loop sequence. A loop length of 1 in the sequence GGUGGUGGUGG had a melting temperature of 60°C, whilst a loop length of 3, 7 or 11 had melting temperatures of 30°C, 19°C or 14°C respectively. Since physiological temperature is 37°C, G2 sequences with loop length of 3 or greater would not form stable G-quadruplexes in vivo. They also analysed thermal stability of G3 G-quadruplexes and found the same relationship of decreasing thermostability with increasing loop length. However, the stability decrease plateaued and all loop lengths up to the 15 nucleotide length tested had melting temperatures above 37°C. It is therefore possible for stable G-quadruplexes to form in vivo between distant (15 nucleotides, and predicted to be more) G3 sequences within mRNA molecules.

Malgowska *et al.*, (2014) investigated the formation of G-quadruplex structures formed from trinucleotide repeat RNA. GGA and GGU repeat sequences formed strong G-quadruplex structures, as measured by several biophysical techniques. GGC2 or GGC4 sequences were found to fold into G-quadruplex and other structures depending on the cation present and the repeat length. GGC2 or GGC4 folds into a G-quadruplex in potassium buffer but not in ammonium or sodium containing buffer. In the ammonium or sodium containing buffer, GGC2 or GGC4 sequences were found to form duplex or hairpin structures.

The presence of quadruplexes in RNA has been subject to extensive debate and diversity in experimental approach. However, there is a growing body of evidence supporting the presence of RNA G-quadruplexes in vitro and in vivo. Many different methods have been used to assess the formation of RNA G-quadruplexes. X-ray crystallography has been used to investigate the fine structure of G-quadruplexes in DNA and RNA. A very high resolution structure has been achieved for the RNA tetraplex CGGGGC4 (0.61Å) (Deng, Xiong & Sundaralingam; 2001). The majority of G-quadruplex structural studies have been performed by NMR. Imino proton resonances of 11-12 ppm are characteristic of guanines involved in G-quartet formation (Blice-Baum & Mihailescu; 2014).

Circular dichroism (CD) is widely used to measure G-quadruplex formation, orientation and thermal decomposition (Guittat *et al.*, 2004). CD measurement of DNA G-quadruplexes is unambiguous, however RNA can form A-form duplexes with complementary RNA or DNA sequences, which give similar spectra to parallel G-quadruplexes. Parallel G-quadruplexes show peak at 262 nm and negative peak at 237 nm (Kumari *et al.*, 2007). It is possible to distinguish G-quadruplex formation in RNA by an additional hypochromism at 295nm (Mergny, Phan & Lacroix; 1998).

A less commonly employed method for measuring G-quadruplex formation in RNA is non-denaturing gel electrophoresis, also known as an electrophoretic shift mobility assay. G-quadruplex formation makes nucleotide sequence more compact relative to single stranded nucleotide sequences, so enhances the speed at which it moves through a non-denaturing gel. This technique does not allow actual identification of the structure formed by a nucleotide sequence, but has been used to illustrate the change in folding conformation relative to buffer conditions such as potassium concentration (Khateb *et al.*, 2007; Fig. 1.6).

G-quadruplexes are predicted to be common in 5' UTRs of mRNAs. A recent study estimates ~3000 human mRNA 5' UTRs contain predicted quadruplex-forming sequences (Kumari *et al.*, 2007). The 5' UTR G-quadruplex of the proto-oncogene, NRAS, was shown to inhibit protein expression by ~80% in vitro (Kumari *et al.*, 2007). 5' UTR hairpins have been shown to inhibit assembly of the pre-initiation complex at the 5' cap (Babendure *et al.*, 2006), and to inhibit mRNA scanning towards the initiation codon (Kozak, 1989). G-quadruplex-mediated repression of translation has recently been shown in vivo. The 5' UTR of Zic-1 contains a G-quadruplex forming sequence, which inhibits protein synthesis by ~80% in HeLa cells (Arora *et al.*, 2008). The authors showed that mutation of the sequence to a non-quadruplex-forming sequence removed protein synthesis inhibition. They demonstrated the effect was inhibiting translation and not transcription, by RT-PCR. The NRAS G-quadruplex must be within ~50-100 nucleotides of the 5' cap to inhibit in vitro translation (Kumari, Bugaut & Balasubramanian, 2008).

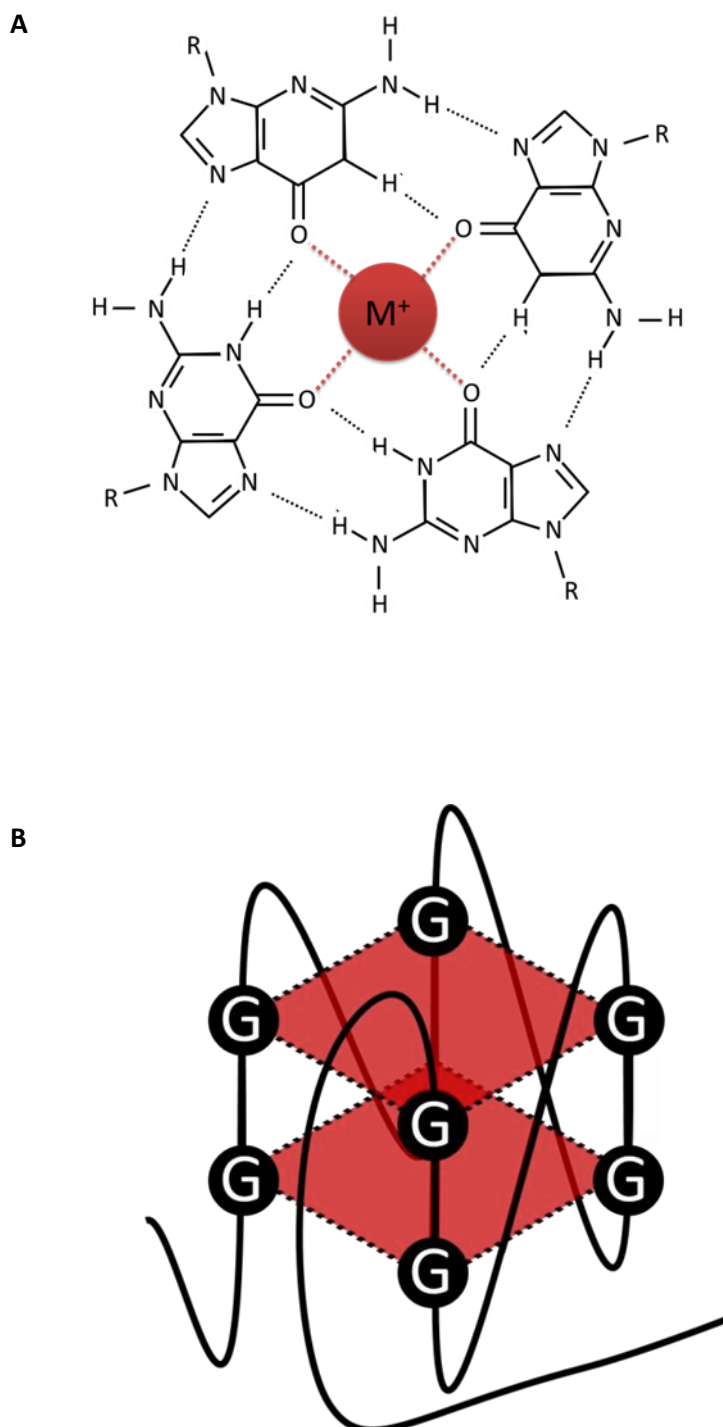


Figure 1.4 Guanine-rich nucleotide sequences form stable G-quadruplex structures. **A)** Guanines accept and donate two electrons with proximal guanines in a planar tetrad. Hydrogen bonds shown with dotted lines. M^+ is any monovalent cation, principally K^+ , but also Na^+ . **B)** Guanine tetrads stack to form four-stranded secondary structures. RNA forms parallel G-quadruplexes as shown in this diagram, where the orientation of RNA strands are parallel.

RNA G-quadruplexes are typically inhibitors of RNA translation (Fig. 1.5). However, G-quadruplexes have recently been shown to play crucial roles in cap-independent translation. An RNA G-quadruplex has been shown to be an essential component of an IRES within the 5' UTR of fibroblast growth factor 2 (*FGF2*) (Bonnal *et al.*, 2003). The IRES activity within the 5'-UTR of human vascular endothelial growth factor (*hVEGF*) is dependent on the presence of a 'conformationally flexible' G-quadruplex. The majority of other IRESs do not contain G-quadruplexes (Morris *et al.*, 2010).

The Fragile X Mental Retardation Protein, FMRP, is a neuronal regulator of translation. Fragile X Syndrome is a result of an expanded 5' UTR CGG repeat. The normal 5' UTR CGG repeat length is around 30 nucleotides and forms G-quadruplex structures (Fig. 1.6) (Khateb *et al.*, 2007). Khateb used electrophoretic mobility shift assays to determine G-quadruplex folding my mRNAs. G-quadruplexes incubated show increased electrophoretic mobility following incubation with 120 mM KCl. Other methods have been used extensively to show nucleotide sequences forming G-quadruplex structures, including nuclear magnetic resonance (NMR), circular dichroism (CD) and increased fluorescence of Mesoporphyrin IX dihydrochloride (NMM). In fragile X-associated tremor ataxia syndrome (FXTAS), the repeat length is expanded typically to 55 - 200. FXTAS is characterised by elevated *fmr1* mRNA expression, often found with various proteins in inclusion bodies. The expanded CGG repeat length (to 55 – 200) in FXTAS causes decreased *fmr1* translation and neurodegeneration. In Fragile X syndrome, the repeats are over 200 and sometimes thousands in length; often methylated, suppressing transcription of the Fragile X mRNA. Decreased FMRP expression means there is dysregulation of mRNA translation.

The mechanism for FMRP binding to specific mRNAs is not fully defined. FMRP has interactions with multiple RBPs and non-coding RNAs, which suggest multiple mechanisms by which FMRP interacts with mRNAs. FMRP has been found in RNPs of the non-coding brain cytoplasmic RNA, BC1. BC1 binds to FMRP via the tudor RNA-binding domains of FMRP N-terminus. The FMRP-BC1 complex has specific effects on local translation of specific mRNAs at the synapse (Lacoux *et al.*, 2012). BC1 RNA is necessary for binding of specific mRNAs by FMRP (including *CamkII α*), whereupon the complex can act to translationally repress the translation of the target mRNA (Napoli *et al.*, 2008).

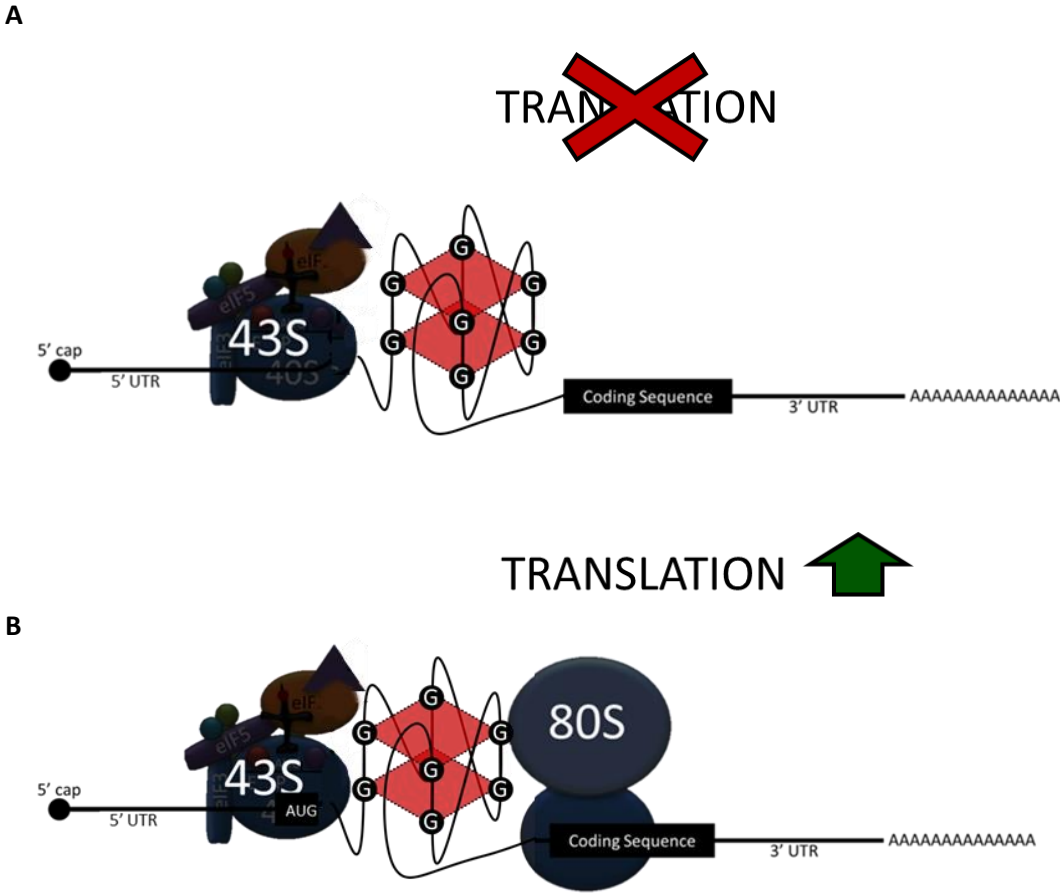


Figure 1.5 A) 5' UTR G-quadruplexes inhibit ribosome scanning and therefore inhibit translation from downstream initiation codons G-quadruplexes can cause **B)** pausing of the scanning ribosome over proximal upstream initiation codons, increasing the probability of translation initiation.

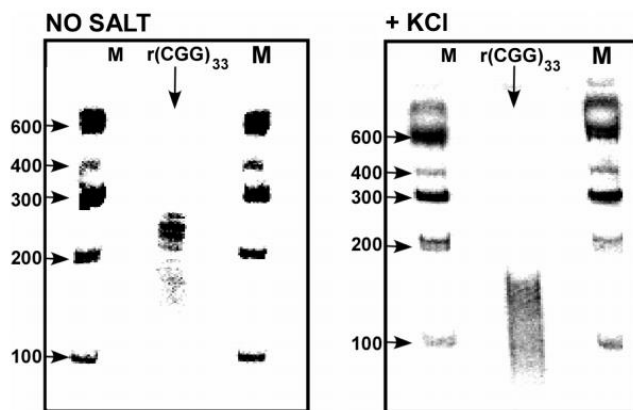


Figure 1.6 Autoradiograms of electrophoretically resolved $5'-^{32}\text{P}\text{FMR1-5'-UTR}(\text{CGG})_{33}$ RNA following incubation at 4°C for 15 min with or without 120 mM KCl. Increased electrophoretic mobility of $5'-^{32}\text{P}\text{FMR1-5'-UTR}(\text{CGG})_{33}$ RNA following incubation with 120mM KCl indicates a conformational compaction, indicative of G-quadruplex formation.

Figure from Khateb et al. (2007)

1.3 RNA-binding proteins and the 5' UTRs of mRNAs

The separation of transcription from translation in eukaryotes affords multiple additional opportunities for gene regulation. From the biogenesis of the newly transcribed pre-mRNA, specific RBPs bind and control the maturation of the mRNA by coordinating splicing, editing and polyadenylation.

RBPs specifically bind RNAs based on recognition of ribonucleotide primary sequence or secondary structure motifs. There are a diverse range of peptide sequences characterised as specific RNA-binding domains of proteins, including the RNA recognition motif (RRM), Arg-Gly-Gly (RGG) box, DEAD/DEAH box, and K-homology (KH) domains I & II. Bioinformatic analysis of the Yeast identified up to 8% of proteins have known RNA-binding domains (Keene *et al.*, 2001), if humans had a similar percentage of proteins with RNA-binding domains, this would be equivalent to more than 2,500 RBPs in the human genome. Most RBPs have multiple RNA-recognition domains which is an indication of the complexity of control of RNA processing. One example of the importance of RBPs in control of gene expression is the poly(A)-binding protein (PABP), which possesses four RRM domains and binds mRNAs with long polyA tails. PABP mediates circularisation of an mRNA with eIF4F complex; required for translation of mRNAs (Coller, Gray & Wickens., 1998).

1.3.1 RNA Helicases resolve secondary structure

The primary rate limiting step in translation of an mRNA is translation initiation. Pre-initiation ribosome scanning of an mRNA by the 43S ribosome is inhibited by secondary structures in the 5' UTR. The scanning 43S ribosome contains an RNA helicase, eukaryotic translation initiation factor 4A (eIF4A or DDX2) which is able to resolve moderate secondary structures. The activity of eIF4A is regulated by eIF4B and eIF4G (Harms *et al.*, 2014). However, it has recently been shown that strong secondary structures require the activity of additional RNA helicases.

The largest family of RNA helicases is the DEAD/DEAH/DDX/DHX/RNA helicase A superfamily 2. DEAD-box helicase proteins have a helicase core consisting of at least

12 conserved motifs. The second motif gives the proteins the DEAD-box name (Asp-Glu-Ala-Asp/His or D-E-A-D/H) (Linder & Jankowsky, 2011).

eIF4A is a DEAD-box helicase which cycles through open and closed conformations relative to binding by eIF4B and eIF4G. However, it has been shown that the DEAH/RHA RNA helicase, DHX29 is essential for translation of mRNAs with highly stable 5' UTR hairpins. In the absence of DHX29, RNA hairpins can enter the mRNA-binding channel of the scanning 43S ribosome, but the hairpins are unable to exit, which ultimately leads to dissociation of the ribosome from the mRNA. The N-terminal region of DHX29 binds the ribosome near the mRNA entrance and expresses nucleoside triphosphatase (NTPase) activity, allowing correct processing of mRNAs through the 43S pre-initiation complex (Dhote *et al.*, 2012). DHX29 is not a processive RNA helicase, and is thought to work by modulating the conformation of the 43S ribosome. DHX29 NTPase activity is specific to double stranded RNA, and has not been shown to unwind quadruplex RNA.

Another DEAH-box helicase protein, DHX36, contains a unique N-terminal domain with specific RNA G-quadruplex-binding activity. It is the principal resolvase of DNA G-quadruplex in HeLa cells, shown to account for >50% of unwinding DNA G-quadruplex (Creacy *et al.*, 2008). Lattmann *et al.*, (2010) showed DHX36 specific recognition of G-quadruplex sequences is dependent on the amino-terminal region of DHX36, the RHAU-specific motif (RSM) – not found in other known RNA helicases. Giri *et al.*, 2011 used electrophoretic mobility shift assays to find high binding affinity of DHX36 to naturally occurring DNA G-quadruplex sequences. They also used a peptide nucleotide trap assay to show ATP dependence of DHX36 for unwinding G-quadruplex sequence, allowing binding to the complementary trap nucleotide sequence. DHX36 has known function in neurons, and is responsible for normal dendritic localisation of pre-miR-134 transcript, the mechanism is unknown (Bicker *et al.*, 2013).

DHX30 is a member of the DEAH superfamily 2 which is highly correlated with Task3 mRNA expression in Breast Cancer primary tumour cells, normalised Pearson's coefficient, 4.51 (Mosca *et al.*, 2010). Xu *et al.*, (2013) found by mass spectrometry, DHX30 bound to (GGGGCC), (CUG), but not (CGG) repeat RNA. The Human Protein Atlas shows high protein expression levels of DHX29, DHX36 in all tissues, apart from adipose and soft tissue. DHX30 is shown as high in only around half the displayed

tissues, including brain, endocrine, muscle, lung, liver and kidney. The Biological General Repository for Interaction Datasets (BioGRID: <http://thebiogrid.org>) was used to identify protein interactors of DHX29, DHX30 and DHX36 (Fig. 1.7, 1.8 & 1.9). DHX29, 30 and 36 interact with RNA-binding proteins. There is evidence for the interaction of DHX29 with eIF3A, a subunit of the largest translation initiation factor involved in regulating translation initiation. DHX29 also binds hnRNP1 which binds heterogeneous nuclear RNA and regulates pre mRNA processing. Also of interest is the interaction of DHX29 with the 60S ribosomal protein L35 (RPL35) and the interaction with 60S ribosomal protein L10 (Fig 1.10). These interactions suggest a complex role for DHX29 in regulating RNA processing. DHX30 is associated with many RNA-binding proteins including hnRNPA1, hnRNP1, eIF3I, Stau1, RPL18, RPL18A, RPL30, RPL10 and RPL37A. DHX36 also interacts with multiple RNA-binding proteins, including hnRNPA1, DDX5 and RPL35.

Specific G-quadruplex-targeting RBPs regulate expression of mRNAs with 5' UTR G-quadruplexes. The heterogeneous nuclear ribonucleoproteins (hnRNPs), CBF- α and hnRNPA2 destabilize RNA G-quadruplexes and relieve translational repression caused by 5' UTR CGG repeats (Khateb *et al.*, 2007).

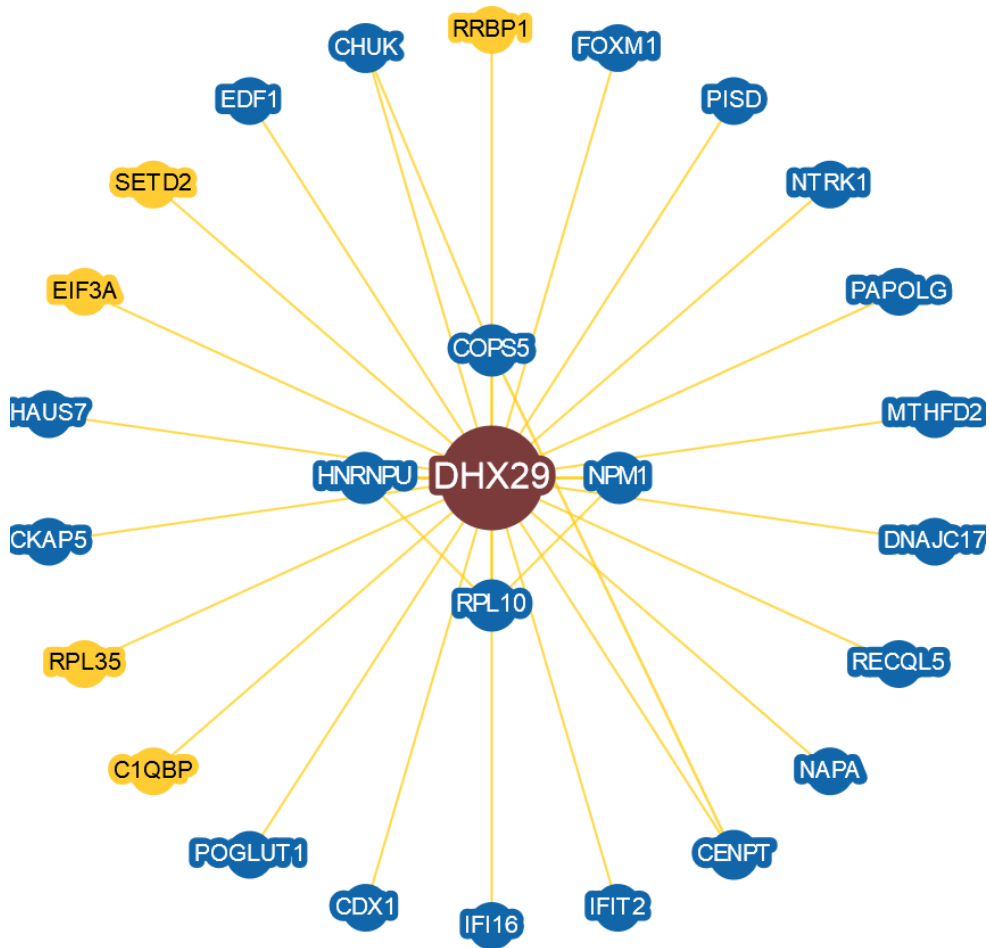


Figure 1.7 Known protein interactors of DHX29 from BioGrid.

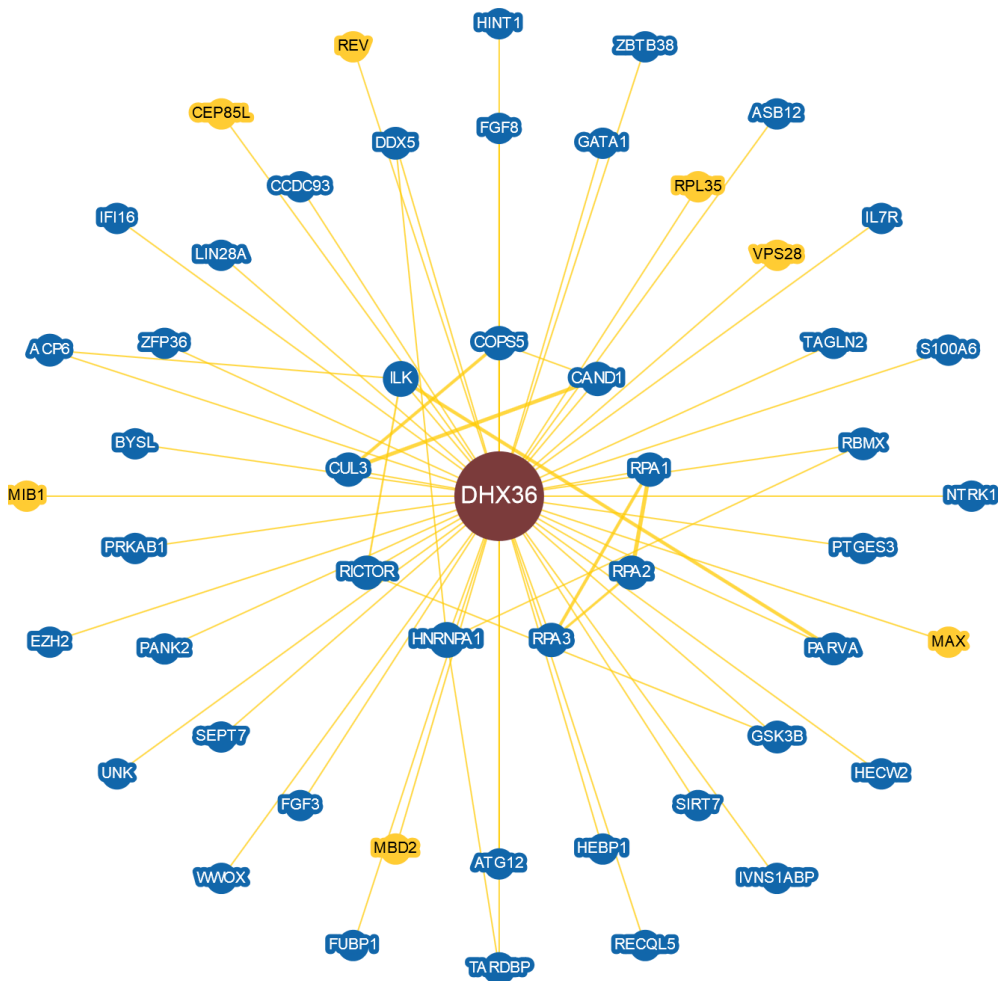


Figure 1.9 Known protein interactors of DHX36 from BioGrid.

1.4 Modulating RNA G-quadruplex effects with small-molecules

Anti-amyloidogenic α -secretase, disintegrin and metalloproteinase 10 (ADAM10) is an important protein in Alzheimer's disease (AD). α -secretase ADAM10 cleaves the amyloid precursor protein and inhibits formation of the primary component of amyloid amyloid plaques in Alzheimers patients, β -peptide (A β). The mRNA of α -secretase ADAM10 contains a 5' UTR G-quadruplex which inhibits its translation (Lammich *et al.*, 2010). G-quadruplex-mediated repression of translation is relieved by treatment with a methylquinolinium derivative small molecule which binds to the 5' UTR G-quadruplex (Dai *et al.*, 2015).

5,10,15,20-tetra(N-methyl-4-pyridyl)porphyrin (TMPyP4) is a cationic porphyrin and unfolds (CGG)_n quadruplexes in vitro (Ofer *et al.*, 2009). TMPyP4 increased the efficiency of translation of a (CGG)₉₉-luciferase construct in HEK293 cells (Ofer *et al.*, 2009). 24 hrs post-transfection with Task3 mutant 5' UTR expression plasmids, TMPyP4 was applied to cell growth media and cells harvested after a further 24 hrs. TMPyP4 was applied to cells at 50 μ M concentration, higher than that used in the Ofer study, 20 μ M, but lower than that used in other studies, up to 100 μ M in HeLa cells (Morris *et al.*, 2012).

Many oncogenes are characterised by G-quadruplex sequences in their 5' UTRs (Wolfe *et al.*, 2014). Manipulation of G-quadruplex helicase activity was suggested as a potential target for cancer therapy. It was demonstrated that Silvestrol and other eIF4A inhibitors including Hippuristanol are able to specifically down-regulate expression of G-quadruplex-containing oncogenes. Deep sequencing identified mRNAs which were translationally down-regulated upon inhibition of eIF4A. These mRNAs were enriched for mRNAs with long 5' UTRs, particularly 12-nucleotide (CGG)₄ repeat sequences, known to be able to form G-quadruplex structures (Malgowska *et al.*, 2014).

1.5 Subcellular localisation of mRNA

The targeting of mRNA to subcellular localisations is an important mechanism for dynamic control of a local proteome. A study of subcellular mRNA localisation found ~71% of 3,000 studied mRNAs were targeted to specific subcellular regions in a single cell, the *Drosophila* embryo (Lecuyer *et al.*, 2007). RBPs act as trans-acting mediators of mRNA subcellular trafficking, recognising cis-acting localisation signals within mRNAs (Fig. 1.7). Specific mRNAs are transported in translationally repressed states as ribonucleoprotein particles, restricting production of the protein to the target site (Besse & Ephrussi, 2008).

Kislauskis, Zhu & Singer (1997) published one of the first major experiments showing subcellular mRNA localisation. Fluorescence in situ hybridisation (FISH) was used to measure the subcellular localisation of the mRNA in fixed chicken embryo fibroblasts (CEFs). FISH revealed β -actin mRNA localised to the lamellipodia of the leading edge of migrating CEFs. The localisation of β -actin mRNA to the leading edge of CEFs was demonstrated to be dependent on the zipcode-binding protein 1 (ZBP1) (Ross *et al.*, 1997). ZBP1 contains four KH domains and one RRM. ZBP1 binds β -actin mRNA at the site of transcription, recognising a 54 nucleotide zipcode sequence in the 3' UTR. ZBP1-bound β -actin mRNA moves to the cytoplasm in a translationally repressed state. Derepression of translation occurs at the target site through phosphorylation by the Src tyrosine kinase of Tyr396, which is proximal to KH domains responsible for ZBP1-binding (Ross *et al.*, 1997).

There is now a wealth of reports on the subcellular localisation and dynamic trafficking of mRNAs within cells. It is an important mechanism for targeting proteins to their sites of function. mRNAs are transported as ribonucleoprotein (RNP) complexes, containing diverse RBPs and non-coding RNAs (reviewed in Kato & Nakamura, 2012). The fate of a specific mRNA is determined by the complement of the RBPs and non-coding RNAs bound to the mRNA.

Following processing of the nascent transcript in the nucleus of a cell to a mature mRNA, they are bound by RBPs to form RNPs. cis-acting elements within the mRNA target specific RBPs to the mRNA, initiating the processes of RNP modelling and remodelling throughout its transport within the cell. The secondary structure of parts of an mRNA can act as cis-acting elements (Patel *et al.*, 2012). Alternative splicing can shuffle these cis-acting elements, causing rearrangements in the binding of RBPs,

leading to differential fate of the mRNA species (Trcek & Singer, 2010). mRNAs are exported from the nucleus via interaction of the RNP with the nuclear pore complex (NPC). It has also been shown, in *Drosophila* neuromuscular junction, large RNPs can transport from the nucleus to the cytoplasm by vesicular budding (Jokhi *et al.*, 2013).

Transport within the cytoplasm can occur once the mRNA has reached the outer surface of the nuclear envelope. Transport can occur via simple diffusion, such as *nanos*, which is localised by diffusion and anchoring of *nanos* mRNA to germ plasm (Forrest & Gavis, 2003). The majority of studies of mRNA intracellular transport have found a dependence on transport along the cytoskeleton by molecular motor proteins. Controlled translation of an mRNA occurs at their target destination. cis-acting elements of an mRNA determine remodelling of the RNP at the destination, binding different trans-acting proteins for regulating translation. One early example of this locally mediated regulation of translation of an mRNA is in *Drosophila*, where the Bruno protein recognises Bruno-response element (BRE) binding sites in the 3' UTR of *oskar* mRNA and prevent binding of the *oskar* mRNA cap by eIF4E, essential for formation of the eIF4F complex, required for translation (Kim-Ha, Kerr and MacDonald, 1995).

Polyadenylation or deadenylation has been demonstrated as a means of controlling the local translation of specific mRNAs. A long poly(A) tail is required for binding of cytoplasmic poly(A) binding proteins, determinant of initiation factor recruitment and circularisation of the mRNA for translation. Cytoplasmic polyadenylation of specific mRNAs has been shown to be crucial in development of many species. Some maternal mRNAs exist in the oocyte with short poly(A) tails, and so are not translated. Upon oocyte maturation or after fertilisation, the poly(A) tail is elongated from ~30 nucleotides to >100 nucleotides. Translational control occurs by CPE-binding protein (CPEB) recognition of cytoplasmic polyadenylation elements (CPEs), uridine-rich sequence elements, within the 3' UTR of specific mRNAs. CPEB binding of mRNAs causes polyA tail elongation, thus promoting translation of the mRNA.

| Gene (mRNA) | Mechanism | Reference |
|---------------|--|---|
| <i>bicoid</i> | Bicoid protein gradient pattern of the anterior-posterior axis of the <i>Drosophila</i> embryo is an essential element in <i>Drosophila</i> embryogenesis. In late <i>Drosophila</i> oogenesis, <i>bicoid</i> mRNA is localised to the anterior of the <i>Drosophila</i> oocyte by continual active transport. | Weil, Forrest & Gavis, 2006 |
| <i>nanos</i> | Nanos protein patterning of the anterior-posterior axis of the <i>Drosophila</i> embryo is an essential element in <i>Drosophila</i> embryogenesis. In late <i>Drosophila</i> oogenesis <i>nanos</i> is localised by diffusion and anchoring of <i>nanos</i> mRNA to germ plasm. | Forrest & Gavis, 2003 |
| <i>oskar</i> | Transported in large complex RNPs with multiple other mRNAs. Kinesin transports <i>osk</i> along microtubules to the plus-end of the <i>Drosophila</i> embryo. | Brendza <i>et al.</i> , 2000; Clark <i>et al.</i> , 1994; Hachet & Ephrussi, 2001 |
| <i>gurken</i> | Kinesin transports <i>grk</i> mRNA along microtubules to the minus-end of the <i>Drosophila</i> embryo. | Januschke <i>et al.</i> , 2002; Delanoue <i>et al.</i> , 2007 |

Table 1.4 Examples of mRNA subcellular localisation studies and their importance in determining cell behaviour.

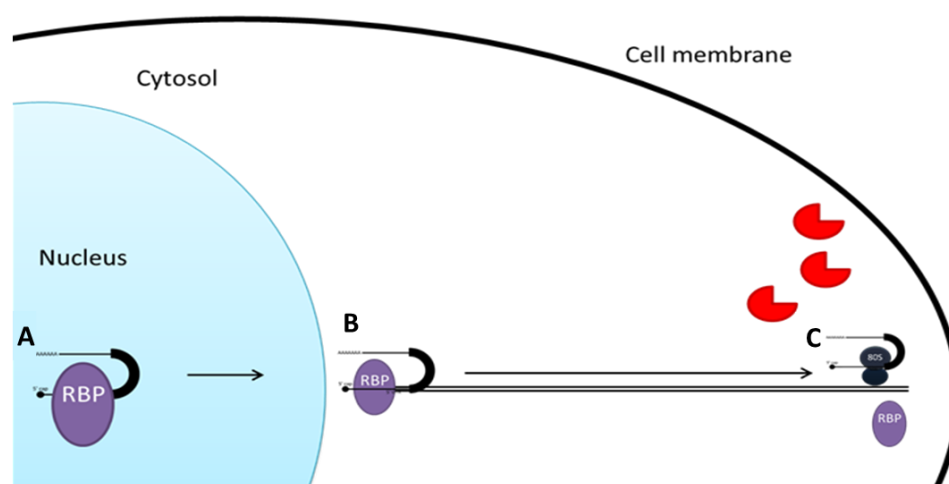


Figure 1.10 The targeting of mRNA to subcellular locations within a cell is mediated by RBPs. **A)** RBPs bind the nascent pre-mRNA transcript in the nucleus and the ribonucleoprotein (RNP) complex is transported out of the nucleus in a translationally repressed state. **B)** The composition of the ribonucleoprotein particle adjusts on binding the molecular motors of the microtubules. **C)** The translational repression of the RNP is relieved at the target site, and local translation of the mRNA is allowed.

1.5.1 mRNA structural motifs determine mRNA targeting

Translation initiation typically occurs in the cytoplasm. Organelles within eukaryotic cells require specific targeting of newly synthesised proteins. For proteins destined for the nucleus, mitochondria, chloroplasts, peroxisomes or cytoplasm, translation elongation and termination occur in the cytoplasm. On release from the ribosome, these proteins are transported to their appropriate organelles, termed posttranslational import. In the case of proteins destined for the cell membrane, endomembranes or secretion, an N-terminal signal peptide on nascent polypeptides (Blobel and Dobberstein, 1975) is recognised by a signal recognition particle (SRP) (Keenan *et al.*, 2001). On binding SRP, translation is paused, whilst the entire complex is directed to the Sec61 complex in the membrane of the ER where translocation can occur. Elongating endomembrane peptides translocate into the ER lumen, whilst integral membrane proteins are inserted into the ER membrane. This is termed co-translational import.

Recently, it has been shown that ribosome subunits and mRNAs can localise to the ER without a signal peptide and in the absence of translation (Chen *et al.*, 2011). mRNA targeting has been seen in yeast (Long *et al.*, 1997), *Drosophila* (MacDougall *et al.*, 2003) and plants (Choi *et al.*, 2000 and Washida *et al.*, 2004). In *Drosophila* embryos, it has been estimated that over two-thirds of mRNAs are specifically localised (Lécuyer *et al.*, 2007). The majority of mRNAs encoding mitochondrial proteins are found proximal to mitochondria, not evenly distributed throughout the cytoplasm (Gadir *et al.*, 2011).

1.6 FMRP is a G-quadruplex binding RBP and its mRNA contains G-quadruplexes

FMRP binds to G-rich RNAs via the FMRP G-quadruplex-recognising domain, C-terminal RGG box. Darnell *et al.*, (2001) showed the binding of FMRP to the G-quadruplex-forming RNA sequence, *sc1* (GCUGCGGUGUGGAAGGAGUGGUCGGGUUGCAGCG), was reliant on the C-terminal RGG box. Binding was decreased by lowering potassium levels or mutating guanines from the G-tracts, demonstrating G-quadruplex-dependence. The autosomal paralogs, FXR1P and FXR2P, expressed in the brain, share significant homology in the C-termini but do not contain the N-terminal G-quadruplex-binding RGG domain of FMRP; they are unable to rescue FXTAS phenotype. Menon and Mihailescu (2007) showed the RGG box of FMRP to be essential for binding to the dendritic semaphorin 3F (S3F) RNA *in vitro*. They showed by circular dichroism spectroscopy, NMR spectroscopy and electrophoretic mobility gel shift assay (EMSA) that the RNA sequence bound by the RGG domain of FMRP forms both G-quadruplex, and stem-loop structures *in vitro*. Both FMRP and its autosomal paralog, FXR1P bind and unwind the G-quadruplex of S3F through their RGG domains. FXR1P unwinds the G-quadruplex with a 3x greater efficiency than FMRP.

Recently it has been shown that *fmr1* 5' UTR CGG repeats cause proximal upstream translation initiation (Todd *et al.*, 2013), generating N-terminal-poly-glycine FMRP (FMRpolyG) as well as poly-alanine peptides out of frame with *fmr1*. The efficiency of this repeat-associated non-AUG-initiated translation (RAN) is proportional to CGG repeat length. FMRpolyG accumulates in ubiquitin-positive inclusion bodies, characteristic of Fragile X patient brains. CGG repeats form G-quadruplex structures (Khateb *et al.*, 2007)), inhibiting ribosome scanning of the 5' UTR to the canonical initiation codon. One study showed a 33 CGG repeat sequence upstream of a luciferase reporter plasmid in HEK293 repressed translation (Khateb *et al.*, 2007). However, coo-expression of the quadruplex-destabilizing proteins, CBF-A and hnRNP A2, relieved this translational repression (Ofer *et al.*, 2009).

It is possible that normal CGG repeat length has evolved in *fmr1* to finely control neuronal FMRP expression. A normal 5' UTR CGG repeat length targets *fmr1* mRNA for local translation at dendritic spines (Muslimov *et al.*, 2011). Heterogenous nuclear

ribonucleoprotein A2 (hnRNP A2) binds the dendritic regulatory RNA, BC1 and mRNA of protein kinase M ζ (PKM ζ). Disruption of the binding motifs in BC1 and PKM ζ ablated dendritic localisation of the RNAs (Muslimov *et al.*, 2011). hnRNP A2 also binds CGG repeat RNA (Sofola *et al.*, 2007). The Muslimov paper (2011) showed expression of FXTAS levels of CGG repeat RNA out-competed BC1 and PKM ζ binding of hnRNP A2. It has also been shown in *Drosophila*, that CGG repeat RNA sequesters RNPs, including hnRNP A2 (Sofola *et al.*, 2007). Muslimov describes the binding sites of hnRNP A2 to BC1 and PKM ζ mRNA as stem-loop structures with a core of tandem G-A base pairs, termed GA motifs. They showed the importance of G-A base pairs in the binding motifs by mutation of these CGG sequences, which disrupted binding of hnRNP A2 to BC1 and PKM ζ mRNA. However, their mutations also disrupted GG pairs in the sequences, which may form G-quadruplex structures common to CGG repeat RNA. Ohashi *et al.*, (2000) found Pur α and Pur β link BC1 RNA to microtubules via the dendrite-targeting motifs. Pur proteins specifically recognise GGN sequences (Knapp *et al.*, 2006), I therefore suggest that the dendritic targeting motif of BC1 is characterised by its G-quadruplex-forming GG sequences, not G-A base pairs.

1.7 Local translation affects synaptic plasticity

Projection neurons connect distant neurons within the brain or to the spinal cord. They have an average of around 10,000 dendritic spines, with an excitatory synapse at each spine (Bramham & Wells, 2007). Individualised regulation of protein synthesis at each synapse goes some way to explaining the incredibly complex processing power of the human brain. Synaptic plasticity refers to the dynamic strengthening and weakening of synapses relative to their activity. It has been described as the basis for memory formation and longevity (Malenka & Bear, 2004). Action potentials stimulate the pre-synaptic membrane of an axon terminal to release neurotransmitters. The primary neurotransmitter in brain is glutamate. These bind receptors in the post-synaptic membrane of a dendritic spine (Fig. 1.11). When glutamate binds AMPA receptors it causes the opening of calcium channels, calcium influx causes depolarisation of the cell. NMDA receptors bind glutamate and glycine neurotransmitters. Activation of AMPA receptors allows influx of the positive sodium ions. This increased positive intracellular charge electrostatically repels Mg^{2+} blockage of the NMDA receptor. Activated NMDA receptors allow influx of sodium and calcium ions. In response to a strong impulse, intracellular calcium increases significantly, Ca^{2+} -calmodulin-dependent protein kinase II (CaMKIIa) is activated, causing the transport of intracellular stores of AMPA receptors to the synaptic membrane. This functions to increase the duration of excitation in the post-synaptic neuron, and is termed Long Term Potentiation (LTP). Under low post-synaptic Ca^{2+} , the phosphatase calcineurin directs AMPA channels from the synaptic membrane for intracellular storage. This functions to inhibit firing of action potentials in the post-synaptic membrane, and is termed Long Term Depression (LTD). The requirement for new protein synthesis during LTP is described in Table 1.5.

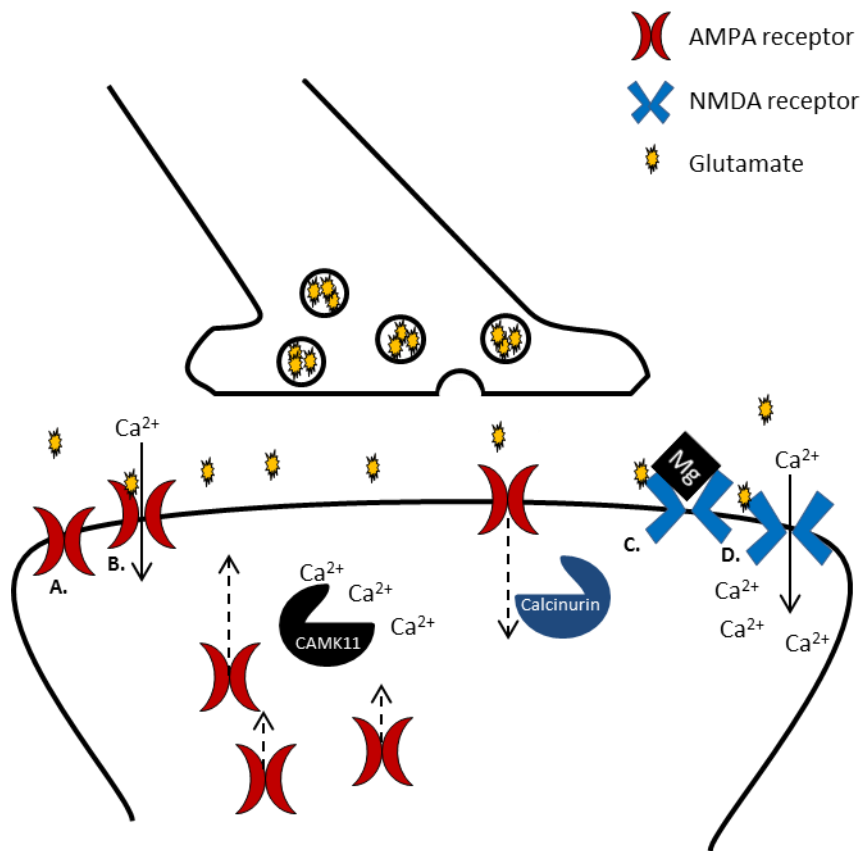


Figure 1.11 Synaptic plasticity is the change in excitability resulting from increases or decreases in their activity. A) AMPA receptors are glutamate receptors (GluR) present in the post-synaptic membrane. B) Glutamate activates AMPA receptors, allowing influx of positive ions, Ca^{2+} and Na^+ . C) NMDA receptors are blocked by Mg^{2+} binding. D) Increased post-synaptic positive charge electrostatically repels Mg^{2+} blockage of the NMDA receptor. Activated NMDA receptors allow influx of sodium and calcium ions. A strong activation of AMPA receptors causes significant increase in intracellular Ca^{2+} . Ca^{2+} -calmodulin-dependent protein kinase II (CaMKIIa) is activated, causing release of AMPA receptors to the synaptic membrane. Duration of excitation in the post-synaptic neuron increases causing LTP. Under low post-synaptic Ca^{2+} , the phosphatase calcineurin directs AMPA channels from the synaptic membrane for intracellular storage. Firing of action potentials in the post-synaptic membrane is inhibited causing LTD.

Synaptic plasticity and learning is dependent on local translation of mRNAs (Kang & Schuman, 1996; Huber *et al.*, 2002). The local translation of Ca²⁺/calmodulin-dependent protein kinase II alpha (CamkII α) mRNA is a well characterised example. CamkII is central to regulating synaptic plasticity. Differential phosphorylation of the amino acids T305 and T306 determine induction of long term potentiation (LTP) and long term depression (LTD) (Lisman, Yasuda & Raghavachari, 2012). During LTP induction, Ca²⁺ influx causes CAMKII activation in dendritic spines by phosphorylation. CAMKII autophosphorylates itself, so maintains activity long after Ca²⁺ concentration decreases within the spine. There is also a translation positive feedback loop for CAMKII expression. The 3' UTR of CamkII α mRNA contains three cis-acting regions including one for binding CPEB (Huang *et al.*, 2003). CamKII activates CPEB1 by phosphorylation and CPEB1 promotes local translation of CamkII mRNA (Fig. 1.12).

Normal synaptic function depends on FMRP repression of translation of many mRNAs in glutamatergic synapses including postsynaptic proteins, glutamate/NMDA receptor subunit NR1, NMDA receptor subunit epsilon-2, and Glutamate receptor 1 - GluR1 (Schutt *et al.*, 2009). Normal translation of dendritically localised mRNAs is controlled by coordination of FMRP and CPEB proteins. Many mRNAs are predicted to be bound by both CPEB and FMRP. Both CPEB and FMRP have been found in neuronal dendrites, and Udagawa *et al.* (2013) demonstrate amelioration of FXS phenotypes in *Fmr1*^{-/-}; *Cpeb1*^{-/-} double-knockout mice.

Specific protein kinases have been shown to affect local translation of mRNAs. For instance, PKR-like ER kinase (PERK) phosphorylates eIF2 α and is required for normal expression of ATF4 in mice brains (Trinh *et al.*, 2012). Knock out of PERK in mice caused decreased eIF2 α phosphorylation and ATF4 and mice showed behaviour similar to schizophrenia. This combined with observed decreased levels of PERK and ATF4 in the frontal cortex of patients with schizophrenia points to a potential therapeutic target for the condition.

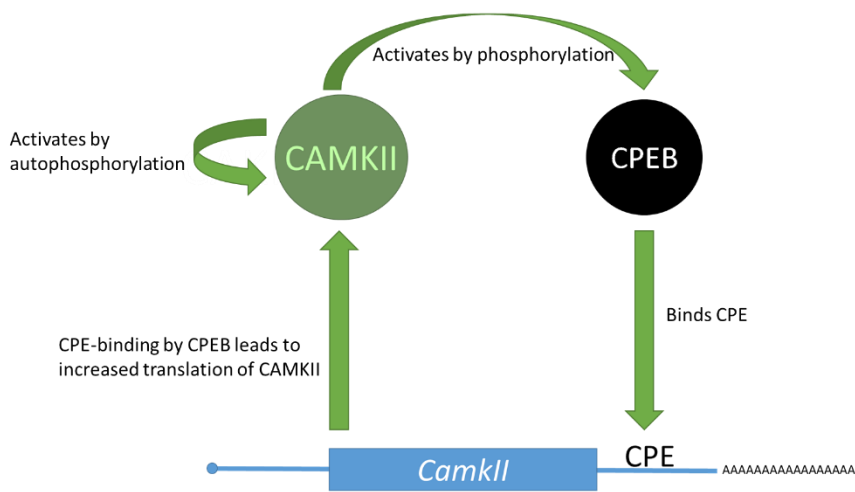


Figure 1.12 Positive feedback loops involved in increased levels of activated CamkII in activated dendritic spines.

| Phase of LTP | Mechanism | Reference |
|---------------------|--|--|
| Early | Ca ²⁺ -calmodulin-dependent protein kinase II (CaMKII α) is activated, causing release of AMPA receptors to the synaptic membrane | Sweatt (1999) |
| Late | New gene transcription and translation for increasing size of synaptic connection. Increased AMPA receptors made and inserted into the post-synaptic membrane. Generation of new synapses. | A mutant mouse was generated with the 3' UTR from the mRNA of CaMKII α deleted. In situ hybridisation analyses of the mutant mice brains showed that CaMKII α mRNA did not localise to dendrites. The mice displayed reduced late-phase long-term potentiation (LTP) as well as impairments to memory consolidation (Miller <i>et al.</i> , 2002). |

Table 1.5 Synthesis of proteins during LTP occurs in the late phase of LTP only. The early phase of LTP releases internal stores of AMPA receptors, increasing the strength of the synapse in this manner without gene transcription/translation.

1.7.1 G-quadruplex mediated delivery of mRNA to synaptic spines for controlled local protein synthesis

Neurons are highly polarised with distal axonal tips reaching up to a metre from the cell body. Initially sparking interest in local translation, polyribosomes were shown to be found in high density clusters at dendritic spines, the sites of excitatory synapses (Steward & Fass, 1983). Local translation has now been shown as prolific across cell types and with a diversity of mRNAs, affecting various behaviours. The conserved significance of local translation is well illustrated by the distribution pattern of local distinct transcriptomes shown in neurons (Andreassi *et al.*, 2010, Cajigas *et al.*, 2012, Gumy *et al.*, 2011, Minis *et al.*, 2014, and Zivraj *et al.*, 2010) as well as migrating fibroblasts (Lawrence and Singer, 1986 and Mili *et al.*, 2008). Neurons possess spatially distinct subcellular compartments and have been used as a model for investigating local translation of mRNA. Translation of specific mRNA away from the soma, in axons or dendrites allows dynamic regulation of the proteome local to synapses or axonal growth cones.

cis-acting localisation signals are contained within the mRNA, either as a specific primary nucleotide sequence, or as a secondary structure. The advantages of differential mRNA targeting for local translation over targeting of proteins are numerous. Multiple copies of a protein may be locally synthesised from a single copy of mRNA. mRNA localisation signals are most commonly found in the untranslated regions (UTR) of an mRNA, therefore not compromising the coding sequence responsible for the peptide sequence of the synthesised protein. The translation of multiple mRNAs can be regulated together in discreet mRNPs, responsive to cell extrinsic or intrinsic signals, allowing rapid modification of the local proteome.

Subramanian *et al.*, 2011 found that of the known dendritic mRNAs, approximately 30% had sequences in their 3' UTRs predicted to form a G-quadruplex. They used RNA structure probing to show G-quadruplex structures in the 3'-UTRS of the mRNAs of PSD-95 and CaMKII α ; important postsynaptic proteins. Mutation of these mRNAs showed delivery of PSD-95 and CaMKII α to neurites of cultured primary cortical neurons was dependent on the presence of the G-quadruplex-forming sequence within their 3' UTRs. The importance of dendritic mRNA localization and local translation was demonstrated in an earlier study by Miller *et al.*, (2002). A mutant

mouse was generated with the 3' UTR from the mRNA of CaMKII α deleted. In situ hybridisation analyses of the mutant mice brains showed that CaMKII α mRNA did not localise to dendrites. The mice displayed reduced late-phase long-term potentiation (LTP) as well as impairments to memory consolidation.

Trans-acting RNA-binding proteins (RBPs) control translation and mediate mRNA targeting. mRNAs are transported and stored in large ribonucleoprotein (mRNP) complexes; specific mRNAs are transported to distinct subcellular compartments in neurons as neuronal RNPs. RBPs bind motor proteins for ATP-dependent transport of neuronal RNPs along filaments. The most comprehensively studied of the G-quadruplex-binding RBPs is FMRP, a protein whose mutation causes fragile X syndrome (FXS), the most common cause of mental retardation. The use of RNA selection suggested FMRP RGG box binds G-quadruplex structures in their target mRNAs (Darnell *et al.*, 2001). It has been shown that the FMRP protein binds a G-quadruplex structure in the coding region of its own mRNA (Schaeffer *et al.*, 2001). However, a later study by Darnell *et al.*, 2011 found no enrichment of G-quadruplex-forming sequences in the mRNAs bound by FMRP; indeed, they found no conserved RNA sequences whatsoever. This suggests a complexity to the formation, trafficking and controlled translation of neuronal RNPs which is presently poorly understood. The cause of fragile X-associated tremor/ataxia syndrome (FXTAS) is an expansion of the CGG repeats in the 5' UTR of fragile x mental retardation-1 (*Fmr1*), the gene coding for FMRP. CGG repeats form G-quadruplex structures (Malgowska *et al.*, 2014). Expansions of this trinucleotide repeat have been shown to cause translation of out-of frame polyglycine or polyalanine peptides whose aggregation is suggested to contribute to FXTAS disease pathologies (Todd *et al.*, 2013). However, it is unclear how much of FXTAS is due to RNA-mediated toxicity and how much may be due to protein inclusions. FXTAS is also characterised by the accumulation of mRNA extremely rich in CGG repeats. The toxicity of this mRNA may lie in its sequestration of RBPs away from their normal duties of mediating the trafficking of dendritically-targeted mRNAs. Disruption of this kind would prevent the dendritic localisation of *fmr1* mRNA, and therefore local synthesis of the FMRP protein. FMRP is required for normal dendritic spine morphology (Comery *et al.*, 1997). In a model of the effects of CGG repeat mRNA overexpression, a (CGG)₂₄ repeat was inserted into the 5' UTR of the non-dendritically localised α -tubulin mRNA and caused localisation to dendritic

spines, whilst a $(CCC)_{24}$ repeat did not cause dendritic localisation (Muslimov *et al.*, 2011).

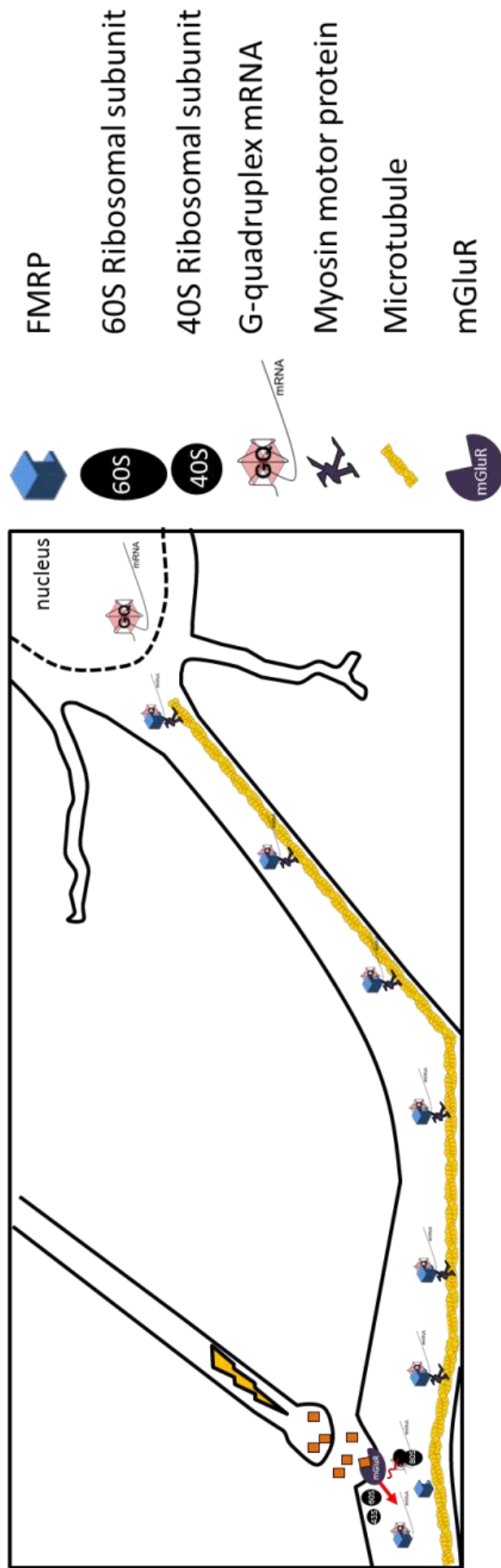


Figure 1.13 The regulation of local translation of G-quadruplex containing mRNAs at active synapses is mediated by FMRP. FMRP binds G-quadruplex mRNA in the nucleus and is part of a neuronal mRNP which is transported along microtubules along dendrites. The mRNA is held in a translationally repressed state by FMRP until activation of the synapse causes dissociation of the mRNA from FMRP, allowing binding by ribosomes for local translation.

High-throughput sequencing of RNA isolated by crosslinking immunoprecipitation (HITS-CLIP) was used to generate a protein-RNA interaction map for FMRP (Darnell *et al.*, 2011). They found that FMRP interacts with the coding region of mRNAs of pre- and postsynaptic proteins. Release of dendritic mRNAs from neuronal RNPs for local translation occurs due to stimulation at activated synapses. In vitro translation assays suggested FMRP stalls translating ribosomes on bound mRNAs, inhibiting elongation. Synaptic activation by mGluR-signalling is suggested to be the cause of FMRP dephosphorylation by S6 kinase-1 (S6K1) (Fig. 1.13). Phosphorylated FMRP has been shown to promote the association of PSD-95 mRNA with Ago2-miR-125a, preventing translation of PSD-95. Dephosphorylated FMRP promotes translation of PSD-95 (Edbauer *et al.*, 2010; Muddashetty *et al.*, 2011).

The composition of neuronal RNPs was investigated by (Kanai *et al.*, 2004). KIF5 is a kinesin-1 motor protein, characterised as trafficking along neuronal microtubules. A proteomic screen of KIF5-associated proteins identified known RBPs such as FMRP and Pur- α , as well as previously unidentified RBPs including hnRNPU and Polypyrimidine tract binding protein (PTB). Many of the hnRNP proteins identified in this study were also shown to amass at activated postsynaptic sites (Zhang *et al.*, 2012). The heterogeneous nuclear ribonucleoprotein A2 (hnRNP A2) complexes with key synaptic mRNAs in neuronal RNPs. hnRNP A2 has been shown to bind CGG repeat RNA (Sofola *et al.*, 2007) which suggests a role for the CGG-quadruplex-forming sequence in assigning mRNAs to neuronal RNPs containing hnRNP A2. Muslimov *et al.*, (2011) demonstrated that G-quadruplex-forming RNAs with CGG triplet repeat expansions bind to hnRNP A2 and prevent dendritic localisation of normally dendritically localised mRNAs. The role of hnRNP A2 once bound to G-quadruplex mRNA is poorly understood, but has been shown to relieve translational inhibition caused by 5' UTR G-quadruplexes in non-neuronal cell culture. Khateb *et al.*, 2007 showed that hnRNP A2 binds G-quadruplex mRNA in transfected HEK293 human cells, and relaxes translational inhibition caused by 5' UTR G-quadruplexes. The relief of translational inhibition may be due to unwinding of the quadruplex resulting from binding of hnRNP A2, or it may be due to the association of the hnRNP A2 – mRNA complex with interacting proteins, potentially with helicase activities. hnRNP A2 may act as a general scaffold protein, recruiting CGG repeat mRNA to protein complexes, including neuronal RNPs in neurons.

The purine rich element binding protein α (Pur- α) is found in neuronal RNPs with FMRP (Chen, Onisko and Napoli 2008). Pur- α specifically binds to G-quadruplex-forming mRNA sequences, and has been found at sites of local translation in dendrites. It has been suggested that Pur- α is required for the dendritic delivery of specific mRNAs to sites of dendritic translation (Johnson *et al.*, 2006). Pur- α was found in the neuronal inclusions characteristic of FXTAS patients. This gave rise to the investigation of the role of Pur- α in regulation of CGG repeat mRNA. It was found that Pur- α specifically binds mRNA CGG repeats in *Drosophila* and mammals (Jin *et al.*, 2007) and over-expression of Pur- α in *Drosophila* prevented neurodegeneration mediated by CGG repeat mRNA. Pur- α therefore plays an important role in normal formation, and targeting of neuronal RNPs, possibly through its recognition of G-quadruplex-forming sequences in mRNAs.

Change in post-synaptic Ca^{2+} causes alterations in the relative membrane expression of neurotransmitter receptors. However, neuronal plasticity also occurs through other mechanisms, including regulation of local translation of synaptic proteins. Polyribosomes were shown to be found in high density clusters at dendritic spines, the sites of excitatory synapses (Steward & Fass, 1983). *Cis*-acting mRNA sequences have been shown to be essential for the correct localisation of mRNAs to dendritic spines. Regulation of translation of synaptic membrane proteins is local and rapid. Mayford *et al.*, 1996, showed mRNA of the α subunit of CaMKIIa localises to dendritic spines due to a targeting sequence in its 3' UTR. A (CGG)₂₄ repeat inserted into the 5' UTR of the non-dendritically localised α -tubulin mRNA caused localisation to dendritic spines, whilst a (CCC)₂₄ repeat did not cause dendritic localisation (Muslimov *et al.*, 2011).

In a generalised view, specific RNA-binding proteins (RNP) bind *cis*-acting mRNA sequences, repress translation initiation and coordinate the migration of the mRNA-RNP along cytoskeletal microtubules towards its destination (Fig. 1.14). Signalling at its destination regulates protein synthesis from the RNP-bound mRNA.

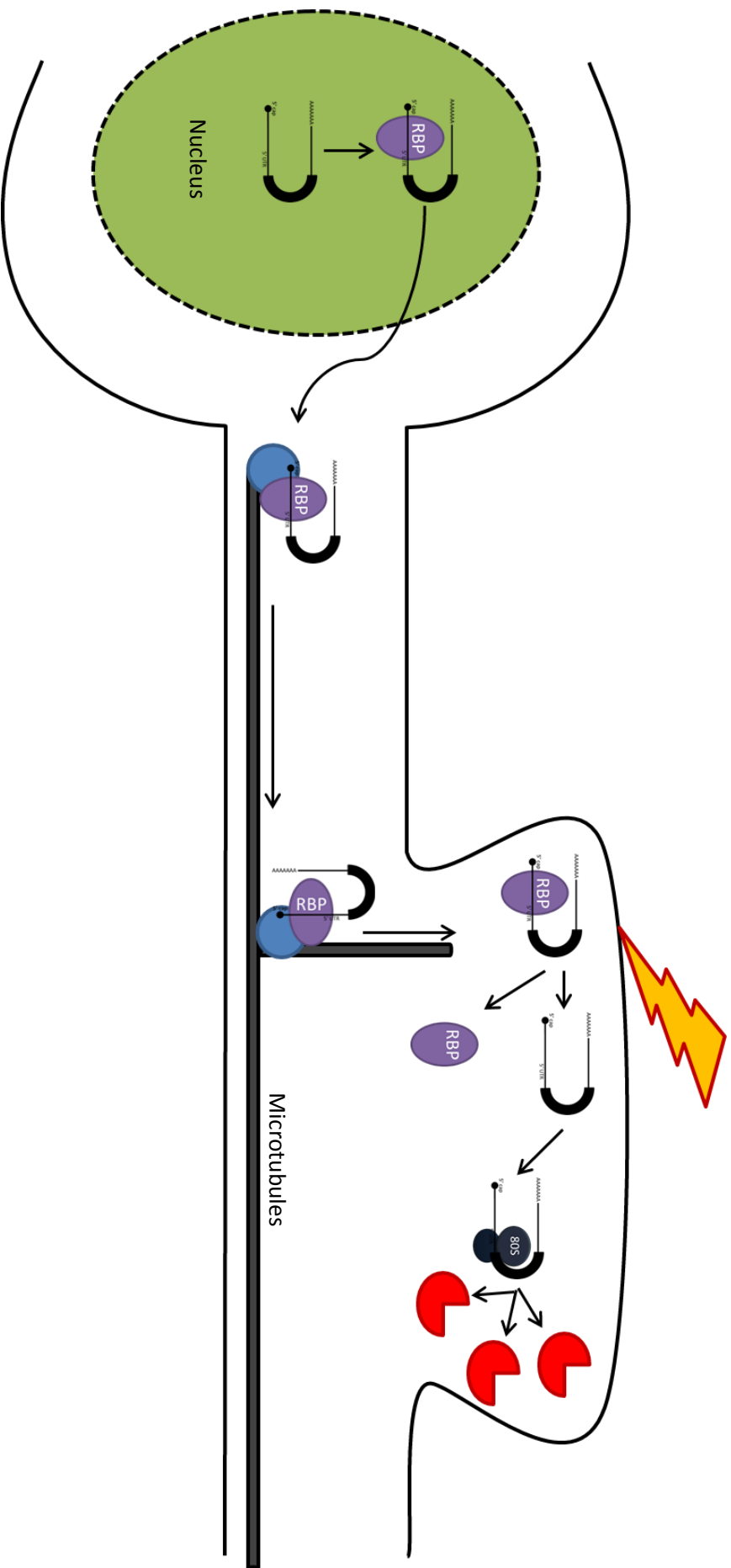


Figure 1.14 Generalised model of mRNA transport and translational control in dendrites. Following transcription, in the nucleus, RNA Binding Proteins (RBPs) bind specific motifs in mRNAs and protect from translation initiation. mRNA is transported in translation repression complexes along microtubules by kinesin/dynein motor proteins. Synaptic activation causes the release of mRNA from repressed complexes, allowing association with translation machinery, and therefore allowing local protein synthesis.

1.7.2 G-quadruplex expansion diseases deregulate processing of G-quadruplex mRNA

Fragile X is associated with CGG repeat expansion. Recently, an expansion of the GGGGCC repeat in the first intron of C9ORF72 has been shown to cause the neurodegenerative diseases, frontotemporal dementia (FTD) (30% of cases) and amyotrophic lateral sclerosis (ALS) (40% of cases) (Renton *et al.*, 2011). Repeats of (GGGGCC)_n RNA form stable G-quadruplex structures (Fratta *et al.*, 2012). Xu *et al.* (2013) showed in *Drosophila*, that neurodegeneration is caused by (GGGGCC)_n RNA. Pur α is found in inclusion bodies of *Drosophila* expressing (GGGGCC)_n RNA as well as in the cerebellum of human carriers of (GGGGCC)_n C9ORF72. They showed that Pur α specifically binds (GGGGCC)_n RNA in *Drosophila* and *Homo sapiens*. Overexpression of Pur α in *Drosophila* or *Mus musculus* neuronal cells relieved neurodegeneration caused by (GGGGCC)_n RNA. It was suggested that in individuals with expanded (GGGGCC)_n C9ORF72, Pur α is sequestered by the (GGGGCC)_n, preventing its normal processing of neuronal RNAs for synaptic translation.

1.8 Two-pore potassium leak channels

Two-pore potassium leak channels (K_{2p}) are responsible for setting and maintaining resting membrane potential in animal and plant cells (Gonzalez *et al.*, 2014). Their expression is under complex regulation, and they play physiologically significant roles in a diversity of tissues, including the central nervous system (CNS), the heart, kidneys and other organs. Potassium channels are typically protein tetramers, however, K_{2p} channels are unique, forming functional channels as dimers. K_{2p} proteins are characterised by four transmembrane domains (M1 – M4) and two pore domains (P1 & P2) and possess intracellular amino and carboxy termini (Fig. 1.15A).

The K_{2p} channel Task3 was shown to be essential for normal neuronal behaviour in mice. The cerebellar granule neurons of wild-type Task3 mice are able to fire continuously at high frequencies, whereas the neurons of Task3 Knock-out mice were not able to sustain high frequency firing (Brickley *et al.*, 2007). Over-expression of potassium leak channels results in membrane hyperpolarisation, inhibiting action potentials. Under-expression results in membrane hypopolarisation, reducing the

threshold needed for an action potential. Regulated membrane expression of K_{2P} channels therefore determines neuron excitability (Mathie *et al.*, 2010).

The voltage kinetics of K_{2P} channels are very similar to that of voltage gated potassium channels. K_{2P} channels are additionally characterised by a constitutive current, hence the term 'leak channel'. However the description of K_{2P} channels as 'leak' channels is not entirely accurate, they are not constitutively open; conductance is relative to intracellular and extracellular ion concentrations. Membrane depolarisation activates K_{2P} channel opening, accompanied by time and voltage-dependant gating. The open probability of K_{2P} channels is additionally diversely controlled by voltage-independent factors. However, their classification as constitutive leak channels is relatively true compared to the other ion channel classes.

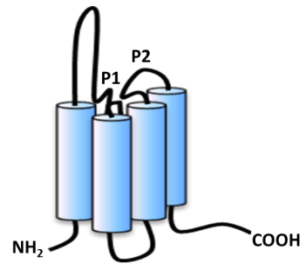
K_{2P} channels have been classified according to sequence homology into six subfamilies (Fig. 1.16). TWIK proteins form weakly inwardly rectifying K_{2P} channels. TREK proteins form lipid and mechanosensitive K_{2P} channels. TASK proteins form K_{2P} channels predominantly sensitive to pH. TALK proteins form K_{2P} channels activated by alkaline pH. The THIK K_{2P} channels are inhibited by halothane anaesthetic. The TRESK subfamily only contains one protein, Kcnk18, and are localised to the CNS (Enyedi and Czirják, 2010).

1.8.1 Potassium leak channels set the baseline membrane potential of neurons

The difference in ions across the membrane of a neuron is a voltage called the membrane potential. The extracellular concentration of sodium is much higher than the intracellular concentration of sodium. The intracellular potassium ion concentration has a much higher intracellular concentration than extracellular concentration. These chemical gradients of sodium and potassium ions is generated by the action of the sodium-potassium pump. The sodium-potassium pump removes three Na^+ ions for every two K^+ ions it brings in to the cell, thus generating a negative voltage across the membrane (negative membrane potential) (Purves *et al.*, 2001). Potassium leak channels in the cell membrane allow K^+ ions to leak out of the cell down its chemical gradient, further increasing the negative membrane potential as more positive charge moves out of the cell. The abundance of potassium leak

channels in the membrane of a neuron therefore sets the baseline membrane potential (Lesage & Lazdunski, 2000). The greater the number of leak channels, the greater the membrane potential, and the lower the number of leak channels, the lower the membrane potential. Two-pore potassium leak channels (K_{2p}) can set the baseline membrane potential of a neuron, therefore determining the sensitivity of a neuron to a stimulus (Gierden *et al.*, 2008).

A)



B) Cell membrane

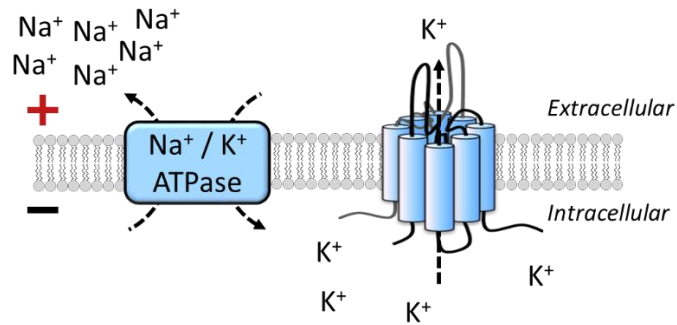


Figure 1.15 **A)** K₂P channels are characterised by their 4 transmembrane domains and two pore domains. K₂P channels possess intracellular amino and carboxy termini. **B)** K₂P channels form homodimers or heterodimers in the cell membrane. K₂P channels set the resting membrane potential of the cell by allowing constitutive leak of potassium from the cell down its chemical gradient.

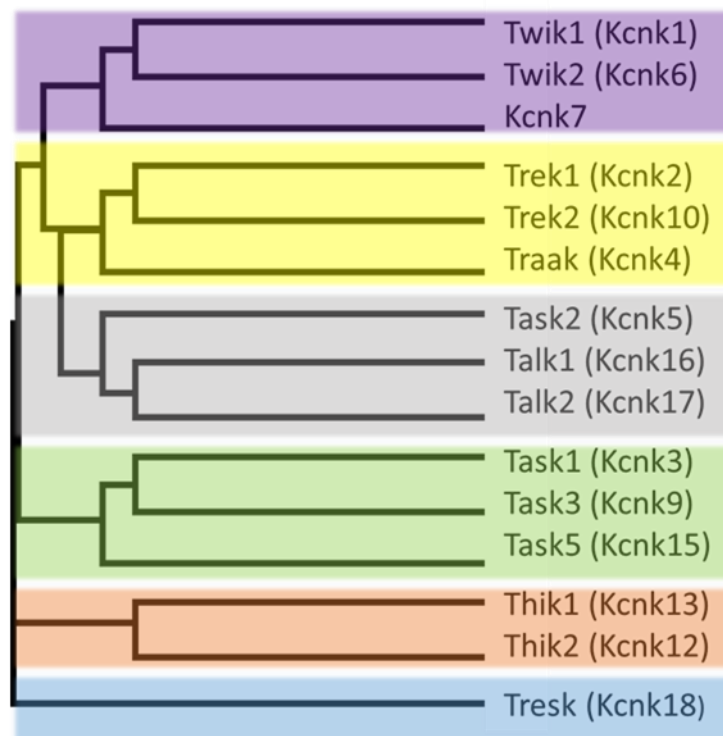


Figure 1.16 K_{2P} channel subfamily classifications. TWIK proteins form weakly inwardly rectifying K_{2P} channels. TREK proteins form lipid and mechanosensitive K_{2P} channels. TALK proteins form K_{2P} channels activated by alkaline pH. TASK proteins form K_{2P} channels predominantly sensitive to pH. The THIK K_{2P} channels are inhibited by halothane anaesthetic. The TRESK clade only contains one protein, Kcnk18, and are localised to the CNS. *Adapted from Enyedi and Czirják, 2010*

1.9 Regulated expression of K_{2P} channel proteins

Control of gene expression of cytoplasmic proteins is less complicated than that of membrane-bound proteins or secreted proteins (Fig. 1.17). pre-mRNA is transcribed in the nucleus and is subject to processing before the mature mRNA exits the nucleus where it is bound by the ribosome and translation occurs, synthesising the encoded protein. Regulation of gene expression of membrane-bound proteins or secreted proteins is more complex. pre-mRNA is transcribed in the nucleus and is subject to processing before the mature mRNA exits the nucleus where it is bound by the ribosome and translation occurs, synthesising the encoded protein. The nascent peptide acts as a signal peptide which causes binding by SRP and translocation to the ER membrane where translation continues, either integrating the protein into the membrane in the case of integral membrane proteins, or enclosing the protein in a membrane vesicle in the case of secreted proteins. The protein is transported in the membranous vesicle to the cell surface for integration or secretion from the cell membrane.

K_{2P} proteins are subject to further regulation of membrane expression. Task channels 1 & 3 have been shown to be subject to control of trafficking between the ER and the cell surface membrane. The N-terminus & C-terminus of Task 1 & 3 contain β -COP recognition motifs, KR and KRR respectively. On binding by β -COP, the protein is retained in the ER membrane, preventing trafficking to the cell surface membrane. However, the C-terminal contains a 14-3-3 binding domain, whereupon binding of 14-3-3 prevents β -COP binding of the C-terminus and promotes forward trafficking of the protein to the cell surface (O' Kelly *et al.*, 2002). The 14-3-3 proteins are highly expressed in the CNS (Sato, Yamamura and Arima, 2004); suggesting ER retention of Task channels may be less prevalent in neuronal cells.

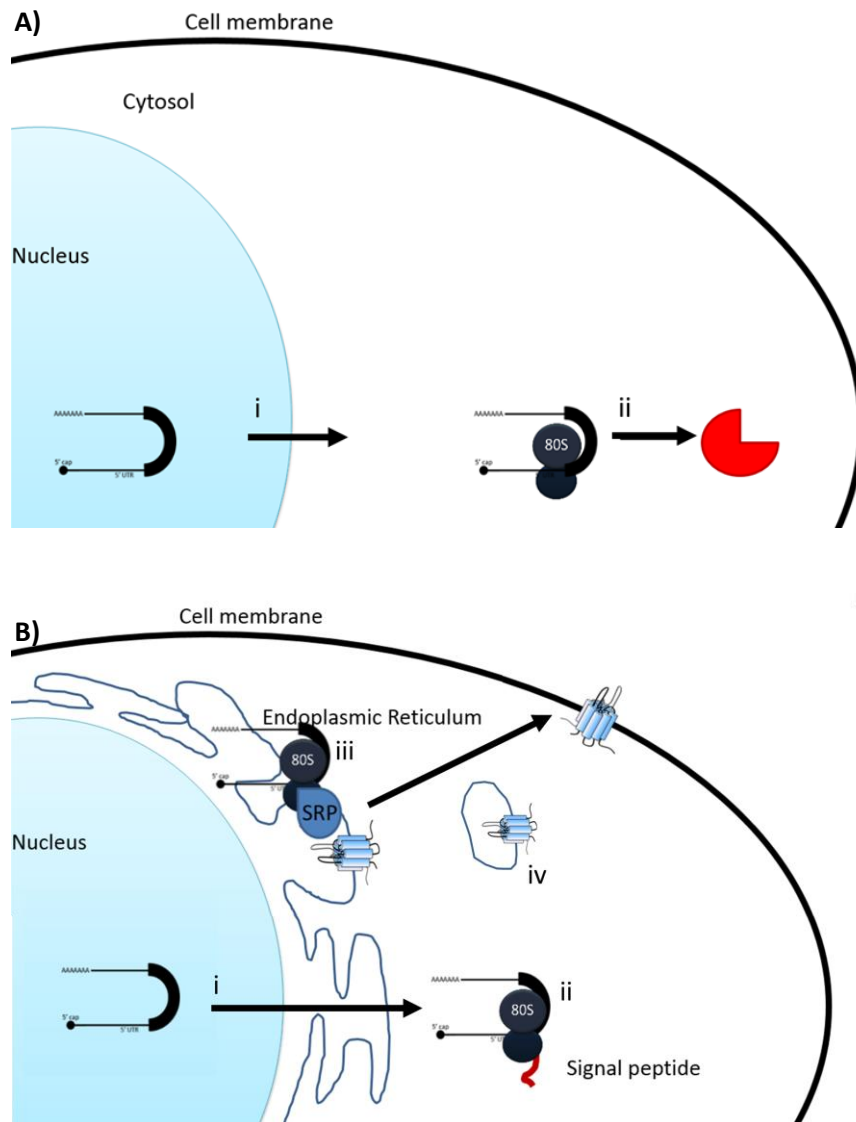


Figure 1.17 Control of gene expression of cytoplasmic proteins is less complicated than that of membrane-bound proteins or secreted proteins. **A)** pre-mRNA is transcribed in the nucleus and is subject to processing before **i)** the mature mRNA exits the nucleus where it is bound by the ribosome and **ii)** translation occurs, synthesising the encoded protein. **B)** Regulation of gene expression of membrane-bound proteins or secreted proteins is more complex. pre-mRNA is transcribed in the nucleus and is subject to processing before **i)** the mature mRNA exits the nucleus where it is bound by the ribosome and **ii)** translation occurs, synthesising the encoded protein. The nascent peptide acts as a signal peptide which causes binding by SRP and **iii)** translocation to the ER membrane where translation continues, either integrating the protein into the membrane in the case of integral membrane proteins, or enclosing the protein in a membrane vesicle in the case of secreted proteins. **iv)** The protein is transported in the membranous vesicle to the cell surface for integration or secretion from the cell membrane.

1.10 Alternative translation initiation in K_{2P} channel, Trek1

Trek1 is expressed primarily in neurons and glial cells of the CNS where they contribute to regulation of resting membrane potential and action potential firing frequency (Gu *et al.*, 2002 and Gnatenco *et al.* 2002). Alternative translation initiation has been shown to regulate ion selectivity in Trek1 (Thomas *et al.*, 2008). Trek2 is translated from the annotated AUG at +1 and from an AUG internal to the CDS, at +169, creating both the full length protein and an N-terminally 56 aa truncated protein. The AUG at +169 is in a favourable context compared to the annotated AUG at +1. The +169 AUG has a purine at -3, whilst the AUG at +1 has a C at -3 which leads to leaky scanning by the ribosome and alternative translation initiation at the internal +169 AUG. The N-terminally truncated Trek1 isoform is permeable to sodium ions as well as potassium ions, causing membrane depolarisation. Thomas *et al.* (2008) suggested the use of alternative translation initiation as a 'natural, epigenetic mechanism for spatial and temporal regulation of neuronal excitability'.

1.11 Bioinformatic screen of mRNAs identified an evolutionarily conserved sequence in the 5' UTR of K₂P channel, Traak

A bioinformatics screen of all human transcripts in the Ensembl genome database identified 5' UTR sequences with a putative N-terminally extended ORF (eORF) Coldwell *et al.*, (publication in preparation). Where translated eORFs >40 amino acids long were identified in frame with the annotated ORF, the transcript was tagged for further analysis. A 40 aa extension is possible to easily distinguish by western blot, and long enough to contain functional motifs. These selected transcripts (~8000) were searched against a parallel dataset from mice for evolutionarily conserved eORFs, which would suggest an increased probability of functional motifs within the eORF. 444 candidate genes with highly conserved putative eORFs between mice and human were identified. To further refine the list of candidate genes for experimental validation, the 444 genes were submitted for tBLASTn top identify sequence homology of the putative eORF peptide sequence with translated mRNA sequences from all eukaryotes. 142 eORFs showed high sequence homology with translated mRNA sequences from distantly related mammals. Each of the 142 genes shortlisted was then subjected to interrogation using a Visual Basic-based macro executed in Microsoft Excel, with data from Ensembl of human 5' UTR and CDS sequences. The macro identifies in frame upstream CUG, GUG and ACG initiation codons in strong contexts. The macro has been named 'ExTATIC' (Extensions and Truncations from Alternative Translation Initiation Codons).

Traak (KCNK4) mRNA was identified by our bioinformatics screen to possess a conserved translated amino acid sequence in its 5' UTR. Traak is an outwardly rectifying channel, allowing potassium to pass down its chemical gradient, out of the cell, enhancing the resting membrane potential. Traak is expressed primarily in neuronal tissues where it is predicted to regulate synapse excitability. The proteins form functional membrane channels as homodimers. Human Traak transcript ENST00000422670 was identified as having a conserved translated 5' UTR sequence with *Pan troglodytes* Traak transcript variant 1 mRNA (Fig. 1.14).

PREDICTED: Pan troglodytes potassium channel, subfamily K, member 4, transcript variant 1 (KCNK4), mRNA
Sequence ID: [reflXM_001164319.3](#) Length: 2034 Number of Matches: 1

Range 1: 430 to 513 [GenBank](#) [Graphics](#) [Next Match](#) [Previous Match](#)

| Score | Expect | Method | Identities | Positives | Gaps | Frame |
|----------------|--------|------------------------------|------------|-------------|----------|-------|
| 55.8 bits(133) | 2e-07 | Compositional matrix adjust. | 27/28(96%) | 28/28(100%) | 0/28(0%) | +1 |
| Query | 16 | TSRGWPAVGSQAAAATTAPQEPPARPLQ | 43 | | | |
| | | TSRGWPAVGS+AAAATTAPQEPPARPLQ | | | | |
| Sbjct | 430 | TSRGWPAVGSRAAAVTIAPQEPPARPLQ | 513 | | | |

Figure 1.18 Alignment of conserved 5' UTR predicted translated amino acid sequence between *Homo sapiens* and *Pan troglodytes*, produced using the NCBI tblastn tool, <http://blast.ncbi.nlm.nih.gov/Blast.cgi>.

This thesis aims to test whether Traak is subject to alternative upstream translation initiation, yielding N-terminally extended Traak proteins. The characteristics of other K_{2P} channel mRNA 5' UTRs may regulate the expression of their genes by control of translation mechanisms. The 5' UTRs of other K_{2P} channels will be examined for translational control mechanisms regulating the protein expression of K_{2P} channels.

1.12 Alternative translation initiation in Fxr2

Fragile X is the most common cause of inherited intellectual disability affecting approximately 1 in 5000 men and 1 in 10,000 women (Coffee et al. 2009). Normal expression of FMRP is essential for normal translation of neuronal RNAs responsible for normal dendritic spine morphology (Comery *et al.*, 1997). Epigenetic silencing of FMRP occurs when transcription of *fmr1* on the X chromosome is suppressed by hypermethylation of an expanded (>230) CGG repeat in the 5' UTR and promoter region of its DNA. Fragile X syndrome (FRAXA) results from this suppression of FMRP expression, leading to dysregulation of neuronal mRNA expression and abnormal spine morphology. Synthesis of FMRP can also be stalled at translation. The translation of *fmr1* mRNA is dependent on the length of the 5' UTR CGG repeat. Fragile X tremor/ataxia syndrome (FXTAS) is caused by premutation CGG repeat lengths (55-200), which are not methylated, and instead cause overexpression of the *fmr1* mRNA (Jacquemont *et al.*, 2003). Premutation CGG repeats causes upstream Repeat Associated Non-AUG (RAN) translation and inhibits translation of the normal FMRP protein with translation initiated at AUG +1. RAN translation from aTICs generate polyglycine-containing protein, FMRpolyG (Todd *et al.*, 2013). FMRpolyG forms neuronal inclusions, indicative of protein-mediated neurodegeneration.

FMRP is involved in the processing of mRNAs for local translation in neurons, partly through recognition of G-quadruplex sequences in target mRNAs via FMRP's RGG

domain. Fmr1 mRNA has also been shown to be subject to G-quadruplex-mediated transport within neurons via a 3' UTR G-quadruplex. Khateb *et al.*, (2007) showed pre-mutation CGG repeats formed G-quadruplex structures. When pre-mutation CGG repeats were placed upstream of a firefly luciferase reporter, luciferase synthesis was greatly inhibited. The same paper also showed over-expression of the hnRNP G-quadruplex destabilising proteins, hnRNP A2 and CBF- α relieved repression of translation of the firefly luciferase reporter in transfected HEK293 cells. Ofer *et al.*, (2009) showed TMPyP4 relieved translational inhibition of the same firefly luciferase reporter by pre-mutation CGG repeat lengths in its 5' UTR.

FMRP interacts with its two paralogs, Fragile X Related Proteins 1 and 2 (FXR1P and FXR2P). Although the functions of these paralogs are unclear, they are thought to compensate for lack of expression of FMRP. Like FMRP, FXR1P is an RBP with RNA G-quadruplex-binding properties responsible for normal mRNA transport and processing. FXR1P is highly expressed in muscle tissue where it is essential for normal muscle development (Davidovic *et al.*, 2008). FXR2P has been implicated in normal learning and memory processes in neurons. Fxr2 KO mice display a similar intellectually disabled phenotype as Fmr1 KO mice (Cavallaro *et al.*, 2008).

Ribosome profiling of mouse embryonic stem cells identified FXR2 to be subject to alternative upstream translation initiation. Ingolia *et al.* (2011) used ribosome profiling to investigate the transcriptome of Mouse Embryonic Stem Cells. The technique used harringtonine to stall ribosomes at sites of translation initiation. Samples were then subjected to nuclease treatment, and ribosome-protected fragments were subjected to deep-sequencing. Results revealed unannotated translation start sites, both AUG and non-AUG, forming uORFs, eORFs and truncated ORFs. The H2G2 Genome Browser (<http://h2g2.ugent.be/biobix.html>) allows searching of this data, as well as comparison with peptide mapping data from N-terminal COFRADIC analysis and vertebrate conservation from the UCSC PhastCons multiple alignments (Siepel *et al.*, 2005, Van Damme *et al.*, 2014). COFRADIC analysis refers to the identification of protein N-terminal peptides by combined fractional diagonal chromatography (Gevaert *et al.*, 2003). The extended FXR2 isoform was found to have an N-terminal methionine, translated from a GUG, in a strong Kozak consensus sequence, at -219 from the annotated AUG at +1.

Fxr2 mRNA, in common with Fmr1, possesses CGG repeats within its 5' UTR. Weisman-Shomer, Naot and Fry; 2000 have shown mRNA GGN repeats can form G-quadruplex structures. Mapping of the G-quadruplex-forming sequences within the 5' UTR of Fxr2 revealed a potential role for the G-quadruplexes in controlling the translation of the normal FXR2P protein, translated from +1 AUG, and a N-terminally extended FXR2P, translated from a GUG, in a strong Kozak consensus sequence, at -219. Fxr2 was found by deep sequencing mRNAs of synaptic neuropil in the hippocampus (Cajigas *et al.*, 2012).

1.13 Aims

The effect of differential expression of K_{2P} proteins in setting the baseline membrane potential is predicted to have significant impact on the sensitivity of neurons (Chapter 1.8.1). The mRNAs of Traak, Task1 and Task3 were found by deep sequencing mRNAs of synaptic neuropil in the hippocampus (Cajigas *et al.*, 2012). Alternative isoforms of the K_{2P} protein, Trek1, are produced by alternative translation initiation, yielding N-terminally different proteins with altered ion permeability. Furthermore, the Coldwell lab has demonstrated the importance of alternative translation initiation from within the 5' UTR of mRNAs from AUGs and non AUGs, and the Coldwell lab have found N-terminally extended protein isoforms with functional consequences. Here, I investigate the potential production of N-terminally diverse K_{2P} proteins Task1, Task3 and Traak by alternative translation initiation (Chapter 1.1)

Secondary structures within the 5' UTR of mRNAs have been shown to determine RBP binding and initiation codon usage (Chapter 1.2). Here, I investigate the potential presence and consequences of secondary structures in the 5' UTRs of Task1 and Task3 mRNA RBPs determine the fate of mRNAs. I will clone significant RBPs for analysis of effects on the translation of products from investigated mRNA sequences.

The 5' UTR of Fxr2 was identified by riboseq to be translated additionally from an upstream GUG codon at -219 (Chapter 1.12). G-quadruplexes have previously been suggested to stall scanning ribosomes over proximal upstream initiation codons, increasing the rate of translation initiation from that codon (Bugaut & Balasubramanian, 2012). I will clone Fxr2 for mutation and analysis of the use of alternative translation initiation codons in transfected cells. We will test the effects of G-quadruplex interacting ligands and RBPs on the expression of Fxr2 isoforms generated from alternative translation initiation at non-AUGs within the 5' UTR.

Chapter Two

Materials and Methods

Chapter 2: Materials and Methods

2.1 Measurement of RNA/DNA concentration

Measurement of RNA and DNA concentrations were made using the Thermo Fisher NanoDrop 2000c UV-Vis spectrophotometer. A 1 μ L sample was loaded onto the NanoDrop platform and nucleic acid concentration calculated by measurement of absorbance at 260/280 nm. The measurement resulted from subtraction of absorbance of a 'blank' buffer-only sample. A 260/280 ratio of \sim 1.8 was taken as 'pure' DNA and a 260/280 ratio of \sim 2.0 was taken as 'pure' RNA.

2.2 PCR techniques

Thin walled Thermo Scientific™ PCR Tubes were used in the Techne TC 3000G thermocycler or MJ research PTC 200. Standard PCR reactions were carried out using Thermo Scientific Phusion High-Fidelity DNA Polymerase or NEB Q5 High fidelity polymerase with standard cycling conditions:

| | Temp. (°C) | Time | Cycles |
|----------------------|------------|--------|--------|
| Initial denaturation | 98 | 30s | 1 |
| Denaturation | 98 | 10s | |
| Primer annealing | \sim 60 | 20s | 35 |
| Extension | 72 | 20s/kB | |
| Final extension | 72 | 8m | 1 |

2.2.1 Slowdown PCR

Slowdown PCR was used, where indicated, to amplify GC-rich template sequences. GC-rich sequences form strong secondary structures. These secondary structures can inhibit PCR by impeding primer-binding or polymerase processing. Increasing the denaturation temperature is not possible in many cases, due to the negative effects on the polymerase's longevity. Slowdown PCR employs a decreased ramp rate (temperature increase towards denaturation temperature) to $2.5^{\circ}\text{C s}^{-1}$ and cooling rate (temperature decrease towards annealing temperature) to $1.5^{\circ}\text{C s}^{-1}$. This is predicted to allow increased denaturation of template DNA and increased primer-binding probability. It was shown to increase PCR efficiency from extremely GC-rich templates (Frey *et al.*, 2008)

2.2.2 PCR primers

Primers used are detailed in the table below (Table2.1).

| qPCR primers | | Application |
|------------------------|--|--|
| k9 qpcr ext f | CGCCGCCGCTTACAACTT ACGTAGAGCGGCTTCTTCT | Attempts to use qPCR to assess relative abundance of extended 5' UTR including GGN repeat Vs coding sequence of Task3. |
| k9 qpcr ext r | G CTCTGTCCCTCATCGTCTG | |
| k9 qpcr dat f | C GCCGCTCATCCTCACTGTT | |
| k9 qpcr dat r | C | |
| 5' RACE primers | | |
| jsK18RACEfromO | GGCAGAGAAGACCACAGC ACCCACCA CGCACGTTCTGCCGCTTCA | RACE of Tresk/Kcnk18 from codon containing initiation AUG codon. |
| jsK3RACEfromO | TCGTC GAGTTTCTCCTCCTCGCGC | |
| K9 RACE Rev | A GGACAGAGTCCGCACGTT | RACE of Task1/kcnk3 |
| K9 nest Rev | CT | RACE of Task3/kcnk9 |
| C-terminal eGFP vector | | |
| eGFP F HindIII/XhoI | TTTTTAAGCTTCTCGAGGT GAGCAAGGGCGAGG TTTTTGGATCCCTACTTGT | Construction of C-terminal eGFP vector for cloning of Task3. eGFP was PCR's from another GFP plasmid, and cloned into pcDNA3.1 leaving 5' terminal HindIII/XhoI for cloning Task3. |
| eGFP R BamHI | ACAGCTCGTCCATGC | |
| pcDNA3.1-FLAG Fix T7 | | |
| Fix T7 FWD | TTTTTTGCTAGCCCTGGGC GCGCCATGCGC TTTTGAGCTCTCTGGCTAA | Primers for restoring a functional T7 promoter sequence to Task3-FLAG plasmids to allow in vitro transcription with T7 polymerase. |
| Fix T7 REV | CTA | |

| N-terminal V5 vector | | |
|-----------------------------------|--|--|
| V5 | AAAAAGGTACCAAGCTTC GTAGAATCGAGACCGAGG AGAGGGTTAGGGATAGGC TTACCCATGGCTAGCAAAA A | Oligonucleotide sequences were annealed and digested with NheI and KpnI for cloning into pcDNA3.1. |
| V5 Comp | TTTTTGCTAGCCATGGGTA AGCCTATCCCTAACCTCT CCTCGGTCTCGATTCTACG AAGCTTGGTACCTTTTT | |
| Fxr2 | | |
| FXR2 FL STOP Sall R | TTTTGTGCGACTTATGAAAC CCCATTACCATACTACC | Cloning of Fxr2 with NheI/Sal1 into pcDNA3.1 3 X FLAG plasmid. |
| FXR2 FL nostop Sall R | TTTTGTGCGACTGAAACCCC ATTCACCATACTACCCAAC | |
| FXR2 -330GUU NheI | TTTTGCTAGCGCTGTTGAG CGGCAGCGGCAGCAGCG | Mutagenic internal primers for selectively mutating out alternative translation initiation codons within the 5' UTR of FXR2. |
| Sall FXR2 R | TTTTGTGACAATAAACCT CCTTTCATCCC | |
| FXR2 -219GTT | GCCGTTTCCCTCACGGTTG CGGAGACCAAG | |
| FXR2 -138GTT | CTGTGGCAGGGCCGCCGT TGGGCCGG | |
| FXR2 1ATT | TGGCGGCCATTGGCGG CCTGG | |
| Task3 | | |
| K9 Database FWD | TAGCAGAACACGAACGTG GG | Cloning of Task3 into |
| K9 3TM HindIII R | TTTTTAAGCTTACTACTGGG AGAAGGCGG | |
| Task3 Rev 3TM EcoRI | TTTTATCGATATGGGCGGC AAGAACAAGAAACACAAG GC | |
| end CDS no STOP Re Task3 EcoRI | AAAAGAATTCAAGCTTACA CTGGGAGAAGGC | |
| KCNK9 Rvr 623 | AAAAGAATTCAACGGACT TCCGGCGTTTCATC | |
| K9 R Sall | TTTTTGTCGACCGAGTTGG TTTCTGGGTCC | |

Task3 GQ Mutation

| | | |
|-------------------------|---|---|
| k9 Quad complement 1-55 | TTTTTGCTAGCCCTCCGCC GCCGCCGCCCTCCTCCT CCGCCGCCGCCGGCGGCC CGCCTGCAGTGGGACGCG CGCGG | Mutation of Task3 5' UTR G-quadruplex containing region transcript positions 1-55 to for experiments testing G-quadruplex structure and effects of G- quadruplex on transcription. |
| k9 Quad NRASQUAD | TTTTTGCTAGCCCCGGGGG GAGGGGGGAGGGGGGAG GGGGGCGGCGCCCGGC GCCACCTGCAGTGGGAC GCGCGCGG | |
| K9 Quad No Quad F | TTTTTGCTAGCGTCCCGTG TGGGAGGGGCGGGTCTG GGTGCGGCCTGCCGCATG ACTCGCTGCAGTGGGACG CGCGCGG | |

Task1

| | | |
|-----------------|-----------------------------------|---|
| NheI Kcnk3 WT F | TTTTGCTAGCGGCGGCGG CGGC | Cloning of Task1/kcnk3 into pcDNA 3.1 3F |
| NheI Kcnk3+1 F | TTTTGCTAGCACGATGAAG CGGCAGAACG | |
| Kcnk3 R XhoI | TTTTCTCGAGCAGCCATGC CCCAGGC | |

| DEAD-box helicases | | |
|------------------------|--|---|
| DHX36 Extract Fwd | CTGCAGTGGGACGCGCGC GG | Extract primers were needed for DHX36 and DHX29 to amplify with high specificity the long amplicons from human brain cDNA. Cloning primers were used to amplify the sequence and add compatible restriction sites to the 5' and 3' ends for ligation into digested C-terminal eGFP plasmid. |
| DHX36 Extract Rev | GCTGGTTCTGACGGGTTG TA | |
| DHX36 HindIII F | TTTTGTCTGACTCAGTTATT CTCTGTTTTTATC | |
| DHX36 XhoI R | TTTTCTCGAGAGTTATGAC TACCATCAGAACTGGG | |
| DHX29 Extract Fwd | GGCATGACCACAGCAGAG TA | |
| DHX29 Extract Rev | ATGTGAAGAGCTCTCGGC TG | |
| DHX29 BamHI Fwd | TTTTGGATCCGGCGGCAA GAACAAGAAAC | |
| DHX29 Sall R | TTTTTTGTCTGAGATGGGCG GCAAGAACAAGAAAC | |
| DHX30 KpnI F | TTTTTCTCGAGTCAGCTGT AATATCCATCCTGG | |
| DHX30 XbaI R | TTTTTGGTACCATGTTTCAG CCTGGACTCATTCA | |
| Purα | | |
| PurA KpnI F | TTTTTTCTAGATCAGTC GTCAGCTGTCTTGCG | PCR amplification of Purα from human brain cDNA, adding KpnI and XhoI restriction sites to the amplicon ends for cloning into N-terminal V5 plasmid. |
| PurA XhoI R | TTTTTGGTACCATGGCG GACCGAGACAG TTTTTCTCGAGTCAATC TTCTCCCCTTCTTCT | |
| GFP-BFP mutagenesis | | |
| eGFP F HindIII/XhoI | TTTTTAAGCTTCTCGAG GTGAGCAAGGGCGAG G | Mutagenesis of Task3-GFP to Task3-BFP. |
| eGFP R BamHI Y66H F | TTTTTGGATCCCTACTT GTACAGCTCGTCCATGC CTGACCCACGGCGTGC | |
| Y145F F | AGCTGGAGTTCAACTA CAACAGC | |

Table 2.1 Primers used for cloning, mutagenesis and qPCR.

2.3 Cloning into pcDNA3.1 CMV 3XFLAG expression plasmids

2.3.1 Restriction Digest

Restriction digests were carried out using enzymes from Promega or New England Biolabs, with their appropriate buffers.

Restriction digests for screening cloned plasmids were setup as follows:

~400ng Plasmid DNA
0.1 μ l BSA
1 μ l 10x Buffer
0.5 μ l Restriction Enzyme 1
0.5 μ l Restriction Enzyme 2 (where necessary)

made up to 10 μ l with dH₂O

Digestions were carried out at 37°C for 1hr.

Restriction digests for cloning were carried out as follows:

~5 μ g Plasmid DNA
0.5 μ l BSA
5 μ l 10x Buffer
2 μ l Restriction Enzyme 1
2 μ l Restriction Enzyme 2 (where necessary)
made up to 50 μ l with dH₂O

And

~5 μ g Insert DNA
0.5 μ l BSA
5 μ l 10x Buffer
2 μ l Restriction Enzyme 1
2 μ l Restriction Enzyme 2
made up to 50 μ l with dH₂O

Digestions were carried out at 37°C for 1.5hr. Digested plasmid DNA was subjected to alkaline phosphatase treatment for 1hr to remove 5' phosphoryl termini which can lead to self-ligation upon treatment with ligase.

Phosphatase treatment was carried out with the following reaction composition:

15 μ l Purified digested DNA

29 μ l dH₂O
5 μ l 10x Buffer
1 μ l TSAP Thermosensitive Alkaline Phosphatase (Promega)

2.3.2 Ligation

Ligations were carried out at room temperature for 1.5hr or at 5°C overnight, using the following reaction setup:

3 µl Purified Digested Insert DNA
1 µl Purified and Phosphatase-treated Digested Plasmid
4 µl dH₂O
1 µl 10x Buffer
1 µl T4 DNA ligase

2.3.3 Clean-up of DNA

Where indicated, DNA was purified following enzymatic reactions or gel electrophoresis, using Macherey Nagel NucleoSpin® Gel and PCR Clean-up kits, according to the manufacturer's instructions:

Two volumes of binding buffer NTI were added to samples. Excised gel slices were dissolved in NTI buffer by heating at 50°C with occasional vortexing. NTI buffer contains chaotropic salts which denature enzymes and increases DNA-binding to the silica membrane of the spin column. The sample was loaded onto a NucleoSpin® Gel and PCR Clean-up Column and subjected to centrifugation for 30 s at 11000 x g. To remove all but the required DNA (bound to the silica membrane), the columns were then washed twice with 700 µl buffer NT3 containing non-chaotropic salts and ethanol. The silica membranes were dried by centrifugation for 1 minute at 11000 x g. After discarding the flow-through and collection tube, the NucleoSpin® Gel and PCR Clean-up Column was placed into 1.5 mL microcentrifuge tube. To elute the DNA, 15 µl Buffer NE (5 mM Tris/HCl, pH 8.5) was applied to the membrane, incubated for 1 minute at room temperature, then eluted into the microcentrifuge tube by centrifugation for 1 minute at 11000 x g.

2.3.4 Transformation of competent cells

DH5α chemically competent *E. coli* were purchased from New England Biolabs. Cells were thawed on ice for 20 minutes. 50 µl cell suspension was added to 2 µl of ligation

reaction in 1.5 mL microcentrifuge tubes and incubated on ice for 30 minutes. Cells were heat-shocked at 42°C for 45 sec and returned to ice for 5 min. 150 µl SOC media (from New England Biolabs) was mixed with cells and then incubated at 37°C for 1 hr. Cells were spread on LB-agar plates containing the antibiotic, ampicillin (100 µg/ml). Plates were incubated overnight at 37°C and refrigerated in the morning.

NEB 1X SOC Outgrowth Medium:

2% Vegetable Peptone

0.5% Yeast Extract

10 mM NaCl

2.5 mM KCl

10 mM MgCl₂

10 mM MgSO₄

20 mM Glucose

500ml LB agar

5g NaCl

5g Tryptone

2.5g Yeast Extract

7.5g Agar

and dH₂O to 500mL

2.4 Cloning into Promega pGEM-T Easy

Blunt-ended PCR products were cloned into pGEM-T Easy (Promega) for sequencing and/or cloning into the mammalian expression vector, pcDNA3.1 CMV 3XFLAG. After pGEM[®]-T Easy is a linearized vector with a 3'-terminal thymidine at both ends to allow efficient ligation of A-tailed PCR products that are produced during amplification with Taq DNA polymerase, or by treating products from a reaction amplified by Phusion or Q5 with ATP and Taq (NEED TO INCLUDE THE TIME AND TEMP HERE). A-tailed products were mixed with pGEM-T Easy and T4 DNA ligase in 2X Rapid Ligation Buffer for 1 hr at room temperature, or 4°C overnight, 50 µl DH5α cells were transformed with 2 µl of each ligation reaction in 1.5ml microcentrifuge tube on ice. Transformation was otherwise carried out as described above. Following transformation, 150 µl SOC media was added to the cells, and allowed to recover at 37°C for 1.5 hrs at 200 rpm. The entire transformation culture was then plated on LB agar containing ampicillin (1µl/ml), IPTG (0.1 mM) and X-Gal (40 µg/ml) and incubated overnight at 37°C. Blue/white screening of colonies allowed identification of colonies where transformation was likely to have been successful; where white colonies were likely to contain the insert. Plasmids were screened for successful cloning by EcoRI digest (two sites surround the insertion point) prior to sequencing using the SP6 Promoter Primer.

2.4.1 Plasmid DNA isolation

Plasmids were purified using Macherey-Nagel NucleoSpin Plasmid Miniprep kits, according to the accompanying instructions. Colonies were picked from Agar plates using sterile 200 µl pipette tips and grown in 2.5 ml in LB-Ampicillin (100 µg/ml) broth overnight with shaking (200 rpm) at 37°C. Bacterial cultures were subjected to centrifugation for 30 s at 11000 x g. The growth medium was discarded and the cell pellet was resuspended in 250 µl Buffer A1. E. coli cells were lysed by mixing with 250 µl Buffer A2 (SDS / alkaline lysis buffer). After 5 minutes, 300 µl Buffer A3 was added to the lysed cells. Buffer A3 is a neutralisation buffer containing chaotropic salts for precipitation of all but the plasmid DNA and favourable conditions for binding of pDNA to the silica membrane of the column. Centrifugation for 5 min at 11,000 x g at room temperature pelleted cell debris. The supernatant was loaded into a NucleoSpin® Plasmid column by centrifugation for 1 min at 11,000 x g. The silica membrane was washed once with 500 µl room temperature buffer AW and twice further with 600 µl buffer A4 to remove salts, metabolites, and soluble cellular components. The silica membrane was dried by centrifugation for 2 min at 11,000 x g. After discarding the flow-through and collection tube, the NucleoSpin® Plasmid Column was placed into 1.5 mL microcentrifuge tube. To elute the DNA, 50 µl Buffer AE (5 mM Tris / HCl, pH 8.5) was applied to the membrane, incubated for 1 minute at room temperature, then eluted into the microcentrifuge tube by centrifugation for 1 minute at 11000 x g. Yield and purity was determined by spectrophotometric measurement using the Nanodrop (See Section 2.1).

2.5 RNA purification from cell lysate

Cultured cells were washed in cold Phosphate buffered saline PBS three times, then scraped into 1ml PBS.

PBS: 140mM NaCl, 2.7mM KCl, 10mM Na₂HPO₄, 1.7mM KH₂P₄O₄,

pH7.4 (adjusted with HCl)

Cells were pelleted using a microcentrifuge, at 2000xg for 5 minutes at 5°C and then processed using the Promega RNA Reliaprep Cell Miniprep System according to the supplier's instructions. The cell pellet was resuspended in BL + TG Buffer (BL contains

guanidine thiocyanate to disrupt nucleoprotein complexes and TG is 1-Thioglycerol to inactivate ribonucleases). A 35 % volume of 100% Isopropanol was then added and mixed by vortexing for 5 seconds. The resulting lysate was loaded onto a ReliaPrep™ Minicolumn and subjected to centrifugation at 13,000 × g for 30 seconds at 20°C–25°C. Ethanolic wash solution (500 µl) was then applied to the ReliaPrep™ Minicolumn and subjected to centrifugation at 13,000 × g for 30 seconds. A 30 µl DNase mix was then incubated on the membrane for 15 minutes at room temperature:

24µl of Yellow Core Buffer
3µl 0.09M MnCl₂
3µl of DNase I enzyme

The membrane was then twice washed with 200µl of ethanolic Column Wash Solution and subjected to centrifugation at 13,000 × g for 15 seconds and 30 seconds respectively. In a clean collection tube, 300 µl ethanolic RNA Wash Solution was applied to the membrane and the column was subjected to centrifugation at 13,000 × g for 2 minutes. The ReliaPrep™ Minicolumn was transferred to a 1.5ml Elution Tube and 30 µl nuclease-free water was applied to the membrane. The ReliaPrep™ Minicolumn was subjected to centrifugation at 13,000 × g for 1 minute, and a sample of the eluted RNA was checked for yield and purity using the Nanodrop, while the remainder was stored at –80°C.

2.6 Reverse Transcription of total RNA to yield cDNA

Thin walled Thermo Scientific™ PCR Tubes were used in the Techne TC 3000G thermocycler or MJ research PTC 200. Total RNA from human brain was acquired from Agilent. The RNA has product code 540005 and was isolated using a modified guanidinium thiocyanate method. Human tissue was obtained using protocols approved by an Institutional Review Board.

2.6.1 Reverse Transcription of total RNA with Maxima H Thermostable Reverse Transcriptase

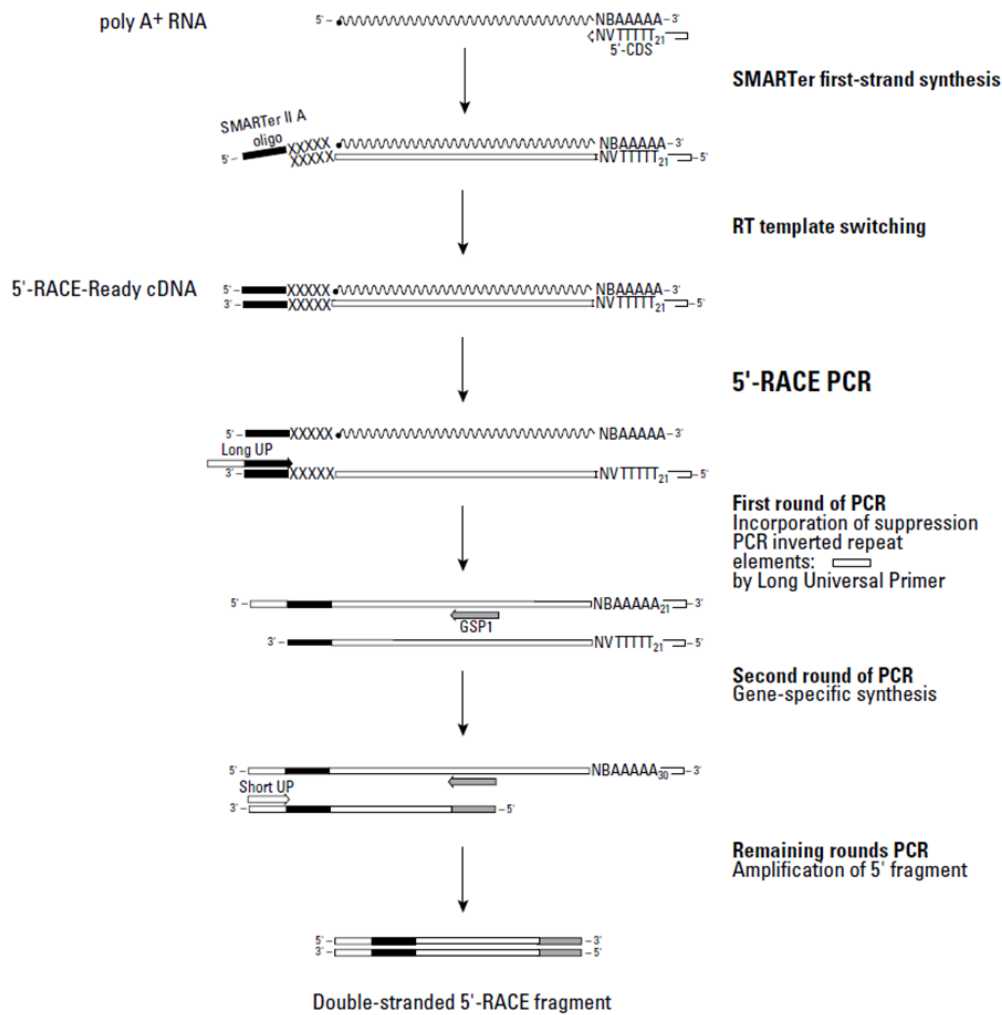
The Thermo Scientific Maxima H Minus Reverse Transcriptase is a mutation of M-MuLV Reverse Transcriptase. The enzyme has 50X higher processivity and has greatly improved thermostability. RNA secondary structures are more efficiently denatured

at temperatures higher than the standard reverse transcription temperature of ~42°C. This enzyme and reaction conditions were chosen for reverse transcription reactions due to the typical high GC content of our targets, and potential secondary structures inhibiting reverse transcription under standard conditions.

5µg total RNA was denatured at 65°C for 5 m. with Oligo(dT)₁₈ primer and dNTP mix. Oligo(dT)₁₈ primers enrich for mRNA by binding poly(A)+ tails of mRNA. This promotes the reverse transcription of full length mRNAs, and acts against reverse transcription of non-coding splice variants. After cooling, RT buffer was added with 40 units of Promega RNasin® Ribonuclease Inhibitor and 200 units of Maxima H Minus Reverse Transcriptase. The reaction mixture was mixed by gentle trituration and incubated for 18 min. at 50°C, followed by 18 min. at 65°C. The reaction was terminated at 85°C for 5 min. They were then cooled to 5°C in the thermocycler prior to storage at -20°C.

2.6.2 Rapid amplification of 5' complementary DNA ends

The rapid amplification of 5' complementary DNA ends (RACE) was used to characterise the expand the known 5' UTR of *Task 3*. The method utilises the terminal transferase activity of the reverse transcriptase enzyme, SMARTscribe (Fig.2.1). Transcription to cDNA begins from a bound oligo(dT) primer at the polyA tail of the mRNA. When the SMARTscribe enzyme reaches the 5' end of the mRNA, it adds known residues to the end of the synthesized first strand cDNA (Fig. 2.1). An oligonucleotide, binds specifically to this known residue and the reverse transcriptase switches template, adding the oligonucleotide sequence to the end of the mRNA template. This extension acts as a primer recognition site for a universal primer. In this way, the entire sequence of an mRNA molecule may be transcribed into cDNA, ready for use as a PCR template. PCR using a gene-specific primer and the universal primer, complementary to the SMARTer II A oligo amplifies from the reverse, gene-specific primer, to the terminal universal primer.



n

Figure 2.1 Schematic of the principal steps in 5' RACE PCR using SMARTer RACE cDNA Amplification Kit (Clontech). Total mRNA from human brain was used as the starting material to generate RACE ready cDNA. cDNA was generated by reverse transcription with SMARTerII A oligonucleotide primer and oligo dT primer. The SMARTer II A oligonucleotide primer extended the mRNA at the 5' end to ensure the very end of the 5' UTR is maintained. The forward reaction of 5'RACE was carried out using universal primer mix (UPM) and the reverse reaction was carried out using gene specific primers.

2.7 Cell culture

HeLa cells were chosen for use in studies of protein expression. HeLa cells are Human Cervical Adenocarcinoma adherent cells. The culture and transfection of HeLa cells using Novagen GeneJuice have been optimised in our lab. HeLa cells were cultured in 10% FCS supplemented DMEM, high glucose, GlutaMAX™ Supplement, HEPES (Gibco®) at 37°C with 5% atmospheric CO₂. Cells were passaged at 70-80% confluence using TrypLE™ Express for dissociation of adherent cells from plate. TrypLE™ Express is a recombinant cell-dissociation enzyme and uses a similar protocol without requirement for deactivation. Washing of cells was carried out using Dulbecco's phosphate buffered saline (DPBS), without Calcium or Magnesium; acquired from Gibco. Plastic ware was gamma irradiated-sterile (Greiner).

2.8 Transient transfection

Cells were transiently transfected using the proprietary transfection reagent, Novagen GeneJuice, according to the manufacturer's instructions. Novagen GeneJuice provides highly efficient transfection and low cytotoxicity. Transfections were carried out on cells grown in 6-well plates, 6cm plates or 10 cm plates. Transfection was carried out 24hr after seeding, with 3:1 Genejuice to µg plasmid DNA. A typical transfection experiment was seeding of 100,000 cells in the well of a 6-well plate. The following day, 1 µg of DNA was transfected with 3 µl GeneJuice diluted in 100 µl Serum Free DMEM. The transfection reaction was scaled appropriately to expression levels of transfected plasmids, as well as the required lysate harvest for protein or RNA analysis. For co-transfection of WT-Task3-FLAG plasmids with RNP-expressing plasmids, 3 µl Genejuice was used to transfect 0.5 µg WT-Task3-FLAG expression plasmids with 0.5 µg RNP-expressing plasmids or empty pcDNA3.1 as a negative control.

2.9 Primary Neuronal Cell Culture

Primary neurons were prepared in accordance with Home Office guidelines by Dr Joanne Bailey, an experienced licenced expert in neuronal cell preparation. Pregnant mice were anaesthetized and decapitated and 18 day old foetuses were removed in Hanks' balanced salt solution (HBS) (Gibco) on ice. Foetuses were decapitated and the meninges and white matter were excised. Brain cortices were isolated in HBS and incubated in 0.25% trypsin for 15 min at 37°C. Cortical cells were dissociated by gentle trituration through a 1000 µl pipette tip.

Cells were plated at low density, approximately 200,000 cells/ml onto 0.1 mg/mL poly-D-lysine – coated coverslips in a 12 well plate. Cells were cultured in Neurobasal medium supplemented with B27 (Gibco) and 0.5 mM L-glutamine. B27 supplement is an optimised supplement used to support the low density growth and viability of CNS neurons (Xie, Markesbery and Lovell, 2000) Half the volume of cell culture media was replaced after 4 days with fresh supplemented Neurobasal medium. Reagents were acquired from Invitrogen.

2.10 Transient Transfection of primary cortical neurons

Cortical neurons were transfected after 8 days in vitro (DIV 8). Cells were transfected on coverslips in 1 ml medium in a 12 well plate. 500 µl (half total volume) of the Neurobasal medium was harvested from cell cultures and maintained at 37°C. 500 ng of plasmid DNA was mixed with 50 µl serum-free DMEM, then mixed by vortexing with 0.5 µl of Lipofectamine 2000 (Invitrogen). The transfection mixture was incubated at RT for 20 minutes before adding drop-wise to cells. Most of the medium was replaced with half fresh and half harvested Neurobasal medium after 45 min. Cells were fixed after 48 hours in culture following transfection.

2.11 Polysome Fractionation

2.11.1 Cell lysis

Cells were transfected 24 hours prior to lysis with WT GQ eUTR-Task3-FLAG or complimentary GQ eUTR-Task3-FLAG (Section xyz) . Cells were incubated with 10µg/ml cycloheximide for 5 minutes then placed on ice and washed three times in ice cold PBS. Cells were then scraped in 1.5ml PBS and pelleted by centrifugation at 2000 x g for 2 minutes. The supernatant was discarded and the cells were re-suspended in 300 µl Polysome cell lysis buffer (10mM Tris-HCl pH7.5, 10mM NaCl, 10mM MgCl₂, 1% Triton X-100, 1% DOC (deoxycholate), 40 units RNasin® Ribonuclease Inhibitor (Promega N2515), 3.3 mM Dithiothreitol (DTT). Lysis reactions were incubated on ice for 2 minutes. Cell debris was pelleted by centrifugation at

13,000 rpm at 4°C for 5 minutes. The supernatant was transferred to a sterile tube and snap frozen at -80°C.

2.11.2 Polysome Gradients

Sucrose density gradients were prepared by dissolving sucrose (Sigma S9378) in polysome gradient buffer (30mM Tris-HCl pH7.5, 100mM NaCl, 10mM MgCl₂) to respective final concentrations of 10% (w/v) 20% (w/v). Sucrose solutions were filter-sterilised (0.4µm). Successive layers of 1.5ml of each sucrose solution were applied to tubes, decreasing in percentage sucrose upwards; snap freezing each layer at -80°C. Sucrose gradients were stored at -20°C, then thawed overnight in a cold room prior to the experiment to allow the formation of a continuous gradient.

2.11.3 Fraction Collection

Cell lysates were thawed on ice and applied to the top of the sucrose density gradients. Gradient tubes were subjected to centrifugation at 37,000 rpm in the Beckman Ultra Centrifuge, using the SW41 swing rotor and buckets for 2.5 hours at 4°C without braking. Gradients were then transferred to ice. Fraction collection tubes were set up containing 30µl 20% SDS and 0.25µg/µl carrier tRNA (Sigma R9001) at 10mg/ml in 0.1M NaCl).

A microfluidic pump was used at 0.75min/tube to pump 60% sucrose into the bottom of the gradient tubes, pushing the sucrose gradient upwards. Polysome-ribosome profiles were generated by UV-Vis absorbance of the pumped sucrose gradient. Proteinase K (Promega V3021) at 5mg/ml was added to collected fractions (20µl per sample) and incubated at 37°C for 2 hours. Collected fractions were snap frozen at -80°C

2.11.4 RNA Extraction

Collected fractions were thawed on ice and mixed with 250µl phenol/chloroform (pH4.5) by vortexing for 1 minute. Samples were then subjected to centrifugation at 12,000 rpm for 10 minutes at 4°C. The aqueous phase was transferred to a sterile tube and mixed with 250µl phenol/chloroform (pH4.5) by vortexing for 1 minute. Samples were then subjected to centrifugation at 12,000 rpm for 10 minutes at 4°C. The aqueous phase was transferred to a sterile tube and mixed with 700µl cold isopropanol. Tubes were inverted 5 times to mix and incubated for 2 hours at -20°C. Samples were subjected to centrifugation at 12,000 rpm for 30 minutes at 4°C. Samples were placed on ice, all isopropanol discarded and pellet mixed 1ml cold 80% ethanol. Samples were then subjected to centrifugation at 12,000 rpm for 30 minutes at 4°C. Samples were placed on ice, all ethanol discarded and the pellet dried by placing the microfuge tube in a 30°C heat block for 30 minutes. Dried pellets were suspended in 20 µl dH₂O and snap frozen at -80°C.

2.12 *In vitro* Transcription for *in vitro* translation

mMESSAGE mMACHINE® T7 Ultra Kit (Ambion) was used to transcribe large quantities of capped RNA. Capped and polyA-tailed RNA was made to optimise representation of *in vivo* mRNA. The structure of the cap analog [m⁷G(5')ppp(5')G] ensures incorporation only at the 5' terminal G of a transcript. The template for transcription was from pcDNA3.1-FLAG expression plasmids. Short linear DNA templates were made by digestion of pcDNA3.1-Task3-FLAG expression plasmids with a restriction enzyme 3' proximal to the C-terminal FLAG-tag, XbaI.

| Component | μl in 20 μl Reaction |
|--------------------------------|----------------------|
| T7 2X NTP/ARCA | 10 |
| 10X T7 Reaction Buffer | 2 |
| linear template DNA (0.5μg/μl) | 2 |
| T7 Enzyme Mix | 2 |
| Nuclease-Free Water | 4 |

Reactions were mixed by gentle trituration and incubated at 37°C for 2hr. To remove the template following the reaction, 1 μl TURBO DNase was added, mixed and incubated for a further 15m at 37°C.

Poly[A] tailing was carried out at 37°C for 45m:

| Component | μl in 100 μl Reaction |
|--------------------------------------|-----------------------|
| mMESSAGE mMACHINE® T7 Ultra reaction | 20 |
| Nuclease-free Water | 36 |
| 5X E-PAP Buffer | 20 |
| 25 mM MnCl ₂ | 10 |
| ATP Solution | 10 |

RNA was purified using PureLink® RNA Mini Kit according to the manufacturer's protocol for purifying RNA from Liquid Samples/RNA Clean-Up (Ambion).

2.13 *In vitro* Transcription for RNA structure analysis

Promega T7 RNA polymerase was used to generate un-capped or polyA tailed RNA for structural analysis by Mesoporphyrin IX dihydrochloride fluorescence.

| Component | μl in 100 μl Reaction |
|---|---|
| Transcription Optimized 5X Buffer | 20 |
| DTT, 100mM | 10 |
| RNasin® Ribonuclease Inhibitor (100 units) (Promega N2515) | 2.5 |
| rNTP mix | 20 |
| Linearised DNA template (1 $\mu\text{g}/\mu\text{l}$) | 2 |
| T7 RNA Polymerase (40 units) | 4 |
| Nuclease-Free Water | 41.5 |

Reactions were incubated for 2 hr at 37°C.

2.14 *In vitro* Translation

In vitro translation with the Flexi® Rabbit Reticulocyte Lysate System (Promega) was used to analyse the effect of K^+ concentration on the translation of G-quadruplex-containing mRNA sequences, generated by *in vitro* transcription. Translation was carried out according to the supplier's protocol apart from RNA templates were not denatured at 65°C for 3 minutes prior to assembling the reaction components on ice. The reaction was incubated at 30°C for 90 minutes. Translation products were diluted with SDS sample buffer before loading on an SDS PAGE gel.

| Component | μl in 25 μl Reaction |
|--|---------------------------------|
| Flexi® Rabbit Reticulocyte Lysate | 16.5 |
| Amino Acid Mixture, Minus Leucine, 1mM | 0.25 |
| Amino Acid Mixture, Minus Methionine, 1mM | 0.25 |
| Potassium Chloride, 2.5M | 0, 0.5, 1.0 |
| DTT, 100mM | 0.5 |
| RNasin® Ribonuclease Inhibitor (20 units) (Promega N2515) | 0.5 |
| RNA substrate | 6 |
| Nuclease-Free Water | 1.0, 0.5, 0 |

2.15 Mesoporphyrin IX dihydrochloride fluorescence

Mesoporphyrin IX has been shown to specifically bind G-quadruplex nucleotide structures in DNA and RNA (Arthanari *et al.*, 1998). Mesoporphyrin IX dihydrochloride (Sigma Aldrich), was used to measure G-quadruplex formation in RNA sequences generated by in-vitro transcription. Fluorescence assays were conducted under the following conditions:

A 200 μ l sample contained:

10 mM Tris HCl, pH 6.4
5 nM NMM
RNA at 10 μ M
with and without 150 mM KCl

Fluorescence was measured using the Horiba Jobin Yvon FluoroMax-4 Bench-top Spectrofluorometer spectra were taken with an excitation wavelength of 399 nm, peak emission wavelength was seen at 614 nm.

2.16 Circular Dichroism

In vitro transcribed RNA was purified using NucleoSpin[®] miRNA (Machery-Nagel), which is optimised for isolation of small RNA (< 200b). The resolution (signal to noise) offered by the Jasco J710 CD spectrometer was insufficient below 245 nm to observe negative peaks at 237 nm, but gave good signal to noise above 245 nm, allowing measurement of changes in peak intensity at 262 nm. RNAs were folded in the presence of 100 mM KCl, 10 mM Tris-HCl and 0.1 mM EDTA (pH 7.5) by heating for 5 min at 95°C followed by cooling to room temperature in an insulated polystyrene box on the bench overnight. Spectra of folded RNA (4 μ M) were measured at room temperature. Spectra were acquired using a Jasco J-810 spectrophotometer with a 1mm cell at a scan speed of 50 nm/min with a response time of 1 s. The spectra were averaged over three scans and the spectrum from a blank sample containing only buffer was subtracted from the data mean. Where the effects of TmPyP4 on structure were analysed, 1 μ l aliquots of TmPyP4 were added to the sample in the cuvette and were mixed by trituration prior to acquisition of new spectra.

2.17 Treatment of transfected cells with TMPyP4

TMPyP4 is a cationic porphyrin and unfolds (CGG)_n quadruplexes in vitro (Ofer *et al.*, 2009). TMPyP4 increased the efficiency of translation of a (CGG)₉₉-luciferase construct in HEK293 cells (Ofer *et al.*, 2009). 24 hrs post-transfection with Task3 mutant 5' UTR expression plasmids, TMPyP4 was dissolved in DMSO and applied to cell growth media and cells harvested after a further 24 hrs. TMPyP4 was applied to cells at 50 µM concentration, higher than that used in the Ofer study, 20µM, but lower than that used in other studies, up to 100 µM in HeLa cells (Morris *et al.*, 2012). Solvent control treatment with DMSO was carried out in parallel to account for effects of DMSO.

2.18 [35S]-methionine incorporation assay

The rate of translation following TMPyP4 treatment was assessed by measuring the radioactivity of HeLa cell lysates grown in media containing [35S]-methionine. 5×10^5 HeLa cells were seeded in triplicate into wells of a 6-well plate in 2ml DMEM and incubated at 37°C for 16 hours prior to treatment with 50 µM TMPyP4 for 24 hours. Media was replaced with DMEM containing 35S-TransLabel (MP Biomedical, France) to 10µCi/ml (0.37MBq/ml) and incubated for 2 hours. Cells were washed 3 X with PBS, scraped into 1ml ice cold PBS and pelleted at 4000 rpm for 3 minutes at 4°C. Cells were lysed using RIPA buffer supplemented with protease inhibitors. Lysates were stored at -20°C overnight.

The activity of the lysates was determined by scintillation counting. 30µl of lysate was spotted onto Whatman filter paper discs and allowed to air dry. Discs were then submersed in 10% (v/v) trichloroacetic acid (TCA) and an excess of unlabelled L-methionine (Sigma) and incubated at room temperature for 15 minutes. Discs were then submersed in 5% TCA (v/v) and heated to 90°C. The samples were cooled and 5% TCA was discarded. The discs were then washed in 100% ethanol followed by 100% acetone. Discs were air dried and then placed in scintillation vials. Discs were submersed in 4ml scintillation fluid (OptiScint 'HiSafe', PerkinElmer) and radioactivity was analysed on a WALLAC 1409 liquid scintillation counter (PerkinElmer) for one minute per sample.

2.19 Cell lysis and immunoblot analyses

Cell lysates were harvested 48 hours after transfection unless otherwise stated. Our standard whole-cell lysis buffer was unable to yield sufficient membrane-protein for SDS-PAGE. M-Per (Pierce) is a whole cell lysis buffer which was used for lysis of HeLa cells transfected with Fxr2 plasmids. Mem-PER (Pierce) was used to solubilize and enrich membrane-associated proteins. The use of Mem-PER allowed for fractionation of membrane-enriched and membrane-depleted fractions. However, lysates made in this way are high in salts and detergents, so required further treatment prior to use in SDS-PAGE.

Initially, lysates were cleaned up, and concentrated where necessary using Stratagene Strataclean Resin, a non-toxic slurry of hydroxylated silica particles which bind amino acids. 2µl of homogenised resin was added to 75 µl membrane cell lysates and vortexed for 1 minute. The resin was then spun down at 2000 rpm for 1 minute. The supernatant was discarded and the resin was resuspended in 50 µl 1x SDS-PAGE loading buffer. 25 µl of sample was loaded per well following 1 hr incubation at 37°C. It is not possible to accurately determine protein concentrations between samples in this way and so equal loading between lanes in SDS PAGE is difficult. Pierce SDS-PAGE Sample Prep Kit was used later to allow assay of protein concentration in lysates.

The method used and detailed above was replaced to reduce cost and handling steps of lysates before separation on SDS PAGE. RIPA buffer was used to lyse whole cells, including a substantial component of membrane-bound proteins. Pierce BCA protein assay reagent was used to quantify protein concentration in samples before normalising and separating on SDS PAGE.

Radioimmunoprecipitation assay (RIPA) buffer

150mM NaCl
1% NP40 (v/v)
0.5% DOC (v/v)
0.1% SDS (w/v)
50 mM Tris-HCl pH8.0

2.19.1 Standardisation of protein concentration

Protein concentrations of cell extracts were standardised based on BioRad Bradford Reagent protein assays for standard cell lysis, or BCA Protein Reagent protein assays for high salt/detergent lysis buffers, MemPER and RIPA buffer.

BSA standards were prepared, diluted with lysis buffer, mixed with assay reagent, and the absorbance at 620 nm was measured using a plate reader. Absorbance at a reference wavelength of 405 nm was deducted from absorbance measured at 620 nm.

2.19.2 SDS-PAGE of protein samples

Lysates were resolved by sodium dodecyl sulphate-polyacrylamide gel electrophoresis (SDS-PAGE). Protein samples were diluted to ~10ug in 15 µl and incubated at 70 °C for 30 minutes in PIERCE Lane Marker Non-Reducing Sample Buffer supplemented with 10% 2-Mercaptoethanol.

5 x PIERCE Lane Marker Non-Reducing Sample Buffer:

Proprietary pink tracking dye in 0.3M Tris-HCl, 5% SDS, 50% glycerol

Protein samples were loaded onto SDS-polyacrylamide gels in Laemmli buffer at 20mA whilst running through the stack, and 30mA thereafter.

Laemmli buffer:
25mM Tris base
192mM glycine
0.1% SDS (w/v)

Stacking gel:
125mM TrisHCl, pH 6.8
4% ProtoGel (30% or 40% (w/v) acrylamide 0.8% (w/v) bisacrylamide)
0.2% (w/v) SDS
0.1% (w/v) APS
0.1% TEMED

Resolving gel:
375mM TrisHCl, pH 8.8
ProtoGel to yield 6 – 15% acrylamide
0.1% (w/v) SDS
0.05% (w/v) APS
0.25% TEMED

Proteins were transferred to nitrocellulose membranes by semi-dry transfer, using BioRad TransBlot Turbo units in Tris-Glycine buffer (0.025M Tris Base and 0.192M Glycine). Membranes were subjected to blocking in 3% BSA TBS-TWEEN (25mM Tris, 3mM KCl, 0.1M NaCl, and 0.1% Tween 20) with gentle shaking for 1 hr. Primary antibodies were applied for a minimum of 2 hr, in TBS-TWEEN with gentle shaking. Membranes were then subjected to 3 X 10 min washes in TBS-TWEEN with gentle shaking. Secondary antibodies were applied for 90 min in TBS-TWEEN with gentle shaking. Finally, 3 X 10 min. washes in TBS-TWEEN with gentle shaking, and 1 X 5 min. wash in dH₂O.

2.19.2 Visualisation of bound secondary antibodies

After binding and washing of the membrane, DyLight™ conjugated secondary antibodies were visualised using an Odyssey® infrared imaging system scanner, to measure absorbance at 700 and 800 nm. Relative quantification of Western Blots was carried out using ImageJ. Scanned images were converted to 256 grey format. The rectangle tool was set to surround the largest of the measured bands, and the mean grey value was measured for each band. Values were processed in Microsoft Excel 2013. The inverted background was deducted from all inverted band measurements. The net value for each band was divided by the value for the actin loading control for that lane. This yielded relative intensities of each band relative to total protein in that lane.

2.20 qPCR of FLAG RNA in transfected cell lysate

Reverse transcription of mRNA was carried out using Maxima H Thermostable Reverse Transcriptase. 1µg total RNA was denatured at 65°C for 5 min with Oligo(dT)18 primer and dNTP mix. After cooling, RT buffer was added with 40 units of Promega RNasin® Ribonuclease Inhibitor and 200 units of Maxima H Minus Reverse Transcriptase. The reaction mixture was mixed by gentle trituration and incubated for 18 min. at 50°C, followed by 18 min. at 65°C. The reaction was terminated at 85°C for 5 min. They were then cooled to 5°C in the thermocycler prior to storage at -20°C.

Quantitative Real Time PCR amplification was performed using SYBR® Select Master Mix (Life Technologies) and Eco qPCR System (illumina). Primers were designed against FLAG and β-actin RNA sequences (section 2.2.4) and expression of FLAG mRNA relative to β-actin mRNA was characterised by relative quantification. Reactions were done in triplicate and mean delta CT values were used for calculating relative abundances.

The Illumina Eco analysis software was used to calculate relative quantification of FLAG Vs Actin cDNA. Relative quantification is calculated by this software using the $\Delta\Delta Cq$ method (Livak *et al.*, 2001). The $\Delta\Delta Cq$ method reports fold difference of a target gene's expression relative to a reference gene and reference sample. The reference gene is β-actin. The reference sample is the untreated control sample; the wild-type GQ eUTR in the case of Task3-FLAG. The $\Delta\Delta Cq$ method assumes equal PCR

efficiencies of the target amplicons. This equates to a similar GC content and length and primer T_a . The amplicons typically targeted in qPCR are small (approximately 100 nucleotides), however, to achieve the requirements set out above regarding GC content and length and primer T_a , longer amplicons were targeted.

| | |
|-------------------------------------|------------|
| SYBR® Select Master Mix (2X) | 5 μ L |
| Forward and Reverse Primers (400nM) | 1 μ L |
| cDNA template (100ng) | 1 μ L |
| Water | 3 μ L |
| <hr/> | |
| Total Volume | 10 μ L |

| <u>Step</u> | <u>Temperature (°C)</u> | <u>Duration (s)</u> | <u>Cycles</u> |
|----------------|-------------------------|---------------------|---------------|
| UDG Activation | 50 | 120 | Hold |
| UP Activation | 95 | 120 | Hold |
| Denature | 95 | 15 | |
| Anneal | 55 | 15 | 40 |
| Extend | 72 | 60 | |

Table 2.2 & 2.3 The composition of qPCR reaction reactions using SYBR® Select Master Mix and cycle conditions using Eco qPCR System.

2.21 Immunofluorescence microscopy

Sterile glass coverslips in six-well plates were seeded with 1×10^5 HeLa cells and transfected as described above. After 48 hr, coverslips were washed three times with PBS and then fixed in 4% (w/v) paraformaldehyde in PBS, pH 7.4 for 15 min. Cells were permeabilised in 0.1% (v/v) Triton X-100 in PBS for 8 min. Blocking was carried out for 10 minutes using 5% Normal Goat Serum (NGS) diluted in PBS. Primary antibody (FLAG M2 or Rabbit anti-V5) was added in NGS-PBS (1:2000) and incubated for 1hr at RT. Slides were then subjected to 5 X PBS washes. Secondary antibody was added together with 0.05% phalloidin-fluorescein isothiocyanate (FITC), to stain actin. Coverslips were mounted on slides with a glue containing 4',6'-diamidino-2-phenylindole hydrochloride (Sigma) (DAPI) to stain nuclei. Mountant was left to set overnight at room temperature, with slides protected from ambient light. Slides were then stored at 4°C in the long term, but allowed to come to room temperature prior to microscopy.

2.22 Fluorescence in situ Hybridization (FISH) of mRNA

Fluorescence *in situ* Hybridization (FISH) allows detection and measurement of subcellular localisation of mRNA in cells. Custom Stellaris FISH probes were designed against eGFP coding sequence Biosearch Technologies. In total, 32 FISH probes were designed and conjugated to CAL Fluor 590. Probes were supplied lyophilised and were resuspended in 400 μ L of TE buffer (10 mM Tris-HCl, 1 mM EDTA, pH 8.0) to generate probe stock at 12.5 μ M. 20 μ l aliquots were stored at -20°C.

2.23 Measurements of mRNA particle distribution in neurons

Measurement of distances of fluorescent mRNA particles from the cell body were made using Volocity 6.0 software (Perkin Elmer). Fluorescence thresholding was used to automatically define regions of interest (ROIs). ROIs with high red fluorescence relative to background were identified as neuronal messenger ribonucleoprotein particles (RNPs). Distance measurements were made using Volocity 6.0 to quantify the size of mRNA particle and distance from the soma.

2.24 Site directed mutagenesis

Where mutation of the target sequence was proximal to the 5' terminus, the mutated sequence, base substitution, deletion or addition was incorporated into the forward cloning primer. This was the case for the majority of mutation reactions. In all other cases, where base substitutions were required, the following method was employed. The mutagenic sequences were incorporated into internal / nested primers and used in a molar ratio of 1:3:1, forward cloning primer : internal mutagenic primer : reverse cloning primer (Fig. 2.2). DNA polymerase binds duplex DNA at the primer-bound site and synthesises the DNA 5' – 3'. In PCR, you can bias the products made at each round by the primer concentrations used. This method uses a large amount of an internal mutagenic primer to bias the amount of mutated DNA sequence in each consecutive PCR round. Some of the products of the fourth round of PCR are the entire cloning sequence from forward cloning primer site to reverse primer cloning site, with the desired internal mutation on both the sense and antisense strands. There is a high probability that DNA of the length of the entire amplicon contains the desired mutation. After 35 cycles, the predicted molar ratio of nucleotide sequences in the PCR reaction of full length amplicons containing the mutation Vs other nucleotide sequences is approximately trillions to one. These amplicons were identified by agarose gel electrophoresis & gel purified prior to cloning. Sequencing of the cloned amplicons confirmed the presence of the desired mutation.

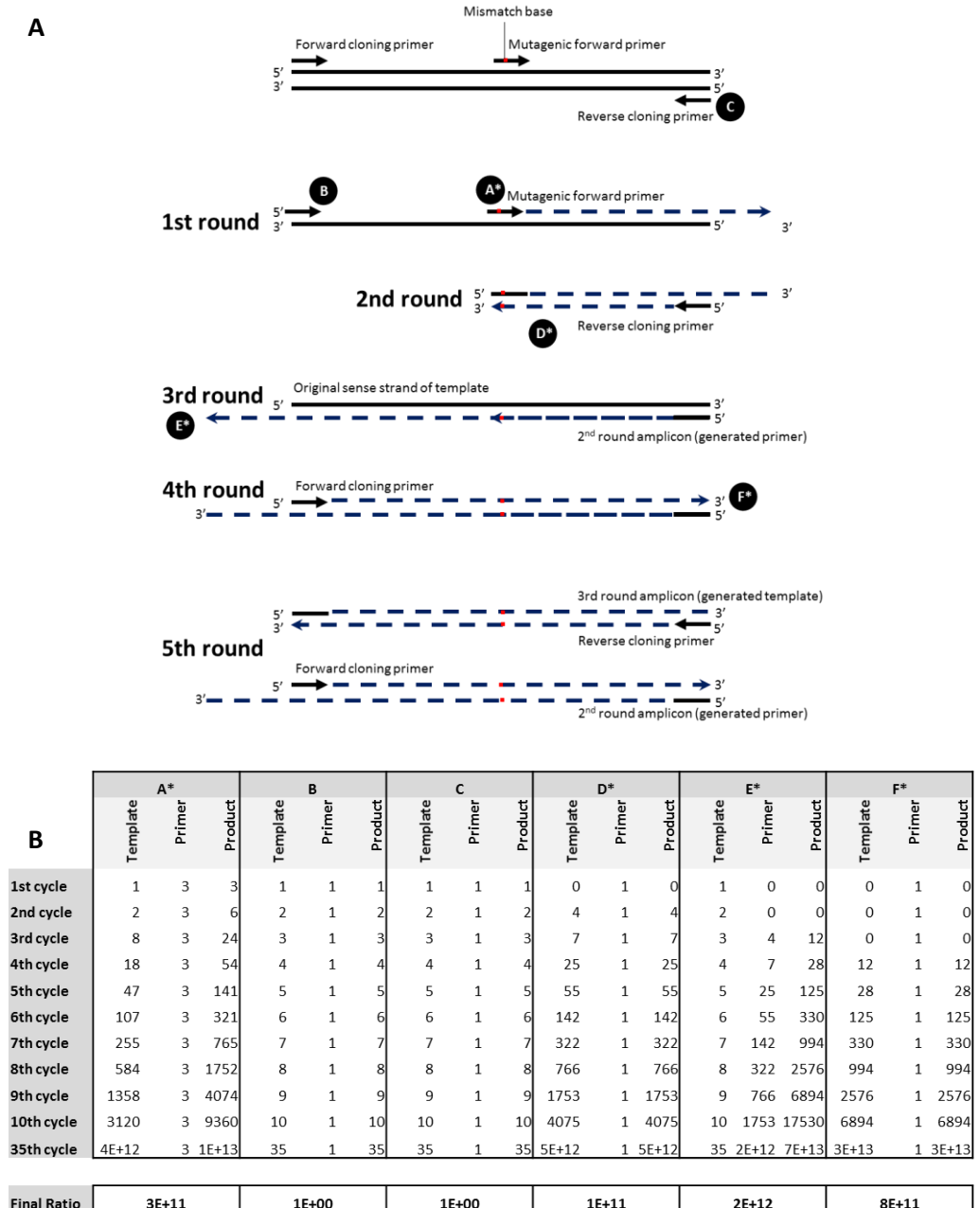


Figure 2.2 Site directed mutagenesis using forward cloning primer, three times molar ratio internal mutagenic primer, and reverse cloning primer. A) Schematic of the PCR mutagenesis reaction. The nucleotide sequences initially present in the reaction or generated during the reactions are labelled A – B. Sequences containing the mutated nucleotide sequence are highlighted with an *. A*, B and C are all products of the 1st round/cycle of PCR. However, A*, containing the mutagenic sequence will be created approximately 3 x more readily than B and C; because the mutagenic primer is at 3 X the concentration of the cloning primers. During the 2nd round/cycle, amplicon D* is produced using amplicon A* as a template. During the 3rd round/cycle of PCR, amplicon D* acts as a primer, binding to the original sense strand of the template. This leads to generation of amplicon E*. F* is produced in the 5th round/cycle of PCR using the forward cloning primer and E* as a template. The table shown in B) illustrates how the bias in molar ratio of mutagenic primer causes accumulation of the mutagenic sequence in the vast majority of amplicons as the PCR cycle number progress. The values given to the template, primer and product for each nucleotide sequence are based on the descriptions here, and the schematic in A).

| Target | Predicted kDa | Antibody Name | Immunogen | Donor Animal | Dilution used | Supplier (and product ID) |
|----------------|---------------|-----------------|--|-------------------|-------------------------|---------------------------|
| β -actin | 42 | β -actin | Slightly modified β -cytoplasmic actin N-terminal peptide, Ac-Asp-Asp-Asp-Ile-Ala-Ala-Leu-Val-Ile-Asp-Asn-Gly-Ser-Gly-Lys, conjugated to KLH | Mouse | WB 1:20000 | Sigma-Aldrich A1978-200UL |
| FLAG | N/A | ANTI-FLAG® M2 | peptide sequence DYKDDDDK | Mouse monoclonal | WB 1:5000 IHC 1:5000 | Sigma-Aldrich F3165-1MG |
| V5 | N/A | V5-tag Antibody | peptide sequence V5-tag | Rabbit polyclonal | IHC 1:5000 | Proteintech 14440-1-AP |

Table 2.4 Details of primary antibodies used in western blot and immunohistochemistry analyses.

Chapter Three

Results

Investigation of putative alternative upstream translation initiation sites in Two-pore potassium leak (K_{2P}) channels

3.1 Introduction

Two-pore potassium leak channels (K_{2P}) are characterised by four transmembrane domains, two pore domains and possess intracellular amino and carboxy termini. K_{2P} channels are responsible for setting and maintaining resting membrane potential in cells. The K_{2P} family is diverse and subfamily members are differentially gated by various stimuli. The expression of K_{2P} family members across tissues is diverse and poorly understood. Regulated membrane expression of K_{2P} channels therefore determines neuron excitability (Mathie *et al.*, 2010). K_{2P} channels are widely expressed in neuronal cells (Honore, 2007) where the influence on membrane potential is most obviously significant. Over-expression of potassium leak channels results in membrane hyperpolarisation, inhibiting action potentials. Under-expression results in membrane hypopolarisation, reducing the threshold needed for an action potential. Researchers at this University have recently described post-translational regulatory mechanisms for membrane expression of K_{2P} channels.

3.1.1 Bioinformatic screen of mRNAs identified an evolutionarily conserved sequence in the 5' UTR of K_{2P} channel, Traak

Traak (KCNK4) mRNA was identified by the Coldwell/Edwards bioinformatics screen (publication in preparation) to possess a conserved translated amino acid sequence in its 5' UTR. Traak is an outwardly rectifying channel, allowing potassium to pass down its chemical gradient, out of the cell, enhancing the resting membrane potential. Traak is expressed primarily in neuronal tissues where it is predicted to regulate synapse excitability. The proteins form functional membrane channels as homodimers. Human Traak transcript ENST00000422670 was identified as having a

conserved translated 5' UTR sequence with *Pan troglodytes* Traak transcript variant 1 mRNA.

3.2 Results

The ExTATIC macro was used to identify alternative upstream initiation codons, in frame with the annotated ORF, and within a strong context. Conservation of translated mRNA sequence from the eORF had been discovered by the bioinformatics analyses described in detail in 'Introduction 1.1'. The macro is limited to identification of CUG, GUG, ACG only in strong contexts. The macro identified one alternative initiation codon identified upstream of the +1 AUG (Fig. 3.2). The codon identified is a GUG in a strong context, G at -3 and G at +4. This putative alternative initiation codon is -99 nucleotides upstream of the +1 AUG, and would yield a 33 aa N-terminally extended TRAAK protein. The macro did not identify another putative alternative initiation codon at -78 to the +1 AUG; GUG in a weaker context, G at -3 and A at +4. Bioinformatics analyses found conserved sequence homology of the putative eORF peptide sequence between humans and chimpanzees (Fig. 3.1).

PREDICTED: Pan troglodytes potassium channel, subfamily K, member 4, transcript variant 1 (KCNK4), mRNA
 Sequence ID: [reflXM_001164319.3](#) Length: 2034 Number of Matches: 1

| Score | Expect | Method | Identities | Positives | Gaps | Frame |
|----------------|------------------------------|------------------------------|------------|-------------|----------|-------|
| 55.8 bits(133) | 2e-07 | Compositional matrix adjust. | 27/28(96%) | 28/28(100%) | 0/28(0%) | +1 |
| Query 16 | TSRGWPAVGSQAAAVTTAPQEPPARPLQ | 43 | | | | |
| | TSRGWPAVGS+AAAVTTAPQEPPARPLQ | | | | | |
| Sbjct 430 | TSRGWPAVGSRAAAVTTAPQEPPARPLQ | 513 | | | | |

Figure 3.1 Alignment of conserved 5' UTR predicted translated amino acid sequence between *Homo sapiens* and *Pan troglodytes*, produced using the NCBI tblastn tool,

| # | Pos | Codon | Context | Strength | eLen/tLen | eSeq/tSeq |
|---|-----|-------|---------|----------|-----------|-----------------------------------|
| 1 | -99 | GTG | GCTGTGG | GTG | 33 | MGSQAAAVTTAPQEPPARPLQAGSGAGPAPGRA |
| 2 | 1 | ATG | GCCATGC | MidR | 0 | |

Figure 3.2 The Microsoft Excel macro (Edwards, unpublished) identified a GUG alternative initiation codon -99 nucleotides upstream of the +1 AUG within the 5' UTR of Traak Transcript ENST00000422670.

3.2.1 Traak was cloned from human brain cDNA into a C-terminal FLAG-fusion expression vector

Traak was amplified from human brain cDNA using forward and reverse primers containing respective NheI and XhoI restriction sites for cloning into pcDNA3.1 3 X FLAG before sequencing and transfection to test expression of the vector. Traak alternative initiation codon constructs were engineered by PCR with mutagenic forward cloning primers. Amplification was targeted to start at each of the identified putative alternative translation initiation start sites, +1, -78, -99 as well as the full length 5' UTR end. Sequences were engineered to begin with an AUG in a strong kozak context; g at -3 and g at +4; g/AUG/g (Fig. 3.4 A). Constructs were cloned into pcDNA3.1 3 X FLAG (Fig. 3.3). The pcDNA3.1 3 X FLAG plasmid was created by Coldwell *et al.*, (2012) and was first used to find a novel CUG alternative translation initiation start site in eIF4GII. A short region of the 5' Traak ORF was cloned into pcDNA3.1 3 X FLAG to allow easy separation of proteins by SDS PAGE. It is easier to separate small differences in small peptides, than the same magnitude differences between larger peptides. The ratio of difference in mass is maximised by using only an N-terminal section of the ORF of Traak. The Traak-FLAG constructs were designed to greatly enhance translation of FLAG-tagged peptides from sites of alternate translation initiation codons to produce peptides of MW corresponding to predicted MWs of putative alternative translation initiation codon products found in the western blot of the wild-type Traak-FLAG transfected cell lysate.

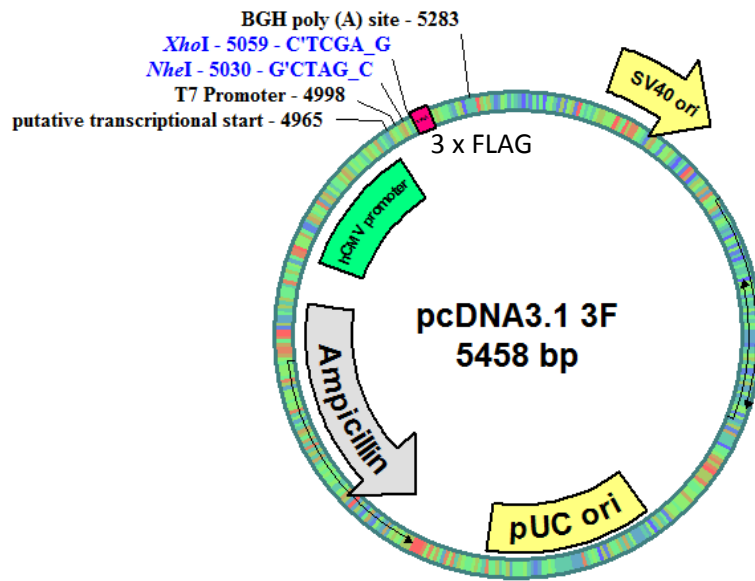


Figure 3.3 Diagram of pcDNA3.1 3F plasmid used as destination vector for cloning candidate genes with an hCMV promoter and 3 x FLAG c-terminal tag. Image constructed with pDRAW.

3.2.2 Investigation of the use of upstream alternative initiation codons in translation of Traak

Transfected HeLa cells were lysed after 48 hr with MemPER to generate membrane-enriched lysate. This method was chosen to increase the yield of membrane proteins for SDS-PAGE analysis, and also indicate intracellular location of proteins; whether Traak-FLAG products were membrane-localised. To improve the running of lysates by SDS-PAGE, the membrane fractions were cleaned with Strataclean resin prior to separation by SDS PAGE and western blot with FLAG antibody and imaging with Licor. The WT-Traak-FLAG transfection lysate showed identical bands to that of +1 g/AUG/g-Traak-FLAG, which is lacking the 5' UTR completely (Fig. 3.4 B). There is only one band produced from expression from of +1 g/AUG/g-Traak-FLAG of 13.3 kDa. The larger MW bands seen from translation from -99 g/AUG/g (16 kDa) or -78 g/AUG/g (15.5 kDa) were not present in the lane WT-Traak-FLAG lane, suggesting translation does not occur from predicted sites of alternative translation initiation, GUG at -78 and GUG at -99.

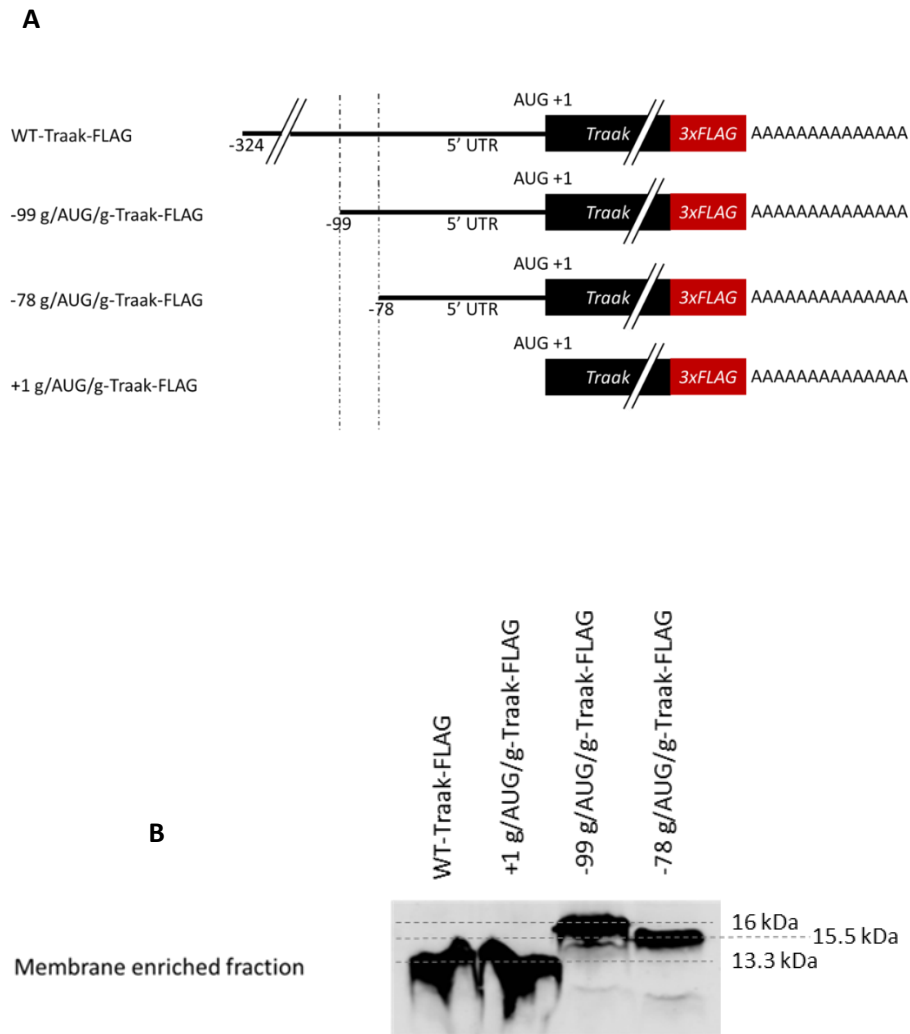


Figure 3.4 A) Traak expression inserts for ligation into pcDNA backbone and transfection in HeLa cells. In mutants, sequence upstream of the alternative initiation codon was deleted and the alternative initiation codon was mutated to *g/AUG/g* to force translation initiation from this site. **B)** Western blot of Traak-FLAG expression plasmids in HeLa cells showed products of equal size between the WT-Traak-FLAG lysate and the 5'-terminally truncated mutants with enhanced initiation codons. Initiation of translation at -99 and -78 yielded peptides which were not seen in the WT-Traak-FLAG-transfected lysate. n = 2

3.3 Analysis of putative alternative upstream translation initiation codons in other K_{2P} channel mRNAs

3.3.1 Acid-sensitive Two Pore Potassium Leak Channels, Task 1 and Task 3

Task1 and Task 3 form functional potassium leak channels as homodimers or heterodimers (Fig. 3.5). Task channels are the main target for volatile anaesthetics, causing decreases in neuronal firing rates (Gruss *et al.*, 2004). Task1 and Task3 do not have predicted signal peptide sequences, instead auxiliary proteins regulate targeting of Task proteins to and from the cell membrane. Binding of the N-terminal dibasic ER retention motif by β coat protein (β COP) prevents targeting from the ER and Golgi to the membrane. The cytosolic adapter protein, phosphorylated 14-3-3 β inhibits β COP binding and binds the C terminus of Task proteins, directing forward trafficking towards membrane expression (O'Kelly *et al.*, 2002). Neuronal signalling has been shown to regulate endocytosis of Task channels. PKC activation by Group I mGluRs cause rapid endocytosis of Task1, mediated by 14-3-3 β in rat cerebellar granule neurons (Gabriel *et al.*, 2012). A missense mutation in TASK-3 disables the channel, resulting in Birk Barel mental retardation dysmorphism syndrome (Barel *et al.*, 2008).

The 5' RACE product of Task 3 (Kcnk9) was carried out according to the method described in Materials and Methods, 2.6.2. I conducted 5' RACE on human brain cDNA using a gene specific primer for Task3. Cloning of the amplified product and sequencing revealed an extended 5' UTR with a 5'-terminal 42 nucleotide (GGN) repeat sequence (Fig. 3.7 A & B) compared to the annotated database sequence ENST00000303015. A similar (GGN) repeat 5' terminal sequence is seen in the database sequence for human *task 1* mRNA (Fig. 3.7 C).

The full 5' UTR of Task 3 mRNA was found by 5' RACE of *Task 3* cDNA from human brain. The most abundant product from the nested PCR (Fig. 3.6 A) was excised and gel-purified for cloning into pGEM-T-Easy (Fig. 3.3).

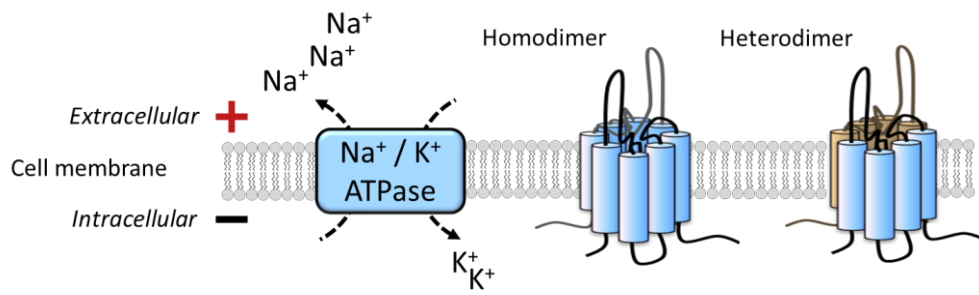


Figure 3.5 Task1 and Task3 proteins form homodimers or heterodimers in the cell membrane. K_{2P} channels set the resting membrane potential of the cell by allowing constitutive leak of potassium from the cell down its chemical gradient.

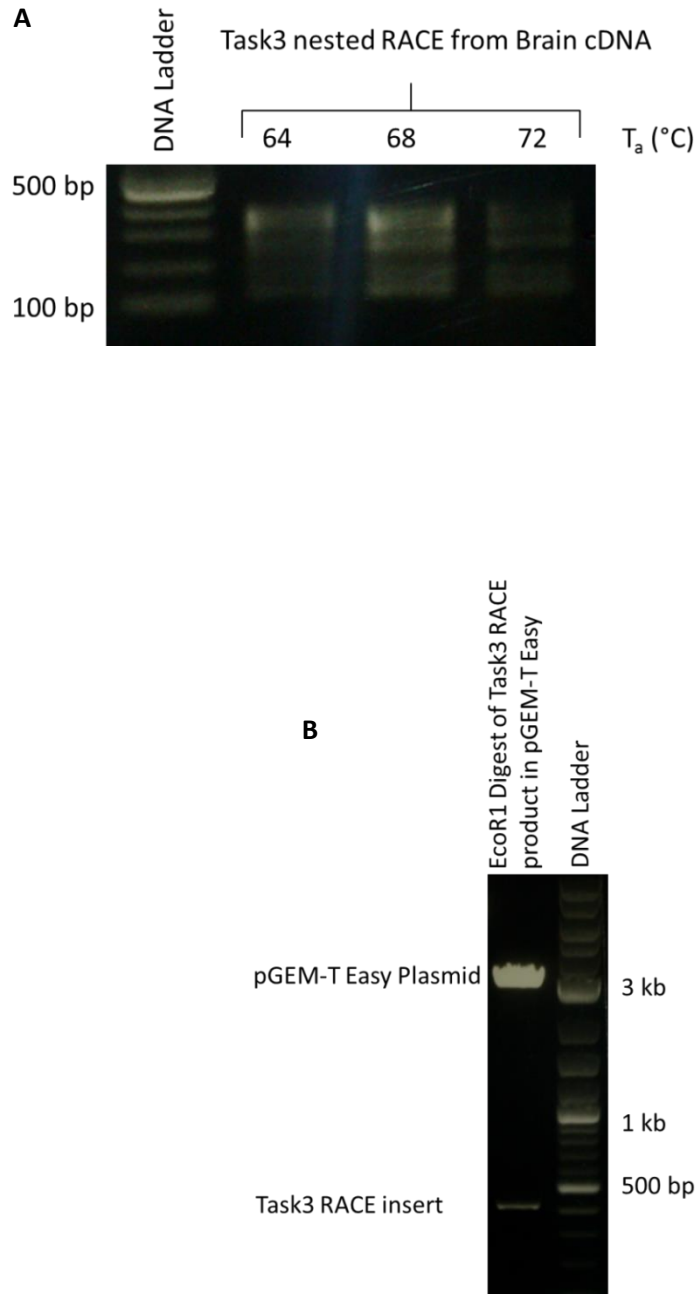


Figure 3.6 A) Task 3 nested RACE products amplified from human brain cDNA and separated by agarose gel electrophoresis. The top (most abundant) band was excised and gel-purified before cloning into pGEM-T Easy. **B)** Clones of Task3 RACE in pGEM-T Easy were screened prior to sequencing by digestion with EcoR1 to check for the correct insert size in transformed DH5 α *E.coli*.

```

5'RACEinBraincDNA5'UTR  GGAGGCGGCGGCGGCGGCGG
EnsemblKCNK95'UTR      -----

5'RACEinBraincDNA5'UTR  CGGAGGAGGAGGCGGCGGCGGCCCGCGCTGcAGTGGGACGCGCGCG
EnsemblKCNK95'UTR      -----

5'RACEinBraincDNA5'UTR  GCTGTGAGCCTGCGGGACATGCCCCCGCGCCGGCTCCTTGCTGGCGGCC
EnsemblKCNK95'UTR      --TGTGAGCCTGCGGGACATGCCCCCGCGCCGGCTCCTTGCTGGCGGCC
*****

5'RACEinBraincDNA5'UTR  ATG
EnsemblKCNK95'UTR      ATG
***

```

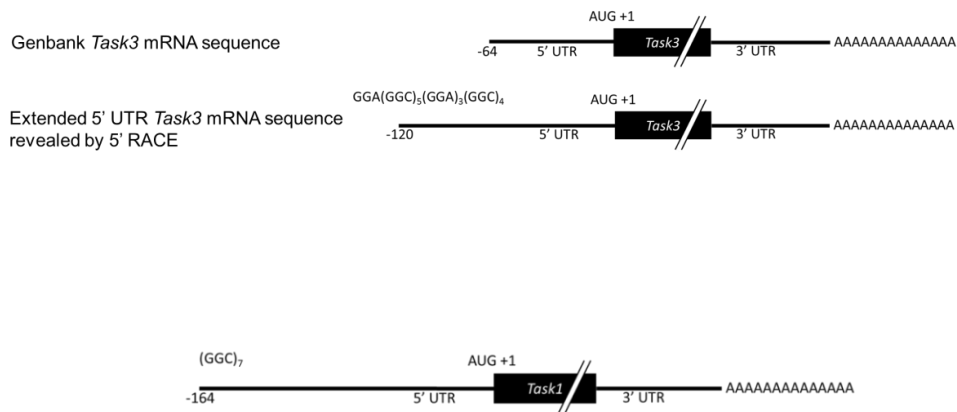


Figure 3.7 A) ClustalW alignment of 5' UTR sequence found by 5' RACE in Brain cDNA against Ensembl Kcnk9 5' UTR ENST00000303015. The annotated AUG and predicted alternative initiation codons are shown as large and bold font. **B)** The 5' RACE product of *task 3* revealed an extended 5' UTR characterised by a 5' terminal 42 nucleotide (GGN) repeat sequence **C)** The Genbank sequence of human *Task 1* mRNA has a 5' terminal (GGN) repeat sequence similar to that seen in the *Task 3* RACE sequence.

3.4.1 Prediction of alternative initiation codons in extended 5' UTR of Task3

Analysis of the extended 5' UTR of Task3 identified a potential in-frame alternative initiation codon upstream of the annotated translation start site. The alternative initiation codon is a CUG at -69 nucleotides from the annotated AUG initiation codon. The existence of a G at -4 of the AIC increases the probability that this codon is used to initiate translation. The presence of a C at +3 of the AIC is not favourable for translation initiation. The strongest context for translation initiation is a G at this +3 position. However, the annotated AUG is in a similar context, with a G at -4 and an A at +3.

3.4.2 Attempts to quantify relative abundance of Task3 extended 5' UTR by qPCR

In order to characterise the relative abundance of the extended 5' UTR task 3 mRNA sequence found by 5' RACE, qPCR was attempted. Primers were designed to the task 3 mRNA from within the extended 5' terminal (GGN) repeats, and to within the coding sequence for the third transmembrane domain. Primers were designed with similar melting temperatures and amplicon length so as to minimise differences in PCR efficiencies (Table 3.3). Test PCR with the qPCR primers in human brain, MCF-7, skeletal muscle and Pooled cDNA (an equimolar mixture of human brain, MCF-7 and skeletal muscle cDNA) showed single bands produced with database qPCR primers, but multiple bands with extended task 3 qPCR primers (Fig. 3.8). The many amplified products from this primer set are likely to include many non-specific products. This disqualifies the use of these primers for qPCR of task-3 transcript abundance. In order to distinguish extended transcripts, with the terminal GGC repeat, the forward primer must be entirely (GGN)_n. The results shown in Figure 3.8 show qPCR cannot be used to accurately quantify the relative abundance of the extended transcript against the database transcript between cDNA of various tissues. Task3 mRNA is highly expressed in cerebellum (RefSeq record), therefore investigations of Task3 mRNA may be improved by analysis of mRNA from cerebellum tissue.

The existence of this extension in endogenous Task3 mRNA could be investigated by high resolution northern blot. This allows detection of down to 10,000 molecules of RNA. However, the sensitivity is still comparatively poor compared to qPCR (Koscianska *et al.*, 2011). There is also the issue that the blotted mRNA may be of a similar size to the sequenced 5' UTR extension, but it may represent a different sequence (such as a splice variant). The use of nuclease protection assays to ascertain the presence of a 5' UTR extension in endogenous Task3 mRNA would be insufficient because it does not inform of transcript size.

| Name | Sequence | Tm (°C) | Amplicon Length |
|---------------|----------------------|---------|-----------------|
| k9 qpcr dat f | CTCTGTCCCTCATCGTCTGC | 65 | 744 |
| k9 qpcr dat r | GCCGCTCATCCTCACTGTTT | 67 | |
| k9 qpcr ext f | GGAGGCGGCGGC | 64 | 780 |
| k9 qpcr ext r | ACGTAGAGCGGCTTCTTCTG | 64 | |

Table 3.1 qPCR primers were designed to the task 3 mRNA from within the extended 5' terminal (GGN) repeats, to within the coding sequence for the third transmembrane domain, k9 qpcr ext f & r. The database mRNA sequence was to be amplified using primers, k9 qpcr dat f & r. Primers were designed with similar melting temperatures and amplicon length so as to minimise differences in PCR

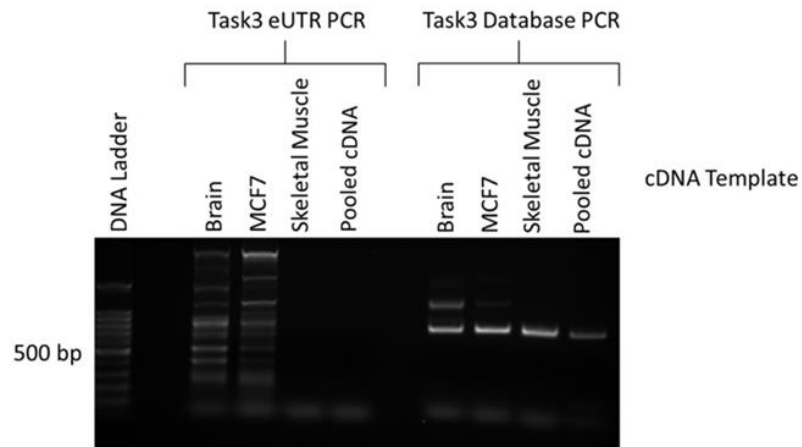
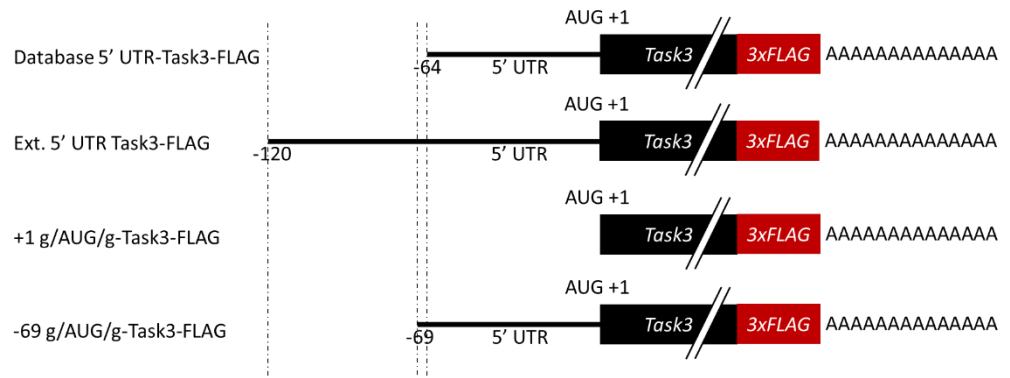


Figure 3.8 Products from test PCR reactions using designed *task 3* qPCR primers. Single products were achieved using task 3 database qPCR primers. The same was not achieved using *task 3* extended UTR qPCR primers.

3.4.3 Attempts to identify the use of alternative initiation codons in Task 3

Task 3 alternative initiation codon constructs were engineered to have an AUG in a strong Kozak context; g at -3 and g at +4; g/AUG/g (Fig. 3.9 A). Constructs were cloned into pcDNA3.1 3 X FLAG (Fig. 3.3) and transfected into HeLa cells. Western blot of Transfected HeLa cells were lysed with Mem-PER and the combined membrane/cytoplasmic fractions were cleaned with Strataclean resin and separated by SDS-PAGE and subjected to western blotting for FLAG-tagged protein expression (Fig. 3.9 B). Expression band patterns were identical between the database sequence and the 5' UTR truncated sequence with g/AUG/g at +1. Expression from the *Task 3* construct with extended 5' UTR sequence yielded undetectable Task3-FLAG expression. Expression from the *Task 3*-FLAG construct with enhanced initiation codon at -69 and deleted 5' sequence showed bands of higher MW than in any other construct. However, the inhibited translation from the eUTR construct prevents analysis of use of the alternative initiation codon, CUG at -69. The CUG at -69 is not in a strong context, there is a G at -3 which would support translation initiation, but a C at +4 which is not favourable to translation initiation. Where expression of Task 3-FLAG is detected, there are two visible bands (Fig. 3.9B). The top band is predicted to be an N-linked glycosylation at N53, a conserved site in both Task 1 and Task 3 (Mant *et al.*, 2013). N-linked glycosylation is critical for Task 1 cell surface expression and a small effect on Task 3 cell surface expression. N-linked glycosylation is thought to increase the stability of K_{2P} proteins.

A)



B)

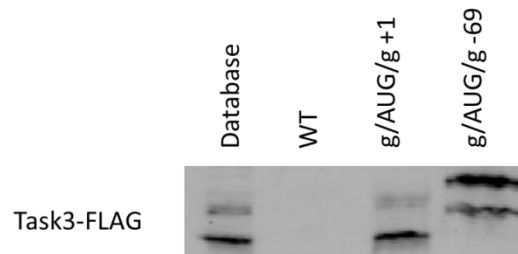


Figure 3.9 A) Expression inserts for ligation into pcDNA backbone and transfection in HeLa cells. In mutants, sequence upstream of the alternative initiation codon were deleted and the alternative initiation codon was mutated to g/AUG/g to force translation initiation from this site. **B)** Western blot of transfected HeLa cell lysates. Expression band patterns were identical between the database sequence and the 5' UTR truncated sequence with g/AUG/g at +1. Expression from the task 3 construct with extended 5' UTR sequence yielded undetectable Task3-FLAG expression. Expression from the task 3-FLAG construct with enhanced initiation codon at -69 and deleted 5' sequence showed bands of higher MW than in any other construct. n = 3. No loading control was used.

3.5 Discussion

Chapter 3 details the investigation of putative eORFs originating from in frame upstream alternative translation initiation. The mRNA of Traak was identified by a bioinformatics workflow designed to identify mRNAs with evolutionarily conserved translated eORF sequences. Characterisation of the codons which may cause translation initiation was carried out using the ExTATIC macro, which identified a GUG alternative upstream initiation codon at -99 from the +1 AUG of the annotated ORF.

Traak was successfully cloned from human brain cDNA into pcDNA3.1 3 X FLAG and sequence verified. Transfection of just this plasmid yields multiple bands by western blot, indicating possible products of alternative translation initiation. The creation of expression plasmids with different 5' UTR sequences allowed the investigation of usage of alternative translation initiation codons. The 5' UTR of Traak-FLAG constructs was truncated to the position of the AIC, and the AIC was mutated to an AUG in a strong context to greatly enhance translation of peptide products predicted to be translated from within the 5' UTR of Traak. Comparison of MW bands suggests alternative translation initiation is not responsible for the multiple bands seen when we transfect Traak-FLAG with a full length, wild-type 5' UTR.

3.5.2 5' RACE revealed a 5' terminal GGN repeat in Task3 mRNA

The 5' UTR of Task3 is short in the database (64 nucleotides in Genbank). 5' RACE was employed to define the true ends of the 5' UTR of Task3 mRNA. The 5' UTR of Task3 was successfully characterised by 5' RACE of human brain cDNA. The ExTATIC macro did not identify alternative initiation codons in strong contexts, however, visual inspection of the 5' UTR did identify an in frame CUG translation initiation codon at -69 from the +1 AUG of the ORF.

The use of the identified alternative translation initiation site at -69 was tested in a similar way to the tests applied to putative translation start sites in the 5' UTR of Traak. The 5' UTR of Task3-FLAG constructs was truncated to the position of the AIC, and the AIC was mutated to an AUG in a strong context to greatly enhance translation of peptide products predicted to be translated from within the 5' UTR of

Task3. Western blot of bands were almost invisible resulting from transfection with Task3-FLAG possessing full length, wild-type 5' UTR. It was not possible to draw conclusions on the origin of peptide masses seen from transfection of the wild-type Task3-FLAG sequence, since the 5' terminal extension found by 5' RACE appears to massively inhibit the synthesis of the Task3-FLAG protein.

3.5.3 Conclusions

1. Results suggest there is no generation of alternative protein isoforms of Traak resulting from the use of identified predicted alternative translation initiation codons within the 5' UTR.
2. The known 5' UTR of Task3 mRNA was extended by 5' RACE and includes a 42 nucleotide terminal GGN repeat.
3. The extended 5' UTR of Task3 inhibits synthesis of the Task3 protein in transfected HeLa cells

Chapter Four

Results

The 5'-terminal (GGN)₁₃ repeat in Task3 mRNA forms a G-quadruplex structure and inhibits translation initiation

4.1 Introduction

Results of 5' RACE (Chapter 3) revealed the mRNA of the K_{2P} channel Task3 is characterised by a 5' UTR terminal (GGN)₁₃ repeat. GGN repeat RNA sequences have been shown to form G-quadruplex structures. Research on the effects of G-quadruplex structures on translation of an mRNA is in its infancy. There is an emerging consensus that G-quadruplex structures can have profound effects on translation of mRNAs. Recent studies have shown G-quadruplex structures to affect translation of mRNA species, whether in the 5' UTR, 3' UTR or its coding region. It was important to investigate the terminal (GGN)₁₃ repeat of Task3 mRNA to ascertain whether the sequence forms a terminal G-quadruplex structure and effects on Task3 protein synthesis.

The profound importance of normal Task3 protein expression on membrane potential highlighted the potential to yield insights into the mechanisms and functions of G-quadruplex mediated translational control in regulating critical cell functions. Investigation of a 5' UTR terminal mRNA G-quadruplex has not been reported to date in the literature. The mechanism of translational control by a 5' terminal G-quadruplex may be different to control exerted by a G-quadruplex elsewhere in the mRNA. A number of RNA-binding proteins have been shown to control translation of an mRNA due to recognition of G-quadruplex structure. DEAH RNA helicase enzymes are responsible for resolving strong RNA secondary structures. Other G-quadruplex recognising RNA-binding proteins have known functions which may be important in the regulation of translation of Task3. This chapter describes the results of experiments to elucidate the function of the 5'-terminal GGN repeat in

Task3 mRNA translation, and molecular mechanisms for modulating G-quadruplex mediated translational control of Task3 protein expression.

4.2 Results

4.2.1 The 5'-terminal (GGN)₁₃ of Task3 mRNA is predicted to form G-quadruplexes

The rules of G-quadruplex formation are not well defined. Current knowledge suggests that larger G-groups and smaller loop sequences are most likely to form stable G-quadruplex structures. The G-group refers to the number of consecutive guanine residues which at each of the four points of the tetrad. The loop length refers to the intervening sequence between G-groups in a tetrad. For instance, a sequence of GGGNNGGGNNGGGNNGGG has a G-group size of 3 and a loop length of 2. For G-quadruplex formation, there are no known lower or upper limits to either the G-group size or the loop length. No empirical data exists for the stability of G-quadruplex structures formed related to their G-group size or the loop length. However, it is generally considered that the G-group must be at least 2 (Kikin, D'Antonio & Bagga, 2006).

We analysed the 5' UTR, including the 5'-terminal (GGN)₁₃ of Task3 mRNA for G-Quadruplex forming sequences using QGRS Mapper, a web-based server for predicting G-quadruplexes in nucleotide sequences (<http://bioinformatics.ramapo.edu/QGRS/index.php>, (Kikin, D'Antonio & Bagga, 2006). The program identifies repeat sequences of 4 or more $\geq G_2$ in nucleotide sequences, with a maximum loop length of 30. QGRS Mapper uses algorithms to generate a G-score based on the loop length and G-group size. Larger G-group sizes and smaller loop lengths produce higher G-scores. The generated G-scores do not represent any real measure of thermodynamic stability of the G-quadruplex but is useful as a rough measurement of the probability of forming stable or less stable G-quadruplexes. The maximum G-score is 105.

Analysis of the 5' UTR, including the 5'-terminal (GGN)₁₃ of Task3 mRNA with QGRS Mapper identified 3 QGRS at the 5' terminus of the 5' UTR (Fig. 4.1). These 3 sequences may stack upon each other to form a much more stable G-quadruplex than each individual G₂-based quadruplex in isolation. G-quadruplexes within the 5' UTR of mRNAs have been shown to affect translation of the protein. The G-quadruplex structures predicted at the 5'-terminus of Task3 mRNA are predicted to inhibit translation of Task3, resulting in depressed expression of the Task3 protein.

4.2.2 Creation of expression vectors to examine properties of the 5' UTR

To test the effect of the (GGN)₁₃ terminal repeat on translation rates of Task3, plasmids were constructed expressing Task3-FLAG with test 5' UTRS. To measure the effect of the (GGN)₁₃ repeat on translation of Task3, it was necessary to create Task3 expression vectors with mutated G-quadruplex sequences for comparison. Task3 with its full wild-type 5' UTR, containing the (GGN)₁₃ repeat, was cloned from the sequenced pGEM-T Easy Task3 plasmid into pcDNA 3.1 3F using a forward mutagenic primer with a 5' terminal NheI restriction site and a reverse primer with a 3' terminal Sall restriction site (Fig. 4.2). Mutagenic primers with 5' terminal NheI restriction sites, were used to generate Task3 sequences with 5' UTRs that differed in the G-quadruplex containing region (nucleotide positions 1-55); a complementary sequence of the G-quadruplex-forming sequence, the 5' UTR with the G-quadruplex sequence deleted, and a positive control mRNA with the G-quadruplex sequence from the NRAS 5' UTR. The plasmid with the GGN repeat sequence deleted was generated to reveal the effect of the G-quadruplex sequence on translation of Task3-FLAG. The length of the 5' UTR is known to affect translation rates of an mRNA (Gray & Hentze, 1994), so I created a Task3-FLAG expression plasmid with a 5' UTR of similar characteristics to the wild-type 5' UTR, but with the GGN repeat sequence mutated to its complementary sequence. The complementary sequence is not predicted to form significant secondary structure, but is of identical length and similar GC content. A Task3-FLAG mRNA with this complementary G-quadruplex sequence was not expected to be under translational inhibition predicted by the wild-type GGN repeat sequence. The NRAS 5' UTR G-quadruplex has been shown to inhibit translation of NRAS (Kumari *et al.*, 2007). We hypothesised that the 5' terminal GGN repeat sequence of Task3 mRNA would have a similar inhibitory effect on mRNA translation as that described for the quadruplex in NRAS mRNA.

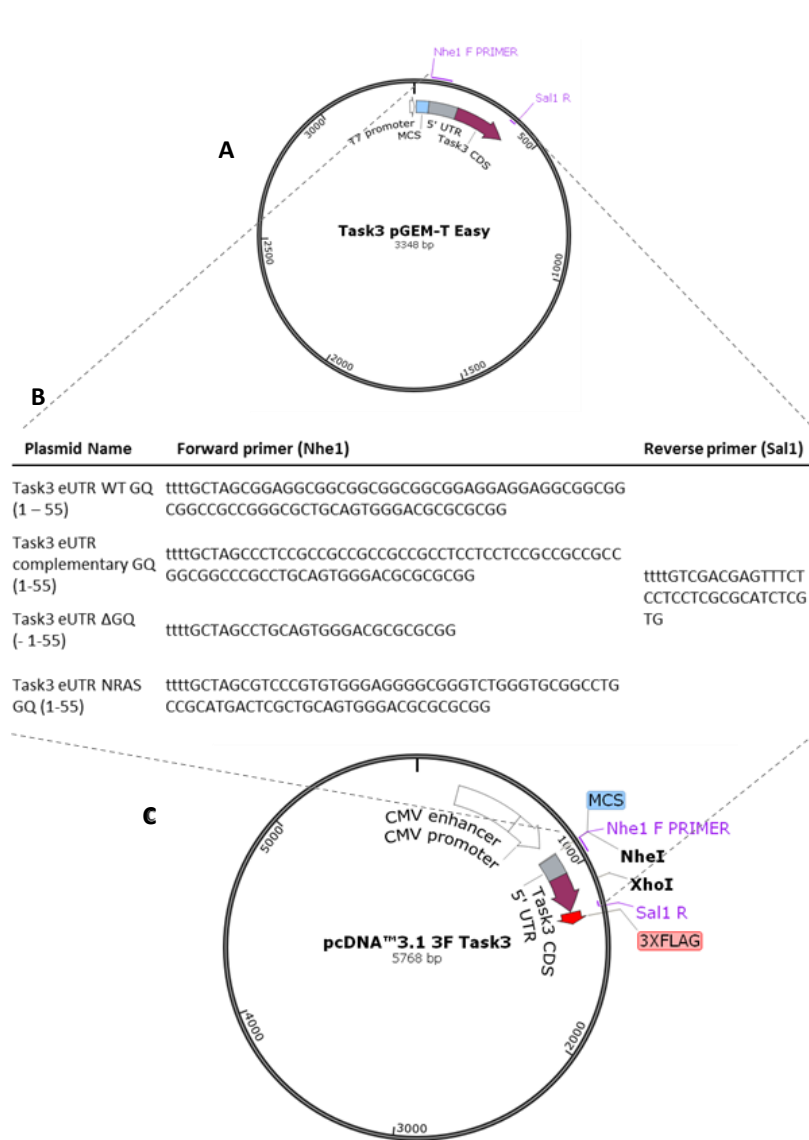


Figure 4.2 FLAG-tagged expression vectors were created for Task3 with mutated 5' UTRS to test G-quadruplex effect on translation of Task3 in transfected cells. The wild-type 5' UTR G-quadruplex region, a complementary sequence of the G-quadruplex-forming sequence, the 5' UTR with the G-quadruplex sequence deleted, and a positive control mRNA with the G-quadruplex sequence from the NRAS 5' UTR

A) The pGEM-T Easy Task3 eUTR plasmid was used as a template for PCR of test Task3 sequences **B)** using forward mutagenic primers with a 5' terminal Nhe1 restriction site and a common reverse primer with a 3' terminal Sal1 restriction site for cloning into **C)** pcDNA3.1 3F.

4.2.3 Task3 translation is inhibited due to the 5'-terminal GGN repeat

We tested whether Task3 expression is under the same G-quadruplex dependent regulation of translation as other proteins with 5' UTR G-quadruplexes, such as *Fmr1*. C-terminally FLAG-tagged *Task 3* expression plasmids with mutated 5' terminal sequences (Fig. 4.3A) were transfected into HeLa cells. HeLa cells were transfected, and after 48 hrs PBS-washed cells were split for RNA and protein expression analysis. RNA was purified with ReliaPrep™ RNA Cell Miniprep System (Promega) and cDNA was generated using Maxima H Minus Reverse Transcriptase (Thermo Scientific) using Oligo(dT) primers. Proteins were harvested using RIPA buffer and expression of the FLAG-tagged Task3 peptide product in HeLa cells was compared with the wild-type G-quadruplex sequence by western blot (Fig. 4.3B). Relative quantification of *Task 3-FLAG* against β -actin mRNA expression was compared by qPCR. The expression of FLAG-tagged Task3 protein was determined by western blot of transfected cell lysate. Primers were designed against the FLAG cDNA sequence for qPCR analysis in order to ascertain whether changes in abundance of FLAG-tagged Task3 protein by western blot were due to changes in the translation of mRNA or changes in the abundance of Task3-FLAG mRNA (Fig 4.3C). No alternative translation initiation products were seen from any of the tested constructs. This was the case for all tested expression constructs of Task3-FLAG with test 5' UTRs, including the complementary 5' UTR (data not shown).

The western blot allows interrogation and identification of the size of protein products resulting from alternative translation initiation sites within an mRNA. However, the ability to accurately and precisely measure the abundance of a protein product is not optimal. An alternative to measurement of protein expression would have been to use an enzymatic reporter of gene expression, such as luciferase. This sort of approach would have allowed greater resolution of the changes in protein abundance. However, the use of FLAG-tagged expression vectors has been optimised in our lab and is further compatible with fluorescence microscopy techniques. The use of Western blot was chosen because it allowed consistency of the plasmids used between experimental techniques, so results can be directly compared between techniques.

Mutated 5' terminal sequences did not affect transcription of *Task 3-FLAG* mRNA. Translation of Task 3-FLAG was greatly inhibited by the presence of the wild type extended 5' terminal sequence and the mutated 5' terminal sequence possessing the G-quadruplex from NRAS 5' UTR (previously shown to inhibit translation (Kumari *et al.*, 2007). Translational repression was relieved by the mutation of the 5' terminal sequence to a complementary sequence, predicted to not form G-quadruplex structures, or with the deletion of the (GGN)₁₃ repeat. This indicated that it is the GGN repeat sequence is responsible for translational repression of Task3, and is not simply inhibition due to a long GC-rich 5' UTR. These results suggest a G-quadruplex structure inhibits the translation of Task3 mRNA. To investigate this further requires biophysical measurements of RNA structure.

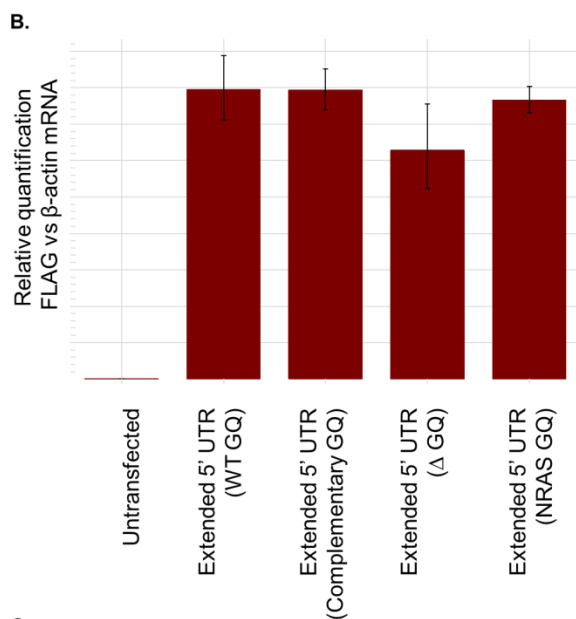
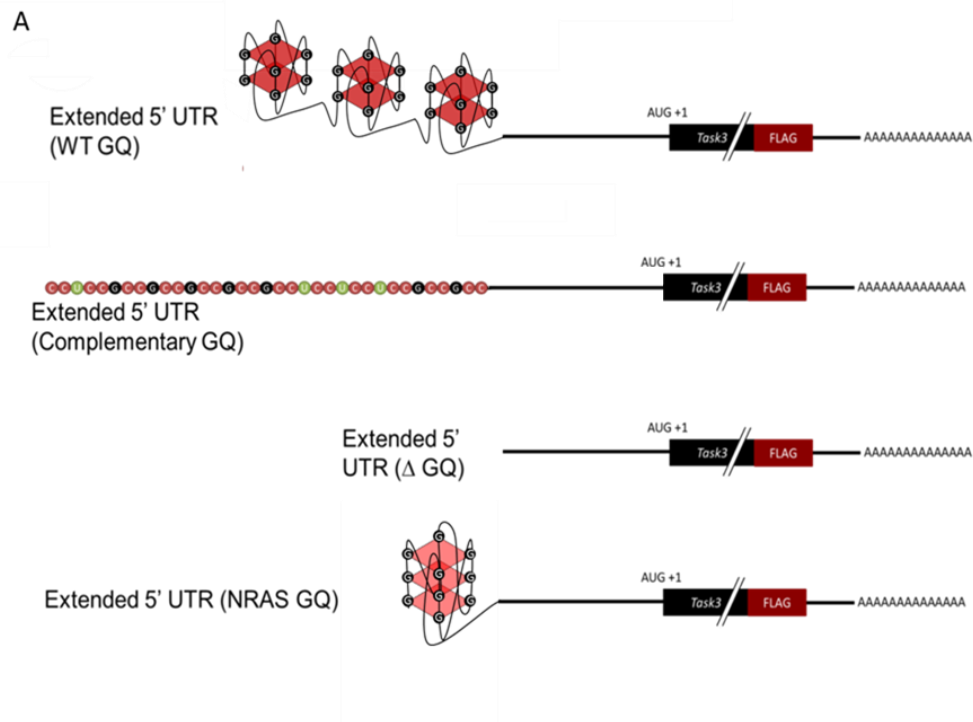


Figure 4.3 The 5' terminal (GGN) repeat sequence forms a quadruplex which inhibits translation of *Task3-FLAG* mRNA. **A)** Mutations were made to analyse the effect of G-quadruplex formation on translation. **B)** Relative quantification of *Task3-FLAG* and β -actin mRNA by qPCR showed no significant effect of mutation of the (GGN)₁₃ terminal repeat. **C)** Translation of Task 3 mRNA to Task 3-FLAG was greatly inhibited by the wild-type (GGN)₁₃ repeat, similar to translation inhibition due to the NRAS G-quadruplex-forming sequence mutant. For clarity, the figure shows only the region of the blot corresponding to the predicted MW of Actin and the unglycosylated Task3-FLAG polypeptide. n=3 technical replicates.

4.2.4 Construction of a Task3-FLAG plasmid with functioning T7 promoter

With the aim of conducting physical studies of the (GGN)₁₃ repeat sequence of Task3 mRNA, predicted to form a G-quadruplex, mRNA was generated by in vitro transcription which required the restoration of a functional T7 promoter sequence present in the original pcDNA3.1 plasmid. The T7 promoter sequence of pcDNA 3.1 3F had been previously deleted as part of optimisation mutagenesis of the original pcDNA 3.1 3F plasmid for other studies in the lab.

A functional T7 promoter sequence was cloned into pcDNA 3.1 3F -Task3 in place of the corresponding sequence excised with SacI and NheI restriction enzymes (Fig. 4.4). A SacI forward primer and a NheI reverse primer were used to copy a functional T7 promoter sequence from the original pcDNA3.1 plasmid for ligation into the newly created pcDNA 3.1 3F -Task3 plasmids lacking functional T7 promoter sequences. The plasmids were sequence verified to confirm the insertion of the T7 promoter site. These new T7 competent plasmids enabled in vitro transcription of the (GGN)₁₃ and mutant Task3 5' terminal sequences for physical studies of secondary structure.

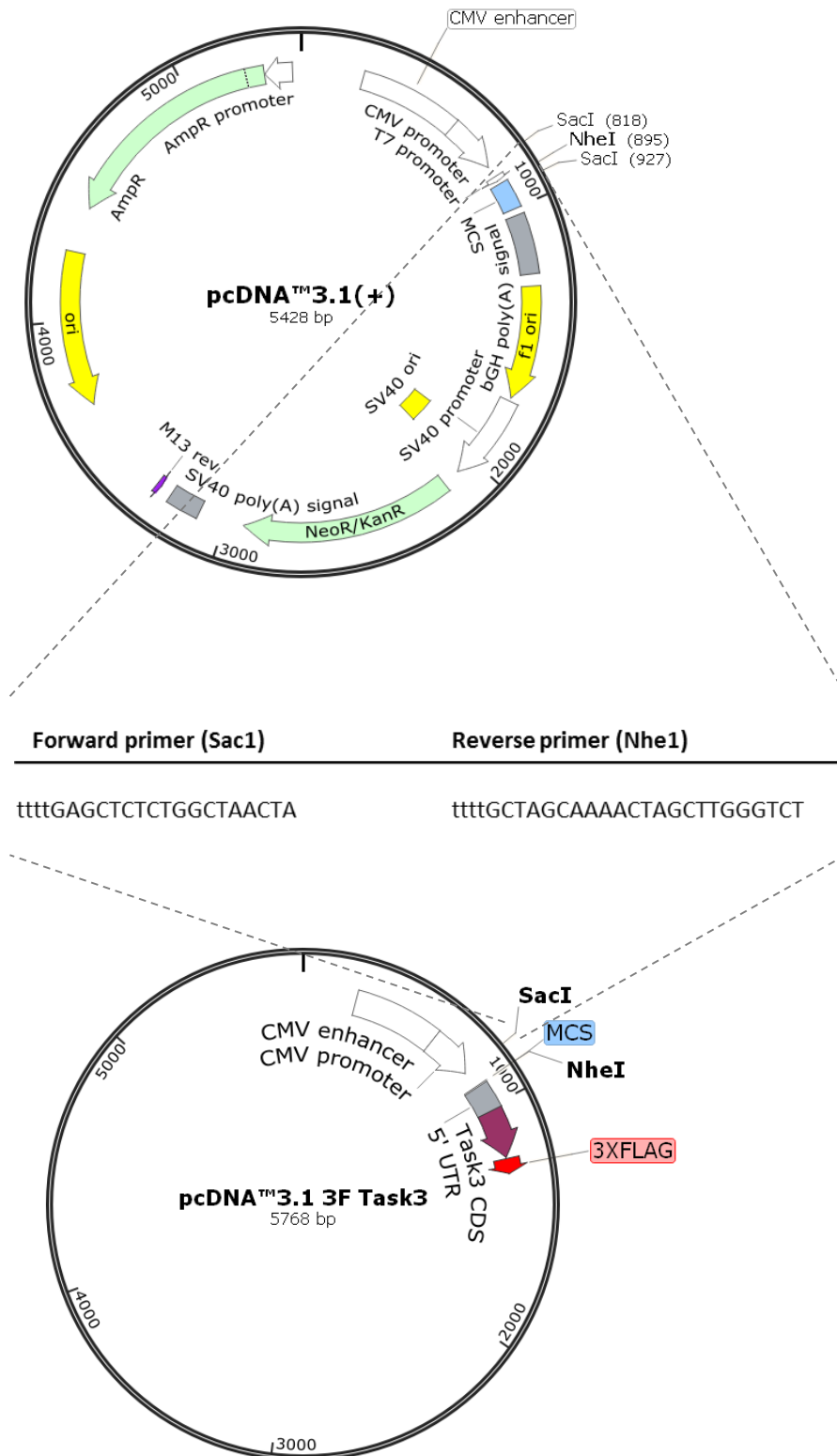


Figure 4.4 A functional T7 promoter sequence was cloned into pcDNA 3.1 3F Task3. A SacI forward primer and a NheI reverse primer were used to copy T7 from the original pcDNA3.1 plasmid for ligation into the newly created pcDNA 3.1 3F Task3 plasmids without functional T7 promoter sequences.

Purified mRNA of the putative G-quadruplex forming region of Task3, as well as the control/mutated forms were generated to enable testing of G-quadruplex structure formation *in vitro*. RNA was synthesised by T7 polymerase *in vitro* transcription from linearized pcDNA3.1 3F Task3 (Fig 4.5) of the wild-type 5' UTR G-quadruplex region, the complementary sequence of the G-quadruplex-forming sequence, a shorter segment of the 5' UTR with the G-quadruplex sequence deleted, and a positive control mRNA with the G-quadruplex sequence from the NRAS 5' UTR. Synthesised RNA was cleaned up using Promega ReliaPrep™ RNA Cell Miniprep for NMM studies and NucleoSpin® miRNA, which gave higher yields of these short RNAs for CD studies.

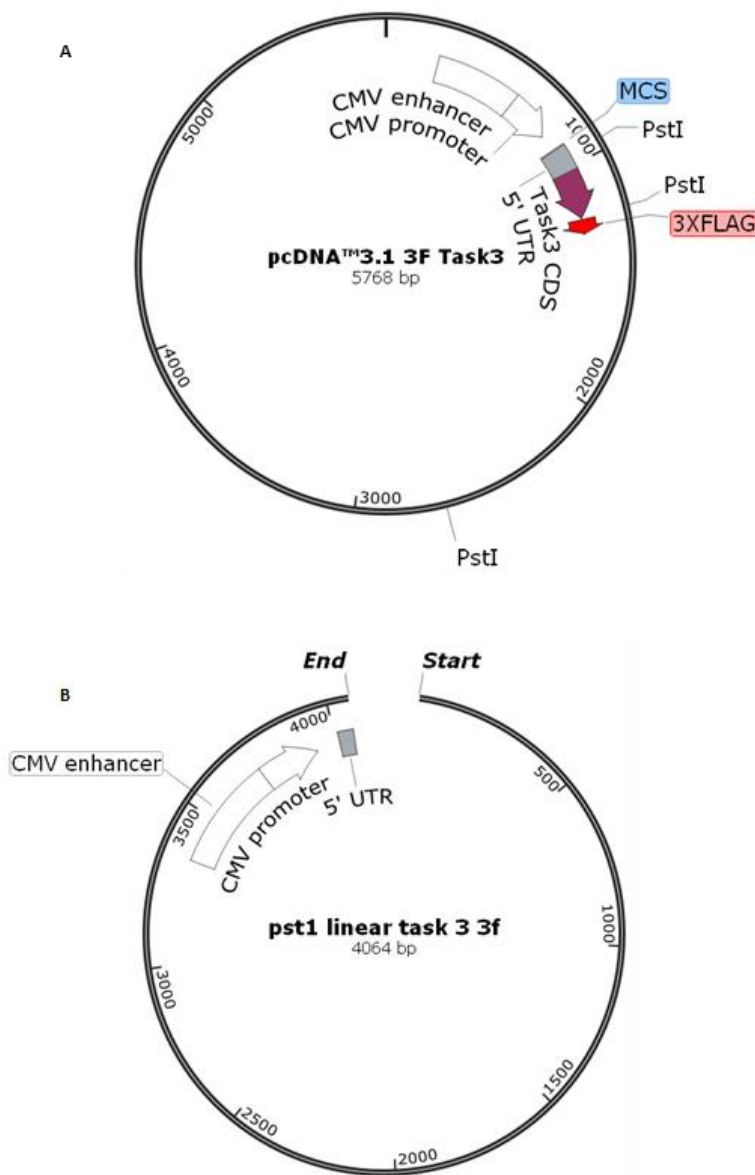


Figure 4.5 Linearized templates for in vitro transcription of 5' UTR terminal sequences were generated by digestion of **A)** pcDNA3.1 3F Task3 plasmids with PstI. **B)** Purified DNA template was used as the template for synthesis of RNA of the wild-type 5' UTR G-quadruplex region, a complementary sequence of the G-quadruplex-forming sequence, the 5' UTR with the G-quadruplex sequence deleted, and a positive control mRNA with the G-quadruplex sequence from the NRAS 5' UTR.

4.2.5 Fluorescence increase of NMM with (GGN)₁₃ RNA indicated G-quadruplex structure

Biophysical techniques allowed the measurement of G-quadruplex folding by (GGN)₁₃ RNA. The cationic porphyrin, Mesoporphyrin IX dihydrochloride (NMM) increases fluorescence when bound to G-quadruplex nucleotide structures (Arthanari *et al.*, 1998) (Fig.4.6).

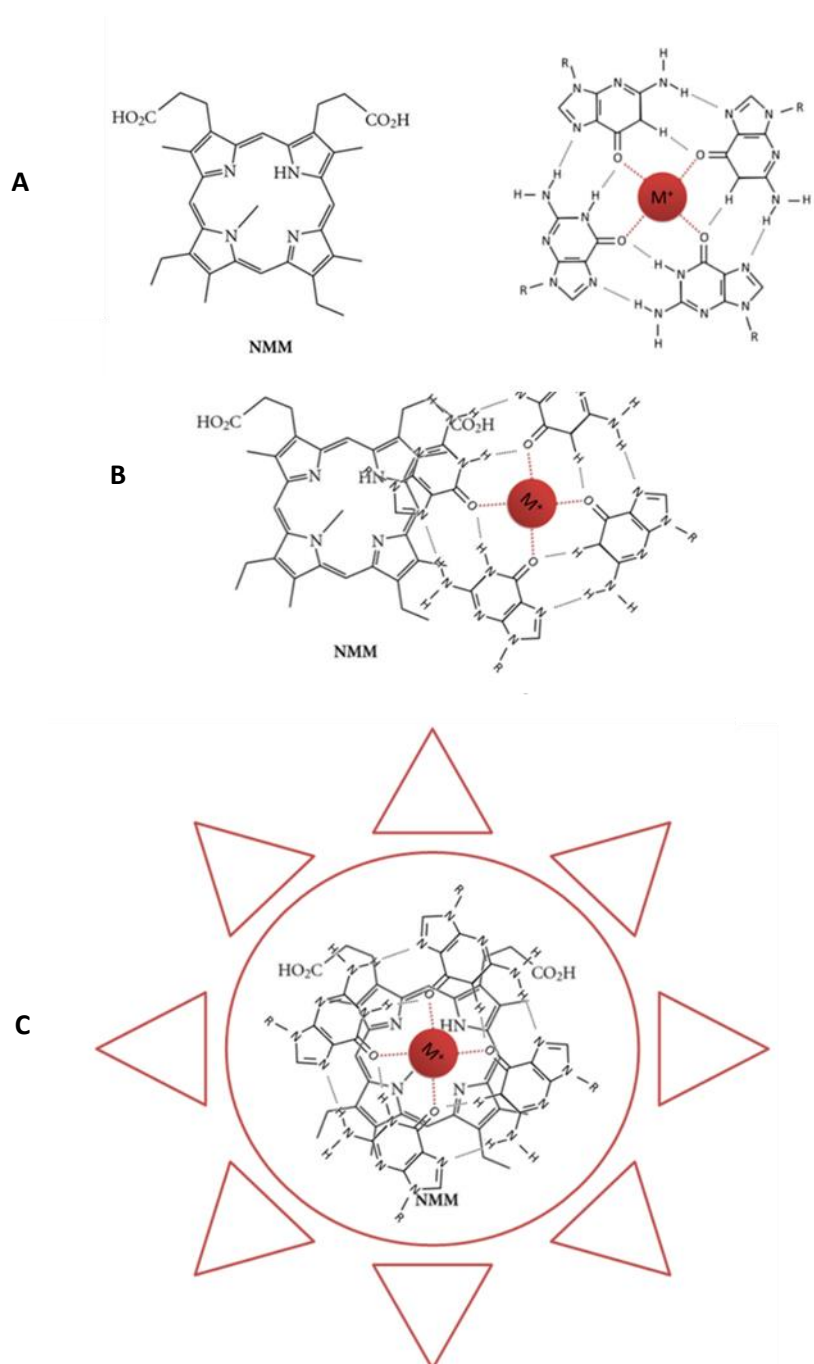


Figure 4.6 NMM increases in fluorescence on binding guanine tetrads of G-quadruplexes. **A)** NMM is a porphyrin which when incubated with G-quadruplex nucleotide structures **B)** binds and **C)** results in increased fluorescence.

Changes in fluorescence of NMM incubated with test RNA was measured using the Horiba Jobin Yvon FluoroMax-4 Bench-top Spectrofluorometer. Spectra were taken with an excitation wavelength of 399 nm, peak emission wavelength was seen at 614 nm. Significant increases in fluorescence intensity of NMM when mixed with WT GQ (GGN)₁₃ RNA, similar to increases when mixed with the positive control G-quadruplex RNA sequence (from NRAS) indicated a G-quadruplex structure. Fluorescence of NMM was further increased in the presence of (GGN)₁₃ RNA by potassium ions added at 150mM KCl (Fig. 4.7), within the physiological normal range. There is a much smaller increase in fluorescence of NMM in the presence of the complimentary G-quadruplex sequence of Task-3 mRNA; (CCN)₁₃. Confirmation that the 5' terminal (GGN)₁₃ sequence of Task3 mRNA forms a G-quadruplex structure was demonstrated by the increased fluorescence of NMM in the presence of RNA from the 5' terminal of Task3 mRNA, (GGN)₁₃, relative to the complementary sequence, negative control RNA, (CCN)₁₃.

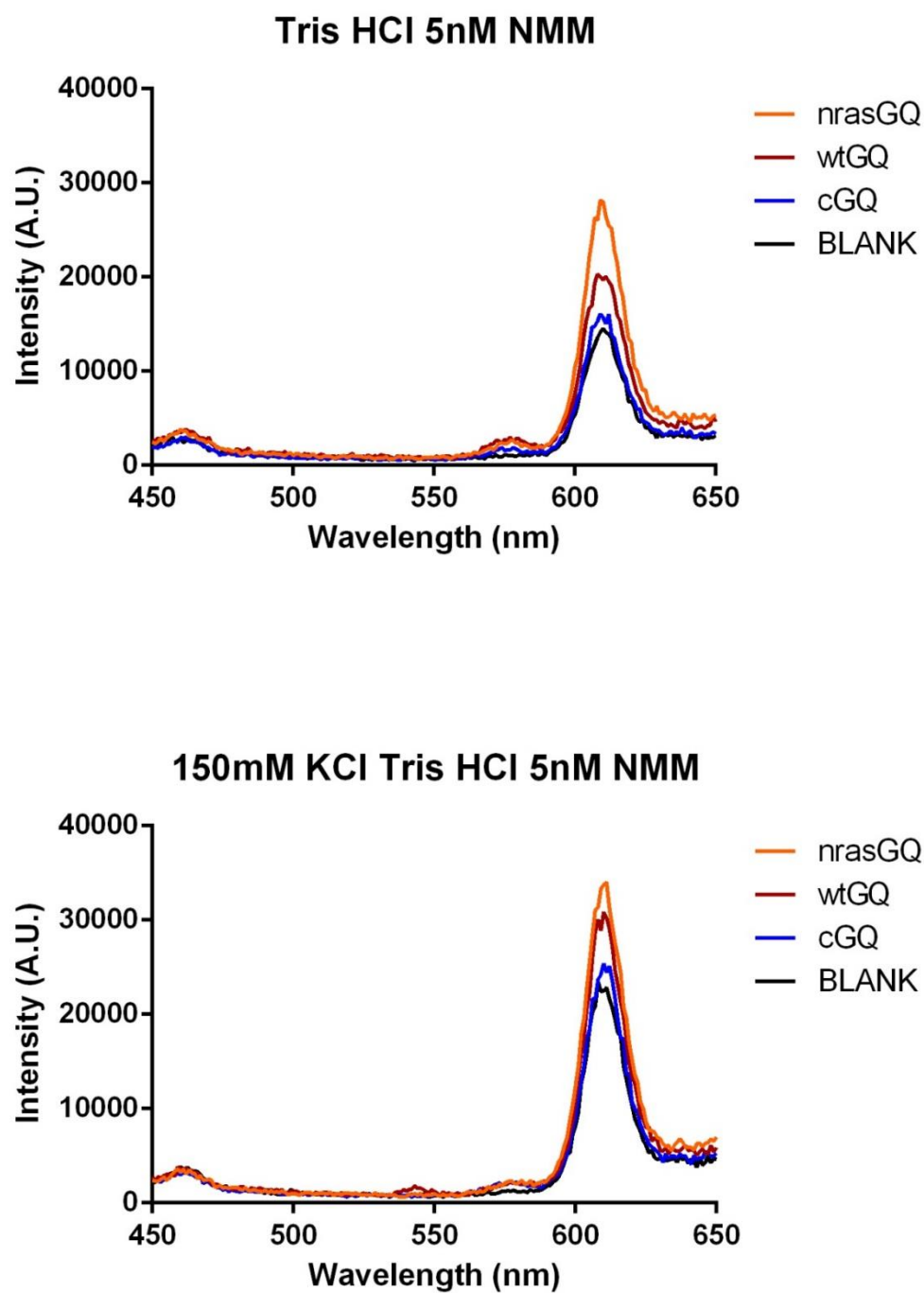


Figure 4.7 Mesoporphyrin IX dihydrochloride increases fluorescence when bound to G-quadruplex nucleotide structures. Fluorescence was measured using the Horiba Jobin Yvon FluoroMax-4 Bench-top Spectrofluorometer spectra were taken with an excitation wavelength of 399 nm, peak emission wavelength was seen at 614 nm. n = 3 technical replicates.

4.2.6 Circular Dichroism (CD) studies confirmed G-quadruplex structure of (GGN)₁₃ RNA

Circular dichroism (CD) is the measurement of differential absorbance of left and right handed circularly polarised light by optically active (chiral) molecules. DNA and RNA secondary structures are chiral molecules and CD has been used extensively to identify the formation of secondary structures in DNA and RNA sequences. The parallel G-quadruplexes of RNA yield distinct CD spectra with a positive difference in absorbance (ΔA) peak at 262 nm and a negative peak at 237 nm (Kumari *et al.*, 2007). CD was used to support the findings by NMM fluorescence change. The resolution (signal to noise) offered by the Jasco J710 CD spectrometer was insufficient below 245 nm to observe negative peaks at 237 nm, but gave good signal to noise above 245 nm, allowing measurement of changes in peak intensity at 262 nm. All measurements were recorded at room temperature using folded RNA samples (4 μ M). Spectra were recorded using a Jasco J-710 spectrophotometer with a 1mm cuvette at a scan speed of 50 nm.min⁻¹ with a response time of 1 s. The spectra were averaged over three scans and the spectrum from a blank sample containing only buffer was subtracted from the averaged data.

Task1 mRNA has a similar 5' GGN repeat to Task3. To test the formation of a G-quadruplex in the Task1 5' UTR, mRNA was synthesised from a linearized T7 Task1-FLAG plasmid. For Task 3 studies, the WT GQ (GGN)₁₃ and control NRAS, and complementary G-quadruplex RNAs were folded in the presence of 100 mM KCl, 10 mM Tris-HCl and 0.1 mM EDTA (pH 7.5) by heating for 5 min at 95°C followed by cooling to room temperature in an insulated polystyrene box on the bench overnight.

Higher CD G-quadruplex signal peak at 263 nm were observed in spectra of WT GQ (GGN)₁₃ RNA compared to complimentary negative control RNA, (CCN)₁₃ sequence. Positive G-quadruplex control NRAS RNA showed a G-quadruplex signal peak at 263nm of similar magnitude to WT GQ (GGN)₁₃ RNA. Task1 5' UTR RNA also showed a G-quadruplex signal peak at 263nm.

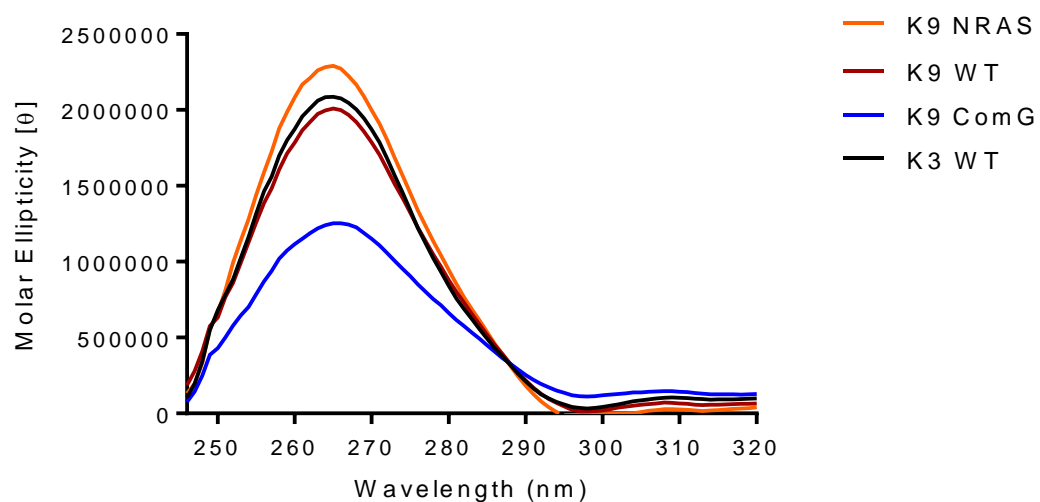


Figure 4.8 Jasco J710 CD spectrometer was used for the measurement of changes in peak intensity at 262 nm, indicative of parallel G-quadruplex structures. Large peak differences in absorbance at 262 nm were seen for WT GQ (GGN)₁₃, control (NRAS GQ) RNA, and Task1 5' UTR RNA. A much smaller peak was measured for the complementary sequence (CCN)₁₃. n = 3 technical replicates

4.2.7 Investigating potassium dependence on *in vitro* translation of Task3 mRNA

Potassium concentration promotes G-quadruplex formation and stability, as observed in Fig. 4.7. I tested the effect of KCl concentration on the translation of 5' terminal mutant task 3-FLAG mRNA. mRNA was *in vitro* transcribed using T7 mMessage Machine Ultra from linearized T7 Task3 pcDNA 3.1 3F plasmids. mRNA was then subjected to *in vitro* translation using Flexi Rabbit Reticulocyte, allowing control over KCl concentration. Translation of task 3-FLAG mRNA was greatly affected by KCl concentration, but independent of 5' terminal (GGN) repeat mutation (Fig. 4.9). These experiments need to be confirmed by repeats with independently prepared RNA transcripts. The results seen here may reflect artefacts associated with RNA synthesis and purification of each transcript. The approach used here may be modified to avoid the lack of clarity observed in the western blotting of protein products of the *in vitro* translation reaction. Measurement of total protein synthesis from a Rabbit Reticulocyte *in vitro* translation reaction can be achieved by ³⁵S-methionine incorporation assay of TCA precipitated protein. The total translation rate seen in the Flexi Rabbit Reticulocyte system should represent the efficiency of translation of the tested mRNAs, as endogenous mRNAs are reduced in the system due to treatment with micrococcal nuclease to destroy endogenous mRNAs. This experiment was not deemed necessary, as the effect on translation of KCl concentration is evidenced in this experiment, and in literature (Weber, Hickey & Baglioni, 1978).

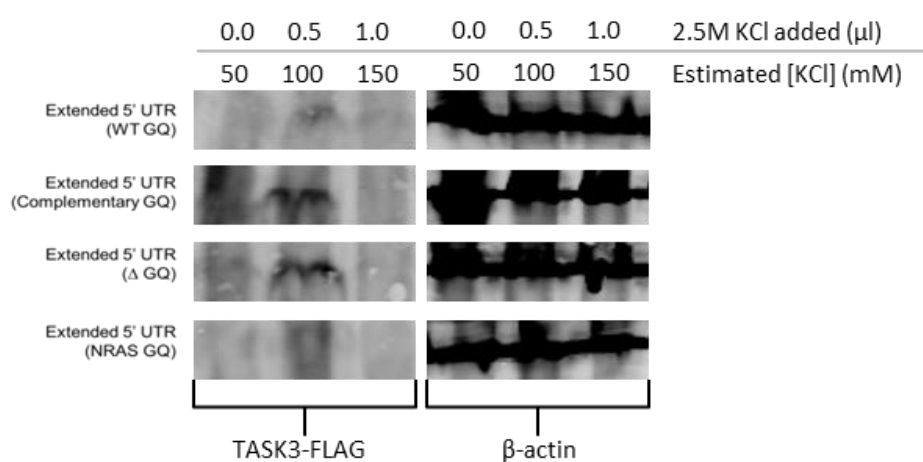


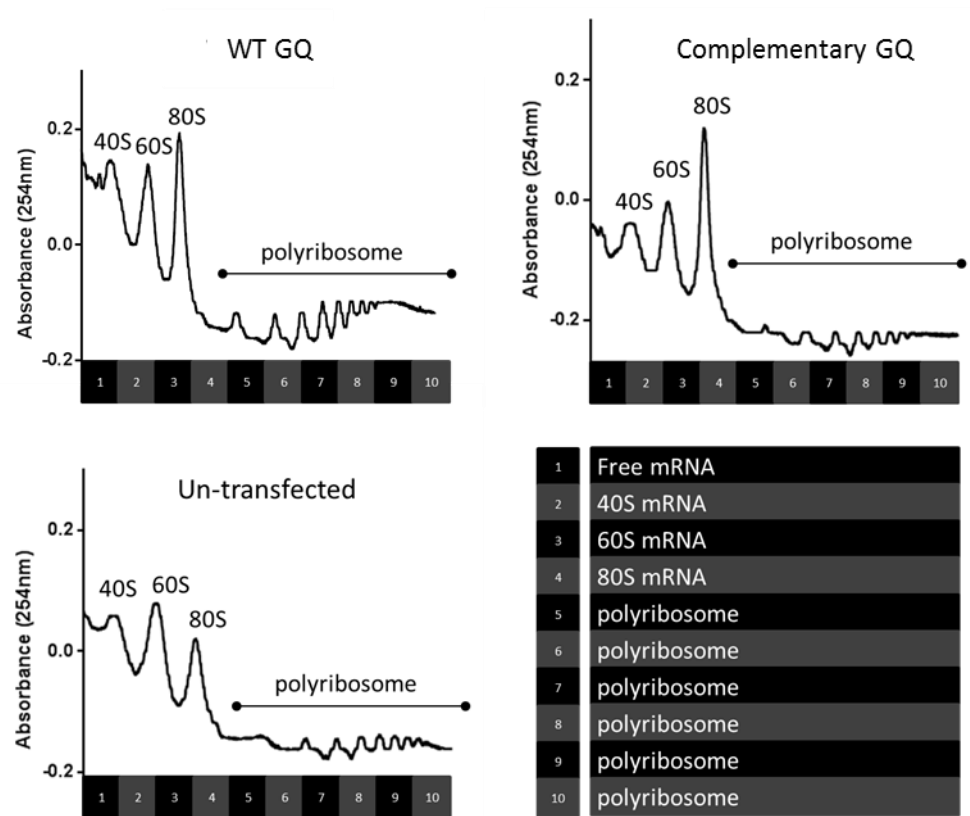
Figure 4.9 Task3-FLAG mRNA was expressed in a 25 μ l Flexi[®] Rabbit Reticulocyte Lysate System with varied KCl concentration. The concentration of KCl affected translation of task 3-FLAG by *in vitro* translation independent of 5' terminal (GGN)₁₃ repeat mutation. TASK3-FLAG expression was compared against endogenous rabbit β -actin protein, which has the same amino acid sequence as human β -actin so was detected by our standard human β -actin antibody.

4.2.9 RT-PCR of FLAG mRNA relative to β -actin mRNA in polysome fractions of transfected HeLa cells suggests an inhibition of translation initiation due to 5'-terminal G-quadruplex

Polysome profiling allows the fractionation of RNA in cell lysates relative to their density. mRNA is separated by centrifugation in a sucrose gradient. The concentration of RNA is mapped along the sucrose gradient by pumping the sucrose gradient through a spectrophotometer and measurement of UV-absorption at 254 nm. It is possible to collect fractions from the polysome gradients, containing mRNA in various stages of translation, from free mRNA to polyribosome mRNA. This principle was used to analyse the stage of translation which is inhibited by the presence of the 5'-terminal G-quadruplex in Task3 mRNA. HeLa cells were transfected 24 hours prior to lysis with WT GQ eUTR-Task3-FLAG or complimentary GQ eUTR-Task3-FLAG. Polysome fractions were collected and RNA isolated for qPCR analysis of the location of Task3-FLAG mRNA in the translation pathway, with and without 5'-terminal G-quadruplex, relative to β -actin mRNA.

Polysome profiles of lysates from HeLa cells transfected with Task3-FLAG constructs or un-transfected showed similar/normal polysome profiles (Fig. 4.10 A). The results are preliminary and have not been repeated. The majority of RNA measured was free RNA, then also of high abundance were discrete peaks representing 40S, 60S and 80S-bound mRNA. Poly-ribosome peaks are very small in comparison and indicate most mRNAs are not in 'active translation'. For this reason, large differences in the concentration of Task3-FLAG relative to β -actin mRNA within the first 4 fractions I have considered as significant. Results of the qPCR of Task3-FLAG relative to β -actin mRNA showed a more than double the amount of WT GQ Task3-FLAG mRNA is stalled prior to 40S-binding compared to complimentary GQ Task3-FLAG (Fig. 4.10 B). This supports the hypothesis that the 5'-terminal G-quadruplex of Task3 mRNA inhibits assembly of the 40S ribosome and therefore impedes translation initiation by this mechanism.

A



B

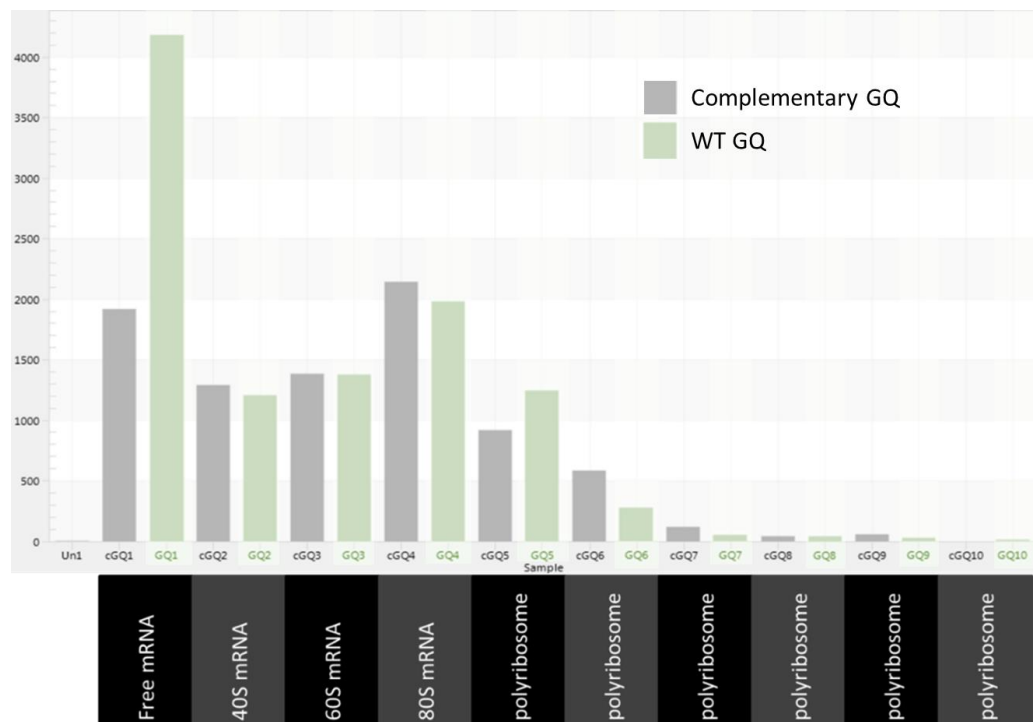


Figure 4.10 A) Polysome profiles were normal for lysates of HeLa cells transfected with WT GQ Task3-FLAG and complimentary GQ Task3-FLAG. **B)** qPCR of FLAG mRNA relative to β -actin mRNA in each fraction showed a greater proportion of WT GQ Task3-FLAG mRNA as free mRNA, unbound by 40S ribosomes. n =1

4.2.10 hnRNPA2 relieved repression of translation of transfected WT Task3

A major family of RNA-binding proteins, heterogeneous nuclear ribonucleoproteins (hnRNPs) were originally described as proteins involved in the maturation of heterogeneous nuclear RNAs (hnRNAs). However, many hnRNPs have been discovered as regulators of mRNA translation (Dreyfuss *et al.* 1993). The hnRNPs, CBF- α and hnRNPA2 have been shown to destabilize DNA and RNA G-quadruplexes *in vitro*. CBF- α and hnRNPA2 were also shown to relieve translational repression caused by CGG repeat RNA in the 5' UTR of a firefly luciferase reporter gene (Khateb *et al.*, 2007).

The pCMV2-Flag-hnRNP A2 vector was kindly given to us by Dr. Michael Fry of Technion-Israel Institute of Technology, Israel. HeLa cells were co-transfected with pCMV2-Flag-hnRNP A2 and WT GQ Task3-FLAG or complimentary GQ Task3-FLAG. Measurement of the western blot band signals indicated that co-transfection of hnRNPA2 relieved translational repression on Task3-FLAG due to its 5' terminal G-quadruplex (Fig. 4.11). Cells transfected with hnRNPA2 constructs did not show increased cell death or any obvious signs of stress.

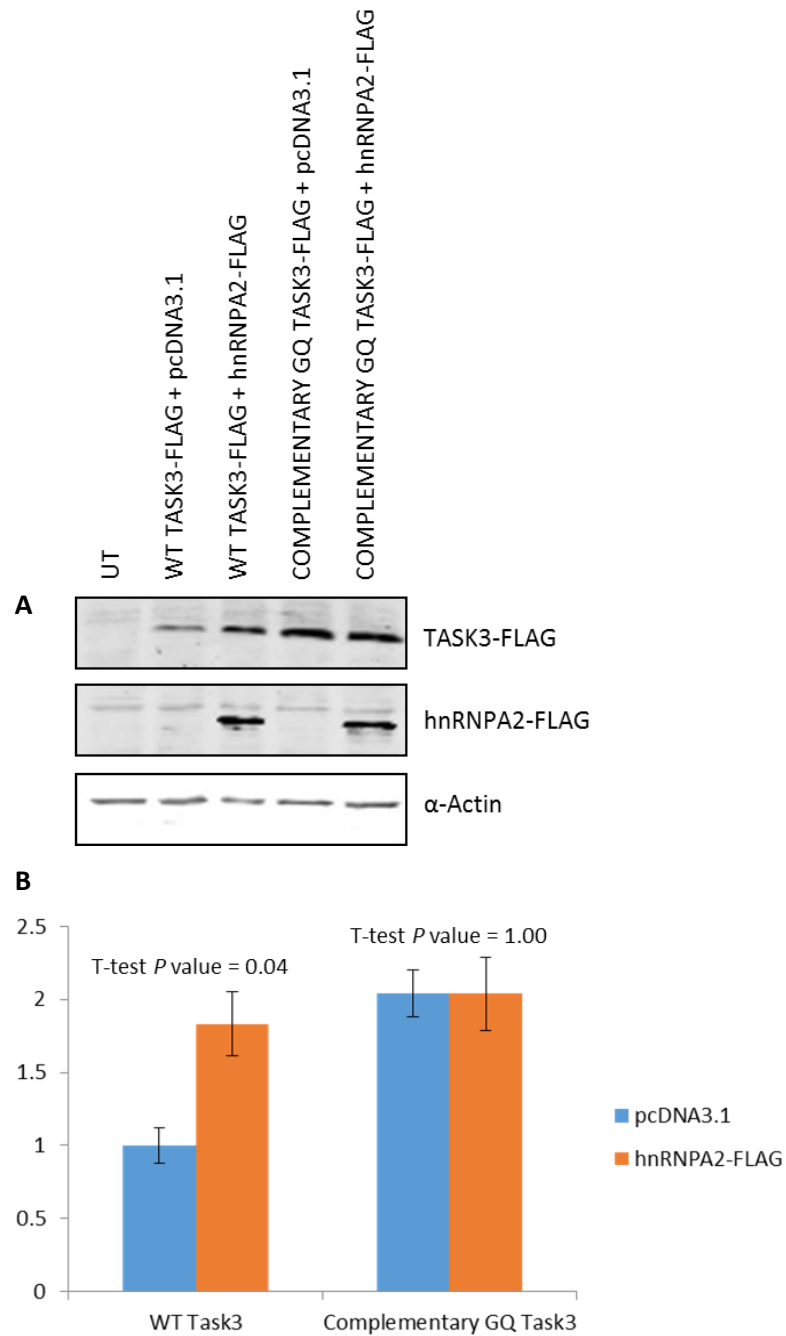


Figure 4.11 A) Western blot of cell lysate from transfected HeLa cells shows Task3-FLAG abundance with and without co-transfection with hnRNPA2. **B)** Graphs represent means and standard deviation, n = 2 biological replicates. Unpaired t-tests were used to compare the quantified abundance of protein between hnRNPA2-FLAG and control pcDNA3.1 cotransfected cells with WT/complementary G-quadruplex 5' UTR Task3 constructs. The difference in abundance of Task3-FLAG in WT-Task3 transfected cells was statistically different ($p < 0.05$) between hnRNPA2-FLAG and control pcDNA3.1 cotransfected cells.

4.2.11 RNA Helicases, DHX29, DHX30, and DHX36 were cloned from human brain cDNA

The DEAH/RNA helicase A (RHA) are members of the superfamily 2 helicase family. Pre-initiation ribosome scanning of an mRNA is inhibited by secondary structures. eIF4A/4B and 4G possess sufficient RNA helicase acidity to unwind medium-stability hairpins. However, it has been shown that the DEAH/RHA RNA helicase, DHX29 is essential for translation of mRNAs with highly stable 5' UTR hairpins. The N-terminal region of DHX29 binds the ribosome near the mRNA entrance and expresses nucleoside triphosphatase (NTPase) activity, allowing exit of hairpins from the scanning 43S pre-initiation complex (Dhote *et al.*, 2012). DHX29 NTPase activity is specific to double stranded RNA, and has not been shown to unwind quadruplex RNA.

DHX36 contains a unique N-terminal domain with specific RNA G-quadruplex-binding activity. It is the principal resolvase of DNA G-quadruplex in HeLa cells, shown to account for >50% of unwinding DNA G-quadruplex (Creacy *et al.*, 2008). DHX30 is a member of the DEAH/RNA helicase A (RHA) superfamily 2 which is highly correlated with Task3 mRNA expression in Breast Cancer primary tumour cells, normalised Pearson's coefficient, 4.51 (Mosca *et al.*, 2010). Xu *et al.*, (2013) found by mass spectrometry, DHX30 bound to (GGGGCC), (CUG), but not (CGG) repeat RNA.

DHX29, DHX30 and DHX36 were all successfully cloned from human brain cDNA into a N-terminal FLAG-tagged, CMV expression vector. Amplification of DHX sequences were achieved using extraction primers and slowdown PCR. This allowed the use of the best optimised, most specific primers for extracting the correct amplicon from the complex cDNA mixture. Slowdown PCR was used to increase specificity of amplification. cDNA was generated from total human brain RNA using Maxima H reverse transcriptase, allowing high temperate denaturation of long, GC rich coding sequences. Immunoblot of FLAG-DHX proteins was compatible with measuring expression of Task3-FLAG because of the difference in molecular weight of the predicted bands by western blot. The DHX helicase proteins are very large, DHX29, 30 and 36 have predicted molecular weights of 155 kDa, 134 kDa and 115 kDa respectively. The Task3-FLAG protein band was measured at approximately 11 kDa. Cells transfected DHX expression constructs did not show increased cell death or any obvious signs of stress at the concentrations used.

4.2.12 DHX helicases differentially change expression of transfected WT Task3 compared to Complementary GQ Task3

HeLa cells were co-transfected with FLAG-DHX29, DHX30 or DHX36, with WT GQ Task3-FLAG or complimentary GQ Task3-FLAG. Measurement of the western blot bands suggest that DHX helicases act to relieve translational repression due to the 5'-G-quadruplex of Task3 (Fig. 4.12). Co-transfection with DHX29 increased abundance of WT GQ Task3-FLAG by 16 % and Complementary GQ Task3-FLAG by 8 %. DHX30 increased abundance of WT Task3-FLAG by 36 % and Complementary GQ Task3-FLAG by 2 %. Co-transfection with DHX36 increased abundance of WT Task3-FLAG by 48 % and Complementary GQ Task3-FLAG by 6 %. Quantification by measurement of western blot band mean intensity is not accurate, but these results do suggest DHX36 can alleviate some of the translational repression afforded by the 5'-terminal G-quadruplex of Task3.

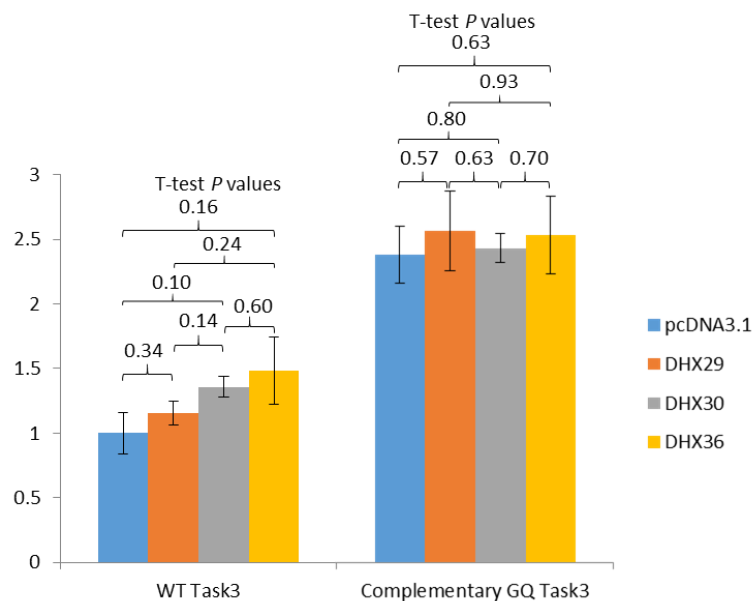
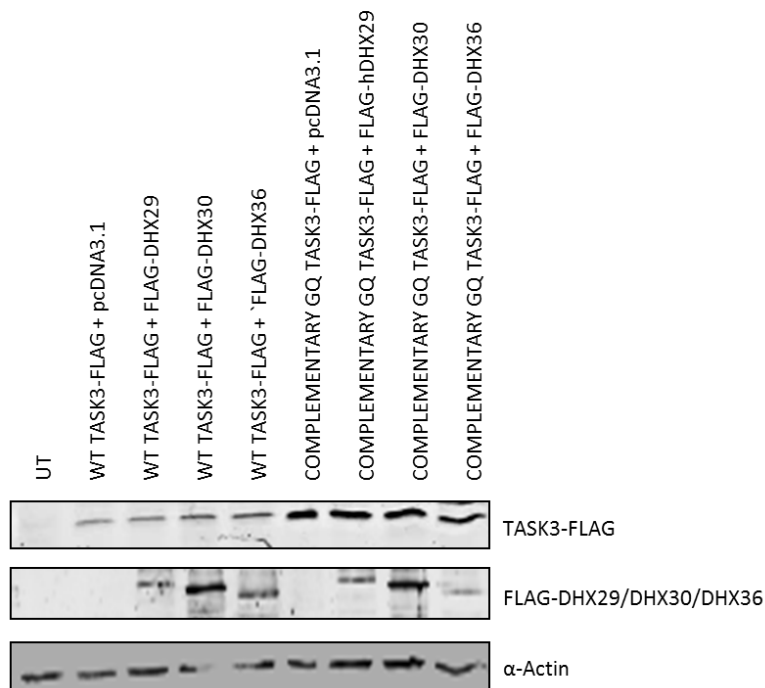


Figure 4.12 Western blot of lysate from cells co-transfected with FLAG-DHX29/30/36 and WT GQ Task3-FLAG/Complementary GQ Task3-FLAG. Graphs represent means and standard deviation, $n = 2$ biological replicates. Unpaired t-tests were used to compare the quantified abundance of Task3-FLAG protein expressed from WT/complementary G-quadruplex 5' UTR Task3 constructs between cells cotransfected with DHX29/30/36 expression vectors cells or control pcDNA3.1. There were no statistically significant differences between hnRNPA2-FLAG and control pcDNA3.1 cotransfected cells ($p < 0.05$) in abundance of Task3-FLAG in WT-Task3 or Complementary GQ Task3 transfected cells cotransfected with DHX29/30/36 expression vectors.

4.2.13 Investigation of the effects of Hippuristanol, an eIF4A inhibitor, on expression of transfected WT Task3 compared to Complementary GQ Task3

The ability of small ligands to control specific gene expression is of major interest for drug development. Recently, Wolfe *et al.*, (2014) showed that many oncogenes are characterised by G-quadruplex sequences in their 5' UTRs. They showed that Silvesterol and other eIF4A inhibitors were able to specifically downregulate expression of oncogenes. The G-quadruplex of the 5' UTR of Task3 inhibits translation of the protein with predicted profound effects on cell physiology. We predicted that the Task3 G-quadruplex requires additional helicase activity than that of eIF4A, the ribosome's endogenous helicase. RNA G-quadruplex structures are very stable and the inhibition of translation of Task3 due to its 5' terminal G-quadruplex has been very strong. We were unable to acquire Silvesterol for testing, however Junichi Tanaka of the University of the Ryukyus, Japan, kindly gifted us Hippuristanol to test, another eIF4A inhibitor also demonstrated by Wolfe *et al.*, to inhibit translation of cancer genes with 5' UTR G-quadruplexes. Results above suggest the Task3 5' terminal (GGN)₁₃ sequence forms a strong G-quadruplex which requires powerful helicase activity to resolve and relieve translational inhibition. It was expected that an eIF4A inhibitor would not dramatically affect Task3-FLAG synthesis in treated transfected cells. HeLa cells were transfected with WT GQ Task3-FLAG or complimentary GQ Task3-FLAG and treated with 10 µM Hippuristanol for 16 hours before lysis for western blot. Measurements of the western blot bands suggest that Hippuristanol did not greatly impact the translation of WT GQ Task3-FLAG (4.13).

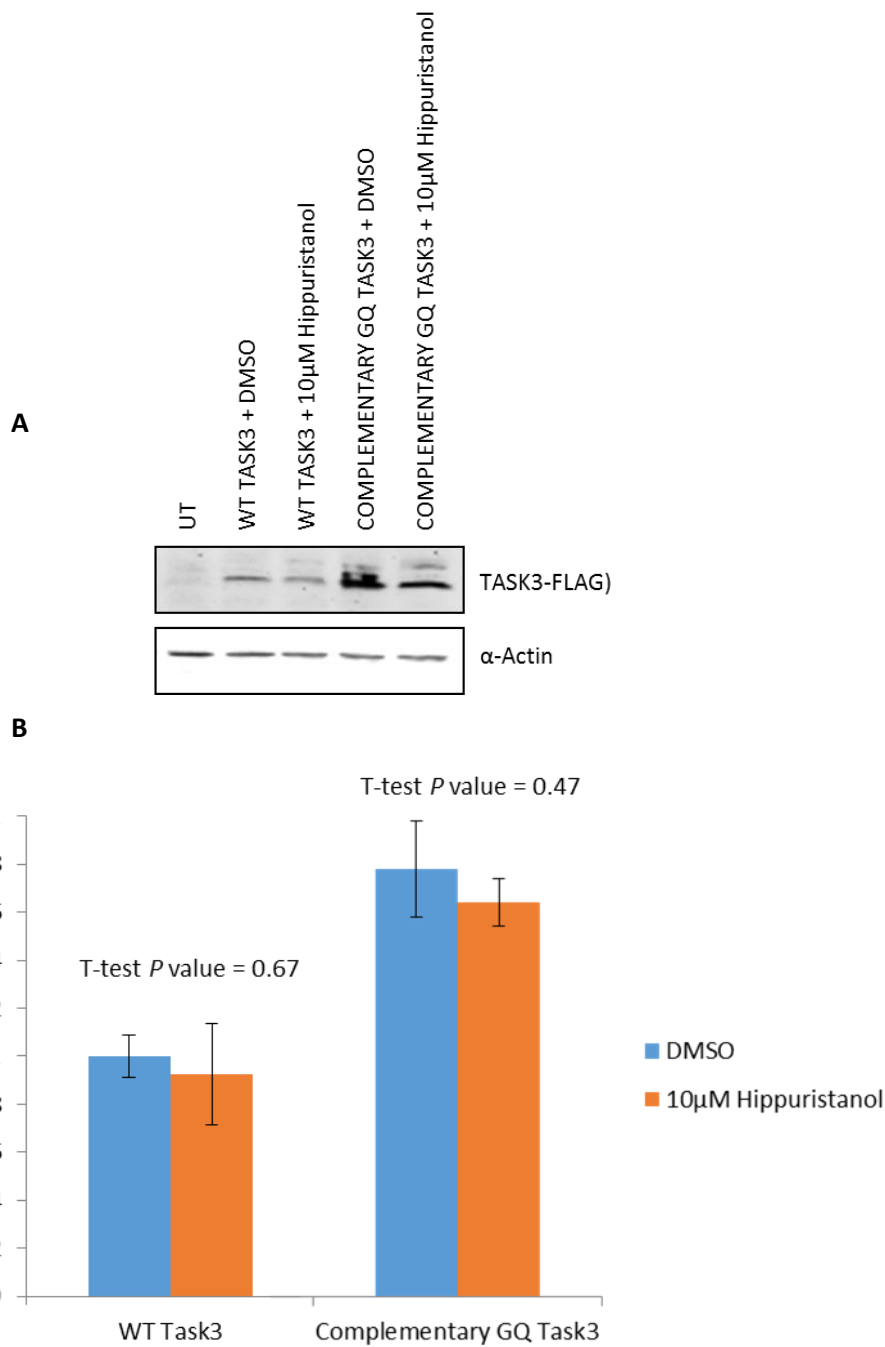


Figure 4.13 A) Western blot of cell lysate from transfected HeLa cells shows Task3-FLAG abundance with and without treatment with 10µM Hippuristanol. **B)** The western blot signal intensities were measured. Graphs represent means and standard deviation, $n = 2$ biological replicates. Unpaired t-tests were used to compare the quantified abundance of Task3-FLAG protein expressed from WT/complementary G-quadruplex 5' UTR Task3 constructs between cells with and without treatment with 10µM Hippuristanol. There were no statistically significant differences in abundance of Task3-FLAG in WT-Task3 or Complementary GQ Task3 transfected cells with and without treatment with 10µM Hippuristanol ($p < 0.05$).

4.2.14 Investigation of the effects of TMPyP4, a G-quadruplex-targetting ligand, on expression of transfected WT Task3 compared to Complementary GQ Task3

The cationic porphyrin, TMPyP4 was shown by Ofer *et al.* (2009) to unfold (CGG)_n quadruplexes in vitro and relieve translational repression due to a 5' UTR G-quadruplex in transfected HEK293 cells. TMPyP4 treatment did not alter protein expression from *Task 3-FLAG* G-quadruplex mutant constructs in transfected HeLa cells (Fig. 4.14 A). The experiment was carried out with n = 3 technical replicates. An unpaired t-test was used for comparison of the CCPM (radioactivity due to 35S-methionine incorporation) between untreated HeLa cells and cells treated with TMPyP4 indicate an approximate 50% inhibition of translation in the presence of 50µM TMPyP4 (Fig. 4.14B).

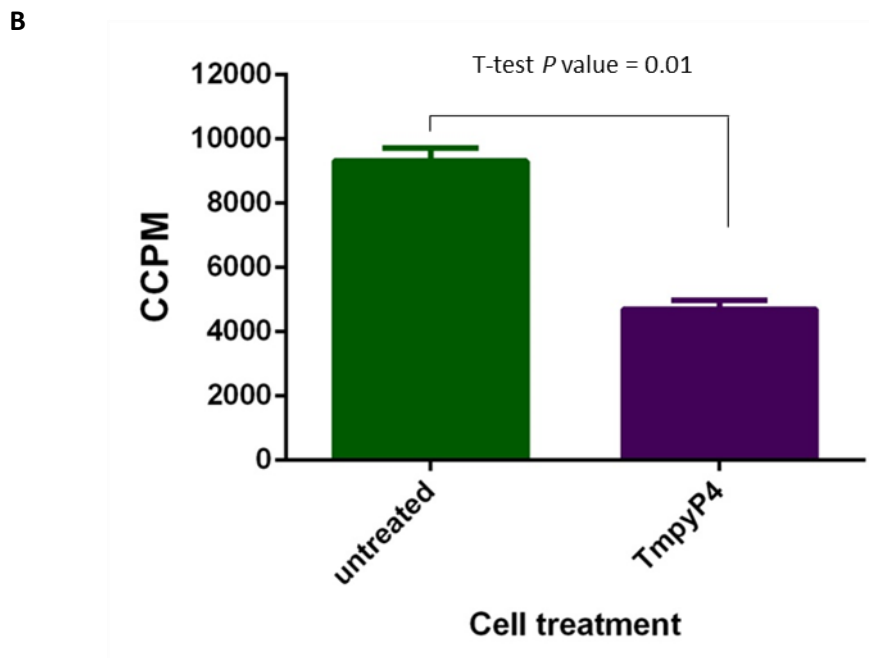
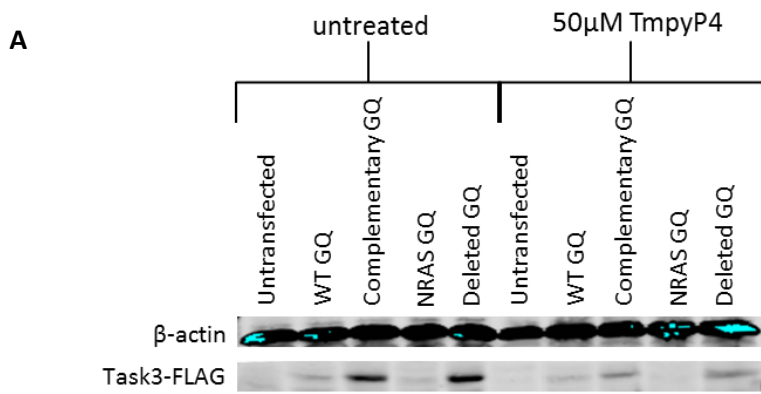


Figure 4.14 The cationic porphyrin, TMPyP4 **A)** showed no sequence-specific inhibition of translation of Task 3-FLAG mRNA mutants. **B)** Graphs represent means and standard deviation, $n = 3$ technical replicates. An unpaired t-test was used to compare the CCPM (radioactivity due to ^{35}S -methionine incorporation) between untreated cells and cells treated with TMPyP4. TMPyP4 treatment caused a ~50% decrease in CCPM, $p=0.01$.

4.2.15 TMPyP4 was shown to unfold (GGN)₁₃ G-quadruplex

The measurement of G-Quadruplex folding by purified *in-vitro* transcribed RNA by CD spectroscopy was carried out on 250µl samples in a 1 mm path cuvette. Following acquisition of the first spectrum, 1 µl of buffer (100 mM KCl, 10 mM Tris-HCl and 0.1 mM EDTA (pH 7.5)) supplemented to 2.5mM TMPyP4 were added to the cuvette containing the measured RNA sample and mixed by 5 inversions prior to recording new spectra at 10µM, 20µM, 50µM, and 100µM. There was no significant change in the peak intensity indicative of G-quadruplex structures, 263nm, at concentrations of 0-50µM TMPyP4. However, upon incubation of (GGN)₁₃ RNA with 100 µM TMPyP4, there was approximately 50% decrease in peak intensity indicative of G-quadruplex structures, 263nm (Fig. 4.15). The RNA was synthesised in a single batch. This experiment should be repeated with a positive and negative control RNA; NRAS and complementary GQ sequences would be suitable. Repeats of this experiment should be carried out using independently prepared batches of RNA from independent reactions and purifications.

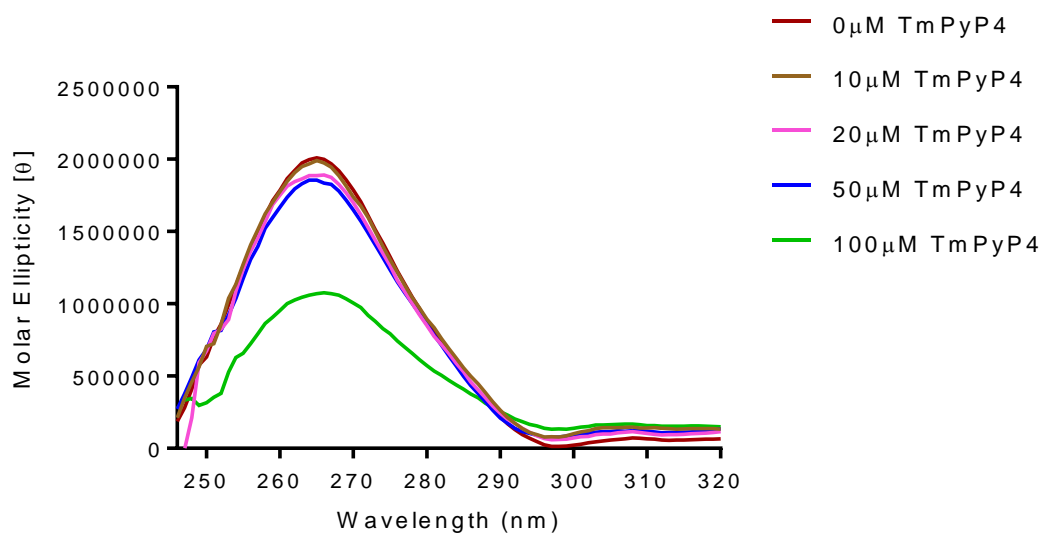


Figure 4.15 The cationic porphyrin, TMPyP4 was shown to unfold (GGN)₁₃ G-quadruplex. Incubation of (GGN)₁₃ RNA with 100µM TMPyP4 reduced the CD G-quadruplex signal peak at 263nm. n = 3 technical replicates.

4.2.16 100µM TMPyP4 partially relieved repression of translation of transfected WT Task3

The cationic porphyrin TMPyP4 was shown to bind and unfold the extremely stable RNA G-quadruplex from the 5' UTR of MT3-MMP mRNA (Morris *et al.*, 2012). CD, 1D 1H NMR and native gel electrophoresis were used to show unfolding of the G-quadruplex in the presence of increasing concentrations of TMPyP4. TMPyP4-mediated unfolding of the G-quadruplex was demonstrated to allow increased protein synthesis. HeLa cells transfected with a dual luciferase bi-cistronic construct showed increased luciferase production from an mRNA with the 5' UTR MT3-MMP G-quadruplex following treatment with TMPyP4.

Here, HeLa cells were transfected with either WT GQ Task3-FLAG or complimentary GQ Task3-FLAG and treated with 100µM TMPyP4 for 16 hours before lysis for western blot. Results of this experiment showed Task3-FLAG abundance increased in cells transfected with WT GQ Task3-FLAG when treated with 100µM TMPyP4 (Fig. 4.16). There was no change in Task3-FLAG abundance in cells transfected with complementary G-quadruplex, (CCN)₁₃, 5' UTR plasmid when treated with 100µM TMPyP4.

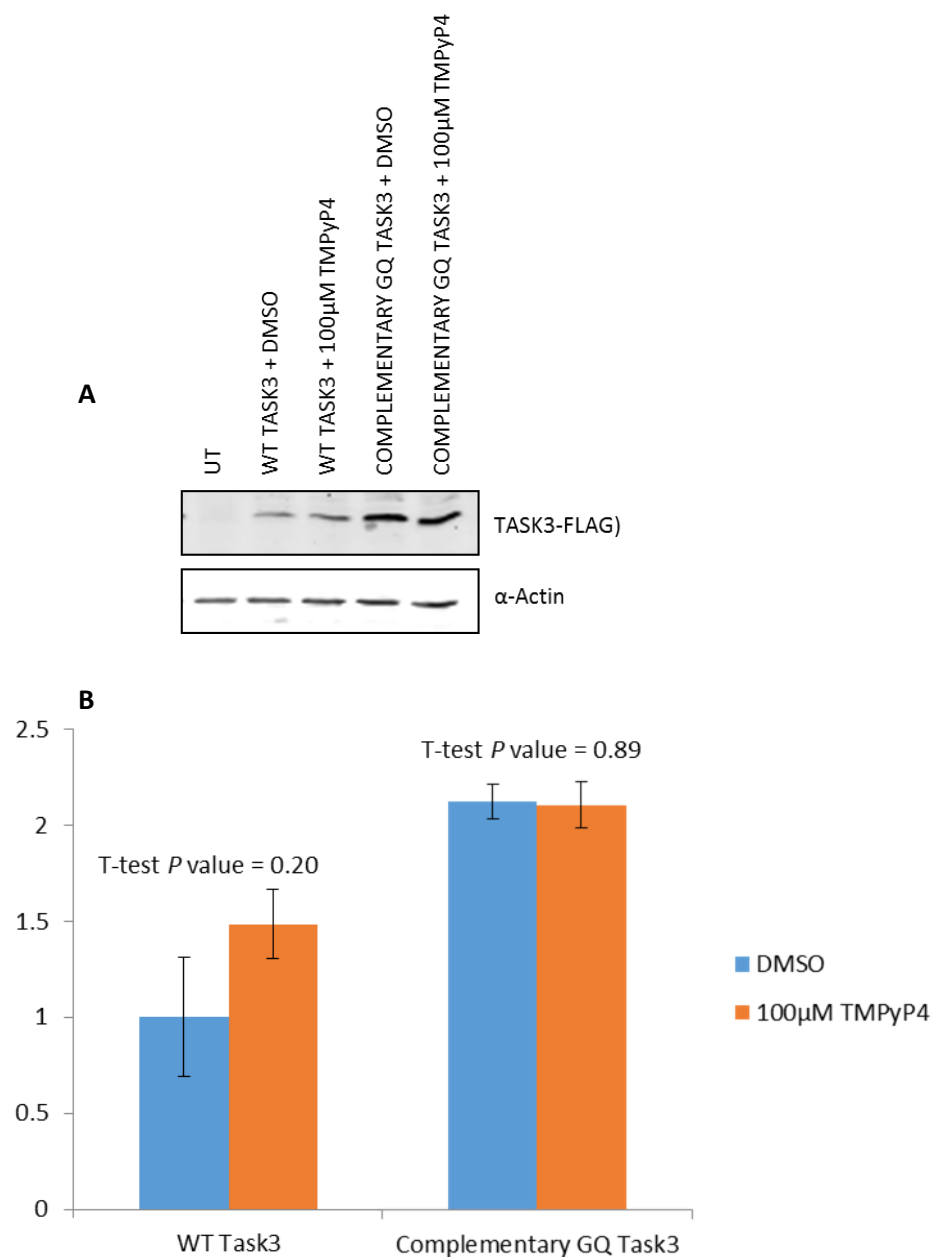


Figure 4.16 A) Western blot of cell lysate from transfected HeLa cells shows Task3-FLAG abundance with and without treatment with 100µM TMPyP4. **B)** The western blot signal intensities were measured. Graphs represent means and standard deviation, $n = 2$ biological replicates. Unpaired t-tests were used to compare the quantified abundance of Task3-FLAG protein expressed from WT/complementary G-quadruplex 5' UTR Task3 constructs between cells with and without treatment with 100µM TMPyP4. There were no statistically significant differences in abundance of Task3-FLAG in WT-Task3 or Complementary GQ Task3 transfected cells with and without treatment with 100µM TMPyP4 ($p < 0.05$).

4.3 Discussion

The mRNA of K_{2P} channel, Task3, has a 5' terminal G-quadruplex which inhibits translation initiation and therefore inhibits Task3 protein expression. K_{2P} channels set the resting membrane potential of mammalian cells; elucidating mechanisms of their controlled expression is of great significance for understanding normal cell behaviour as well as identifying potential pharmaceutical targets. Specific RBPs have been shown to regulate expression of mRNAs with 5' UTR G-quadruplexes. In this chapter, I have demonstrated the ability of specific RBPs to regulate the translation of Task3 mRNA in a G-quadruplex dependent manner. The ability to modulate translation of mRNAs with 5' UTR G-quadruplexes with small ligands has been of great interest in recent reports (Wolfe *et al.*, 2014, Zamiri *et al.*, 2014). The cationic porphyrin, TMPyP4, unfolded the Task3 G-quadruplex *in vitro* and allowed increased Task3-FLAG protein synthesis in transfected HeLa cells.

4.3.1 The 5'-terminal (GGN)₁₃ of Task3 mRNA forms a G-Quadruplex which inhibits translation initiation

The 5'-terminal (GGN)₁₃ of Task3 mRNA was analysed for G-Quadruplex forming sequences using QGRS Mapper (Kiken *et al.*, 2006). The program identified 3 QGRS within the (GGN)₁₃ 5' terminus (Fig. 4.1). 5' UTR G-quadruplexes have been shown to inhibit translation of the mRNA. We hypothesised that the 5'-terminal G-quadruplex of Task3 mRNA inhibits translation of Task3, having a negative impact on Task3 protein levels.

Expression vectors of Task3-FLAG with test 5' UTRS were constructed to test the effect of the (GGN)₁₃ terminal G-quadruplex on translation rates of Task3. The test 5' UTRs were mutations of the wild-type (GGN)₁₃ sequence of the 5' UTR. Mutagenic primers were used to generate Task3-FLAG plasmids with 5' UTRs different in the predicted G-quadruplex region (nucleotide positions 1-55) (Fig. 4.2). To test the expression of Task3-FLAG would be without the (GGN)₁₃ terminal sequence, predicted to form a G-quadruplex, a plasmid with a mutated 5' UTR with positions 1-55 deleted was created. To test for the effect of a long GC-rich region predicted to form a G-quadruplex against one with similar GC content, but not expected to form a G-quadruplex, at the 5'-terminus of the UTR a mutant was created with positions 1-55 replaced with the complementary sequence of the G-quadruplex-forming sequence (CCN)₁₃. A positive G-quadruplex control Task3-FLAG plasmid with the G-

quadruplex sequence from the NRAS 5' UTR inserted at positions 1-55. The expression of C-terminally FLAG-tagged Task3 protein was investigated by western blot of transfected HeLa cell lysate. qPCR analysis showed changes in Task3-FLAG protein abundances due to changes in the translation of mRNA, not changes in the abundance of Task3-FLAG mRNA (Fig 4.4).

Task 3-FLAG translation was greatly inhibited by the (GGN)₁₃ terminal sequence, predicted to form a G-quadruplex. Inhibition of translation was similar to that of the mutant with positive control G-quadruplex from NRAS 5' UTR, previously shown to inhibit translation (Kumari *et al.*, 2007). Repression of Task3-FLAG translation was relieved by removal of the (GGN) repeat or mutation of positions 1-55 to the complementary sequence, predicted to not form G-quadruplex structures. These results suggested the (GGN)₁₃ terminal sequence of Task3 mRNA forms a G-quadruplex similar to that of the NRAS 5' UTR and with similar inhibitory effect on translation of the mRNA. To compare the effects of the predicted G-quadruplex-forming sequence of Task3 5' UTR with already published effects of double stranded secondary structures, it would be useful to repeat experiments shown in Fig 4.7 & 4.8 with a control RNA of a 5' UTR secondary structure of known consequence on translation.

Biophysical investigations characterised the structure of the (GGN)₁₃ terminal sequence of Task3 mRNA. Initially, it was necessary to replace the absent T7 promotor sequence present in the original pcDNA3.1 plasmid. T7 Polymerase was used for *in vitro* transcription of GGN and mutant Task3 5' terminal sequences (positions 1-55). Increased fluorescence of NMM incubated with WT GQ (GGN)₁₃ RNA confirmed formation of a G-quadruplex structure (Arthanari *et al.*, 1998). NMM increased in fluorescence when incubated with the positive control G-quadruplex RNA sequence RNA sequence from NRAS (Fig. 4.7). Incubation of NMM with negative control RNA sequences did not result in increased fluorescence. Circular dichroism (CD) was used to support findings of NMM studies of G-quadruplex formation. G-quadruplex structures are chiral, and differentially absorb left and right handed circular light at 262 nm. Spectra of WT GQ (GGN)₁₃ RNA showed high CD G-quadruplex signal peak at 262 nm, similar to that of the positive control G-quadruplex RNA sequence from NRAS (Fig. 4.8). The negative control, (CCN)₁₃ RNA sequence had much lower peaks at 262 nm. Positive G-quadruplex control RNA

showed a G-quadruplex signal peak at 262nm of similar magnitude to WT GQ (GGN)₁₃ RNA. Task1 5' UTR RNA also showed a G-quadruplex signal peak at 263nm.

Polysome profiling was used to investigate where in the translation pathway, inhibition was occurring due to the 5'-terminal G-quadruplex of Task3 (Fig. 4.11). qPCR was used to measure the differential in abundance of Task3-FLAG RNA at each polysome fraction between lysates from HeLa cells transfected with WT GQ eUTR-Task3-FLAG or complimentary GQ eUTR-Task3-FLAG. Results suggested more than double the amount of WT GQ Task3-FLAG mRNA is stalled prior to 40S-binding compared to complimentary GQ Task3-FLAG (Fig. 4.6 B). The 5'-terminal G-quadruplex of Task3 mRNA may inhibit translation by retarding assembly of the 40S ribosome at the 5' cap.

4.3.2 Specific G-quadruplex-targeting RBPs can modulate translational control of Task3

Specific G-quadruplex-targeting RBPs regulate expression of mRNAs with 5' UTR G-quadruplexes. Results in this chapter showed regulation of Task3 mRNA translation by specific RBPs in a G-quadruplex dependent manner. Characterisation of proteins involved in the regulation of mRNAs with regulatory 5' UTR G-quadruplexes is important for understanding normal cell signalling and for identifying putative therapeutic targets.

The heterogeneous nuclear ribonucleoproteins (hnRNPs), CBF- α and hnRNP A2 destabilize RNA G-quadruplexes and relieve translational repression caused by 5' UTR CGG repeats (Khateb *et al.*, 2007). Western blot of lysate from HeLa cells co-transfected with pCMV2-Flag-hnRNP A2 and WT GQ Task3-FLAG or complimentary GQ Task3-FLAG showed hnRNP A2 was able to greatly reduce inhibition of translation of Task3 due to its 5'-terminal G-quadruplex (Fig. 4.12). hnRNP A2 increased the Task3-FLAG detected in lysate from cells co-transfected with WT GQ Task3-FLAG, and hnRNP A2 did not change the abundance of Task3-FLAG detected in cells co-transfected with complimentary GQ Task3-FLAG. To validate that these proteins act upon translation and not mRNA stability, qPCR analysis of the abundance of Task3-FLAG mRNA should be also carried out.

Highly stable RNA hairpins inhibit translation of an mRNA and require additional helicase activity beyond that of the ribosome's endogenous eIF4A/4B and 4G proteins. Translation of mRNAs with highly stable 5' UTR hairpins is facilitated by the DEAH/RHA RNA helicase, DHX29. The ability of DHX29 to aid unwinding of G-quadruplexes is unknown. The DEAH/RHA RNA helicase, DHX36, is the major DNA G-quadruplex helicase in HeLa cells (Creacy *et al.*, 2008). DHX29, DHX30 and DHX36 were cloned into a N-terminal FLAG-tagged, CMV expression vector.

Co-transfection with FLAG-DHX plasmids and WT GQ Task3-FLAG or complementary GQ Task3-FLAG showed differential efficiency of DHX helicases in relieving translational repression due to the 5'-G-quadruplex of Task3 (Fig. 4.13). Most significantly, co-transfection with DHX36 increased abundance of WT Task3-FLAG by 48 % but only 6 % increase was seen when co-transfected with complementary GQ Task3-FLAG. A complex network of helicases may participate in the regulation of Task3 translation *in vivo*. The composition of Task3-RBP complexes may be investigated *in vivo* by RNA IP (RIP) of antibody-captured RBPs from cell lysate. The presence of Task3 mRNA in complex with specific RBPs could be measured by qPCR of an easily amplifiable, specific section of the Task3 mRNA.

4.3.3 TMPyP4 unfolded Task3 5'-terminal G-quadruplex and relieved translational repression

Wolfe *et al.*, (2014) demonstrated the controlled translation of oncogenes with 5' UTR G-quadruplexes by the eIF4A inhibitor, Silvestrol. K_{2p} levels are of critical importance to cell physiology, so drugs which could modulate translation of Task3 could have a significant impact on treatment of disease associated with abnormal resting membrane potential, including neurological disorders. The strong inhibition of Task3-FLAG translation due to the presence of the 5' G-quadruplex, coupled with evidence above on the ability of strong helicase enzymes to have limited success in relieving translational inhibition meant we predicted an eIF4A inhibitor would have little noticeable effect on Task3-FLAG protein synthesis. Hippuristanol an eIF4A inhibitor was tested for effectiveness in modulating expression of Task3-FLAG protein in transfected HeLa cells. Results showed no real difference in expression of Task3-FLAG protein between cells transfected with WT GQ Task3-FLAG or complementary GQ Task3-FLAG with or without Hippuristanol treatment (Fig. 4.14).

The cationic porphyrin, TMPyP4 has been shown to unfold (CGG)_n quadruplexes *in vitro* and relieve translational repression due to a 5' UTR G-quadruplex in transfected HEK293 cells (Ofer *et al.* 2009). Results demonstrated 100 μM TMPyP4 may have unfolded the (GGN)₁₃ G-quadruplex (Fig. 4.16) and partially relieved repression of translation of transfected WT GQ Task3-FLAG (Fig. 4.17). However, this may reflect a different biological reason, such as an induced stress response from high TMPyP4 concentrations, and general decrease in translation rates. TMPyP4 at 100 μM was seen to preferentially increase expression of WT GQ Task3-FLAG, but not complementary GQ Task3-FLAG in transfected HeLa cells. However, its use as a therapeutic agent may be compromised by the fact that it was also shown that TMPyP4 reduces global translation in HeLa cells treated at 50 μM (Fig. 4.15B). The concentration of TMPyP4 required to effect the measured G-quadruplex structure was higher than the concentration used to treat cells. The effect of TMPyP4 on global translation is toxic to cells and therefore any observations based on the proposed relaxation of G-quadruplex structure due to treatment with TMPyP4 must be treated cautiously.

4.3.4 Conclusions

1. The formation of a G-quadruplex structure by the 5' terminal GGN repeat of Task3 mRNA was supported by increased fluorescence of NMM and further supported by CD spectra consistent with G-quadruplex formation
2. DHX helicase genes were cloned from human brain cDNA into FLAG-tagged expression vectors
3. Co-transfection of HeLa cells with Task3-FLAG and DHX helicases suggest an increase in Task3-FLAG protein synthesis in the presence of DHX helicases, with DHX36 showing the greatest effect. This may be further validated by repeated experiments.
4. Treatment of transfected HeLa cells with the eIF4A inhibitor, Hippuristanol, did not appear to affect synthesis of Task3-FLAG protein. This may be further validated by repeated experiments.
5. It had previously been reported that TMPyP4 relaxes G-quadruplex structures and alleviates repression of translation due to G-quadruplex structures within the 5' UTR of specific mRNAs. However, we found TMPyP4 globally decreased translation rates in HeLa cells. 100 μM TMPyP4 was required to reduce the G-quadruplex CD spectra of GGN repeat RNA *in vitro*.

The treatment of cells transfected with Task3-FLAG constructs with 100 μ M TMPyP4 showed no change in abundance of Task3-FLAG protein with or without G-quadruplex coding sequence.

Chapter Five

Results

The 5'-terminal G-quadruplex in Task3 mRNA potentially mediates local translation in neurons

5.1 Introduction

G-quadruplex structures have been shown to effect mRNA subcellular targeting and direct protein synthesis at the synapse (Subramanian *et al.*, 2011). The unaltered subcellular localisation of Task3-FLAG transfected HeLa cells suggests the *Task3* 5' UTR G-quadruplex does not affect mRNA trafficking in HeLa cells. However, any effect of the G-quadruplex on mRNA trafficking may be masked by the N-terminal di-basic ER-retention signal present in the expressed fusion proteins. The Task3-FLAG fusion proteins also lack the C-terminal 14-3-3 recognition site, which enables forward trafficking of TASK3 to the membrane. To further investigate the effects of the 5'-terminal G-quadruplex on mRNA localisation, in-situ fluorescence hybridisation of mRNA was used. This allowed direct measurement of mRNA localisation changes due to the 5'-terminal G-quadruplex of Task3 mRNA.

The translation of specific messenger RNA (mRNA) at distinct subcellular localisations allows modification of the local proteome, independent of general translation in the cell. Environmental cues lead to rapid changes in discrete local proteomes. The complex regulation of local translation involves controlled mRNA targeting and transport as well as stimulus-controlled translation of the message. Spatially

differentiated translation of mRNA allows dynamic regulation of the local proteome. Neurons make use of complex, poorly understood mechanisms for controlling the packaging, targeting and controlled local translation of specific mRNAs. Aberrations to these processes are responsible for neurological diseases (Kelleher and Bear, 2008, Jung *et al.*, 2012, Ramaswami *et al.*, 2013).

5.2 Results

5.2.1 The 5'-terminal G-quadruplex does not affect subcellular localisation of Task3 protein in transfected HeLa cells

Western blot showed deletion or substitution with complementary 5' UTR G-quadruplex-forming sequence altered the quantity of Task 3-FLAG product, but not size. Protein localisation was tested and found to be unaltered. Similar Task3-FLAG was observed in HeLa cells transfected with WT GQ (Fig. 5.1) and Δ GQ *Task3-FLAG* constructs (Fig. 5.1). Task 3-FLAG was highly expressed in ER and Golgi, consistent with previous research regarding an ER retention signal within Task3. Many of the K_{2P} channels possess N-terminal dibasic sites which are recognised by coatamer proteins (β -COP) and cause retention of the K_{2P} channel in the ER. Membrane expression of TASK1 and TASK3 is regulated by phosphorylation of a serine in the intracellular C-terminal tail. The 14-3-3 adaptor protein binds the phosphorylated channel, inhibits β -COP binding and enables trafficking to the cell membrane (O'Kelly *et al.*, 2002). The Task3-FLAG constructs expressed lacked the C-terminal 14-3-3 binding site responsible for decreased ER retention and increased membrane expression (Rajan, Preisig-Müller & Wischmeyer, 2002).

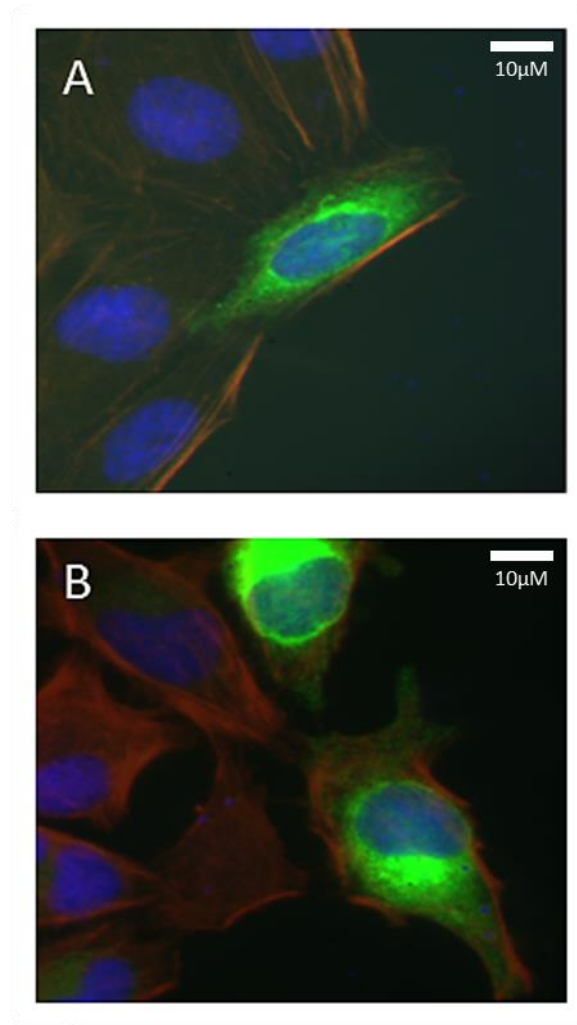


Figure 5.1 Task3-FLAG (green) expression in HeLa cells transfected with **A)** WT GQ and **B)** Δ GQ *Task3-FLAG* constructs. DAPI nuclear stain (blue). Actin (red).

5.2.2 Creation of Task3-GFP expression vectors

The N-terminal G-quadruplex of Task3 may act as a motif for RBP-mediated subcellular trafficking. The distribution of an mRNA molecule can be detected by fluorescence in situ hybridisation. Stellaris FISH was chosen as the best technique to detect Task3 mRNA subcellular distribution. The technique uses 30-40 short DNA probes labelled with a single fluorophore, able to detect individual molecules of mRNA without amplification (Orjalo, Johansson & Ruth, 2011). In order to maximise the value of the probe set, and the reproducibility of the technique with other target genes, Stellaris probes were to be targeted to the target gene's fusion tag. The FLAG sequence is too short (24 nucleotides) to allow the design of Stellaris FISH probes sets, therefore Task3 was fused with GFP, a well-established, characterised, large epitope tag (717 nucleotides). Task3-GFP fusion expression vectors have been used successfully in our lab for investigations of Task3 subcellular localisation (Mant, Williams & O'Kelly, 2013). The simultaneous detection of Task3 protein and FISH detection of Task3 mRNA was made simple by the creation of C-terminally tagged Task3-GFP fusion proteins. Task3-GFP protein localisation can be easily measured without the use of fluorescently labelled antibodies. Task3 protein expression has a critical effect on cellular potassium homeostasis, overexpression of functional Task3 ultimately causes apoptosis, not conducive to investigation of mRNA trafficking. To investigate the effect of the 5' terminal G-quadruplex on mRNA trafficking, it was therefore decided that the C-terminal (4th) transmembrane domain and Task3's C-terminal intracellular tail would be deleted, and replaced with a GFP fusion epitope tag (Fig. 5.2) to create a non-functional chimera.



Figure 5.2 The C-terminal (4th) transmembrane domain and C-terminal intracellular tail Task3's were deleted, and replaced with a GFP fusion epitope tag.

Previously our lab has used N-terminal Task3 GFP fusion proteins. For investigation of the effects of the mRNA's 5' G-quadruplex, an N-terminal GFP tag would not be useful. The first step was the creation of a C-terminal GFP-fusion expression vector. To make this most useful as an addition to the lab's arsenal, it was designed to be similar to the pcDNA3.13F plasmid used extensively in the lab already. The enhanced GFP sequence from the lab's N-terminal GFP expression vector was cloned into the pcDNA3.1 vector, with upstream restriction sites for simple compatible cloning from existing plasmids (Fig. S1). The Task3 5' UTR sequences, with wild-type 5' UTR and with complimentary 1-55, were cut with NheI/XhoI from the Task3-FLAG expression vectors used above (Fig. S2). A C-terminal (3 transmembrane) region of Task3 was PCR amplified from a full length Task3 expression vector using a forward primer from the AUG at +1 and reverse primer with a HindIII restriction site. This region was then cut with XhoI and annealed to the Task3 5' UTR sequences cut with NheI/XhoI in Fig. S2. The C-terminal region of Task3 was amplified from the lab's N-terminal GFP Task3 expression vector (Fig. S3). The N & C termini were ligated (Fig. S4) to form the PCR template for amplification of the full length sequence to be cloned into the newly created C-terminal GFP-fusion vector (Fig. 5.3).

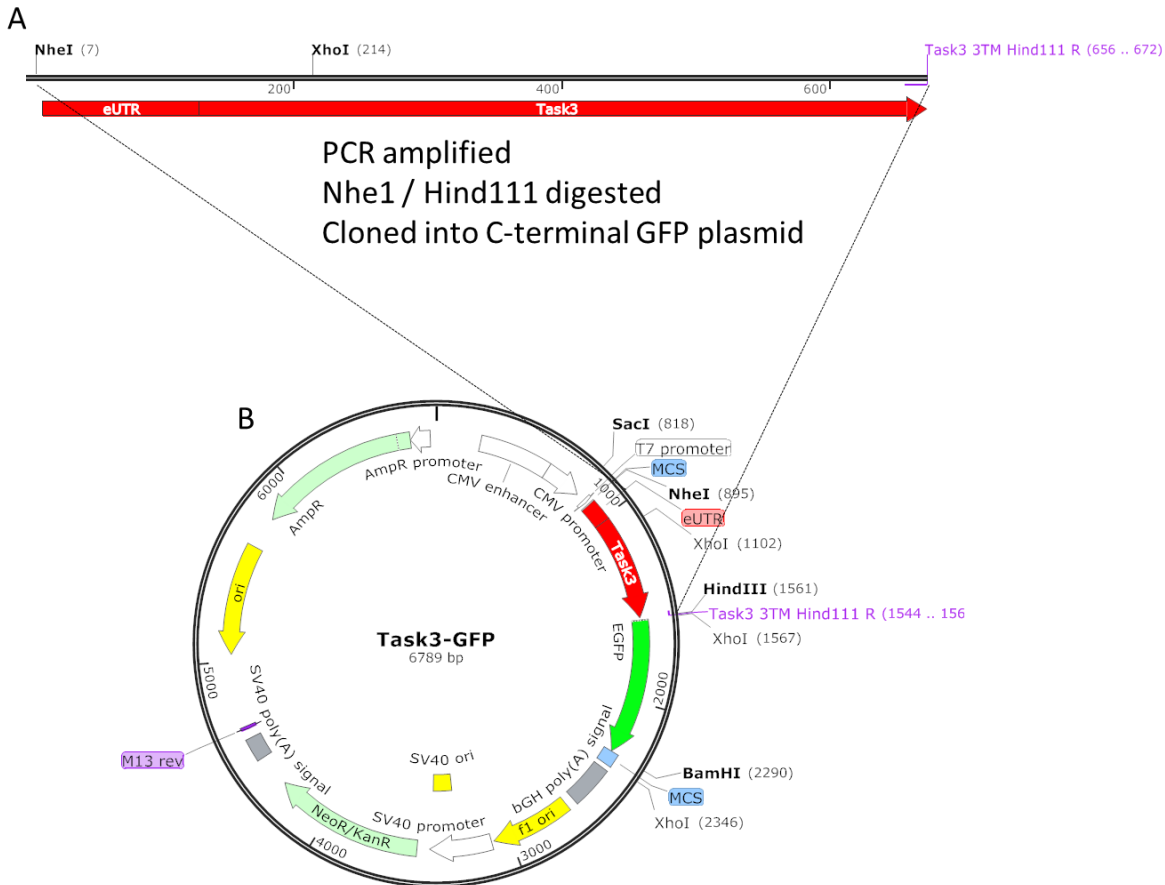


Figure 5.3 A) The ligated Task3 construct was PCR amplified using NheI forward primer and HindIII reverse primer. Following gel purification of the PCR product, the fragment and C-terminal GFP expression vectors were digested with NheI and HindIII for cloning. **B)** The resulting plasmid, Task3-GFP was used for fluorescence studies of mRNA and protein localisation.

WT GQ Task3-GFP and complimentary GQ Task3-GFP plasmids were transfected into HeLa cells and the expression of the expressed protein was detected by fluorescence microscopy. The distribution of the proteins was similar to that seen for FLAG-tagged constructs, the majority of expressed Task3-GFP was localised to the ER and golgi (Fig. 5.4).

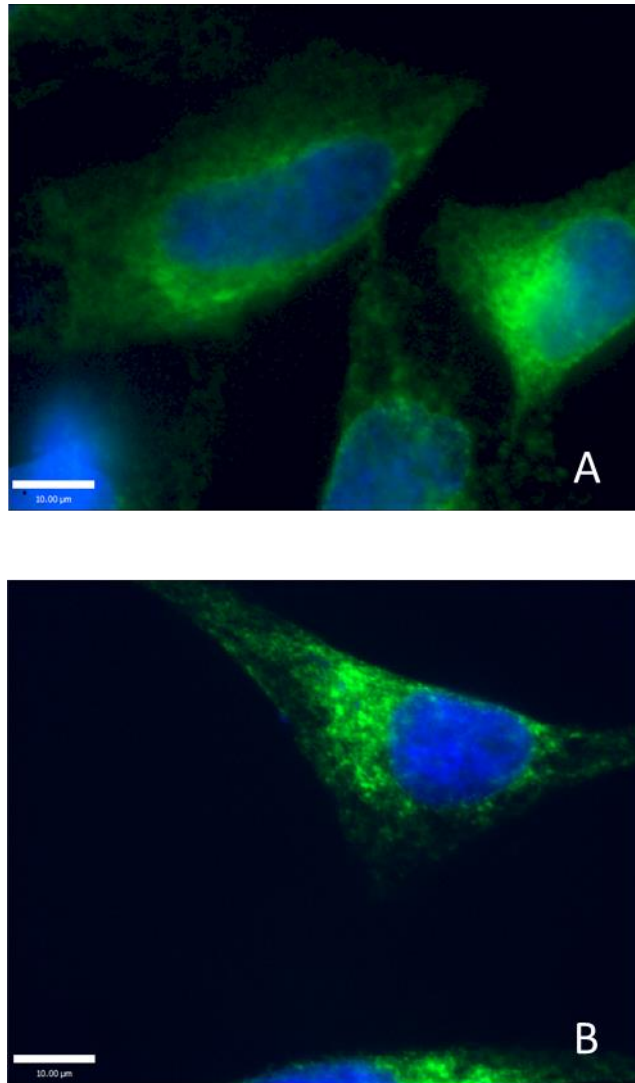


Figure 5.4 HeLa cells were transfected with **A)** WT GQ Task3-GFP and **B)** complementary GQ Task3-GFP; the 5'-terminal 1-55 replaced with the complementary nucleotide sequence. Nucleus in blue (DAPI). Experiment repeated four times and transfection efficiency was approximately 50 - 70%.

5.2.3 Design of Stellaris probes for FISH of Task3-GFP mRNA

G-quadruplexes have been shown to direct differential subcellular localisation of the mRNA (Subramanian *et al.*, 2011). Task3 mRNA is highly expressed in neuronal tissues. The 5'-terminal G-quadruplex in Task3 mRNA is predicted to mediate localisation of mRNA to neurites. Stellaris RNA FISH is a cutting edge technique designed to improve signal to noise compared to conventional FISH techniques. Up to 50 fluorescently labelled short (20 nucleotide) DNA oligonucleotides with similar T_m are designed complementary to non-overlapping regions of the RNA target using the online tool (<https://www.biosearchtech.com/stellarisdesigner/>) (Fig 5.5). Improved signal to noise afforded by the Stellaris technique enables increased sensitivity and specificity, making it ideal for characterising an mRNA's subcellular localisation. The buffers and low annealing temperatures are compatible with detection of protein localisation by fluorescence-labelled antibodies.

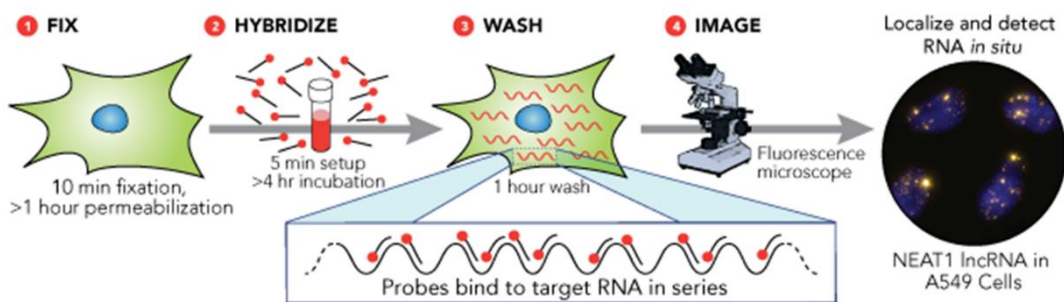


Figure 5.5 The principles of Stellaris probes for FISH imaging of RNA localisation in cells.

The eGFP sequence was chosen as the target sequence for RNA detection and localisation of mRNA from transfected Task3 plasmids. The Stellaris probes are stable at -80C for over a year, so the designed probes could be used in other experiments within our group, without the need to design and test unique probe sets. The added advantage of targeting the GFP sequence is the lack of homologous coding sequences in the human genome, so the probability of off-target binding is reduced. The GFP sequence is at the C-terminus of the Task3-GFP constructs, so the effects of secondary structures within the 5' UTR on binding of FISH probes is minimised. This method allows for un-biased comparison of mRNA localisation due to changes in sequences within the 5' UTR. The Stellaris FISH probes were used for measuring the difference in mRNA localisation of the wild-type Task3 mRNA, characterised by its 5' terminal G-quadruplex in transfected cells and the negative control mRNA; the same

Task3-GFP construct, with the 5'-terminal 1-55 replaced with the complementary sequence, shown not to form a G-quadruplex (Fig 5.6).

The online tool provided for Stellaris FISH probe design was unable to design a complete set of unique probes for eGFP. However, specialists at Biosearch had designed and validated a set of eGFP probes, which we were able to purchase. A set of 38 unique probes of 20 nucleotides in length were labelled with CALflourRED590. This fluorophore was chosen as the excitation and emission peaks best match the filters of our Zeiss Axioplan 2 fluorescence microscope.

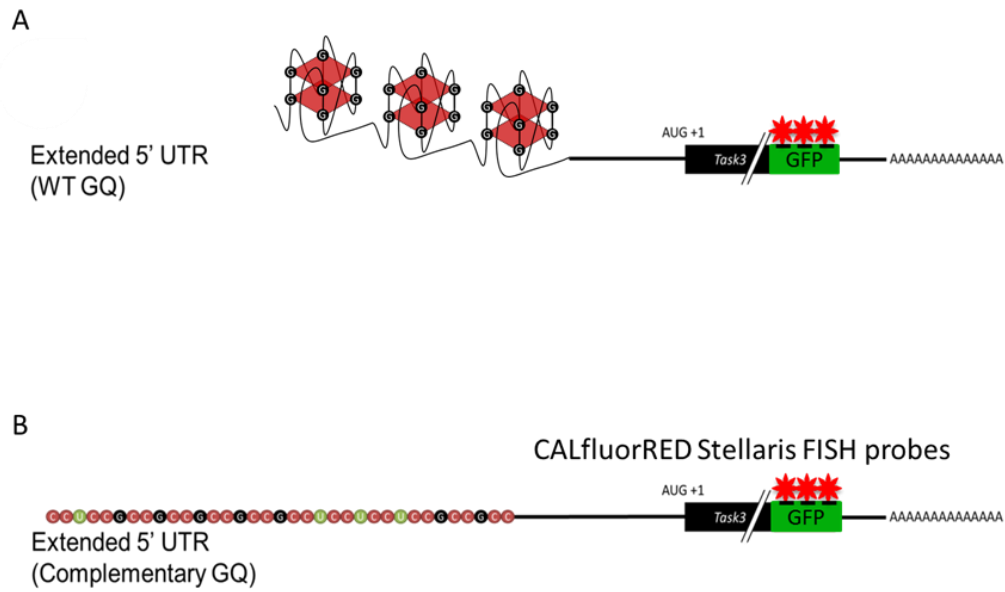


Figure 5.6 The Stellaris FISH probes were used for detection of **A)** the wild-type Task3 mRNA, characterised by its 5' terminal G-quadruplex in transfected cells. **B)** The negative control for the effect of the 5'-terminal G-quadruplex on mRNA localisation is the same Task3-GFP construct, with the 5'-terminal 1-55 replaced with the complementary sequence, shown not to form a G-quadruplex.

5.2.4 Detection of the subcellular localisation of Task3-GFP mRNA by Stellaris FISH

HeLa cells offer high transfection efficiency and are well characterised for fluorescence microscopy studies. HeLa cells were transfected with wild-type G-quadruplex Task3-GFP and the negative control; complementary sequence 1-55. The Stellaris FISH probes for eGFP were used to measure the difference in mRNA localisation by immunofluorescence microscopy. Task3-GFP protein produced from mRNA of the test expression vectors is measurable without the need for antibody probing.

The mRNA and protein of wild-type G-quadruplex Task3-GFP and the negative control were similarly distributed in transfected HeLa cells (Fig. 5.7). FISH signal was considered to be specific to Task3-GFP mRNA due to no signal observed in control untransfected preparations. The mRNA localised throughout the cytoplasm, with some granules proximal to the ER. These are likely to be P-bodies, formed due to the overexpression of the mRNA. HeLa take up a relatively large amount of DNA at transfection, and typically express high levels of transfected protein. Confocal microscopy was used to achieve greatest resolution of subcellular localisation of Task3-GFP mRNA, although it is recommended to use wide-field microscopy with Stellaris probes, because of the low signal expected from detection of endogenous, lowly expressed mRNAs.

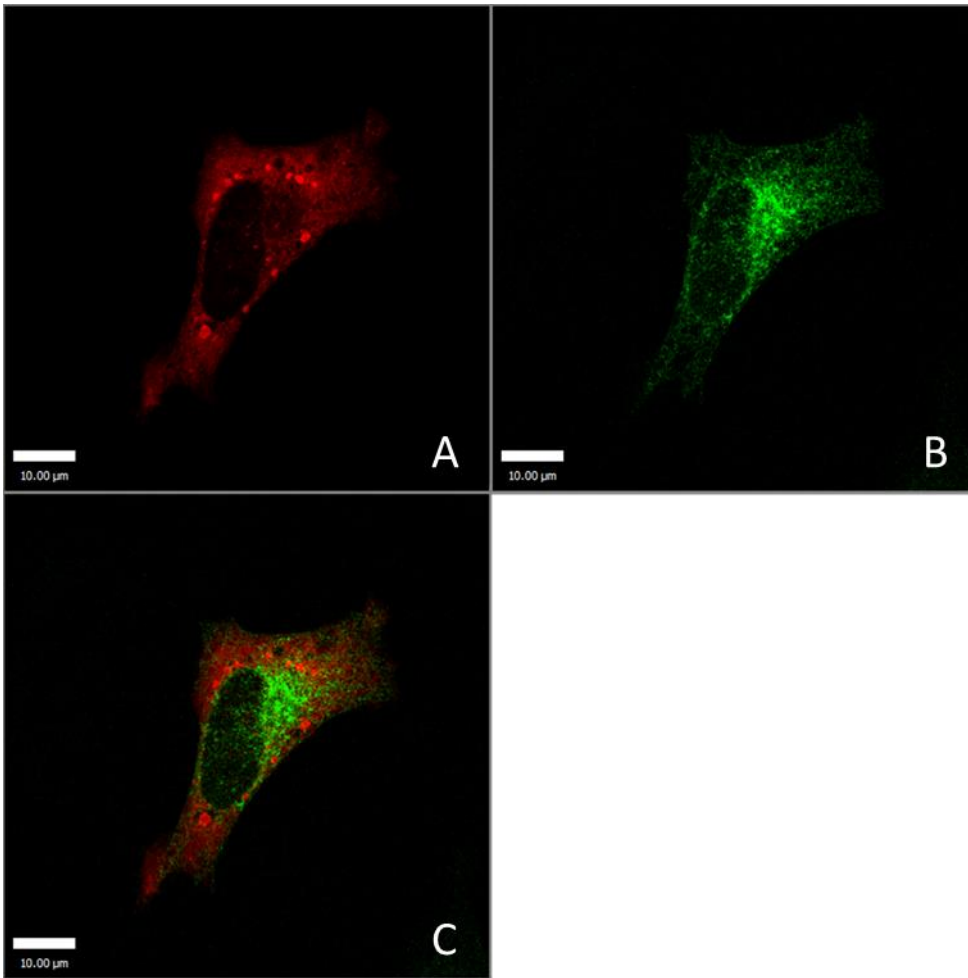


Figure 5.7 Expression of WT GQ Task3-GFP mRNA **A)** in red, detected by Stellaris GFP probe set. **B)** GFP signal (green) and **C)** merge of green and red channels to show relative distribution of WT GQ Task3-GFP mRNA and its protein. Image acquired using Leica SP8 confocal microscope.

5.2.5 The 5'-terminal G-quadruplex in Task3 mRNA mediates localisation of mRNA to neurite particles in transfected primary neurons

Task3 is highly expressed in neuronal cells and is able to exert control over local membrane potential. It is therefore of great interest to investigate whether the 5' terminal G-quadruplex of Task3 mRNA causes differential localisation in neurons, which would suggest a role of Task3 in controlling local excitability within discrete subcellular regions of neurons, such as dendritic spines.

To investigate the effect of the 5' terminal G-quadruplex on Task3-GFP mRNA subcellular localisation, primary cultures of mouse cortical neurons were transfected with wild-type G-quadruplex Task3-GFP and the negative control; complementary sequence 1-55. The Stellaris FISH probes for eGFP were used to measure the difference in mRNA localisation by wide-field fluorescence microscopy. The distance between Stellaris FISH signal particle and the cell soma was quantified using Volocity 6.0 distance measurement tool. The detection of Task3 mRNA particles in neurons transfected with wild-type GQ Task3-GFP, was distributed along the lengths of neurites, a long way from the cell soma (Fig. 5.8 & Fig. 5.9). Task3 mRNA was only detected close to the cell soma in neurons transfected complementary GQ Task3-GFP (Fig. 5.10 & Fig. 5.11). The experiments in Fig. 5.8 – 5.11 were conducted three times and transfection efficiency was approximately 3%, meaning a total number of cells for comparison of 5-10 per experiment. This meant only a small number of transfected healthy neurons were observed.

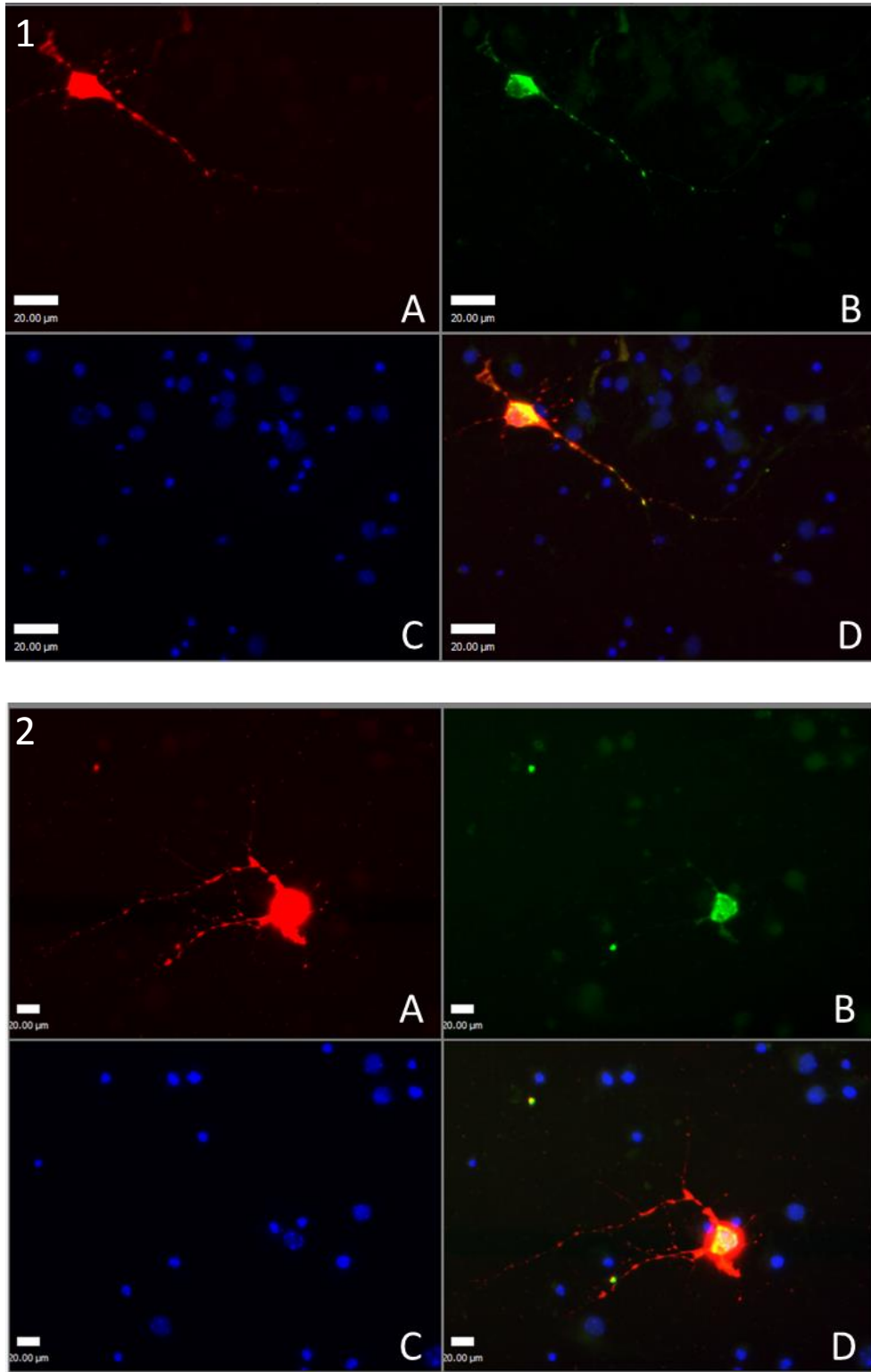


Figure 5.8 1 & 2 The WT G-quadruplex Task3-GFP mRNA is localised to discrete particles along neurites of transfected primary cortical neurons. **A)** mRNA detected by Stellaris CALfluorRED590 FISH probes against eGFP. **B)** Task3-GFP expression. **C)** DAPI nuclear stain. **D)** Merge of 3 channels. The experiment was conducted three times and transfection efficiency was approximately 3%.

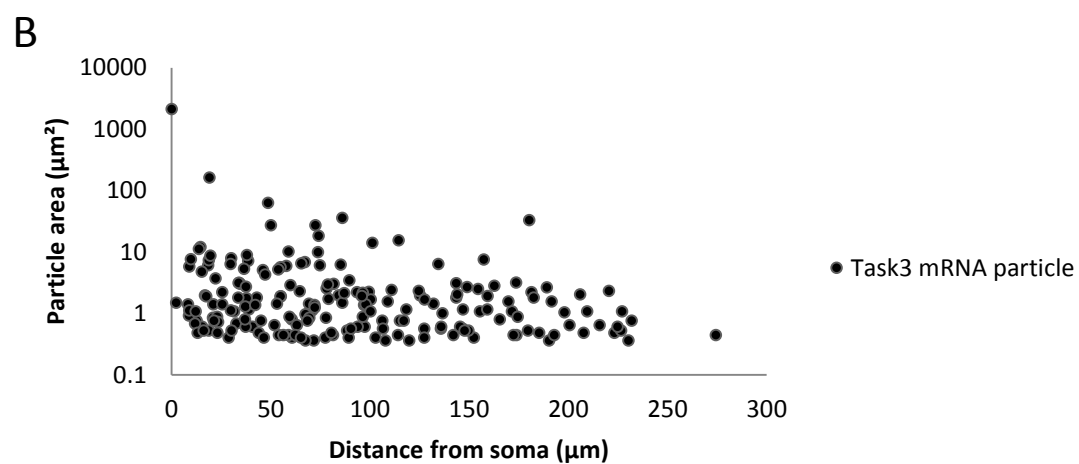
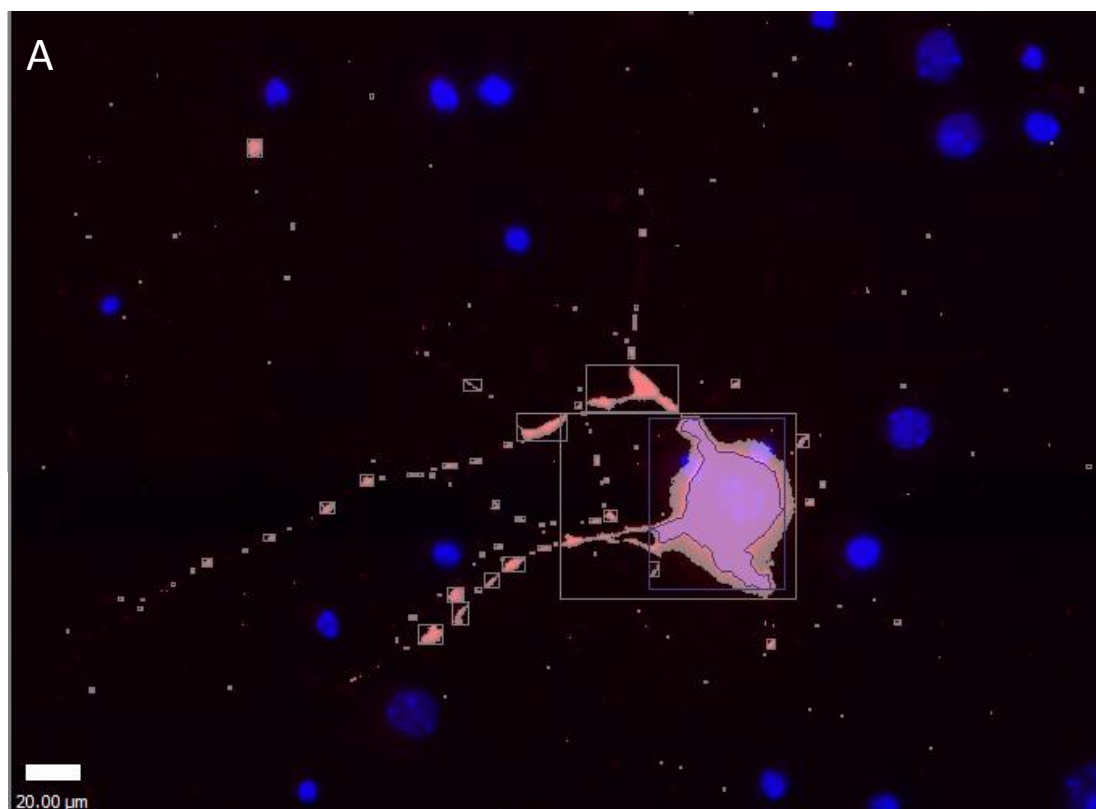


Figure 5.9 The distribution of WT G-quadruplex Task3-GFP mRNA was measured using Volocity image analysis software from Perkin Elmer. A) Fluorescence thresholding was used to automatically define regions of interest (ROIs), in this case, high red fluorescence, representing WT G-quadruplex Task3-GFP mRNA localisation (ROIs) coloured in white). The soma of the cell is defined by the lilac region. B) Distance measurements were made using Volocity to quantify the size of Task3 mRNA particle and distance from the soma.

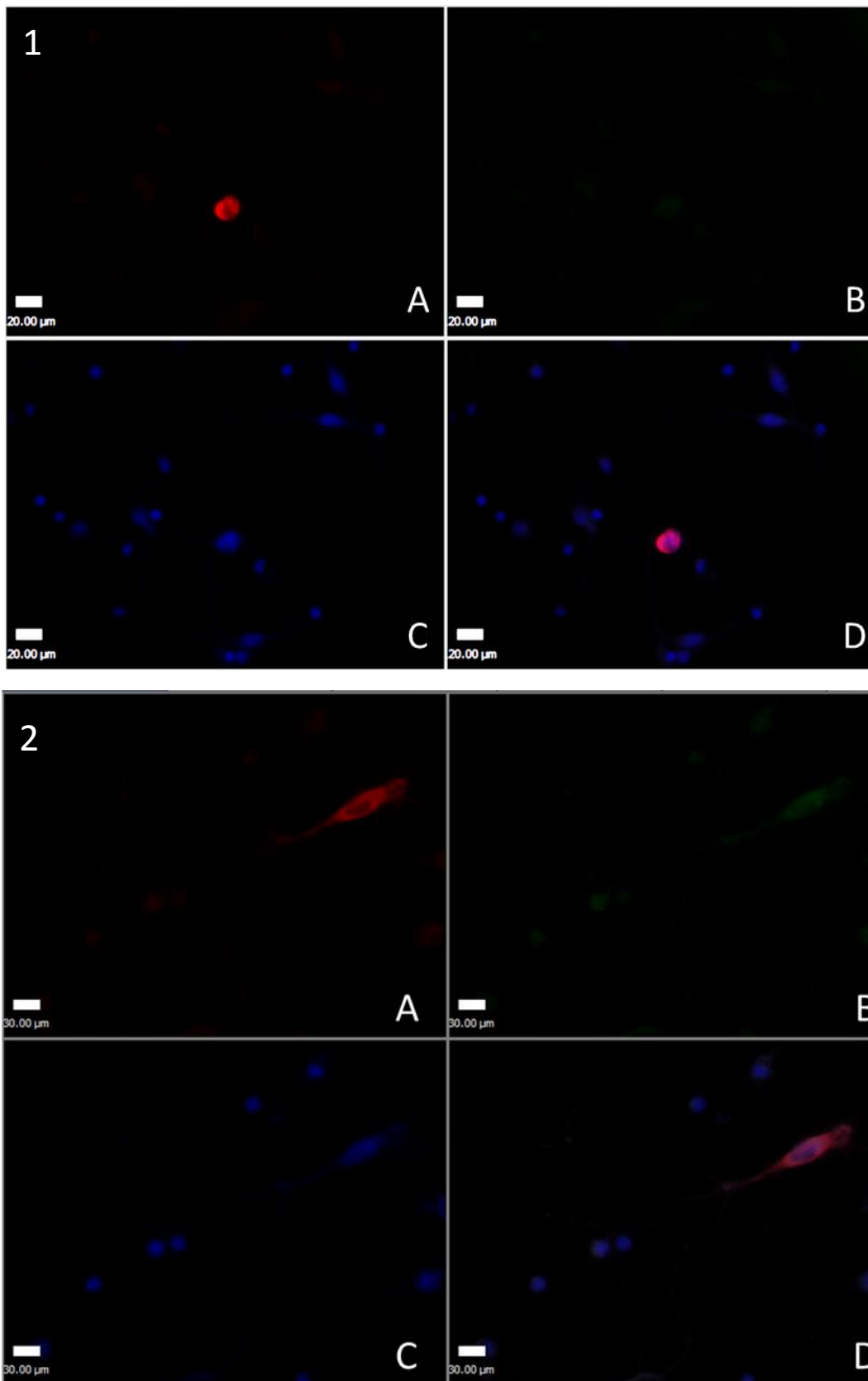


Figure 5.10 1 & 2 The complimentary 1-55 Task3-GFP mRNA is localised to the soma of transfected primary cortical neurons. **A)** mRNA detected by Stellaris CALfluorRED590 FISH probes against eGFP. **B)** Task3-GFP expression. **C)** DAPI nuclear stain. **D)** Merge of 3 channels. The experiment was conducted three times and transfection efficiency was approximately 3%.

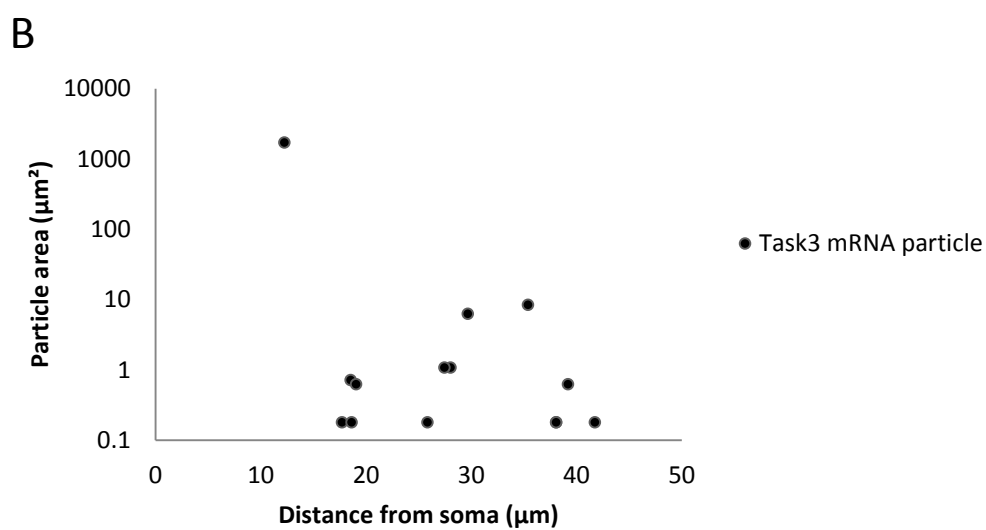
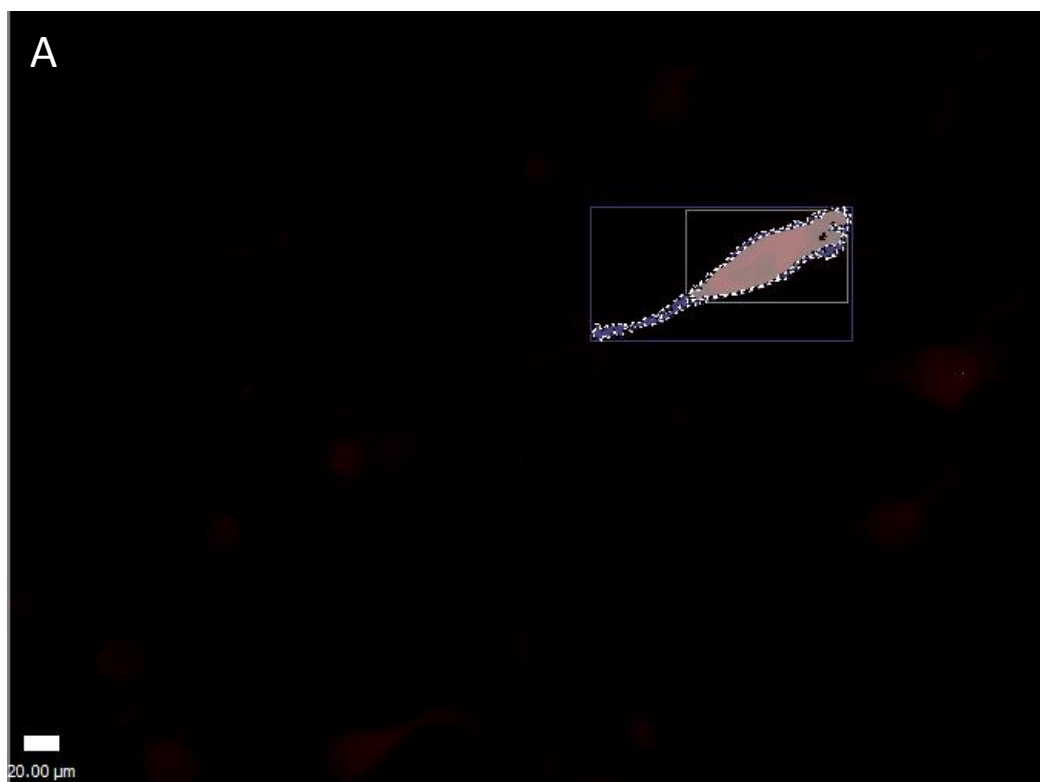


Figure 5.11 The distribution of the complimentary 1-55 Task3-GFP mRNA was measured using Volocity image analysis software from Perkin Elmer. A) Fluorescence thresholding was used to automatically define regions of interest (ROIs), in this case, high red fluorescence, representing WT G-quadruplex Task3-GFP mRNA localisation (ROIs) coloured in white). The soma of the cell is defined by the lilac region. B) Distance measurements were made using Volocity to quantify the size of Task3 mRNA particle and distance from the soma.

5.2.6 Task3-GFP expression vectors were mutated to Task3-BFP for RBP co-localisation experiments

GFP was the most suitable of the fluorescent proteins as an epitope tag for experiments above due to its high fluorescence and compatibility with DAPI nuclear stain and red Stellaris probe set. However, in order to examine co-localisation of RBPs with Task3 mRNA, the use of the three channels in our Zeiss Axioplan 2 fluorescence microscope must be used differently. The Stellaris probe set was expensive and its use in measuring Task3 mRNA localisation has been successful. The Coldwell lab has optimised the use of two secondary Alexafluor antibodies to measure primary antibody binding of target proteins, 488 and 550nm, green and red. A blue secondary antibody was tested, but gave a low signal. A far-red antibody was also tested, but emission and excitation spectra overlapped with the Stellaris 590 probe set. This means that the red channel is occupied with Stellaris CALfluorRed590 and the green channel is used for the 488 nm Alexafluor secondary antibody, for measuring RBPs. Simultaneous measurement of RBPs and Task3 protein translated from transfected plasmids required a change of the Task3 epitope tag to blue. Blue Fluorescent Protein (BFP) is less fluorescent than GFP, however, measurement of the Task3 protein is not the principal question. Instead, we were looking for RBP co-localisation with the Task3 mRNA.

Our GFP is Enhanced GFP (eGFP), with the mutations F64L and S65T. Mutation of GFP Y66H changed colour to blue, a Blue Fluorescent Protein (eBFP). Mutation Y145F has been shown to double the brightness of eBFP (Patterson *et al.*, 1997), so we also mutated our sequence Y145F (Fig. 5.12). The Stellaris probe set against eGFP consists of 38 short DNA probes which do not overlap on the target sequence, so the maximum number of mismatches caused by the mutation to eBFP is two; which is predicted to have only very minor impact on the detection power of the probe set. The two Task3-eBFP plasmids were expressed in HeLa cells to test detection of eBFP signal using wide-field fluorescence microscopy (Fig. 5.13).

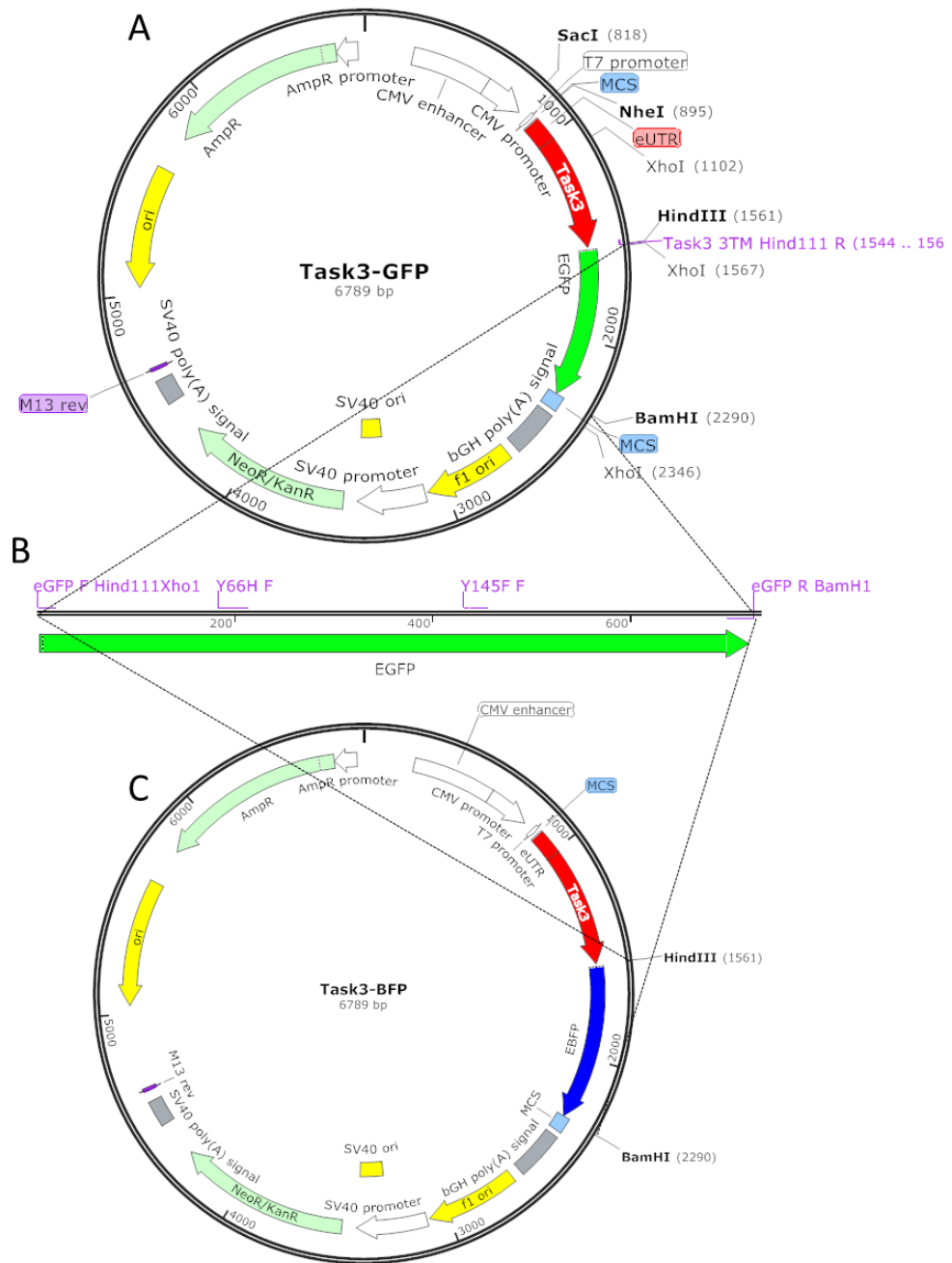


Figure 5.12 A) Task3-GFP expression vectors were mutated to Task3-BFP for RBP co-localisation experiments by PCR **B)** first with 3:1 mutagenic primer Y66H : eGFP F HindIII XhoI and eGFP R BamHI, then using the purified PCR product as the template for a second mutagenesis round, 3:1 mutagenic primer Y145F : eGFP F HindIII XhoI and eGFP R BamHI **C)** Task3-GFP and purified PCR product digested with HindIII and BamHI for ligation.

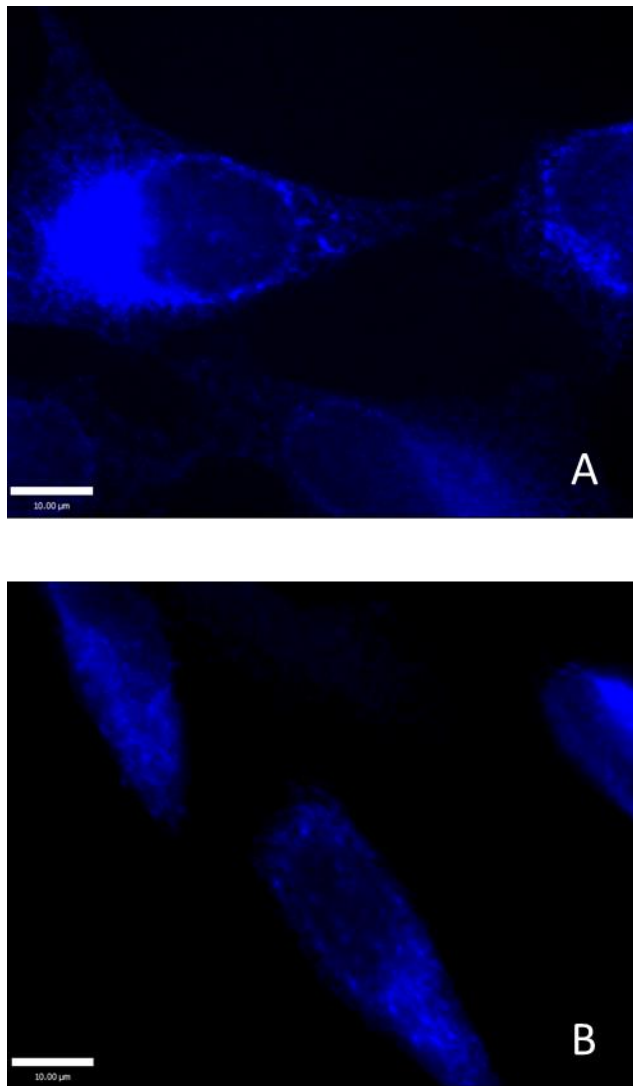


Figure 5.13 HeLa cells were transfected with **A)** WT GQ Task3-BFP and **B)** complementary GQ Task3-BFP; the 5'-terminal 1-55 replaced with the complementary nucleotide sequence.

5.2.7 hnRNPA2 expression does not alter Task3-BFP mRNA localisation in transfected HeLa cells

The heterogeneous nuclear ribonucleoprotein A2 (hnRNP A2) was shown to affect translation rates of Task3-FLAG, dependent on its 5'-terminal G-quadruplex (Chapter 4). hnRNP A2 has been shown to bind CGG repeat RNA (Sofola *et al.*, 2007) and synaptic mRNAs in neuronal RNPs. hnRNP A2 sequestration by (CGG) repeat RNA prevents dendritic localisation of normally dendritically localised mRNAs (Muslimov *et al.*, 2011). hnRNP A2-binding of G-quadruplex mRNA appears to be an important regulator of G-quadruplex-containing mRNAs. To investigate whether hnRNP A2 affects the subcellular trafficking of Task3 mRNA, pCMV2-Flag-hnRNP A2 was co-transfected with Task3-BFP in HeLa cells. Stellaris GFP probes were used to image Task3-BFP mRNA localisation, and hnRNP A2 localisation was measured by probing with FLAG primary antibody and 488 nm Alexafluor secondary antibody (Fig. 5.14). FLAG-hnRNP A2 localised primarily to nuclei of transfected HeLa cells, away from the detected mRNA of WT GQ Task3-BFP, in the cytoplasm. However, some FLAG-hnRNP A2 also localised to the cytoplasm, and was distributed in a similar way to Task3-BFP mRNA. Further investigations are required. The resolution is insufficient to accurately measure co-localisation of the molecules, but is sufficient to whether the molecules localise to similar subcellular organelles.

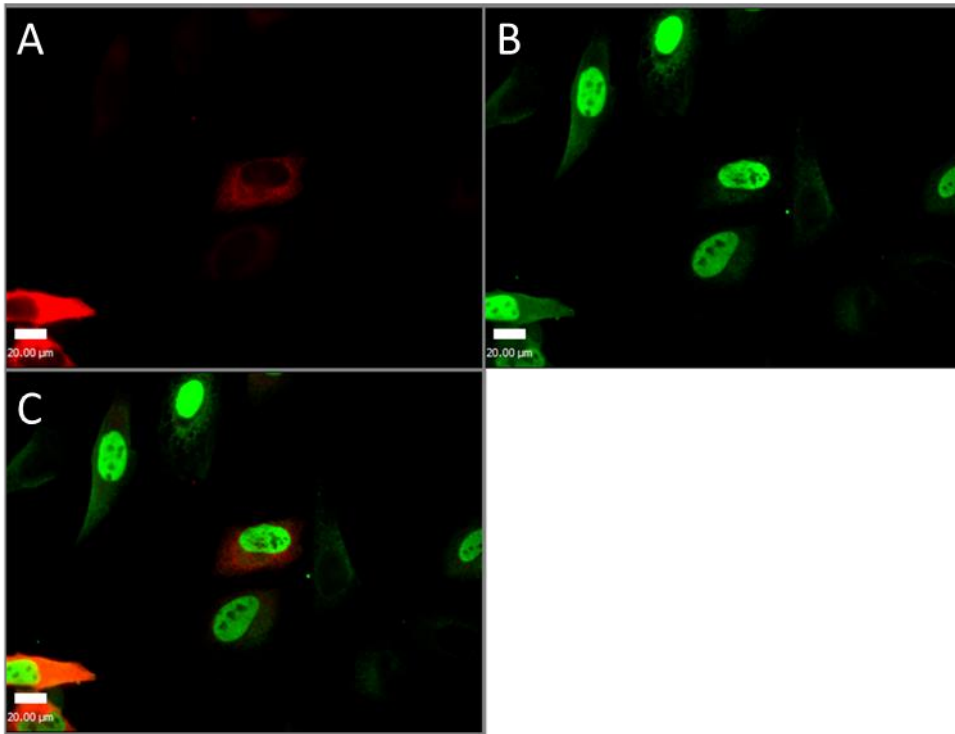


Figure 5.14 Measurement of the subcellular localisation of hnRNP A2 protein with Task3 mRNA **A)** Task3-BFP mRNA detected with Stellaris CALfluorRED 590 probes against GFP. **B)** hnRNP A2 localisation was measured by probing with FLAG primary antibody and 488 nm Alexafluor secondary antibody **C)** Merge of A & B.

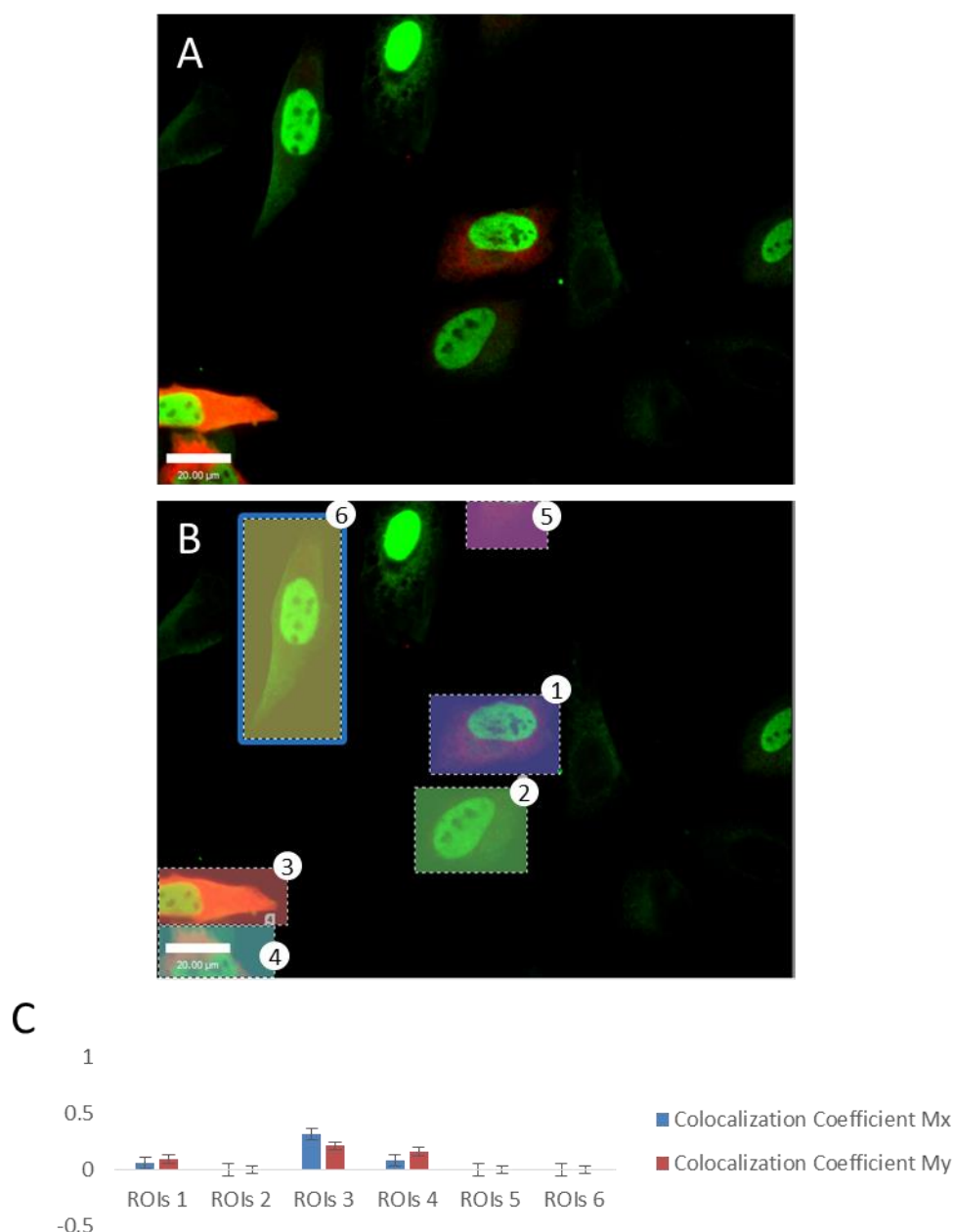


Figure 5.15 The majority of transfected hnRNP A2 localises to the nucleus, away from Task3-BFP mRNA, which is predominantly localised to outside the nucleus. **A)** Merge of Task3-BFP mRNA (red) and FLAG-hnRNP A2 (green). **B)** ROIs selected around co-transfected cells for colocalisation measurements with Volocity software. **C)** Graph showing the colocalisation coefficients, Mx and My, for Task3-BFP mRNA (red) and FLAG-hnRNP A2 (green) in ROIs 1 – 6. However, the resolution afforded by this technique does not allow for measurement of actual colocalisation of molecules, but does allow for measurement of similarity in subcellular distribution.

5.2.8 V5-Pur- α has a similar subcellular expression pattern as mRNA of transfected Task3-BFP in HeLa cells

The purine rich element binding protein α (Pur- α) specifically binds to CGG repeat G-quadruplex-forming mRNA sequences in *Drosophila* and mammals (Jin *et al.*, 2007). Pur- α is a component of neuronal RNPs, involved in the delivery of specific mRNAs to sites of dendritic translation (Johnson *et al.*, 2006). Over-expression of Pur- α in *Drosophila* prevents neurodegeneration mediated by CGG repeat mRNA (Jin *et al.*, 2007). Co-localisation of transfected V5-Pur- α with mRNA of transfected Task3-BFP would suggest a role for Pur- α in the regulation of Task-3 mRNA trafficking. Pur- α was cloned from human brain cDNA and ligated into a pcDNA3.1 plasmid with the V5-coding sequence inserted upstream of the MCS. V5-Pur- α was co-transfected in HeLa cells with WT G-quadruplex Task3-BFP. Stellaris GFP probes were used to image Task3-BFP mRNA localisation, and Pur- α localisation was measured by probing with V5 primary antibody and 488 nm Alexafluor secondary antibody. Results showed a high degree of co-localisation of V5-Pur- α and Task3-BFP mRNA (Fig. 5.16 and 5.17).

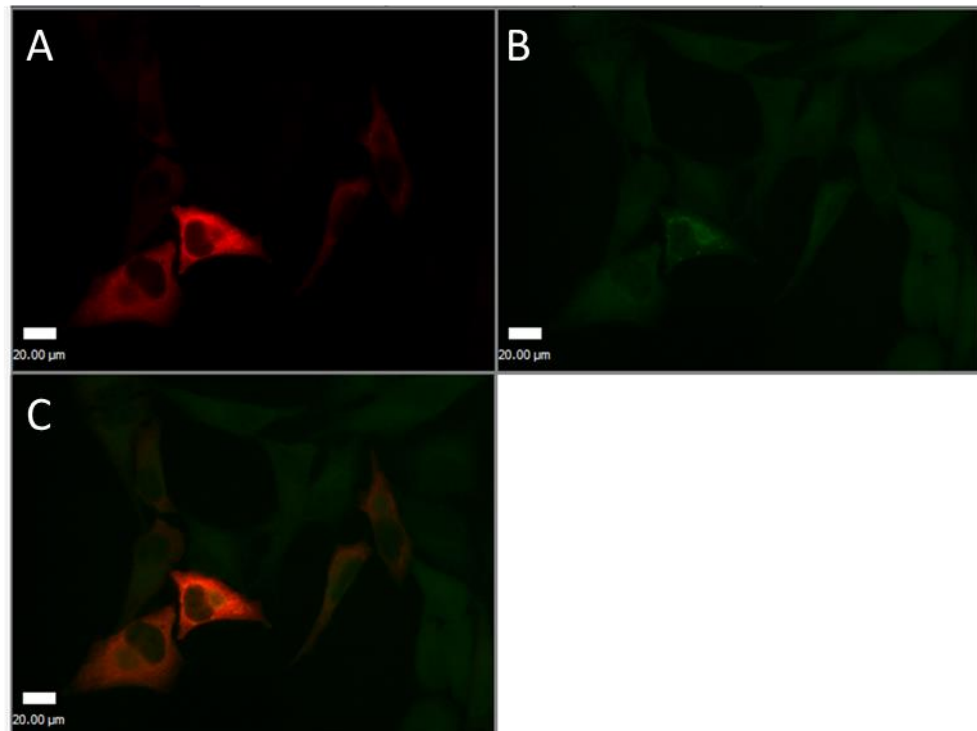


Figure 5.16 Measurement of the interaction of V5-Pur- α with Task3 mRNA **A)** Task3-BFP mRNA detected with Stellaris CALfluorRED 590 probes against GFP. **B)** V5-Pur- α localisation was measured by probing with V5 primary antibody and 488 nm Alexafluor secondary antibody **C)** Merge of A & B suggests similar subcellular distribution. However, the resolution afforded by this technique does not allow for measurement of actual co-localisation of molecules, but does allow for measurement of similarity in subcellular distribution.

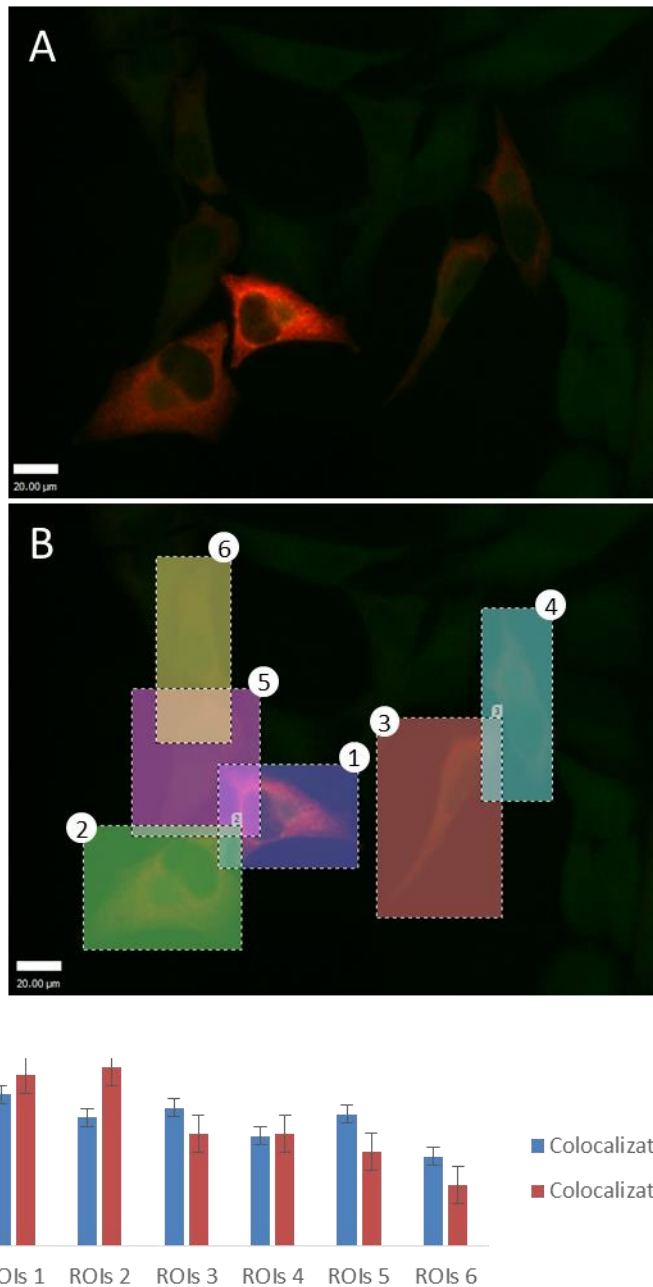


Figure 5.17 V5-Pur- α co-localises with mRNA of transfected Task3-BFP in HeLa cells. **A)** Merge of Task3-BFP mRNA (red) and V5-Pur- α (green). **B)** ROIs selected around co-transfected cells for co-localisation measurements with Volocity software. **C)** Graph showing the colocalisation coefficients, Mx and My, for Task3-BFP mRNA (red) and V5-Pur- α (green) in ROIs 1 – 6. The resolution afforded by this technique does not allow for measurement of actual co-localisation of molecules, but does allow for measurement of similarity in subcellular distribution.

5.2.9 Co-transfection of neurons with RBPs and Task3-BFP were unsuccessful

The role of hnRNP A2 and Pur- α in the regulation of Task3 mRNA transport and translation are predicted to be most relevant in neuronal cells, where these RBPs are known to be involved in neuronal RNP formation and transport. Co-expression of tagged RBPs in HeLa cells gives some idea of their roles in Task3 mRNA trafficking and translational control, and is relatively easy to execute because of the high transfection efficiency, high metabolic rate and robustness of HeLa cells. Cultures of primary neurons are difficult to transfect, with 5% transfection being an excellent result. The transfection of these cells is impaired in the presence of antibiotics, and the cells are also very susceptible to bacterial infection due to the method of cell culture preparation from whole mice. The health/robustness of primary neuron cultures is variable between dissections. Expression of transfected plasmids is lower than in HeLa cells, and so detection of expressed proteins and RNA by FISH is more difficult. Transfection of primary cortical neurons with pCMV2-Flag-hnRNP A2 or V5-Pur- α with Task3-BFP was attempted but did not produce useful results. Persistence in attempting these experiments is likely to reveal greater understanding of the roles of hnRNP A2 and Pur- α in the regulation of Task3 mRNA transport and translation.

5.3 Discussion

Chapter 4 determined that Task3 mRNA has a 5' terminal G-quadruplex which inhibits its translation. Task3 expression regulates the resting membrane potential of mammalian cells. Specific RBPs were shown to regulate expression of transfected Task3-FLAG protein dependent on the 5' terminal G-quadruplex. In this chapter, I have demonstrated that the 5'-terminal G-quadruplex of Task3 mRNA does not affect mRNA or protein localisation in HeLa cells.

In neurons, the local translation of mRNAs at activated synapses allows remodelling of the local proteome. Specific mRNAs are transported in a translationally repressed state in large RNPs, known as neuronal RNPs or neuronal mRNPs (messenger RNPs). mRNAs with G-quadruplexes in their untranslated regions have been found in neuronal RNPs.

Transport of specific mRNAs in neuronal RNPs is dependent on RBP recognition of their G-quadruplex sequences. hnRNP A2 has been found in free RNPs and ribosome associated RNPs at resting synapses in cultured hippocampal neurons (Leal, Afonso and Duarte, 2014). Synapse activation increases detectable hnRNP A2 in dendrites, partially dependent on endogenous BDNF release. Brain-derived neurotrophic factor (BDNF) is required for many forms of synaptic plasticity including long-term synaptic potentiation (LTP) (Leal, Comprido & Duarte 2014). hnRNP A2 has been identified as a KIF5-associated protein (Kanai *et al.*, 2004), implicating hnRNP A2 in the trafficking of particles along neuronal microtubules. CaMKII α and Arc are key protein determinants of synaptic plasticity; mRNAs encoding these proteins contain hnRNP A2 response element (A2RE). Dendritic localisation of CaMKII α and Arc is dependent on hnRNP A2 expression (Gao *et al.*, 2008). The hnRNP A2 protein was shown in Chapter 4 to partially relieve translation repression of Task3 mRNA due to its 5'-terminal G-quadruplex. Furthermore, hnRNP A2 binds CGG repeat RNA (Sofola *et al.*, 2007., Muslimov *et al.*, 2011). Here, we have shown hnRNP A2 primarily localises to the nucleus in transfected HeLa cells, away from Task3-BFP mRNA. hnRNP A2 has previously been found primarily in the nucleus (Cui *et al.*, 2010). Han *et al.*, (2010) found endogenous hnRNP A2 to be almost exclusively nuclear in HeLa cells. They also found a large proportion of endogenous hnRNP A2 localised throughout neurites of neurons.

Pur- α has been identified as a KIF5-associated protein (Kanai *et al.*, 2004), suggesting a role of Pur- α in the trafficking of neuronal RNPs. A genetic inactivation of Pur- α in mouse causes aberrant localisation of normally dendritically localised mRNAs. This demonstrates a requirement of Pur- α for dendritic transport of mRNAs essential for normal neuronal development (Johnson *et al.*, 2006). In this chapter we have found V5-Pur- α co-localises with Task3-BFP Task3-BFP mRNA in transfected HeLa cells. Further investigation is needed on the co-localisation of Pur- α and hnRNP A2 with Task3 mRNA in neurons. The identification of RBPs differentially associated with Task3 mRNA throughout subcellular regions of neurons will help characterise and understand the mechanisms by which Task3 mRNA is delivered to neurite particles and its translational control.

This chapter details experiments showing G-quadruplex-mediated delivery of Task3 mRNA to discrete RNPs throughout neurites of primary neurons. Further investigation is needed into the role of RBPs in targeting Task3 mRNA to neurites. The results of Chapter 4 should be investigated as potential modifiers of G-quadruplex-mediated neurite delivery of Task3, and other mRNAs with 5' UTR G-quadruplexes. TMPyP4 should be tested for effects on Task3 mRNA trafficking and translation in neurons. The role of DEAH RNA helicases should also be examined.

5.3.1 Conclusions

1. Expression vectors were cloned for GFP-Task3 fusion proteins.
2. Stellaris FISH probes specifically detect GFP-Task3 mRNA in transfected HeLa cells and neurons. No fluorescence was measured with the FISH probes in untransfected control cells.
3. Transfection of primary cortical neurons with GFP-Task3 expression vectors had a transfection efficiency of approximately 3%. In successfully transfected cells, GFP-Task3 mRNA was measured in the neurites of neurons. However, this needs to be repeated at a much larger scale to validate this result. Higher resolution techniques including single molecule FRET would allow greater measurement of the subcellular localisation of Task3 mRNA.
4. The study of RNPs containing Task3 mRNA requires further research. RNA immunoprecipitation (RIP) could be used to map *in vivo* RNA-protein

interactions of neuronal subcellular regions. The RBPs, Pur α , hnRNPA2 and DHX proteins may be immunoprecipitated together with interacting RNA for identification of bound RNA molecules, including Task3.

Chapter Six

Results

G-quadruplex mediated alternative translation initiation generates N-terminally diverse FXR2 proteins

6.1 Introduction

COFRADIC analysis and vertebrate conservation from the UCSC PhastCons multiple alignments (Siepel *et al.*, 2005, Van Damme *et al.*, 2014). COFRADIC analysis refers to the identification of protein N-terminal peptides by combined fractional diagonal chromatography (Gevaert *et al.*, 2003). The extended FXR2 isoform was found to have an N-terminal methionine, translated from a GUG, in a strong Kozak consensus sequence, at -219 from the annotated AUG at +1.

Fxr2 mRNA, in common with Fmr1, possesses CGG repeats within its 5' UTR. We and others (Weisman-Shomer, Naot and Fry; 2000) have shown mRNA GGN repeats can form G-quadruplex structures (Chapter 4). Mapping of the G-quadruplex-forming sequences within the 5' UTR of Fxr2 revealed a potential role for the G-quadruplexes in controlling the translation of the normal FXR2P protein, translated from +1 AUG, and a N-terminally extended FXR2P, translated from a GUG, in a strong Kozak consensus sequence, at -219. G-quadruplexes have previously been suggested to stall scanning ribosomes over proximal upstream initiation codons, increasing the rate of translation initiation from that codon (Bugaut & Balasubramanian, 2012).

Fragile X is the most common cause of inherited intellectual disability affecting approximately 1 in 5000 men and 1 in 10,000 women (Coffee *et al.* 2009). Normal expression of FMRP is essential for normal translation of neuronal RNAs responsible for normal dendritic spine morphology (Comery *et al.*, 1997). Epigenetic silencing of FMRP occurs when transcription of *fmr1* on the X chromosome is suppressed by hypermethylation of an expanded (>230) CGG repeat in the 5' UTR and promoter region of its DNA. Fragile X syndrome (FRAXA) results from this suppression of FMRP

expression, leading to dysregulation of neuronal mRNA expression and abnormal spine morphology. Synthesis of FMRP can also be stalled at translation. The translation of *fmr1* mRNA is dependent on the length of the 5' UTR CGG repeat. Fragile X tremor/ataxia syndrome (FXTAS) is caused by premutation CGG repeat lengths (55-200), which are not methylated, and instead cause overexpression of the *fmr1* mRNA (Jacquemont *et al.*, 2003). Premutation CGG repeats causes upstream Repeat Associated Non-AUG (RAN) translation and inhibits translation of the normal FMRP protein with translation initiated at AUG +1. RAN translation from aTICs generate polyglycine-containing protein, FMRpolyG (Todd *et al.*, 2013). FMRpolyG forms neuronal inclusions, indicative of protein-mediated neurodegeneration.

FMRP is involved in the processing of mRNAs for local translation in neurons, partly through recognition of G-quadruplex sequences in target mRNAs via FMRP's RGG domain. *Fmr1* mRNA has also been shown to be subject to G-quadruplex-mediated transport within neurons via a 3' UTR G-quadruplex. Khateb *et al.*, (2007) showed premutation CGG repeats formed G-quadruplex structures. When premutation CGG repeats were placed upstream of a firefly luciferase reporter, luciferase synthesis was greatly inhibited. The same paper also showed over-expression of the hnRNP G-quadruplex destabilising proteins, hnRNP A2 and CBF- α relieved repression of translation of the firefly luciferase reporter in transfected HEK293 cells. Ofer *et al.*, (2009) showed TMPyP4 relieved translational inhibition of the same firefly luciferase reporter by premutation CGG repeat lengths in its 5' UTR.

FMRP interacts with its two paralogs, Fragile X Related Proteins 1 and 2 (FXR1P and FXR2P). Although the functions of these paralogs are unclear, they are thought to compensate for lack of expression of FMRP. Like FMRP, FXR1P is an RBP with RNA G-quadruplex-binding properties responsible for normal mRNA transport and processing. FXR1P is highly expressed in muscle tissue where it is essential for normal muscle development (Davidovic *et al.*, 2008). FXR2P has been implicated in normal learning and memory processes in neurons. *Fxr2* KO mice display a similar intellectually disabled phenotype as *Fmr1* KO mice (Cavallaro *et al.*, 2008).

Ribosome profiling of mouse embryonic stem cells identified FXR2 to be subject to alternative upstream translation initiation. Ingolia *et al* (2011) used ribosome profiling to investigate the translome of Mouse Embryonic Stem Cells. The technique used harringtonine to stall ribosomes at sites of translation initiation.

Samples were then subjected to nuclease treatment, and ribosome-protected fragments were subjected to deep-sequencing. Results revealed unannotated translation start sites, both AUG and non-AUG, forming uORFs, eORFs and truncated ORFs. The H2G2 Genome Browser (<http://h2g2.ugent.be/biobix.html>) allows searching of this data, as well as comparison with peptide mapping data from N-terminal COFRADIC analysis and vertebrate conservation from the UCSC PhastCons multiple alignments (Siepel *et al.*, 2005, Van Damme *et al.*, 2014). COFRADIC analysis refers to the identification of protein N-terminal peptides by combined fractional diagonal chromatography (Gevaert *et al.*, 2003). The extended FXR2 isoform was found to have an N-terminal methionine, translated from a GUG, in a strong Kozak consensus sequence, at -219 from the annotated AUG at +1.

Fxr2 mRNA, in common with Fmr1, possesses CGG repeats within its 5' UTR. We and others (Weisman-Shomer, Naot and Fry; 2000) have shown mRNA GGN repeats can form G-quadruplex structures (Chapter 4). Mapping of the G-quadruplex-forming sequences within the 5' UTR of Fxr2 revealed a potential role for the G-quadruplexes in controlling the translation of the normal FXR2P protein, translated from +1 AUG, and a N-terminally extended FXR2P, translated from a GUG, in a strong Kozak consensus sequence, at -219. G-quadruplexes have previously been suggested to stall scanning ribosomes over proximal upstream initiation codons, increasing the rate of translation initiation from that codon (Bugaut & Balasubramanian, 2012).

6.2 Results

The 5' UTR of Fxr2 was identified by riboseq to be translated additionally from an upstream GUG codon at -219. Characterisation of alternative translation initiation sites using the ExTATIC macro identified a further two GUGs upstream and in frame of the annotated AUG at +1. The alternative initiation codons are at -138, -219 and -330 nucleotides upstream of the AUG initiation codon at +1 in the annotated CDS (Fig. 6.1).

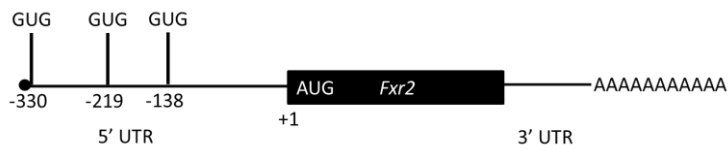


Figure 6.1 Diagram of the arrangement of in-frame upstream AICs in the 5' UTR of Fxr2 mRNA. There are three GUG AICs in frame of the CDS of Fxr2, at -138, -219 and -330 nucleotides upstream of the AUG initiation codon at +1 in the annotated CDS.

6.2.1 Fxr2-FLAG expression vectors were cloned from human brain cDNA

The Coldwell lab has a range of well-established techniques for investigating the usage of alternative translation initiation codons within an mRNA. Here, an initial assay of translation from 5' UTR AICs was employed. Fxr2 was cloned from human brain cDNA into pcDNA3.1-3xFLAG plasmid vector and mutated forms were created to test expression of Fxr2-FLAG protein products from alternative initiation codons. A truncated 5' portion of the CDS (252 nucleotides) was cloned in frame with the 3XFLAG sequence in pcDNA3.1 (Fig. 6.2). The truncation of the CDS has advantage over analysing expression from a full length CDS in that relative differences in molecular weight of bands are easy to resolve at the lower molecular weights, by western blot, produced from shortened transcripts compared to full length constructs. The predicted molecular weight of an Fxr2-FLAG protein from +1 AUG is 15 kDa. We generated a FLAG-tagged Fxr2 expression vector (WT FXR2, Fig. 6.3 A) and mutated vectors, with the -219 GUG mutated to an AUG in a strong context, with no preceding 5' sequence (-219 GUG-AUG FXR2, Fig. 6.3 B). We also created an Fxr2-FLAG plasmid with the 5' UTR deleted (Δ 5' UTR FXR2, Fig. 6.3 C). The WT FXR2 sequence was cloned using a forward cloning primer containing the very 5' terminal 5' UTR nucleotide sequence. The truncated, mutated GUG-AUG at -219, construct was created using a forward primer targeting the sequence starting immediately downstream of the -219 GUG codon, with a 5' Nhe1 site followed by an AUG codon. This 219 GUG-AUG FXR2 was designed to increase translation from the -219 position in the *fxr2* 5' UTR, and allow comparison with bands produced from cells transfected with the WT FXR2 construct. The Δ 5' UTR FXR2 was generated by targeting the forward cloning primer to the sequence beginning at the +1 AUG position, with the

cloning restriction site immediately upstream, thus deleting the 5' UTR. Comparison of the MW products from cells transfected with the Δ 5' UTR FXR2 enables identification of MW bands resulting from alternative translation initiation events in the 5' UTR, or potentially other effects of the 5' UTR.

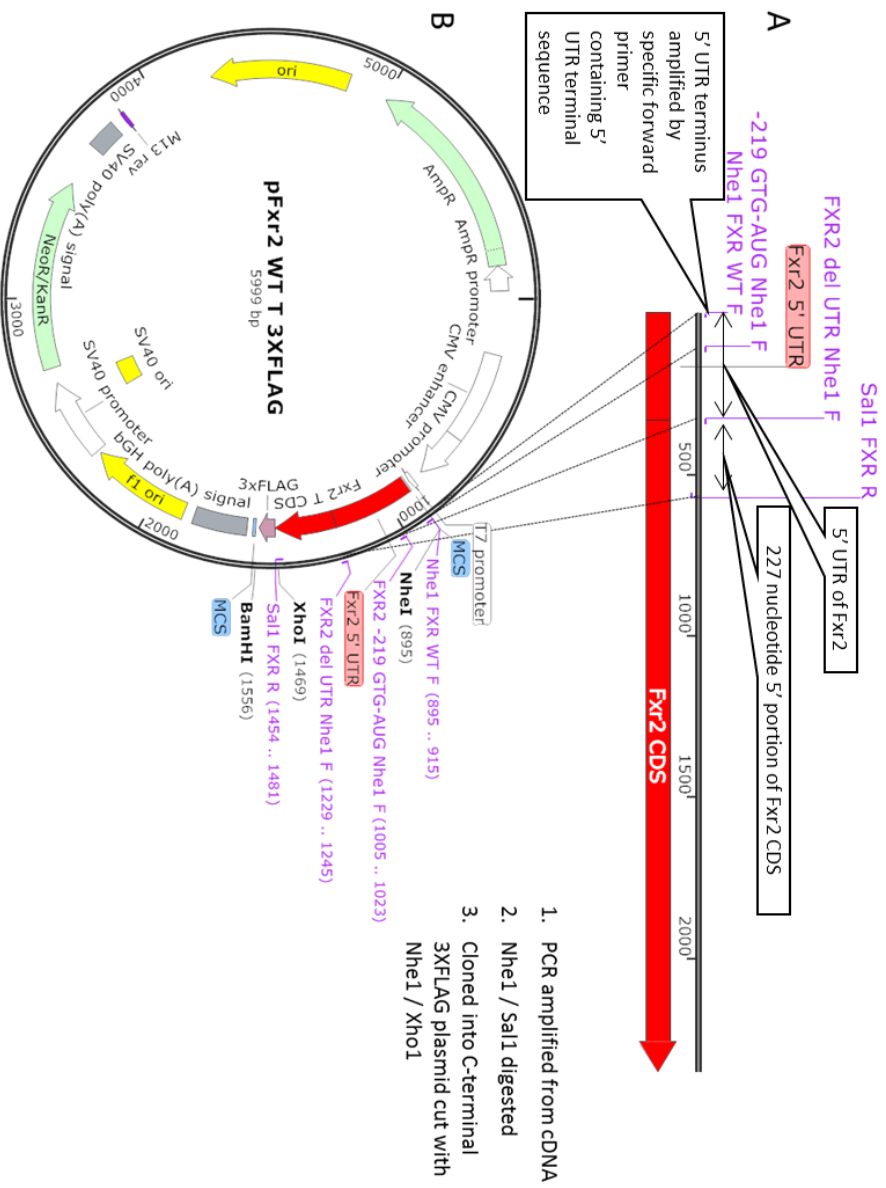


Figure 6.2 Fxr2 5'UTR test plasmids were generated **A)** using PCR products of a portion of the N-terminus coding sequence, and either no 5' UTR, a 5' UTR truncated at -219 with translation initiation codon, GUG mutated to AUG; and a full length 5' UTR with native (wild type) sequence. **B)** The purified PCR products were digested with Sal1 and Nhe1 for cloning into Nhe1 / Xho1 digested pCDNA3.1-3XFLAG expression vector.

6.2.2 Western blot of transfected HeLa cells lysate suggests Fxr2 is predominantly translated from -219 GUG

Western blot identified initiation codons corresponding to the MW of N-terminally extended Fxr2-FLAG proteins from translation initiation codon mutant vectors (Fig. 6.3). The majority of protein produced from the Fxr2-FLAG plasmid corresponds to the major band seen from the -219 GUG-AUG mutant plasmid. This indicates -219 as the main translation initiation codon in Fxr2 mRNA.

The MW of bands detected by western blot of lysates from cells transfected with these plasmids allowed identification of initiation codon usage. Results seen in figure 6.3 indicate Fxr2 is primarily translated from the codon identified by Riboseq, -219 GUG, as the most intense band is produced from the WT FXR2 plasmid at position of the predicted MW of the protein translated from -219 GUG (Fig. 6.3 D). The most abundant band in WT FXR2 is still present when the sequence upstream of the -219 GUG is removed (-219 GUG-AUG FXR2). Deletion of the 5' UTR caused the disappearance of the most abundant bands from seen from translation of WT FXR2 and -219 GUG-AUG FXR2, and the only band observed in the Δ 5' UTR FXR2 corresponds to the predicted MW of the translated peptide, initiating at +1 AUG. This band is present at very low abundance in lanes transfected with WT FXR2 and -219 GUG-AUG FXR2; this suggests the majority of ribosomes initiate translation at upstream AICs, mostly -219 GUG, and do not scan as far as the +1 AUG.

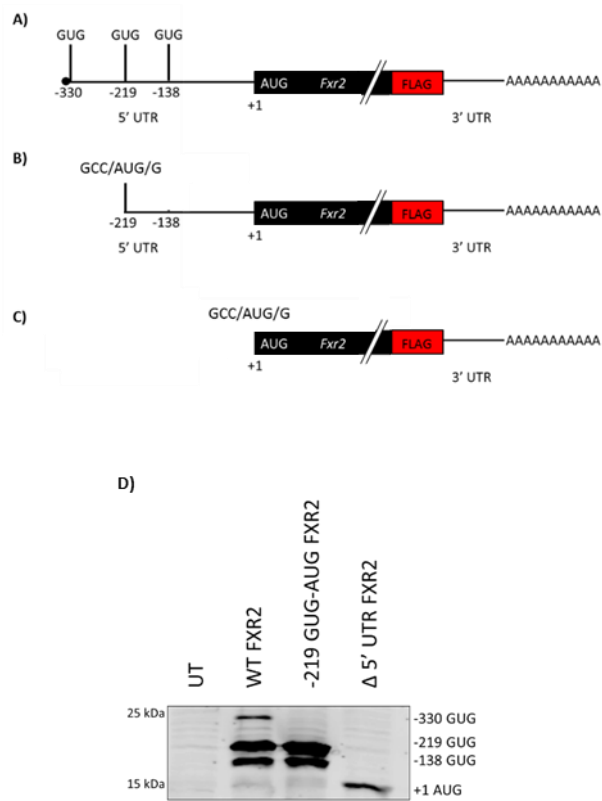


Figure 6.3 Western blot of lysates from HeLa cells transfected with **A)** wild-type 5' UTR Fxr2-FLAG, **B)** a truncated 5' UTR with the GUG at -219 mutated to an AUG, and **C)** an Fxr2-FLAG construct without the 5' UTR. **D)** The size of the bands detected using FLAG antibody are indicated on the left of the image, and the alternative initiation codon positions corresponding to observed peptide masses are indicated to the right of the image. The Western Blot was not quantified, as no loading control (β -actin) was measured. This experiment identifies the pattern of MW products expressed from constructs with test 5' UTRs. n =1

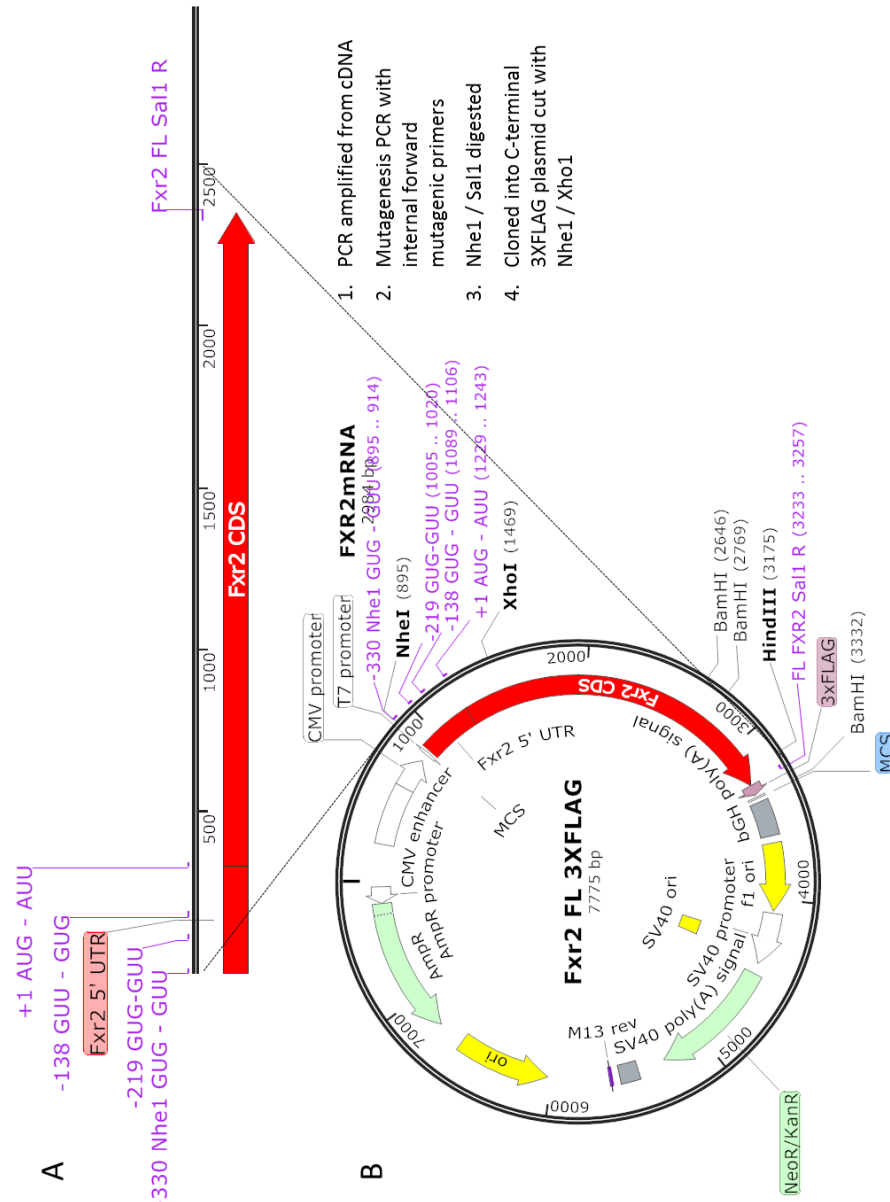


Figure 6.4 Full length coding sequence Fxr2 5' UTR test plasmids were generated **A**) using PCR products of the full protein coding sequence the full length 5' UTR with native (wild type) sequence, and variants with all but one initiation codon mutated out. **B**) The purified PCR products were digested with Sal1 and Nhe1 for cloning into Nhe1 / Xho1 digested pcDNA3.1-3XFLAG expression vector.

6.2.2 The -219 GUG initiates translation of Fxr2 in the absence of other initiation codons

To investigate whether translation initiates mainly from -219 GUG in a more natural state, full-length Fxr2 was cloned from human cDNA and the 5' UTR sequence was mutated to test sequences. Test 5' UTR sequences were created by use of mutagenic internal primers, mutating all but the target alternative translation initiation codon (Fig. 6.4). Test constructs were transfected into HeLa cells and SH-SY5Y neuroblastoma cells. SH-SY5Y are a commonly used model of neuronal cells, and are easy to transfect to high efficiencies, similar to efficiencies achieved in HeLa cells. Transfection of primary neurons is only achieved with low efficiency. It is easy to generate large quantities of SH-SY5Y cells in culture for transfection experiments, whereas, preparation of primary neuronal cultures requires far greater resource to achieve the same number of cells for transfection. However, it was deemed suitable to look at the use of alternative translation initiation codons in Fxr2 in a context more closely resembling a neuronal cell.

Western blot of lysates from HeLa cells and SH-SY5Y cells transfected with test plasmids confirmed the high strength of translation initiation from -219 relative to +1 AUG and other alternative upstream GUGs (Fig. 6.5).

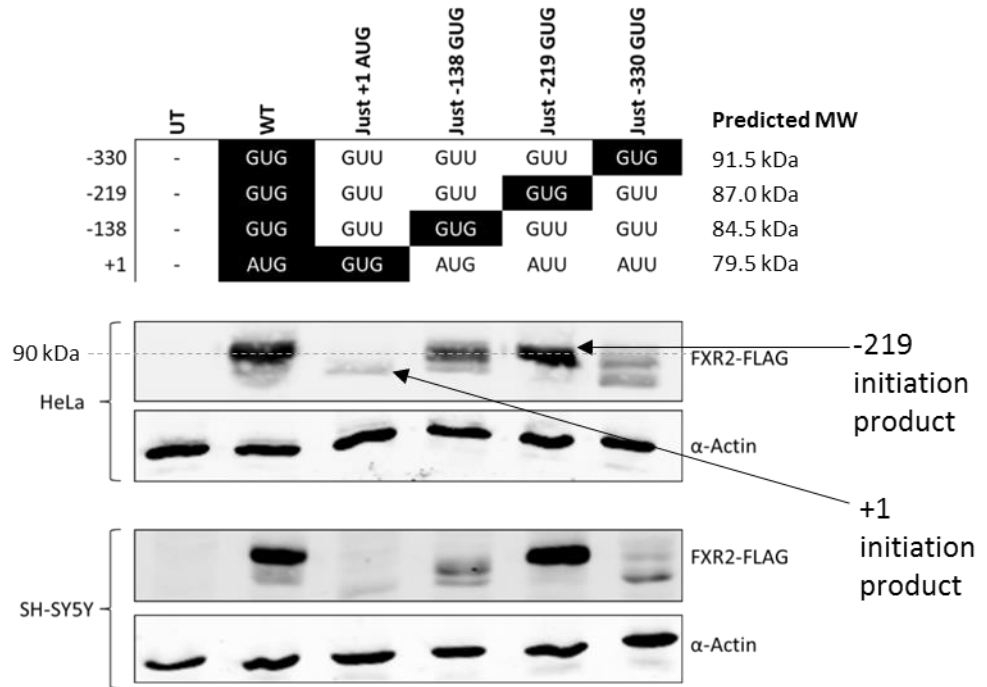


Figure 6.5 Western blot of lysates from HeLa cells transfected with Fxr2 plasmids of the full protein coding sequence with the full length 5' UTR with native (wild type) sequence, and variants with all but one initiation codon mutated out. Fxr2-FLAG bands detected in each lane represent the translation of protein from that initiation codon, in the absence of contextual AICs. Blots not quantified. n = 1.

6.2.3 There are multiple putative G-quadruplex-forming sequences in the 5' UTR of Fxr2 mRNA

The 5' UTR of Fxr2 is very GC rich. QGRS Mapper was used to analyse the 5' UTR of the 5' UTR of FXR2 mRNA for putative G-quadruplex-forming sequences. Multiple QGRS were identified within the 5' UTR and some predicted G-quadruplexes were identified immediately upstream or downstream of putative translation initiation sites. The alternative translation initiation site found by Riboseq, at -219, has a QGRS immediately downstream, but a QGRS-free region 15 bases upstream (Fig 6.6).

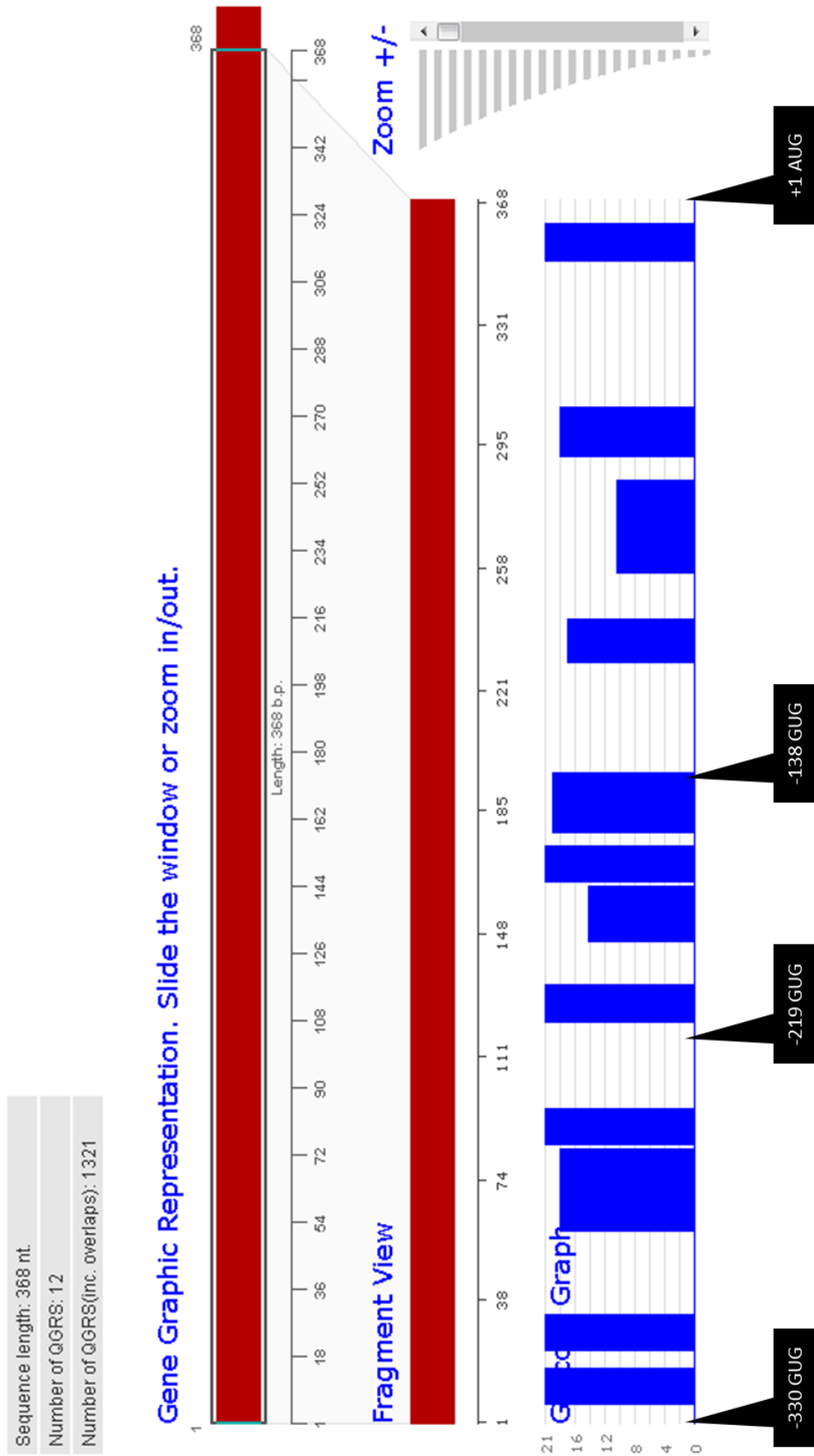


Figure 6.6 QGRS Mapper was used to analyse the 5' UTR of the 5' UTR of FXR2 mRNA. Multiple QGRS were identified within the 5' UTR. Some predicted G-quadruplexes were identified immediately upstream or downstream of putative translation initiation sites. The alternative translation initiation site found by Riboseq, at -219, has a QGRS immediately downstream, but a QGRS-free region 15 bases upstream.

6.2.4 Creation of purified RNA of the wild-type Fxr2 5' UTR

In order to measure the physical characteristics of the 5' UTR secondary structure, it was necessary to *in vitro* transcribe and purify mRNA. Purified mRNA of the 5' UTR of Fxr2 mRNA was synthesised by T7 polymerase *in vitro* transcription from linearized pcDNA3.1 3F Fxr2 (Fig 6.7).

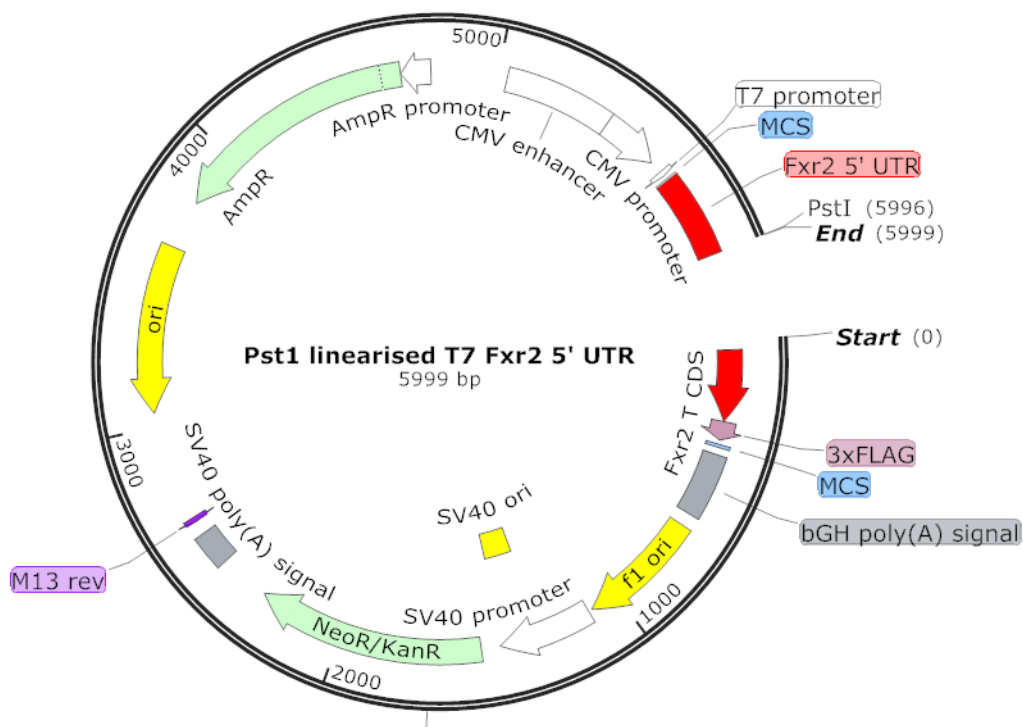


Figure 6.7 A linearized template for *in vitro* transcription of Fxr2 5' UTR sequence was generated by digestion of pcDNA3.1 3F Fxr2 with PstI. Purified DNA template was used as the template for synthesis of RNA of the wild-type 5' UTR of Fxr2.

6.2.5 CD spectroscopy showed G-quadruplex structures in the 5' UTR of Fxr2 mRNA, destabilised by TMPyP4

Jasco J710 CD spectrometer was used for the measurement of changes in peak intensity at 262 nm, indicative of parallel G-quadruplex structures. Large peak differences in absorbance at 262 nm were seen for Fxr2 5' UTR. The peak at 262 nm was reduced by the addition of TMPyP4 (Fig. 6.8). This needs to be repeated with positive and negative control RNAs. The NRAS G-quadruplex RNA sequence used in the analysis of the G-quadruplex of Task3 in Chapter 4 would be suitable as a positive control. The experiment needs repeating to ensure reproducibility of the results observed.

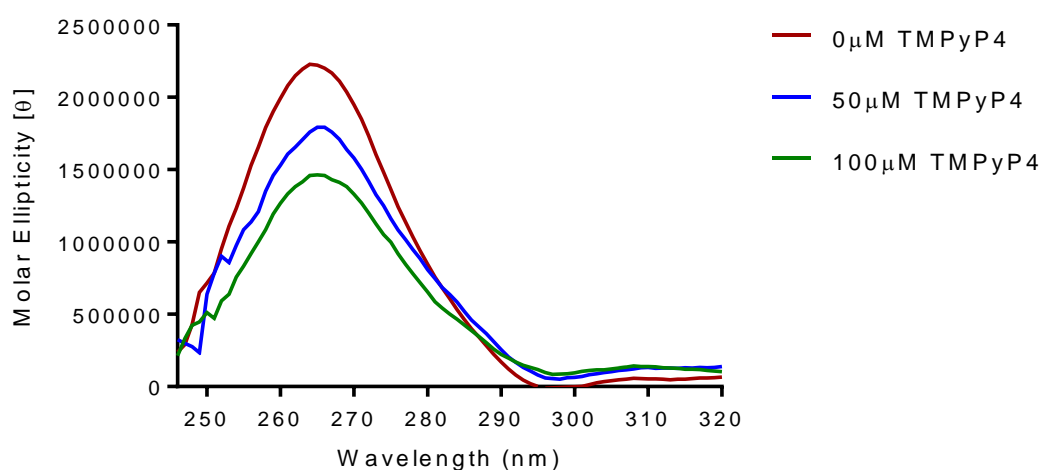


Figure 6.8 Jasco J710 CD spectrometer was used for the measurement of changes in peak intensity at 262 nm, indicative of parallel G-quadruplex structures. Large peak differences in absorbance at 262 nm were seen for Fxr2 5' UTR. The peak at 262 nm was reduced by the addition of TMPyP4.

6.2.6 TMPyP4 and Hippuristanol modulate expression of extended and normal length Fxr2p

In Chapter 4, we tested the ability of small molecule ligands, TMPyP4 and Hippuristanol to modify the expression of Task3 in a G-quadruplex-dependent fashion. Although Ofer *et al.* (2009) published the ability of TMPyP4 to unfold (CGG)_n quadruplexes *in vitro*, we show in Chapter 4.2.14 that TMPyP4 halves the global rate of translation in HeLa cells at half the concentration needed to relax G-quadruplex structures (Chapter 4.2.15). This suggests that differences in translation rate of specific mRNAs, such as *fxr2* test constructs here, may not be due to unwinding of the G-quadruplex structures by TMPyP4, but instead may be a result of changes in cell biology resulting from cell stress. TMPyP4 was able to relieve some of the translational inhibition resulting from its mRNA's 5' terminal G-quadruplex. However, there was no major change in translation of Task3-FLAG following Hippuristanol treatment of transfected cells.

Western blot of cell lysate from transfected HeLa cells shows Fxr2-FLAG abundance with and without treatment with 100μM TMPyP4 or 10μM Hippuristanol (Fig. 6.9). The western blot signal intensities were measured and show a very small decrease in FXR2-FLAG translation from -219 GUG Vs +1 AUG upon TMPyP4 treatment. Hippuristanol treatment showed a minor increase in synthesis of Fxr2-FLAG from -219 GUG relative to +1 AUG. This suggests that there are different structures within the 5' UTR of Fxr2 compared to Task3's 5' UTR, or it might reflect the different positions of the G-quadruplexes in Fxr2 5' UTR relative to Task3 mRNA.

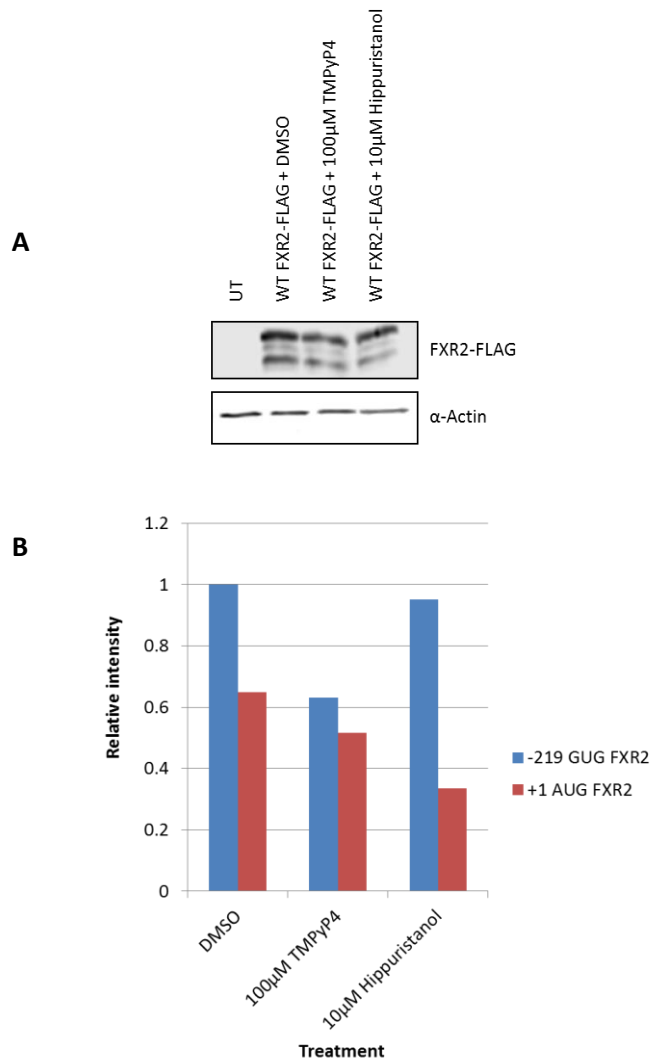


Figure 6.9 **A)** Western blot of cell lysate from transfected HeLa cells shows Fxr2-FLAG abundance with and without treatment with 100µM TMPyP4 or 10µM Hippuristanol. **B)** The western blot signal intensities were measured and show a relative decrease in FXR2-FLAG translation from -219 GUG Vs +1 AUG upon TMPyP4 treatment. Hippuristanol treatment increased synthesis of Fxr2-FLAG from -219 GUG relative to +1 AUG. n = 1

6.2.7 Co-transfection of Fxr2p with FLAG-tagged DHX expression constructs modulated expression of extended and normal length Fxr2p

Chapter 4 describes the effects of DEAH RNA helicases on the translation of Task3 mRNA relative to a G-quadruplex at its 5' terminus. We hypothesised that DHX proteins may regulate unfolding of G-quadruplex structures within the 5' UTR of Fxr2 mRNA, and potentially, differentially regulate translation initiation from alternative sites within the 5' UTR. FLAG-DHX expression vectors were co-transfected with wild-type 5' UTRFxr2-FLAG in HeLa cells. Western blot of cell lysate from transfected HeLa cells showed Fxr2-FLAG abundance with and without co-transfection with FLAG-DHX29/30/36. FLAG bands were measured relative to actin at positions corresponding to the MW of peptides translated from -219 and +1 AICs. Co-transfection with FLAG-DHX29/30/36 differentially increased synthesis of Fxr2-FLAG from +1 AUG relative to -219 GUG (Fig. 6.10). These are preliminary results and need to be repeated to achieve statistically reliable results. In these preliminary results, DHX29 had the most minor effect on changing the ratio of translated Fxr2 isoforms, DHX30 showed a moderate effect, and DHX36 displayed the largest shift in ratio of extended Fxr2 Vs annotated Fxr2 protein.

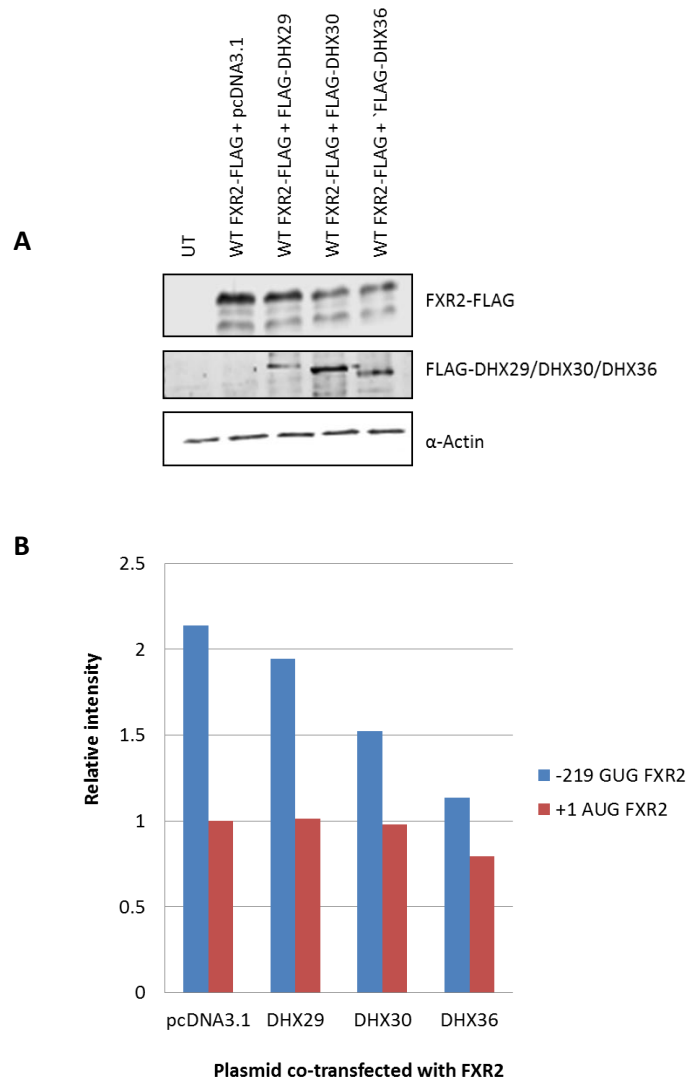


Figure 6.10 A) Western blot of cell lysate from transfected HeLa cells shows Fxr2-FLAG abundance with and without co-transfection with FLAG-DHX29/30/36. **B)** Measurement of FLAG bands at positions corresponding to the MW of peptides translated from -219 and +1 AICs. Co-transfection with FLAG-DHX29/30/36 differentially increased synthesis of Fxr2-FLAG from +1 AUG relative to -219 GUG. n = 1

6.2.8 Investigating subcellular localisation of Fxr2 protein isoforms

The N-terminal extension of Fxr2 protein resulting from translation initiation at -219 GUG, may cause differential subcellular localisation. The N-terminal extension of proteins derived from upstream alternative translation initiation have been found to differentially localise to subcellular locations (Coldwell *et al.*, paper in preparation). Wide field fluorescence microscopy of HeLa cells and primary neurons transfected with Fxr2-FLAG with 5' UTR and without 5' UTR was used to investigate differential protein expression of Fxr2 and Fxr2 with N-terminal extension, resulting from translation initiation at -219 GUG compared to Fxr2 protein produced from annotated initiation codon, +1 AUG. In transfected HeLa cells, Fxr2-FLAG translated predominantly from -219 appears more cytosolic relative to nuclear than Fxr2-FLAG translated mostly from +1 AUG (Fig. 6.11). However, these plasmids do not produce purely 1 N-terminal isoform of Fxr2 (Fig. 6.5). The plasmid for +1 isoform also shows some production of a larger isoform by western blot of transfected HeLa cell lysate. This complicates interpretation of these results. There was no significant difference in subcellular distribution of Fxr2 isoforms in transfected primary neurons (Fig. 6.12). Fxr2 was seen throughout the soma and neurites.

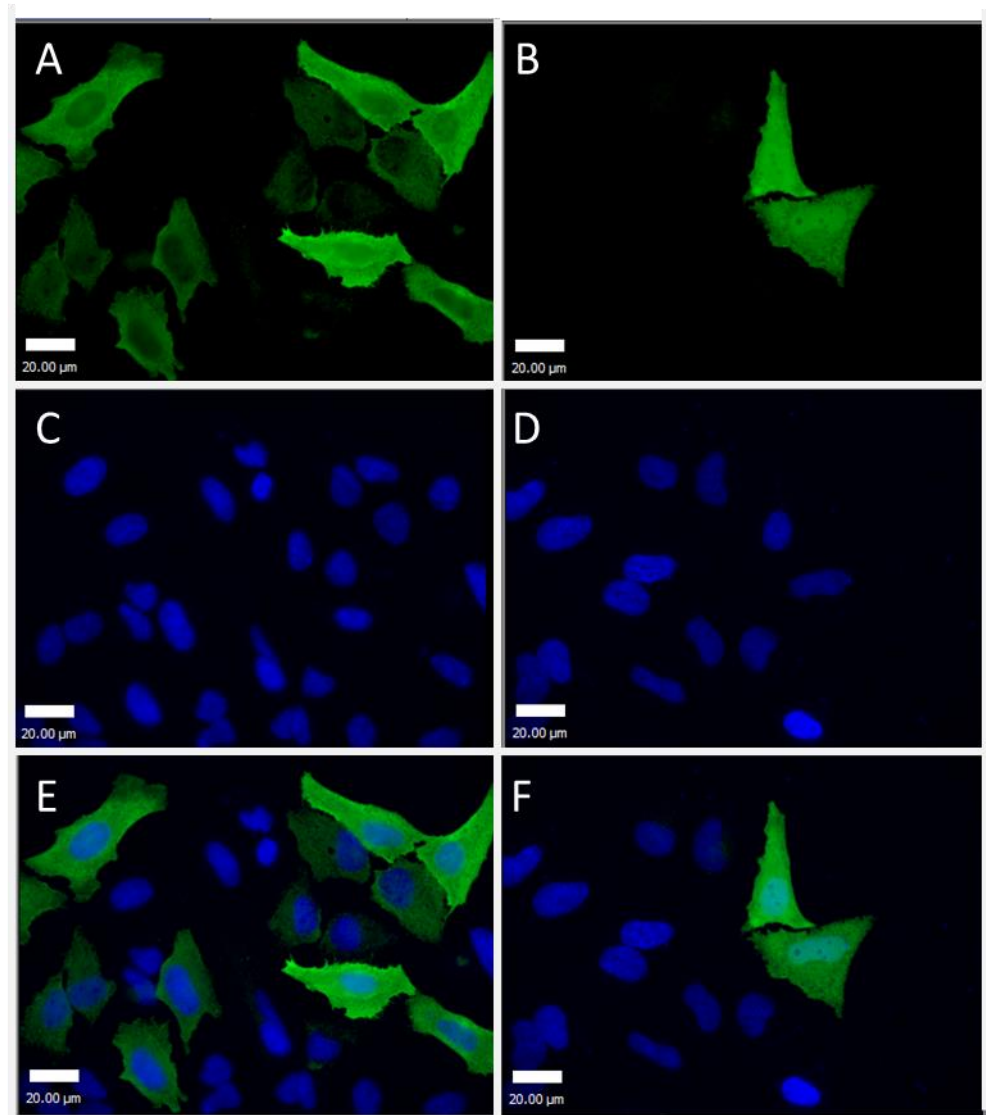


Figure 6.11 HeLa cells transfected with Fxr2-FLAG with 5' UTR (**A, C, E**) and without 5' UTR (**B, D, F**). Fxr2-FLAG translated predominantly from -219 appears more cytosolic relative to nuclear than Fxr2-FLAG translated only from +1 AUG.

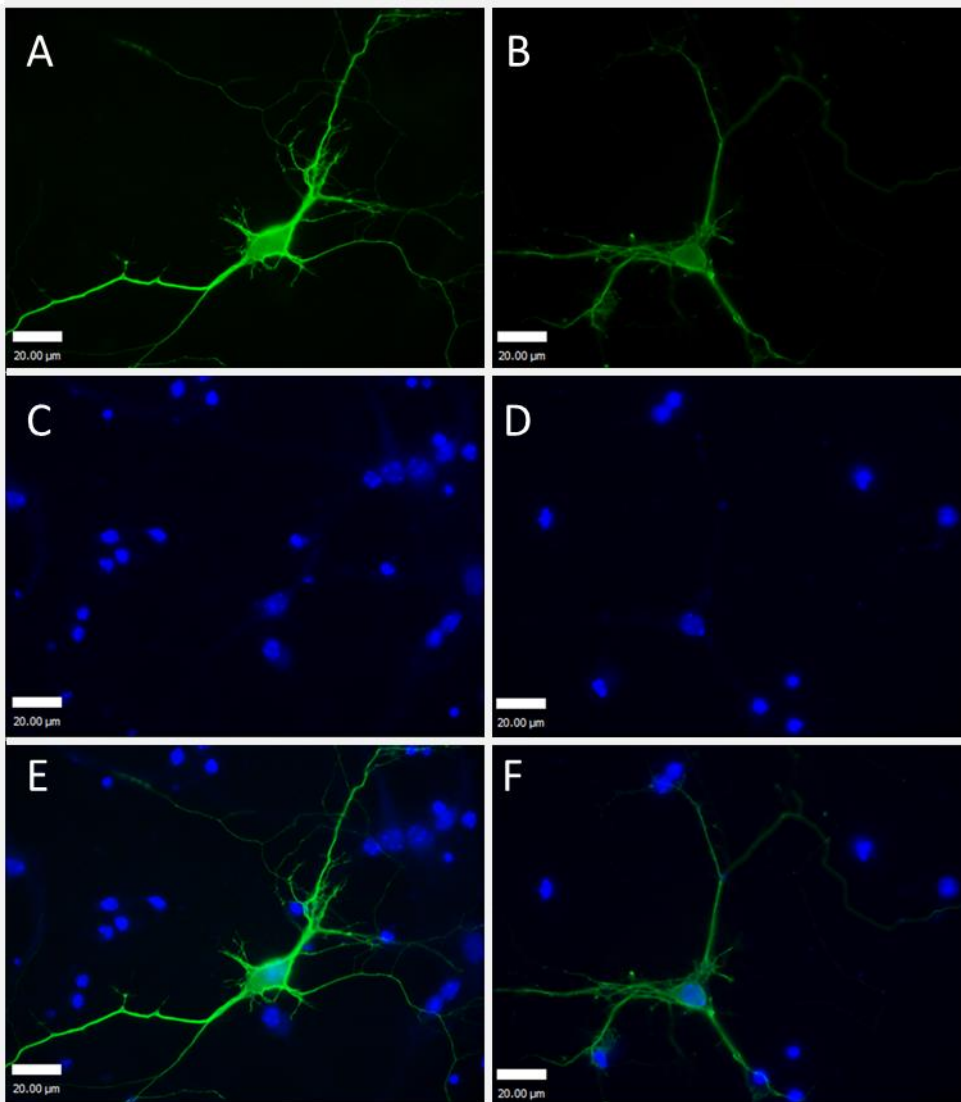


Figure 6.12 Primary cortical neurons were transfected with Fxr2-FLAG with 5' UTR (**A, C, E**) and without 5' UTR (**B, D, F**). There is no significant difference in localisation of Fxr2-FLAG translated predominantly from -219 appears more cytosolic relative Fxr2-FLAG translated only from +1 AUG.

6.3 Discussion

Chapter six details an investigation of the role of G-quadruplex structures in directing translation initiation from aTICs within the 5' UTR of Fxr2. Alternative translation initiation has never been published in Fxr2. As a paralog of FMRP and of increasingly known significance in neuron behaviour, it is important to characterise the synthesis of Fxr2p protein. Fxr2 has a predicted molecular weight of 74 kDa, however, most antibodies show a band, or two bands around 90 kDa. This difference in observed and predicted molecular weight potentially indicates extension of the protein. Searching for Fxr2 in riboseq database indicated Fxr2 to be translated additionally from an upstream GUG codon at -219. Here, the use of alternative translation initiation codons within the 5' UTR has been investigated.

Fxr2 was cloned from human brain cDNA using reverse transcription PCR. CD spectroscopy of *in vitro* transcribed RNA was carried out to analyse the formation of G-quadruplex structures within the 5' UTR of Fxr2 mRNA. CD spectroscopy was also carried out in the presence of TMPyP4 to assess the ability of TMPyP4 to destabilise the G-quadruplex structure in Fxr2. However, the ability of TMPyP4 to destabilise G-quadruplexes in transfected HeLa cells is questionable, due to the reduction in global translation of HeLa cells seen in Chapter 4.2.14. FLAG-tagged Fxr2 expression vectors were created to analyse, by western blot of transfected HeLa cells lysate, the protein isoforms generated from three upstream GUG aTICs. Mutagenesis of putative aTICs showed Fxr2 is predominantly translated from GUG -219 of the annotated AUG initiation codon. Fxr2 is translated mostly from the upstream aTIC at -219 which results in production of a larger, N-terminally extended Fxr2 protein. It is possible that all native protein may be produced from the -219 GUG codon, protein mass spectrometry could be used to investigate the abundance of specific isoforms in different tissue types. The abundance of this N-terminally extended Fxr2 protein could be probed *in vivo* with a specific antibody generated against the N-terminal extension amino acid sequence of the extended isoform. Results from these probe experiments could be compared with total Fxr2P protein detected using an antibody specific to the annotated coding sequence of Fxr2P.

The results suggest alternative translation initiation in Fxr2 mRNA is dependent on G-quadruplex structures within the 5' UTR. The ability of G-quadruplex-targeted

chemicals and RBPs to modulate expression of FLAG-tagged Fxr2p in transfected HeLa cells was carried out using TMPyP4/ Hippuristanol or co-transfection with FLAG-tagged DHX expression constructs. The extended Fxr2p isoform, translated from the -219 GUG has a 73 aa N-terminal extension. The DHX helicases co-expressed in HeLa cells transfected with Fxr2 constructs decreased the synthesis of the longer isoform of Fxr2 (translated from the -219 GUG) relative to the shorter isoform, produced from the +1 AUG of the CDS. DHX36 showed the greatest changes to relative expression of the isoforms, reducing the expression of the N-terminally extended Fxr2p. DHX36 contains an N-terminal domain with specific RNA G-quadruplex-binding activity. It is the main helicase for resolution of DNA G-quadruplex structures in HeLa cells. The impact of DHX36 expression on the translation of Fxr2 isoforms suggests a dependence of translation of the longer isoform, from the -219 GUG, on a G-quadruplex structure. DHX36 may be resolving the G-quadruplex structure in these constructs and removing the directing of the ribosome for translation initiation at -219 GUG; caused by the predicted G-quadruplex sequence. Mutation of the G-quadruplex forming sequence in the 5' UTR of Fxr2 to a sequence predicted not to form a G-quadruplex would be a negative control for the effects of the predicted G-quadruplex structure in these experiments.

Changes to subcellular localisation of the extended protein compared to the normal Fxr2p protein were investigated by immunofluorescence microscopy of transfected HeLa cells and primary neurons. However, the results are preliminary and needs to be repeated on a larger scale to assess differences in subcellular localisation of the protein due to different N-terminal isoforms produced by alternative translation initiation.

6.3.1 Conclusions

1. Fxr2 was cloned into pcDNA 3.1 3xFLAG from human brain cDNA and sequence verified. Constructs were made with mutations within the 5' UTR to test for use of alternative translation initiation codons in synthesis of alternative protein isoforms.
2. The -219 GUG alternative initiation codon identified by ribose analysis was validated in our experiments as the source of translation of N-terminally extended Fxr2p isoforms.

3. The mRNA of Fxr2 5' UTR showed CD spectra corresponding to RNA G-quadruplex structure. However, this needs to be further validated with the use of control RNA molecules, and repeats with independently synthesised batches of RNA.
4. DHX helicases showed some effect on the relative translation of the longer and shorter Fxr2p isoforms when cotransfected in HeLa cells. DHX36 had the greatest effect, reducing the relative expression of the longer Fxr2p isoform, translated from the -219 GUG, in comparison to the shorter isoform, translated from the +1 AUG.

Chapter Seven

Final Discussion

Summary

Regulation of gene expression at the level of translation can greatly impact the abundance, location, isoforms and functions of proteins. Control of the local proteome is particularly important in neurons due to their subcellular organisation and the role of protein synthesis in late LTP (Chapter 1.7). The 5' UTR of mRNAs can direct alternative translation initiation and subcellular localisation (Chapter 1.5). The results presented here address potential regulation of translation of genes of significance to neuronal cell behaviour, K_{2P} channels and Fxr2.

The 5' UTR of an mRNA can provide significant control over the fate of an mRNA. The primary sequence determines the site of translation initiation (Kozak, 1986; Nakagawa *et al.* 2007). The strongest initiation codon is an AUG in a strong Kozak consensus sequence, however, translation also starts from many near-cognate alternative initiation codons such as CUG, GUG and ACG (Chapter 1.1). Translation initiation in the 5' UTR, in-frame with the coding sequence, generates eORFs; N-terminally extended proteins (Coldwell *et al.*, 2012). The context of an initiation codon is hugely significant in determining the rate at which the codon initiates translation, and the primary sequence of a 5' UTR can also contain RBP-binding motifs. The secondary structure of the 5' UTR can modify the translation of an mRNA (Gray & Hentze, 1994), where a strong secondary structure within the 5' UTR can slow ribosome scanning and therefore reduce the rate of translation initiation. Secondary structures can also act as RBP-binding motifs (Darnell *et al.*, 2001) and G-quadruplexes are known to be targets of RBPs in neurons. Differential binding by RBPs can affect alternative subcellular localisation, alternative splicing and specific translational control.

The regulated expression of K_{2p} channels is critical in determining the resting membrane potential of cells (Chapter 1.8), so it is essential to characterise mechanisms which control the expression of K_{2p} channels. This thesis details investigations of 5' UTR primary sequence and secondary structure effects on the expression of K_{2p} leak channels, Traak, Task1 and Task3. The generation of alternative isoforms of Fxr2p due to alternative translation from upstream GUG codons is also investigated. The role of G-quadruplex structure within the 5' UTR of Fxr2 mRNA may direct ribosomes to initiation codons.

Significance of research to neurons

RNA targeting to subcellular localisations is an important mechanism for dynamic control of a local proteome which is important in local protein synthesis characteristic of late LTP in neurons (Chapter 1.7). G-quadruplex structures have been shown to effect mRNA subcellular targeting and direct protein synthesis at the synapse. Furthermore, Task3 mRNA has been found by deep sequencing in the synaptic neuropil. Any change in the abundance of Task3 protein in the membrane alters the resting membrane potential and therefore the sensitivity. Because the 5' UTR CGG repeat targets *fmr1* mRNA for local translation at dendritic spines (Muslimov *et al.*, 2011), it is important to investigate the potential targeting of Task3 mRNA to dendritic spines due to its 5' GGN repeat sequence

Normal synaptic function depends on FMRP repression of translation of many mRNAs in glutamatergic synapses including postsynaptic proteins (Chapter 1.7). Normal translation of dendritically localised mRNAs is controlled by coordination of FMRP and CPEB proteins. FMRP interacts with its paralog, Fxr2p. Fxr2p is thought to compensate for lack of expression of FMRP. *Fxr2* KO mice display a similar intellectually disabled phenotype as *Fmr1* KO mice (Cavallaro *et al.*, 2008). FXR2, is involved in normal learning and memory processes in neurons and knock out of FXR2 causes intellectual disability. Chapter 6 describes the identification of multiple in-frame GUG alternative initiation codons in the 5' UTR of Fxr2 which generates N-terminally extended Fxr2 protein. The protein produced from Fxr2 mRNA, and the mechanisms controlling translation of its mRNA need to be characterised in order to further our understanding of this neuronal protein.

Principal findings

The K_{2P} mRNA, Task3, was found to have a longer 5' UTR than in databases. The reason this may have been missed in sequencing for databases is the GC-richness of this extension. I conducted 5' RACE on human brain cDNA using a gene specific primer for Task3. Cloning of the amplified product of 5' RACE from human brain cDNA and sequencing revealed an extended 5' UTR with a 5'-terminal 42 nucleotide (GGN) repeat sequence. This extended 5' UTR was inhibitory of translation of Task3 (Fig. 4.3). The 42 nucleotide (GGN) repeat sequence was shown to form a G-quadruplex structure (Fig. 4.7 & 4.8). Task1 also has a G-quadruplex-forming GGN repeat sequence in its 5' UTR (Fig. 4.8).

Rbps with documented G-quadruplex mediated activity were tested for their effects on translation of Task3 mRNA. hnRNPA2 has been shown to destabilize RNA G-quadruplexes *in vitro*. DHX36 contains a unique N-terminal domain with specific RNA G-quadruplex-binding activity. It is the principal resolvase of DNA G-quadruplex in HeLa cells. hnRNP A2 and DHX36 relieved translational repression of Task3 translation (Fig. 4.11 & Fig. 4.11). DHX36 has been found in neuronal RNPs and also is responsible for normal dendritic localisation of miR transcripts, the mechanism is unknown (Chapter 1.3.1). The role of DHX36 in control of Task3 mRNA fate may be important in regulating synaptic excitability.

Preliminary results of FISH of GFP-labelled Task3 expression in transfected primary cortical neurons suggest the GGN repeat of the 5' UTR of Task3 is essential for neurite targeting of Task3 mRNA. Higher resolution and techniques and more repeats are required to validate neurite targeting of Task3 mRNA. Measurement of the localisation of the endogenous mRNA would also be required to validate the existence of this trafficking of Task3 mRNA in untransfected neurons.

7.1 5' UTR sequences can regulate expression of K_{2P} leak channels

Alternative translation initiation at an AUG downstream and in frame with the annotated +1 AUG has been shown to change channel permeability of the K_{2P}

channel, Trek1 (Chapter 1.10). Another K_{2P} channel mRNA (Traak) was identified, by our bioinformatics screening process, to contain a putative alternative translation initiation codon within its 5' UTR (Chapter 1.11). We tested whether N-terminally extended proteins were translated from the identified alternative initiation codon by transfection of HeLa cells with Traak-FLAG constructs mutated to have strong translation initiation codons at potential alternative initiation codons within the 5' UTR (Chapter 3.2.2). Western blot of protein products from the mutated constructs allowed comparison with protein bands detected from expression of Traak-FLAG with a wild-type 5' UTR. The higher MW protein bands representative of eORFs, expressed from Traak-FLAG constructs mutated to have strong translation initiation codons at potential alternative initiation codons were not present in the lysate from cells expressing Traak-FLAG with a wild-type 5' UTR.

However, the 5' UTRs of K_{2P} channels are poorly annotated in databases, and so 5' RACE was used to characterise the 5' UTR of Task3 (Chapter 3.5.2). The 5' UTR of Task3 was discovered to be longer than the annotated 5' UTR of the database sequences and characterised by a 5' terminal (GGN)₁₃ repeat. It would be useful to know the relative abundance of Task3 transcripts with the extended 5' UTR, including the terminal (GGN)₁₃ repeat. We attempted to design a qPCR assay to compare the levels of mRNA of the coding sequence of Task3, with the level of a Task3 transcript containing the terminal (GGN)₁₃ repeat. However, it was not possible to design primers capable of specifically amplifying transcripts containing the 5' terminal (GGN)₁₃ repeat (Fig. 3.9). Indeed, an external company specialising in the design of qPCR primers deemed it impossible to design qPCR primers for this purpose. The terminal (GGN)₁₃ repeat sequence is too GC-rich and not specific to Task3 mRNA. There are no established methods capable of assessing the relative abundance of a transcript containing an intensely GC rich 5' terminal region in comparison with overall abundance of a specific transcript.

7.2 A 5'-terminal G-quadruplex modulates translation of Task3

The extended 5' UTR of Task3 also contains a putative alternative translation initiation codon, -69 CUG. We attempted to determine whether translation initiates from this CUG, and in doing so creates an N-terminally extended Task3 protein.

Task3-FLAG with a wild-type (extended) 5' UTR were expressed in HeLa cells and bands detected by western blot were compared with the MW of bands from Task3-FLAG constructs with -69 CUG-AUG mutation, in a Kozak consensus sequence. However, expression from the Task 3 construct with extended 5' UTR sequence yielded undetectable Task3-FLAG expression and so comparison was not possible (Chapter 3.4.3). The 5' (GGN)₁₃ repeat was identified as the cause for the inhibition of Task3-FLAG synthesis in this assay. Translation of Task3-FLAG was shown to be dependent on the 5' (GGN)₁₃ repeat sequence. The Task3-FLAG protein expressed from constructs containing the WT 5' (GGN)₁₃ repeat is greatly reduced compared to constructs with the (GGN)₁₃ repeat deleted or containing the complementary sequence, 5' (CCN)₁₃ (Fig. 4.3). The inhibited protein synthesis was similar to when the (GGN)₁₃ repeat was substituted with the G-quadruplex sequence from the NRAS 5' UTR; which has been shown to inhibit translation of NRAS (Kumari, Bugaut & Balasubramanian, 2008). The transcript levels were measured by RT-PCR and found to be unchanged between constructs.

G-quadruplex formation was measured by increased fluorescence of Mesoporphyrin IX dihydrochloride (NMM) and positive difference in the circular dichroism (CD) absorbance ($\Delta\Delta$) peak at 262 nm when incubated with in-vitro synthesised (GGN)₁₃ RNA. RT-PCR of Task3-FLAG mRNA relative to β -actin mRNA in polysome fractions of transfected HeLa cells suggests the inhibition of Task3 protein synthesis results from an inhibition of translation initiation due to the 5'-terminal G-quadruplex. The inhibition of Task3 protein synthesis can be modulated by RNA-binding proteins. hnRNP A2 was shown to relieve translational inhibition, and the DEAH/RHA RNA helicases, DHX29, DHX30 and DHX36 differentially regulate translation from Task3 mRNA dependent on the presence of the 5' terminal G-quadruplex (Chapter 4.2.11). The cationic porphyrin, TMPyP4, was able to melt (GGN)₁₃ in vitro, and partially relieved repression of translation of transfected WT Task3-FLAG. eIF4A inhibitors have recently been suggested to inhibit the translation of mRNAs with >(GGN)₄ 5' UTR repeats (Wolfe *et al.*, 2014), however, we found 10 μ M Hippuristanol was unable to modulate expression of WT Task3-FLAG.

The role of the 5'-terminal G-quadruplex of Task3 mRNA is likely to be complex. The key principle is that this G-quadruplex inhibits translation of the mRNA, which has critical effects on cell physiology by determining membrane potential. The G-quadruplex adds multiple levels of control of gene expression. The abilities of G-

quadruplex-binding RBPs to modulate expression of Task3 have been demonstrated (Chapter 4.2.10, and 4.2.12).

7.3 Neurite localisation of Task3 mRNA may be determined by a 5' terminal G-quadruplex

Task3 is highly expressed in neuronal cells where the constitutive leak of potassium out of the cell increases local membrane potential. Chapter 5 describes detection of Task3-GFP mRNA by Fluorescence In Situ Hybridisation (FISH) in transfected primary cortical neurons. It was found that the 5'-terminal G-quadruplex in Task3 mRNA mediates localisation of its mRNA to discrete neurite particles (Fig. 5.10). The roles of G-quadruplex-interacting RBPs, hnRNP A2 and Pur α , in the trafficking of Task3 mRNA was investigated, however, the mechanism of neurite delivery of Task3 mRNA requires further investigation. Dysregulation of this mechanism is predicted to cause perturbations to individual synapse excitability and therefore contribute to neuronal phenotypes.

7.4 G-quadruplex mediated translation initiation from upstream AICs generates N-terminally extended FXR2 protein

Mutagenesis of alternative initiation codons suggests -219 GUG is the main source of translation initiation of Fxr2. The 5' UTR of Fxr2 contains multiple G-quadruplex-forming sequences (Fig. 6.6 and 6.8). We used techniques developed for investigating the G-quadruplex-mediated regulation of Task3 expression to investigate potential control of translation from initiation codons within the 5' UTR of Fxr2.

We investigated the ability of RBPs and small ligands to modulate translation initiation from AICs in Fxr2. Treatment of HeLa cells transfected with Fxr2-FLAG with the eIF4A helicase inhibitor, 10 μ M Hippuristanol caused a shift in the relative abundance of proteins of MW corresponding to translation initiation from +1 or -219 initiation codons (Fig. 6.9). Hippuristanol did not produce a measurable effect on translation of Task3-FLAG, which indicates a difference in the structures or associated translational control mechanisms between the 5' terminal (GGN)₁₃ repeat of Task3 mRNA and the G-rich 5' UTR of Fxr2. Investigation of the roles of the N-terminal extension of FXR2 protein would be useful to determine functional effects of

differential translation initiation from -219/+1 in a G-quadruplex-dependent fashion. The ability of TmPyP4 to disrupt G-quadruplex structure was not observed in the biophysical studies presented here. The TmPyP4 cannot be considered to relax the G-quadruplex structure of Fxr2 mRNA, therefore, interpretation of the result is limited.

The co-expression of DHX helicases in HeLa cells transfected with Fxr2 constructs decreased the synthesis of the longer isoform of Fxr2 (translated from the -219 GUG) relative to the shorter isoform, produced from the +1 AUG of the CDS. DHX36 contains an N-terminal domain with specific RNA G-quadruplex-binding activity (discussed in Chapter 1.3.1). It is the main helicase for resolution of DNA G-quadruplex structures in HeLa cells. DHX36 showed the largest changes to relative expression of the isoforms, reducing the relative abundance of the N-terminally extended Fxr2p. The impact of DHX36 expression on the translation of Fxr2 isoforms suggests a dependence of translation of the longer isoform, from the -219 GUG, on a G-quadruplex structure. DHX36 may be resolving the G-quadruplex structure in these constructs and removing the directing of the ribosome for translation initiation at -219 GUG; caused by the predicted G-quadruplex sequence.

7.5 Suggestions for continued research

The significance of control of gene expression by 5' UTR G-quadruplexes is increasingly recognised. One study estimates ~3000 human mRNA 5' UTRs contain predicted quadruplex-forming sequences (Kumari *et al.*, 2007). They may all form G-quadruplexes in vivo, and reveals an additional layer of control of gene expression hitherto unknown. The published roles of 5' UTR G-quadruplexes is already diverse and complex. Some of the RBPs which are able to modulate gene expression control by G-quadruplexes have been identified, but there are likely to be many more as yet unidentified. We have investigated herein some of the best characterised G-quadruplex-recognising RBPs, but their roles and mechanisms are not fully characterised. To identify RBPs specifically associated with Task3 mRNA in different subcellular fractions of neurons, an RNA pull-down assay could be used. The mRNA of Task3 could be end-labelled with biotin and incubated with lysate from subcellular fractions of neuronal cells. RNA-protein complexes recovered using streptavidin beads, and RBPs identified using mass spectrometry. We have also shown how small ligands, such as TmPyP4 and Hippuristanol, can modulate gene expression in a G-quadruplex dependent fashion. We have also further characterised the properties of TmPyP4 in resolving G-quadruplex structures. In Chapter 4.2.15 we show TmPyP4 is

able to resolve a GGN RNA G-quadruplex, characteristic of the 5' terminal sequence of Task3 mRNA. However, the concentration of TMPyP4 required to achieve this relaxation of the structure, is twice the concentration shown in Chapter 4.2.14 to half the global translation rate in HeLa cells. There are likely many more small ligands which could be tested for altering the expression of Task3. The exact shape of the G-quadruplex, its context within the mRNA sequence, and position of the G-quadruplex relative to the 5' CAP and initiation codons amplifies the scope of investigations necessary.

The characterisation of the mechanisms and results of local Task3 translation in neurons would be of great importance. Other groups have used advanced FISH techniques to examine control and effects of local translation in neurons. Park *et al.*, (2014) used single molecule FISH of cultured hippocampal neurons from transgenic mice expressing labelled β -actin mRNA to identify the release of β -actin mRNA from dendritic mRNPs following depolarization of the neurons with potassium chloride. Buxbaum *et al.*, (2014) used single molecule FISH of cultured hippocampal neurons to show increased detection of β -actin mRNA in neurites in response to chemically induced long-term potentiation (cLTP). This effect was reversed by blocking NMDA receptors. Protease treatment of cells produced a similar increase in detected β -actin mRNA by FISH. It is suggested that neuronal stimulation causes the 'unmasking' of mRNAs from mRNPs, allowing binding of the mRNA by ribosomes for translation. Synaptic activation may also control the release of Task3 mRNA from neuronal RNPs. The technique we have used with Stellaris FISH probes gives high signal to noise, but is not suitable for single molecule FISH of endogenously expressed Task3 mRNA. The mRNA of Task3 in neurons is many times lower than the abundance of β -actin mRNA. However, measurement should be possible using FISH techniques with a signal amplification protocol, such as the ViewRNA ISH Cell Assay (Affymetrix) which uses branch DNA signal amplification (bDNA) for tunable amplification of bound oligo probes, prior to binding of fluorescently labelled probes. How RNA detection techniques could be applied in the dynamic situation of an active synapse would be an exciting possibility, but one that is likely to be several leaps in technology away.

Local translation is essential for normal neurophysiology. The neurite targeting of Task3 is predicted to be highly important in regulating local synaptic excitability due to the direct effect of Task3 expression on local membrane potential. We can

measure the changes in membrane potential local to specific synapses using patch clamping. The application of patch clamping to synapses in cultured primary neurons expressing labelled Task3 with the full 5' UTR and primary neurons expressing labelled Task3 with no 5' UTR would allow investigation of the effect of changes to local translation in response to synapse activation.

We have shown that the localisation of Task3 mRNA to discrete neurite particles is dependent on a 5' terminal G-quadruplex. 5' UTR G-quadruplexes may mediate the delivery of other mRNAs to neurite particles. Finally, the Coldwell lab has conducted preliminary bioinformatics search of known neuronal mRNAs for 5' UTR G-quadruplexes and identified multiple genes which may be trafficked to neurites via pathways involving RBPs common to targeting of Task3 mRNA. The group intend to follow up these new avenues with the techniques and tools generated during the work on this PhD project, and so further investigate these novel areas of exciting research.

Chapter Eight

References

Abdelmohsen, K. (2012) Modulation of Gene Expression by RNA Binding Proteins: mRNA Stability and Translation

Andreassi, C., Zimmermann, C., Mitter, R., Fusco, S., De Vita, S., Saiardi, A. and Riccio, A. (2010) An NGF-responsive element targets myo-inositol monophosphatase-1 mRNA to sympathetic neuron axons. *Nature neuroscience*. *13*, 291-301

Andres-Enguix, I., Shang, L., Stansfeld, P. J., Morahan, J. M., Sansom, M. S., Lafreniere, R. G., Roy, B., Griffiths, L. R., Rouleau, G. A. and Ebers, G. C. (2012) Functional analysis of missense variants in the TRESK (KCNK18) K⁺ channel. *Scientific reports*. *2*

Arora, A., Dutkiewicz, M., Scaria, V., Hariharan, M., Maiti, S. and Kurreck, J. (2008) Inhibition of translation in living eukaryotic cells by an RNA G-quadruplex motif. *RNA*. *14*, 1290-129

- Arthanari, H., Basu, S., Kawano, T. L. and Bolton, P. H. (1998) Fluorescent dyes specific for quadruplex DNA. *Nucleic acids research*. *26*, 3724-3728
- Babendure, J. R., Babendure, J. L., Ding, J.-H. and Tsien, R. Y. (2006) Control of mammalian translation by mRNA structure near caps. *RNA*. *12*, 851-861
- Barel, O., Shalev, S. A., Ofir, R., Cohen, A., Zlotogora, J., Shorer, Z., Mazor, G., Finer, G., Khateeb, S., Zilberberg, N. and Birk, O. S. (2008) Maternally inherited Birk Barel mental retardation dysmorphism syndrome caused by a mutation in the genomically imprinted potassium channel KCNK9. *American journal of human genetics*. *83*, 193-199
- Bartel, D. P. (2004) MicroRNAs: genomics, biogenesis, mechanism, and function. *Cell*. *116*, 281-297
- Bicker, S., Khudayberdiev, S., Weiß, K., Zocher, K., Baumeister, S. and Schrott, G., (2013) The DEAH-box helicase DHX36 mediates dendritic localization of the neuronal precursor-microRNA-134. *Genes & development*, *27*(9), pp.991-996.
- Blice-Baum, A.C. and Mihailescu, M.R. (2014) Biophysical characterization of G-quadruplex forming FMR1 mRNA and of its interactions with different fragile X mental retardation protein isoforms. *Rna*, *20*(1), pp.103-114.
- Blobel, G. and Dobberstein, B. (1975) Transfer of proteins across membranes. I. Presence of proteolytically processed and unprocessed nascent immunoglobulin light chains on membrane-bound ribosomes of murine myeloma. *The Journal of Cell Biology*. *67*, 835-851
- Bonnal, S., Schaeffer, C., Créancier, L., Clamens, S., Moine, H., Prats, A.-C. and Vagner, S. (2003) A single internal ribosome entry site containing a G quartet RNA structure drives fibroblast growth factor 2 gene expression at four alternative translation initiation codons. *Journal of Biological Chemistry*. *278*, 39330-39336
- Bradley, C.A., Padovan, J.C., Thompson, T.L., Benoit, C.A., Chait, B.T. and Rhoads, R.E., (2002) Mass spectrometric analysis of the N terminus of translational initiation factor eIF4G-1 reveals novel isoforms. *Journal of Biological Chemistry*, *277*(15), pp.12559-12571.
- Bramham, C. R. and Wells, D. G. (2007) Dendritic mRNA: transport, translation and function. *Nature Reviews Neuroscience*. *8*, 776-789
- Brendza, R.P., Serbus, L.R., Duffy, J.B. and Saxton, W.M. (2000) A function for kinesin I in the posterior transport of oskar mRNA and Stauf protein. *Science*, *289*(5487), pp.2120-2122.
- Brickley, S. G., Aller, M. I., Sandu, C., Veale, E. L., Alder, F. G., Sambhi, H., Mathie, A. and Wisden, W. (2007) TASK-3 two-pore domain potassium channels enable sustained high-frequency firing in cerebellar granule neurons. *The Journal of Neuroscience*. *27*, 9329-9340
- Bugaut, A. and Balasubramanian, S. (2012) 5'-UTR RNA G-quadruplexes: translation regulation and targeting. *Nucleic acids research*. *40*, 4727-4741
- Buxbaum, A. R., Wu, B. and Singer, R. H. (2014) Single β -Actin mRNA Detection in Neurons Reveals a Mechanism for Regulating Its Translatability. *Science*. *343*, 419-422

- Cajigas, I. J., Tushev, G., Will, T. J., tom Dieck, S., Fuerst, N. and Schuman, E. M. (2012) The local transcriptome in the synaptic neuropil revealed by deep sequencing and high-resolution imaging. *Neuron*. 74, 453
- Cavallaro, S., Paratore, S., Fradale, F., de Vrij, F. M., Willemsen, R. and Oostra, B. A. (2008) Genes and pathways differentially expressed in the brains of Fxr2 knockout mice. *Neurobiology of disease*. 32, 510-520
- Chen, H. and Chan, D. C. (2004) Mitochondrial dynamics in mammals. *Current topics in developmental biology*. 59, 119-144
- Chen, N., Onisko, B. and Napoli, J. L. (2008) The nuclear transcription factor RAR α associates with neuronal RNA granules and suppresses translation. *Journal of Biological Chemistry*. 283, 20841-20847
- Chen, Q., Jagannathan, S., Reid, D. W., Zheng, T. and Nicchitta, C. V. (2011) Hierarchical regulation of mRNA partitioning between the cytoplasm and the endoplasmic reticulum of mammalian cells. *Molecular biology of the cell*. 22, 2646-2658
- Cheung, Y.N., Maag, D., Mitchell, S.F., Fekete, C.A., Algire, M.A., Takacs, J.E., Shirokikh, N., Pestova, T., Lorsch, J.R. and Hinnebusch, A.G. (2007) Dissociation of eIF1 from the 40S ribosomal subunit is a key step in start codon selection in vivo. *Genes & development*, 21(10), pp.1217-1230.
- Choi, S.-B., Wang, C., Muench, D. G., Ozawa, K., Franceschi, V. R., Wu, Y. and Okita, T. W. (2000) Messenger RNA targeting of rice seed storage proteins to specific ER subdomains. *Nature*. 407, 765-767
- Chowdhury, S., Ragaz, C., Kreuger, E. and Narberhaus, F. (2003) Temperature-controlled structural alterations of an RNA thermometer. *Journal of Biological Chemistry*. 278, 47915
- Clark, I., Giniger, E., Ruohola-Baker, H., Jan, L.Y. and Jan, Y.N. (1994) Transient posterior localization of a kinesin fusion protein reflects anteroposterior polarity of the *Drosophila* oocyte. *Current Biology*, 4(4), pp.289-300.
- Coffee, B., Keith, K., Albizua, I., Malone, T., Mowrey, J., Sherman, S. L. and Warren, S. T. (2009) Incidence of Fragile X Syndrome by Newborn Screening for Methylated FMR1 DNA. *American journal of human genetics*. 85, 503-514
- Coldwell, M.J., Sack, U., Cowan, J.L., Barrett, R.M., Vlasak, M., Sivakumaran, K. and Morley, S.J. (2012) Multiple isoforms of the translation initiation factor eIF4GII are generated via use of alternative promoters, splice sites and a non-canonical initiation codon. *Biochemical Journal*, 448(1), pp.1-11.
- Coller, J. and Parker, R. (2004) Eukaryotic mRNA decapping. *Annual review of biochemistry*. 73, 861-890
- Collie, G. W. and Parkinson, G. N. (2011) The application of DNA and RNA G-quadruplexes to therapeutic medicines. *Chemical Society Reviews*. 40, 5867-5892
- Comery, T. A., Harris, J. B., Willems, P. J., Oostra, B. A., Irwin, S. A., Weiler, I. J. and Greenough, W. T. (1997) Abnormal dendritic spines in fragile X knockout mice: maturation and pruning deficits. *Proceedings of the National Academy of Sciences*. 94, 5401-5404
- Cui, H., Wu, F., Sun, Y., Fan, G. and Wang, Q. (2010) Up-regulation and subcellular localization of hnRNP A2/B1 in the development of hepatocellular carcinoma. *BMC Cancer*. 10, 356

- Czirják, G., Tóth, Z. E. and Enyedi, P. (2004) The two-pore domain K⁺ channel, TRESK, is activated by the cytoplasmic calcium signal through calcineurin. *Journal of Biological Chemistry*. 279, 18550-18558
- Dai, J., Liu, Z.-Q., Wang, X.-Q., Lin, J., Yao, P.-F., Huang, S.-L., Ou, T.-M., Tan, J.-H., Li, D. and Gu, L.-Q. (2015) Discovery of Small Molecules for Up-Regulating the Translation of Anti-amyloidogenic Secretase, a Disintegrin and Metalloproteinase 10 (ADAM10), by Binding to the G-Quadruplex-Forming Sequence in the 5' Untranslated Region (UTR) of Its mRNA. *Journal of medicinal chemistry*. 58, 3875-3891
- Darnell, J. C., Jensen, K. B., Jin, P., Brown, V., Warren, S. T. and Darnell, R. B. (2001) Fragile X mental retardation protein targets G quartet mRNAs important for neuronal function. *Cell*. 107, 489-499
- Darnell, J. C., Van Driesche, S. J., Zhang, C., Hung, K. Y. S., Mele, A., Fraser, C. E., Stone, E. F., Chen, C., Fak, J. J. and Chi, S. W. (2011) FMRP stalls ribosomal translocation on mRNAs linked to synaptic function and autism. *Cell*. 146, 247-261
- Davidovic, L., Sacconi, S., Bechara, E. G., Delplace, S., Allegra, M., Desnuelle, C. and Bardoni, B. (2008) Alteration of expression of muscle specific isoforms of the fragile X related protein 1 (FXR1P) in facioscapulohumeral muscular dystrophy patients. *Journal of medical genetics*. 45, 679-685
- Delanoue, R., Herpers, B., Soetaert, J., Davis, I. and Rabouille, C. (2007) Drosophila Squid/hnRNP helps Dynein switch from a gurken mRNA transport motor to an ultrastructural static anchor in sponge bodies. *Developmental cell*, 13(4), pp.523-538.
- Deng, J.P., Xiong, Y. and Sundaralingam, M. (2001) January. Ultra-high resolution crystal structure of a RNA tetraplex r (cggggc)(4). In *BIOPHYSICAL JOURNAL* (Vol. 80, No. 1, pp. 480A-480A). 9650 ROCKVILLE PIKE, BETHESDA, MD 20814-3998 USA: BIOPHYSICAL SOCIETY.
- Derry, M., Yanagiya, A., Martineau, Y. and Sonenberg, N. (2006) Regulation of poly (A)-binding protein through PABP-interacting proteins. In *Cold Spring Harbor symposia on quantitative biology* pp. 537-543, Cold Spring Harbor Laboratory Press
- Dhote, V., Sweeney, T. R., Kim, N., Hellen, C. U. and Pestova, T. V. (2012) Roles of individual domains in the function of DHX29, an essential factor required for translation of structured mammalian mRNAs. *Proceedings of the National Academy of Sciences*. 109, E3150-E3159
- Dreyfus, M. and Régnier, P. (2002) The poly (A) tail of mRNAs: bodyguard in eukaryotes, scavenger in bacteria. *Cell*. 111, 611-613
- Dreyfuss, G., Matunis, M. J., Pinol-Roma, S. and Burd, C. G. (1993) hnRNP proteins and the biogenesis of mRNA. *Annu Rev Biochem*. 62, 289-321
- Edbauer, D., Neilson, J. R., Foster, K. A., Wang, C.-F., Seeburg, D. P., Batterton, M. N., Tada, T., Dolan, B. M., Sharp, P. A. and Sheng, M. (2010) Regulation of synaptic structure and function by FMRP-associated microRNAs miR-125b and miR-132. *Neuron*. 65, 373-384
- Enyedi, P. and Czirják, G. (2010) Molecular background of leak K⁺ currents: two-pore domain potassium channels. *Physiological reviews*. 90, 559-605
- Fekete, C.A., Mitchell, S.F., Cherkasova, V.A., Applefield, D., Algire, M.A., Maag, D., Saini, A.K., Lorsch, J.R. and Hinnebusch, A.G. (2007) N- and C-terminal residues of

- eIF1A have opposing effects on the fidelity of start codon selection. *The EMBO journal*, 26(6), pp.1602-1614.
- Frey, U. H., Bachmann, H. S., Peters, J. and Siffert, W. (2008) PCR-amplification of GC-rich regions: 'slowdown PCR'. *Nature protocols*. 3, 1312-1317
- Gabriel, L., Lvov, A., Orthodoxou, D., Rittenhouse, A. R., Kobertz, W. R. and Melikian, H. E. (2012) The acid-sensitive, anesthetic-activated potassium leak channel, KCNK3, is regulated by 14-3-3beta-dependent, protein kinase C (PKC)-mediated endocytic trafficking. *J Biol Chem*. 287, 32354-32366
- Gadir, N., Haim-Vilmovsky, L., Kraut-Cohen, J. and Gerst, J. E. (2011) Localization of mRNAs coding for mitochondrial proteins in the yeast *Saccharomyces cerevisiae*. *RNA*. 17, 1551-1565
- Gao, Y., Tatavarty, V., Korza, G., Levin, M. K. and Carson, J. H. (2008) Multiplexed dendritic targeting of alpha calcium calmodulin-dependent protein kinase II, neurogranin, and activity-regulated cytoskeleton-associated protein RNAs by the A2 pathway. *Mol Biol Cell*. 19, 2311-2327
- Gevaert, K., Goethals, M., Martens, L., Van Damme, J., Staes, A., Thomas, G. R. and Vandekerckhove, J. (2003) Exploring proteomes and analyzing protein processing by mass spectrometric identification of sorted N-terminal peptides. *Nature biotechnology*. 21, 566-569
- Gierten, J., Ficker, E., Bloehs, R., Schlömer, K., Kathöfer, S., Scholz, E., Zitron, E., Kiesecker, C., Bauer, A., Becker, R. and Katus, H.A., 2008. Regulation of two-pore-domain (K2P) potassium leak channels by the tyrosine kinase inhibitor genistein. *British journal of pharmacology*, 154(8), pp.1680-1690.
- Giri, B., Smaldino, P.J., Thys, R.G., Creacy, S.D., Routh, E.D., Hantgan, R.R., Lattmann, S., Nagamine, Y., Akman, S.A. and Vaughn, J.P. (2011) G4 resolvase 1 tightly binds and unwinds unimolecular G4-DNA. *Nucleic acids research*, 39(16), pp.7161-7178.
- Goldstein, S. A. N., Bockenhauer, D., O Kelly, I. and Zilberberg, N. (2001) Potassium leak channels and the KCNK family of two-P-domain subunits. *Nature Reviews Neuroscience*. 2, 175-184
- González, W., Valdebenito, B., Caballero, J., Riadi, G., Riedelsberger, J., Martínez, G., Ramírez, D., Zúñiga, L., Sepúlveda, F. V. and Dreyer, I. (2014) K_{2P} channels in plants and animals. *Pflügers Archiv-European Journal of Physiology*. 467, 1091-1104
- Graveley, B. R. (2001) Alternative splicing: increasing diversity in the proteomic world. *TRENDS in Genetics*. 17, 100-107
- Gray, N. K., Coller, J. M., Dickson, K. S. and Wickens, M. (2000) Multiple portions of poly (A)-binding protein stimulate translation in vivo. *The EMBO Journal*. 19, 4723-4733
- Gray, N. K. and Hentze, M. W. (1994) Regulation of protein synthesis by mRNA structure. *Molecular biology reports*. 19, 195-200
- Gruss, M., Bushell, T. J., Bright, D. P., Lieb, W. R., Mathie, A. and Franks, N. P. (2004) Two-pore-domain K⁺ channels are a novel target for the anesthetic gases xenon, nitrous oxide, and cyclopropane. *Molecular pharmacology*. 65, 443-452
- Gu, W., Schlichthörl, G., Hirsch, J. R., Engels, H., Karschin, C., Karschin, A., Derst, C., Steinlein, O. K. and Daut, J. (2002) Expression pattern and functional characteristics of two novel splice variants of the two-pore-domain potassium channel TREK-2. *The Journal of physiology*. 539, 657-668

- Guittat, L., Lacroix, L., Gomez, D., Arimondo, P.B., de Cian, A., Pennarun, G., Amrane, S., Alberti, P., Lemerteleur, T., Aouali, N. and Morjani, H. (2004) Quadruplex structures and quadruplex ligands.
- Gumy, L. F., Yeo, G. S., Tung, Y.-C. L., Zivraj, K. H., Willis, D., Coppola, G., Lam, B. Y., Twiss, J. L., Holt, C. E. and Fawcett, J. W. (2011) Transcriptome analysis of embryonic and adult sensory axons reveals changes in mRNA repertoire localization. *RNA*. *17*, 85-98
- Hachet, O. and Ephrussi, A. (2001) *Drosophila* Y14 shuttles to the posterior of the oocyte and is required for oskar mRNA transport. *Current biology*, *11*(21), pp.1666-1674.
- Han, S. P., Friend, L. R., Carson, J. H., Korza, G., Barbarese, E., Maggipinto, M., Hatfield, J. T., Rothnagel, J. A. and Smith, R. (2010) Differential subcellular distributions and trafficking functions of hnRNP A2/B1 spliceforms. *Traffic*. *11*, 886-898
- Harms, U., Andreou, A. Z., Gubaev, A. and Klostermeier, D. (2014) eIF4B, eIF4G and RNA regulate eIF4A activity in translation initiation by modulating the eIF4A conformational cycle. *Nucleic acids research*. *42*, 7911-7922
- Hellen, C. U. T. and Sarnow, P. (2001) Internal ribosome entry sites in eukaryotic mRNA molecules. *Genes & development*. *15*, 1593-1612
- Hinnebusch, A. G. (2011) Molecular mechanism of scanning and start codon selection in eukaryotes. *Microbiology and Molecular Biology Reviews*. *75*, 434-467
- Honoré, E. (2007) The neuronal background K_{2P} channels: focus on TREK1. *Nature reviews neuroscience*. *8*, 251-261
- Huang, Y.S., Carson, J.H., Barbarese, E. and Richter, J.D., 2003. Facilitation of dendritic mRNA transport by CPEB. *Genes & development*, *17*(5), pp.638-653.
- Huber, K.M., Gallagher, S.M., Warren, S.T. and Bear, M.F., 2002. Altered synaptic plasticity in a mouse model of fragile X mental retardation. *Proceedings of the National Academy of Sciences*, *99*(11), pp.7746-7750.
- Imataka, H., Gradi, A. and Sonenberg, N. (1998) A newly identified N-terminal amino acid sequence of human eIF4G binds poly (A)-binding protein and functions in poly (A)-dependent translation. *The EMBO journal*. *17*, 7480-7489
- Ingolia, N. T., Lareau, L. F. and Weissman, J. S. (2011) Ribosome profiling of mouse embryonic stem cells reveals the complexity and dynamics of mammalian proteomes. *Cell*. *147*, 789-802
- Jackson, R. J., Hellen, C. U. and Pestova, T. V. (2010) The mechanism of eukaryotic translation initiation and principles of its regulation. *Nature reviews Molecular cell biology*. *11*, 113-127
- Jacquemont, S., Hagerman, R. J., Leehey, M., Grigsby, J., Zhang, L., Brunberg, J. A., Greco, C., Des Portes, V., Jardini, T., Levine, R., Berry-Kravis, E., Brown, W. T., Schaeffer, S., Kissel, J., Tassone, F. and Hagerman, P. J. (2003) Fragile X premutation tremor/ataxia syndrome: molecular, clinical, and neuroimaging correlates. *American journal of human genetics*. *72*, 869-878
- Januschke, J., Gervais, L., Dass, S., Kaltschmidt, J.A., Lopez-Schier, H., Johnston, D.S., Brand, A.H., Roth, S. and Guichet, A. (2002) Polar transport in the *Drosophila* oocyte requires Dynein and Kinesin I cooperation. *Current Biology*, *12*(23), pp.1971-1981.

- Jin, P., Duan, R., Qurashi, A., Qin, Y., Tian, D., Rosser, T. C., Liu, H., Feng, Y. and Warren, S. T. (2007) Pur α binds to rCGG repeats and modulates repeat-mediated neurodegeneration in a Drosophila model of fragile X tremor/ataxia syndrome. *Neuron*. 55, 556-564
- Joachim, A., Benz, A. and Hartig, J. S. (2009) A comparison of DNA and RNA quadruplex structures and stabilities. *Bioorganic & medicinal chemistry*. 17, 6811-6815
- Johnson, E. M., Kinoshita, Y., Weinreb, D. B., Wortman, M. J., Simon, R., Khalili, K., Winckler, B. and Gordon, J. (2006) Role of Pur α in targeting mRNA to sites of translation in hippocampal neuronal dendrites. *Journal of neuroscience research*. 83, 929-943
- Jokhi, V., Ashley, J., Nunnari, J., Noma, A., Ito, N., Wakabayashi-Ito, N., Moore, M.J. and Budnik, V. (2013) Torsin mediates primary envelopment of large ribonucleoprotein granules at the nuclear envelope. *Cell reports*, 3(4), pp.988-995.
- Jung, H., Yoon, B. C. and Holt, C. E. (2012) Axonal mRNA localization and local protein synthesis in nervous system assembly, maintenance and repair. *Nature Reviews Neuroscience*. 13, 308-324
- Kanai, Y., Dohmae, N. and Hirokawa, N. (2004) Kinesin transports RNA: isolation and characterization of an RNA-transporting granule. *Neuron*. 43, 513-525
- Kang, D., Kim, G. T., Kim, E. J., La, J. H., Lee, J. S., Lee, E. S., Park, J. Y., Hong, S. G. and Han, J. (2008) Lamotrigine inhibits TRESK regulated by G-protein coupled receptor agonists. *Biochem Biophys Res Commun*. 367, 609-615
- Kang, H. and Schuman, E.M., 1996. A requirement for local protein synthesis in neurotrophin-induced hippocampal synaptic plasticity. *Science*, 273(5280), p.1402.
- Keene, J. D. (2001) Ribonucleoprotein infrastructure regulating the flow of genetic information between the genome and the proteome. *Proceedings of the National Academy of Sciences*. 98, 7018-7024
- Kelleher, R. J. and Bear, M. F. (2008) The autistic neuron: troubled translation? *Cell*. 135, 401-406
- Khateb, S., Weisman-Shomer, P., Hershco-Shani, I., Ludwig, A. L. and Fry, M. (2007) The tetraplex (CGG) n destabilizing proteins hnRNP A2 and CBF-A enhance the in vivo translation of fragile X premutation mRNA. *Nucleic acids research*. 35, 5775-5788
- Kikin, O., D'Antonio, L. and Bagga, P. S. (2006) QGRS Mapper: a web-based server for predicting G-quadruplexes in nucleotide sequences. *Nucleic Acids Res*. 34, W676-682
- Kim, Y., Gnatenco, C., Bang, H. and Kim, D. (2001) Localization of TREK-2 K⁺ channel domains that regulate channel kinetics and sensitivity to pressure, fatty acids and pH. *Pflügers Archiv European Journal of Physiology*. 442, 952-960
- Kim-Ha, J., Kerr, K. and Macdonald, P.M., 1995. Translational regulation of oskar mRNA by bruno, an ovarian RNA-binding protein, is essential. *Cell*, 81(3), pp.403-412.
- Kindler, C. H. and Yost, C. S. (2005) Two-Pore Domain Potassium Channels: New Sites of Local Anesthetic Action and Toxicity. *Regional Anesthesia and Pain Medicine*. 30, 260-274
- Knapp, A. M., Ramsey, J. E., Wang, S.-X., Godburn, K. E., Strauch, A. R. and Kelm, R. J. (2006) Nucleoprotein interactions governing cell type-dependent repression of the mouse smooth muscle α -actin promoter by single-stranded DNA-binding proteins Pur α and Pur β . *Journal of Biological Chemistry*. 281, 7907-7918

- Koscianska, E., Starega-Roslan, J., Czubala, K. and Krzyzosiak, W.J., 2011. High-resolution northern blot for a reliable analysis of microRNAs and their precursors. *The Scientific World Journal*, 11, pp.102-117.
- Kozak, M. (1986) Point mutations define a sequence flanking the AUG initiator codon that modulates translation by eukaryotic ribosomes. *Cell*. 44, 283-292
- Kozak, M. (1987) At least six nucleotides preceding the AUG initiator codon enhance translation in mammalian cells. *Journal of molecular biology*. 196, 947-950
- Kozak, M. (1987) An analysis of 5'-noncoding sequences from 699 vertebrate messenger RNAs. *Nucleic acids research*. 15, 8125-8148
- Kozak, M., 1989. The scanning model for translation: an update. *The Journal of cell biology*, 108(2), pp.229-241.
- Kumari, S., Bugaut, A. and Balasubramanian, S. (2008) Position and Stability Are Determining Factors for Translation Repression by an RNA G-Quadruplex-Forming Sequence within the 5' UTR of the NRAS Proto-oncogene. *Biochemistry*. 47, 12664-12669
- Kumari, S., Bugaut, A., Huppert, J. L. and Balasubramanian, S. (2007) An RNA G-quadruplex in the 5' UTR of the NRAS proto-oncogene modulates translation. *Nature chemical biology*. 3, 218-221
- Lacoux, C., Di Marino, D., Boyl, P.P., Zalfa, F., Yan, B., Ciotti, M.T., Falconi, M., Urlaub, H., Achsel, T., Mougin, A. and Caizergues-Ferrer, M., 2012. BC1-FMRP interaction is modulated by 2'-O-methylation: RNA-binding activity of the tudor domain and translational regulation at synapses. *Nucleic acids research*, 40(9), pp.4086-4096.
- Lammich, S., Buell, D., Zilow, S., Ludwig, A.-K., Nuscher, B., Lichtenthaler, S. F., Prinzen, C., Fahrenholz, F. and Haass, C. (2010) Expression of the anti-amyloidogenic secretase ADAM10 is suppressed by its 5'-untranslated region. *Journal of Biological Chemistry*. 285, 15753-15760
- Lattmann, S., Giri, B., Vaughn, J.P., Akman, S.A. and Nagamine, Y., 2010. Role of the amino terminal RHAU-specific motif in the recognition and resolution of guanine quadruplex-RNA by the DEAH-box RNA helicase RHAU. *Nucleic acids research*, 38(18), pp.6219-6233.
- Lawrence, J. B. and Singer, R. H. (1986) Intracellular localization of messenger RNAs for cytoskeletal proteins. *Cell*. 45, 407-415
- Lécuyer, E., Yoshida, H., Parthasarathy, N., Alm, C., Babak, T., Cerovina, T., Hughes, T., Tomancak, P. and Krause, H. (2007) Global analysis of mRNA localization reveals a prominent role in organizing cellular architecture and function. *Cell*. 131, 174
- Lesage, F., Guillemare, E., Fink, M., Duprat, F., Lazdunski, M., Romey, G. and Barhanin, J. (1996) TWIK-1, a ubiquitous human weakly inward rectifying K⁺ channel with a novel structure. *The EMBO journal*. 15, 1004
- Lesage, F., Lauritzen, I., Duprat, F., Reyes, R., Fink, M., Heurteaux, C. and Lazdunski, M. (1997) The structure, function and distribution of the mouse TWIK-1 K channel. *FEBS letters*. 402, 28-32
- Lesage, F. and Lazdunski, M., 2000. Molecular and functional properties of two-pore-domain potassium channels. *American Journal of Physiology-Renal Physiology*, 279(5), pp.F793-F801.

- Li, J., Li, Q., Xie, C., Zhou, H., Wang, Y., Zhang, N., Shao, H., Chan, S. C., Peng, X. and Lin, S.-C. (2004) β -actin is required for mitochondria clustering and ROS generation in TNF-induced, caspase-independent cell death. *Journal of cell science*. *117*, 4673-4680
- Li, P. T. X., Viereggs, J. and Tinoco Jr, I. (2008) How RNA unfolds and refolds. *Annu. Rev. Biochem.* *77*, 77-100
- Linder, P. and Jankowsky, E. (2011) From unwinding to clamping—the DEAD box RNA helicase family. *Nature reviews Molecular cell biology*. *12*, 505-516
- Lisman, J., Yasuda, R. and Raghavachari, S., 2012. Mechanisms of CaMKII action in long-term potentiation. *Nature reviews neuroscience*, *13*(3), pp.169-182.
- Livak, K. J. and Schmittgen, T. D. (2001) Analysis of relative gene expression data using real-time quantitative PCR and the 2⁻ $\Delta\Delta$ CT method. *methods*. *25*, 402-408
- Lodish, H., Berk, A., Zipursky, S. L., Matsudaira, P., Baltimore, D. and Darnell, J. (2000) Processing of Eukaryotic mRNA.
- Long, R. M., Singer, R. H., Meng, X., Gonzalez, I., Nasmyth, K. and Jansen, R.-P. (1997) Mating type switching in yeast controlled by asymmetric localization of ASH1 mRNA. *Science*. *277*, 383-387
- MacDougall, N., Clark, A., MacDougall, E. and Davis, I. (2003) *Drosophila* gurken (TGF α) mRNA localizes as particles that move within the oocyte in two dynein-dependent steps. *Developmental cell*. *4*, 307-319
- Malenka, R. C. and Bear, M. F. (2004) LTP and LTD: an embarrassment of riches. *Neuron*. *44*, 5-21
- Malgowska, M., Gudanis, D., Kierzek, R., Wyszko, E., Gabelica, V. and Gdaniec, Z. (2014) Distinctive structural motifs of RNA G-quadruplexes composed of AGG, CGG and UGG trinucleotide repeats. *Nucleic acids research*. *42*, 10196-10207
- Mant, A., Williams, S., Roncoroni, L., Lowry, E., Johnson, D. and O'Kelly, I. (2013) N-glycosylation-dependent control of functional expression of background potassium channels K_{2p}3.1 and K_{2p}9.1. *J Biol Chem*. *288*, 3251-3264
- Mark, J. C., Ulrike, S., Joanne, L. C., Rachel, M. B., Markete, V., Keiley, S. and Simon, J. M. (2012) Multiple isoforms of the translation initiation factor eIF4GII are generated via use of alternative promoters, splice sites and a non-canonical initiation codon. *Biochemical Journal*. *448*, 1-11
- Mathie, A., Rees, K. A., El Hachmane, M. F. and Veale, E. L. (2010) Trafficking of neuronal two pore domain potassium channels. *Current neuropharmacology*. *8*, 276
- Mayford, M., Baranes, D., Podsypanina, K. and Kandel, E. R. (1996) The 3'-untranslated region of CaMKII α is a cis-acting signal for the localization and translation of mRNA in dendrites. *Proceedings of the National Academy of Sciences*. *93*, 13250-13255
- Menon, L. and Mihailescu, M.-R. (2007) Interactions of the G quartet forming semaphorin 3F RNA with the RGG box domain of the fragile X protein family. *Nucleic acids research*. *35*, 5379-5392
- Mergny, J.L., Phan, A.T. and Lacroix, L., 1998. Following G-quartet formation by UV-spectroscopy. *FEBS letters*, *435*(1), pp.74-78.
- Mili, S., Moissoglu, K. and Macara, I. G. (2008) Genome-wide screen reveals APC-associated RNAs enriched in cell protrusions. *Nature*. *453*, 115-119

- Miller, S., Yasuda, M., Coats, J. K., Jones, Y., Martone, M. E. and Mayford, M. (2002) Disruption of dendritic translation of CaMKII α impairs stabilization of synaptic plasticity and memory consolidation. *Neuron*. *36*, 507-519
- Minis, A., Dahary, D., Manor, O., Leshkowitz, D., Pilpel, Y. and Yaron, A. (2014) Subcellular transcriptomics—Dissection of the mRNA composition in the axonal compartment of sensory neurons. *Developmental neurobiology*. *74*, 365-381
- Morris, M. J., Negishi, Y., Paszint, C., Schonhoft, J. D. and Basu, S. (2010) An RNA G-quadruplex is essential for cap-independent translation initiation in human VEGF IRES. *Journal of the American Chemical Society*. *132*, 17831-17839
- Morris, M. J., Wingate, K. L., Silwal, J., Leeper, T. C. and Basu, S. (2012) The porphyrin TmPyP4 unfolds the extremely stable G-quadruplex in MT3-MMP mRNA and alleviates its repressive effect to enhance translation in eukaryotic cells. *Nucleic acids research*. *40*, 4137-4145
- Muddashetty, R. S., Nalavadi, V. C., Gross, C., Yao, X., Xing, L., Laur, O., Warren, S. T. and Bassell, G. J. (2011) Reversible inhibition of PSD-95 mRNA translation by miR-125a, FMRP phosphorylation, and mGluR signaling. *Molecular cell*. *42*, 673-688
- Muslimov, I. A., Patel, M. V., Rose, A. and Tiedge, H. (2011) Spatial code recognition in neuronal RNA targeting: Role of RNA–hnRNP A2 interactions. *The Journal of cell biology*. *194*, 441-457
- Nagel, J., Gulyaev, A., Öistämö, K., Gerdes, K. and Pleij, C. (2002) A pH-jump approach for investigating secondary structure refolding kinetics in RNA. *Nucleic acids research*. *30*, 63-63
- Nakamura, M. T., and Nara, T. Y. (2002) Gene regulation of mammalian desaturases. *Biochem Soc Trans*. *30*, 1076-1079
- Nakagawa, S., Niimura, Y., Gojobori, T., Tanaka, H. and Miura, K.-i. (2008) Diversity of preferred nucleotide sequences around the translation initiation codon in eukaryote genomes. *Nucleic acids research*. *36*, 861-871
- Napoli, I., Mercaldo, V., Boyl, P.P., Eleuteri, B., Zalfa, F., De Rubeis, S., Di Marino, D., Mohr, E., Massimi, M., Falconi, M. and Witke, W., 2008. The fragile X syndrome protein represses activity-dependent translation through CYFIP1, a new 4E-BP. *Cell*, *134*(6), pp.1042-1054.
- Nechooshtan, G., Elgrably-Weiss, M., Sheaffer, A., Westhof, E. and Altuvia, S. (2009) A pH-responsive riboregulator. *Genes & development*. *23*, 2650-2662
- Nilsen, T. W. and Graveley, B. R. (2010) Expansion of the eukaryotic proteome by alternative splicing. *Nature*. *463*, 457-463
- Ofer, N., Weisman-Shomer, P., Shklover, J. and Fry, M. (2009) The quadruplex r (CGG)_n destabilizing cationic porphyrin TMPyP4 cooperates with hnRNPs to increase the translation efficiency of fragile X premutation mRNA. *Nucleic acids research*. *37*, 2712-2722
- Ohashi, S., Kobayashi, S., Omori, A., Ohara, S., Omae, A., Muramatsu, T., Li, Y. and Anzai, K. (2000) The Single-Stranded DNA- and RNA-Binding Proteins Pur α and Pur β Link BC1 RNA to Microtubules Through Binding to the Dendrite-Targeting RNA Motifs. *Journal of neurochemistry*. *75*, 1781-1790

- Olsen, C.M., Lee, H.T. and Marky, L.A., 2008. Unfolding Thermodynamics of Intramolecular G-Quadruplexes: Base Sequence Contributions of the Loops†. *The Journal of Physical Chemistry B*, 113(9), pp.2587-2595.
- O'Kelly, I., Butler, M. H., Zilberberg, N. and Goldstein, S. A. (2002) Forward transport. 14-3-3 binding overcomes retention in endoplasmic reticulum by dibasic signals. *Cell*. 111, 577-588
- Pandey, S., Agarwala, P. and Maiti, S., 2013. Effect of loops and G-quartets on the stability of RNA G-quadruplexes. *The Journal of Physical Chemistry B*, 117(23), pp.6896-6905.
- Park, H. Y., Lim, H., Yoon, Y. J., Follenzi, A., Nwokafor, C., Lopez-Jones, M., Meng, X. and Singer, R. H. (2014) Visualization of Dynamics of Single Endogenous mRNA Labeled in Live Mouse. *Science*. 343, 422-424
- Passmore, L.A., Schmeing, T.M., Maag, D., Applefield, D.J., Acker, M.G., Algire, M.A., Lorsch, J.R. and Ramakrishnan, V., 2007. The eukaryotic translation initiation factors eIF1 and eIF1A induce an open conformation of the 40S ribosome. *Molecular cell*, 26(1), pp.41-50.
- Patel, A. J., Honoré, E., Maingret, F., Lesage, F., Fink, M., Duprat, F. and Lazdunski, M. (1998) A mammalian two pore domain mechano-gated S-like K⁺ channel. *The EMBO journal*. 17, 4283-4290
- Patel, V.L., Mitra, S., Harris, R., Buxbaum, A.R., Lionnet, T., Brenowitz, M., Girvin, M., Levy, M., Almo, S.C., Singer, R.H. and Chao, J.A., 2012. Spatial arrangement of an RNA zipcode identifies mRNAs under post-transcriptional control. *Genes & development*, 26(1), pp.43-53.
- Patterson, G. H., Knobel, S. M., Sharif, W. D., Kain, S. R. and Piston, D. W. (1997) Use of the green fluorescent protein and its mutants in quantitative fluorescence microscopy. *Biophys J*. 73, 2782-2790
- Peabody, D. S. (1989) Translation initiation at non-AUG triplets in mammalian cells. *Journal of Biological Chemistry*. 264, 5031-5035
- Pestova, T. V., Hellen, C. and Shatsky, I. N. (1996) Canonical eukaryotic initiation factors determine initiation of translation by internal ribosomal entry. *Molecular and Cellular Biology*. 16, 6859-6869
- Pestova, T. V., Lorsch, J. R. and Hellen, C. U. (2007) The Mechanism of Translation Initiation in Eukaryotes. *Cold Spring Harbor Monograph Archive*. 48, 87-128
- Pestova, T. V., Shatsky, I. N. and Hellen, C. (1996) Functional dissection of eukaryotic initiation factor 4F: the 4A subunit and the central domain of the 4G subunit are sufficient to mediate internal entry of 43S preinitiation complexes. *Molecular and Cellular Biology*. 16, 6870-6878
- Pisareva, V. P., Pisarev, A. V., Komar, A. A., Hellen, C. U. and Pestova, T. V. (2008) Translation initiation on mammalian mRNAs with structured 5'-UTRs requires DEXH-box protein DHX29. *Cell*. 135, 1237
- Rajan, S., Plant, L. D., Rabin, M. L., Butler, M. H. and Goldstein, S. A. (2005) Sumoylation silences the plasma membrane leak K⁺ channel K_{2p1}. *Cell*. 1, 121
- Rajan, S., Preisig-Müller, R., Wischmeyer, E., Nehring, R., Hanley, P., Renigunta, V., Musset, B., Schlichthörl, G., Derst, C. and Karschin, A. (2002) Interaction with 14-3-3 proteins promotes functional expression of the potassium channels TASK-1 and TASK-3. *The Journal of physiology*. 545, 13-26

- Ramaswami, M., Taylor, J. P. and Parker, R. (2013) Altered ribostasis: RNA-protein granules in degenerative disorders. *Cell*. *154*, 727-736
- Richter, Joel D., Gary J. Bassell, and Eric Klann. (2015) Dysregulation and restoration of translational homeostasis in fragile X syndrome. *Nature Reviews Neuroscience*
- Ross, A. F., Oleynikov, Y., Kislauskis, E. H., Taneja, K. L. and Singer, R. H. (1997) Characterization of a beta-actin mRNA zipcode-binding protein. *Molecular and Cellular Biology*. *17*, 2158-2165
- Satoh, J.-i., Yamamura, T. and Arima, K. (2004) The 14-3-3 protein ϵ isoform expressed in reactive astrocytes in demyelinating lesions of multiple sclerosis binds to vimentin and glial fibrillary acidic protein in cultured human astrocytes. *The American journal of pathology*. *165*, 577-592
- Schaeffer, C., Bardoni, B., Mandel, J. L., Ehresmann, B., Ehresmann, C. and Moine, H. (2001) The fragile X mental retardation protein binds specifically to its mRNA via a purine quartet motif. *The EMBO Journal*. *20*, 4803-4813
- Schütt, J., Falley, K., Richter, D., Kreienkamp, H.J. and Kindler, S. (2009) Fragile X mental retardation protein regulates the levels of scaffold proteins and glutamate receptors in postsynaptic densities. *Journal of Biological Chemistry*, *284*(38), pp.25479-25487.
- Siepel, A., Bejerano, G., Pedersen, J. S., Hinrichs, A. S., Hou, M., Rosenbloom, K., Clawson, H., Spieth, J., Hillier, L. W., Richards, S., Weinstock, G. M., Wilson, R. K., Gibbs, R. A., Kent, W. J., Miller, W. and Haussler, D. (2005) Evolutionarily conserved elements in vertebrate, insect, worm, and yeast genomes. *Genome Res*. *15*, 1034-1050
- Sofola, O., Jin, P., Qin, Y., Duan, R., Liu, H., de Haro, M., Nelson, D. and Botas, J. (2007) RNA-Binding proteins hnRNP A2/B1 and CUGBP1 suppress fragile X CGG premutation repeat-induced neurodegeneration in a Drosophila model of FXTAS. *Neuron*. *55*, 565-571
- Sonenberg, N. (2008) eIF4E, the mRNA cap-binding protein: from basic discovery to translational research This paper is one of a selection of papers published in this Special Issue, entitled CSBMCB-Systems and Chemical Biology, and has undergone the Journal's usual peer review process. *Biochemistry and cell biology*. *86*, 178-183
- Steward, O. and Fass, B. (1983) Polyribosomes associated with dendritic spines in the denervated dentate gyrus: evidence for local regulation of protein synthesis during reinnervation. *Progress in brain research*. *58*, 131-136
- Steward, O. and Ribak, C. (1986) Polyribosomes associated with synaptic specializations on axon initial segments: localization of protein-synthetic machinery at inhibitory synapses. *The Journal of Neuroscience*. *6*, 3079-3085
- Subramanian, M., Rage, F., Tabet, R., Flatter, E., Mandel, J. L. and Moine, H. (2011) G-quadruplex RNA structure as a signal for neurite mRNA targeting. *EMBO reports*. *12*, 697-704
- Sudhakar, A., Ramachandran, A., Ghosh, S., Hasnain, S.E., Kaufman, R.J. and Ramaiah, K.V., 2000. Phosphorylation of serine 51 in initiation factor 2 α (eIF2 α) promotes complex formation between eIF2 α (P) and eIF2B and causes inhibition in the guanine nucleotide exchange activity of eIF2B. *Biochemistry*, *39*(42), pp.12929-12938.
- Sweatt, J.D., 1999. Toward a molecular explanation for long-term potentiation. *Learning & Memory*, *6*(5), pp.399-416.

- Talley, E. M., Solorzano, G., Lei, Q., Kim, D. and Bayliss, D. A. (2001) Cns distribution of members of the two-pore-domain (KCNK) potassium channel family. *The Journal of neuroscience : the official journal of the Society for Neuroscience*. *21*, 7491-7505
- Tan, Z. J. and Chen, S. J. (2011) Salt Contribution to RNA Tertiary Structure Folding Stability. *Biophysical Journal*. *101*, 176
- Taylor, A. M., Berchtold, N. C., Perreau, V. M., Tu, C. H., Jeon, N. L. and Cotman, C. W. (2009) Axonal mRNA in uninjured and regenerating cortical mammalian axons. *The Journal of Neuroscience*. *29*, 4697-4707
- Thomas, D., Plant, L. D., Wilkens, C. M., McCrossan, Z. A. and Goldstein, S. A. N. (2008) Alternative Translation Initiation in Rat Brain Yields K_{2p}2.1 Potassium Channels Permeable to Sodium. *Neuron*. *58*, 859-870
- Timchenko, N.A., Wang, G.L. and Timchenko, L.T., 2005. RNA CUG-binding protein 1 increases translation of 20-kDa isoform of CCAAT/enhancer-binding protein β by interacting with the α and β subunits of eukaryotic initiation translation factor 2. *Journal of Biological Chemistry*, *280*(21), pp.20
- Todd, P. K., Oh, S. Y., Krans, A., He, F., Sellier, C., Frazer, M., Renoux, A. J., Chen, K.-c., Scaglione, K. M. and Basrur, V. (2013) CGG repeat-associated translation mediates neurodegeneration in fragile X tremor ataxia syndrome. *Neuron*. *78*, 440-455
- Trcek, T. and Singer, R.H., 2010. The cytoplasmic fate of an mRNP is determined cotranscriptionally: exception or rule?. *Genes & development*, *24*(17), pp.1827-1831.549-20557.
- Trinh, M.A., Kaphzan, H., Wek, R.C., Pierre, P., Cavener, D.R. and Klann, E., 2012. Brain-specific disruption of the eIF2 α kinase PERK decreases ATF4 expression and impairs behavioral flexibility. *Cell reports*, *1*(6), pp.676-688.
- Van Damme, P., Gawron, D., Van Crielinge, W. and Menschaert, G. (2014) N-terminal proteomics and ribosome profiling provide a comprehensive view of the alternative translation initiation landscape in mice and men. *Molecular & cellular proteomics : MCP*. *13*, 1245-1261
- Varani, G. and McClain, W. H. (2000) The G·U wobble base pair. *EMBO reports*. *1*, 18-23
- Varshavsky, A. (2011) The N-end rule pathway and regulation by proteolysis. *Protein Science*. *20*, 1298-1345
- Vattem, K.M. and Wek, R.C., 2004. Reinitiation involving upstream ORFs regulates ATF4 mRNA translation in mammalian cells. *Proceedings of the National Academy of Sciences of the United States of America*, *101*(31), pp.11269-11274.
- Wan, J. and Qian, S.-B. (2014) TISdb: a database for alternative translation initiation in mammalian cells. *Nucleic acids research*. *42*, D845-D850
- Wang, G.-S. and Cooper, T. A. (2007) Splicing in disease: disruption of the splicing code and the decoding machinery. *Nature Reviews Genetics*. *8*, 749-761
- Wang, W., Putra, A., Schools, G. P., Ma, B., Chen, H., Kaczmarek, L. K., Barhanin, J., Lesage, F. and Zhou, M. (2013) The contribution of TWIK-1 channels to astrocyte K⁺ current is limited by retention in intracellular compartments. *Frontiers in cellular neuroscience*. *7*
- Washida, H., Sugino, A., Messing, J., Esen, A. and Okita, T. W. (2004) Asymmetric localization of seed storage protein RNAs to distinct subdomains of the endoplasmic reticulum in developing maize endosperm cells. *Plant and cell physiology*. *45*, 1830-1837

- Weber, L.A., Hickey, E.D. and Baglioni, C.O.R.R.A.D.O., 1978. Influence of potassium salt concentration and temperature on inhibition of mRNA translation by 7-methylguanosine^{5'}-monophosphate. *Journal of Biological Chemistry*, 253(1), pp.178-183.
- Weisman-Shomer, P., Naot, Y. and Fry, M. (2000) Tetrahelical forms of the fragile X syndrome expanded sequence d(CGG)(n) are destabilized by two heterogeneous nuclear ribonucleoprotein-related telomeric DNA-binding proteins. *J Biol Chem*. 275, 2231-2238
- Weil, T.T., Forrest, K.M. and Gavis, E.R., 2006. Localization of bicoid mRNA in late oocytes is maintained by continual active transport. *Developmental cell*, 11(2), pp.251-262.
- Wek, R.C., Jiang, H-Y., and Anthony, T.G., 2006. Coping with stress: eIF2 kinases and translational control. *Biochemical Society Transactions* 34.1 : 7-11.
- Wilkie, G. S., Dickson, K. S. and Gray, N. K. (2003) Regulation of mRNA translation by 5'-and 3'-UTR-binding factors. *Trends in biochemical sciences*. 28, 182-188
- Wolfe, A. L., Singh, K., Zhong, Y., Drewe, P., Rajasekhar, V. K., Sanghvi, V. R., Mavrakis, K. J., Jiang, M., Roderick, J. E. and Van der Meulen, J. (2014) RNA G-quadruplexes cause eIF4A-dependent oncogene translation in cancer. *Nature*. 513, 65-70
- Xu, Z., Poidevin, M., Li, X., Li, Y., Shu, L., Nelson, D. L., Li, H., Hales, C. M., Gearing, M., Wingo, T. S. and Jin, P. (2013) Expanded GGGGCC repeat RNA associated with amyotrophic lateral sclerosis and frontotemporal dementia causes neurodegeneration. *Proc Natl Acad Sci U S A*. 110, 7778-7783
- Zamiri, B., Reddy, K., Macgregor, R. B., Jr. and Pearson, C. E. (2014) TMPyP4 porphyrin distorts RNA G-quadruplex structures of the disease-associated r(GGGGCC)n repeat of the C9orf72 gene and blocks interaction of RNA-binding proteins. *J Biol Chem*. 289, 4653-4659
- Zhang, Y., Matt, L., Patriarchi, T., Malik, Z. A., Chowdhury, D., Park, D. K., Renieri, A., Ames, J. B. and Hell, J. W. (2014) Capping of the N-terminus of PSD-95 by calmodulin triggers its postsynaptic release. *The EMBO Journal*. 33, 1341-1353
- Zivraj, K. H., Tung, Y. C. L., Piper, M., Gumy, L., Fawcett, J. W., Yeo, G. S. and Holt, C. E. (2010) Subcellular profiling reveals distinct and developmentally regulated repertoire of growth cone mRNAs. *The Journal of Neuroscience*. 30, 15464-1

Chapter Nine

Supplementary Figures

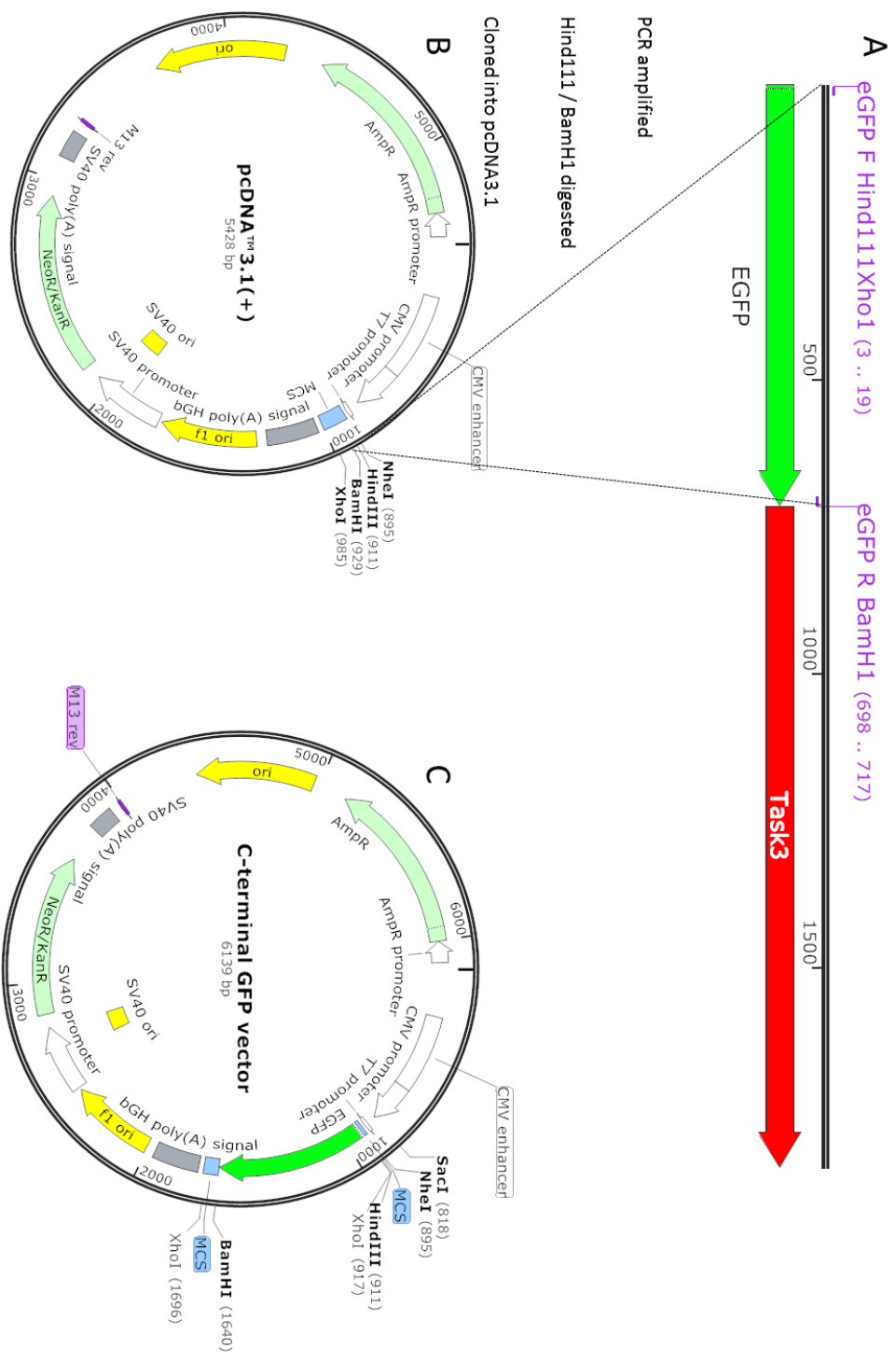


Figure S1 The enhanced GFP sequence was amplified **A**) from the lab's N-terminal GFP expression vector using a HindIII and XhoI forward primer, and a BamHI reverse primer for cloning into **B**) the pCDNA3.1 vector. **C**) NheI/XhoI restriction sites upstream and in frame with the GFP sequence allows simple cloning from existing plasmids.

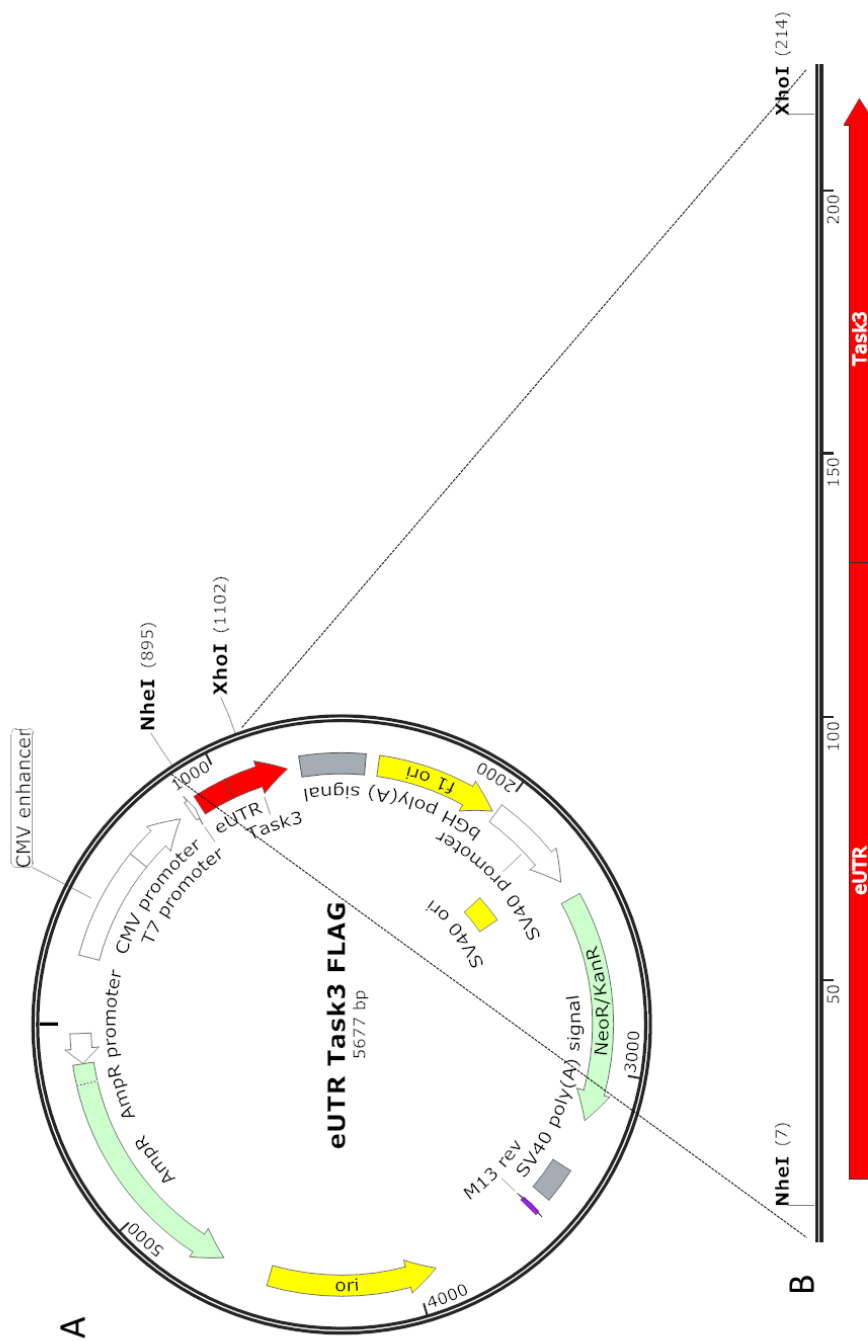


Figure S2 Task3-GFP test plasmids were generated using the 5' UTR sequences cut from existing Task3-FLAG plasmids. **B)** The purified sequence is characterised by NheI and XhoI terminal restriction sites. The XhoI site was used for ligation to the C-terminus of Task3.

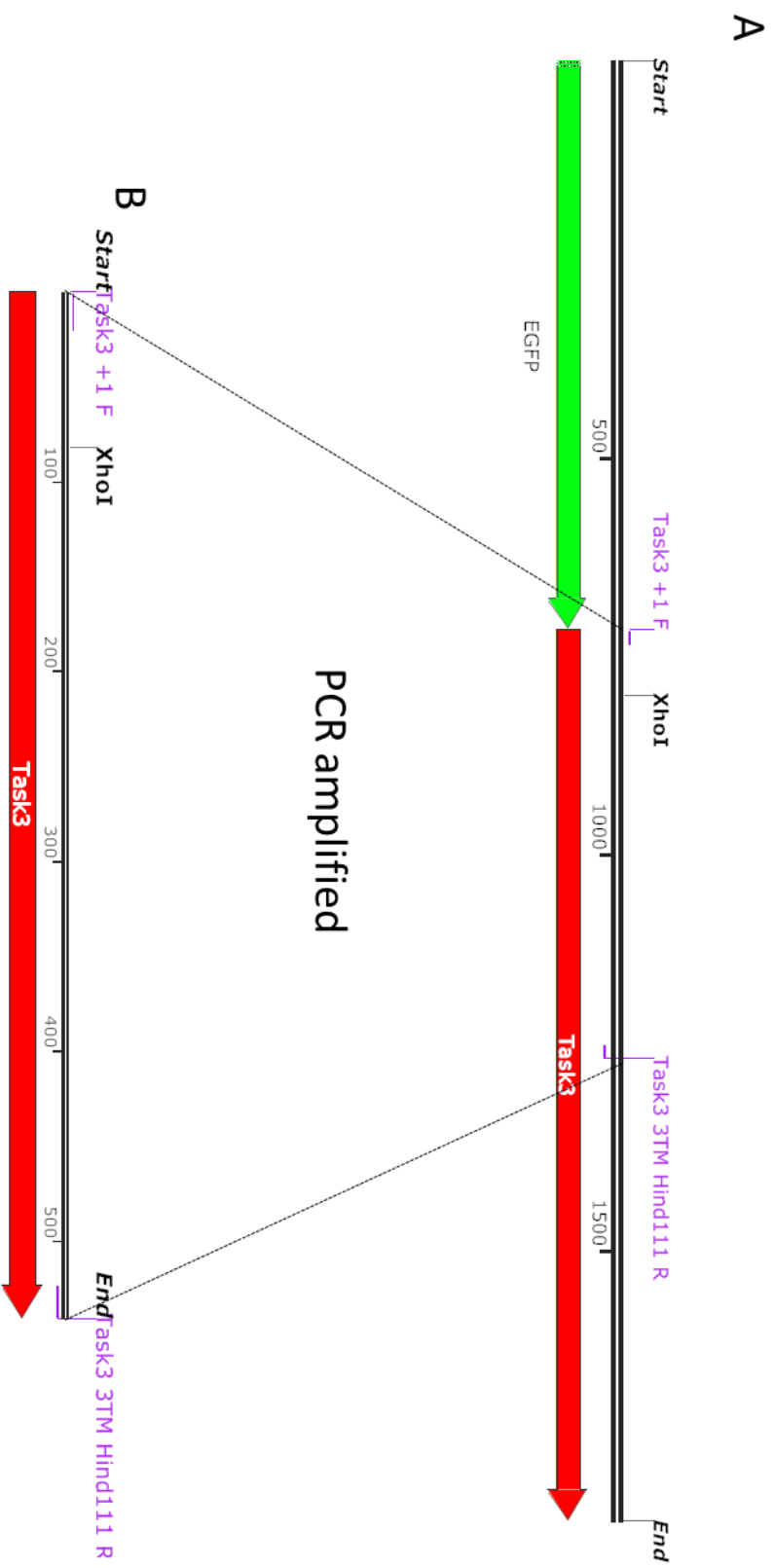


Figure S3 A) The lab's N-terminal GFP Task3 expression vector was used as a template for the amplification of **B)** the C-terminus of Task3, for ligation to the N-terminus, including its 5' UTR sequences. PCR of the C-terminal, or coding sequence, of Task3 was achieved using the Task3 HindIII reverse primer and the Task3 NheI forward primer from the +1 AUG start codon position.

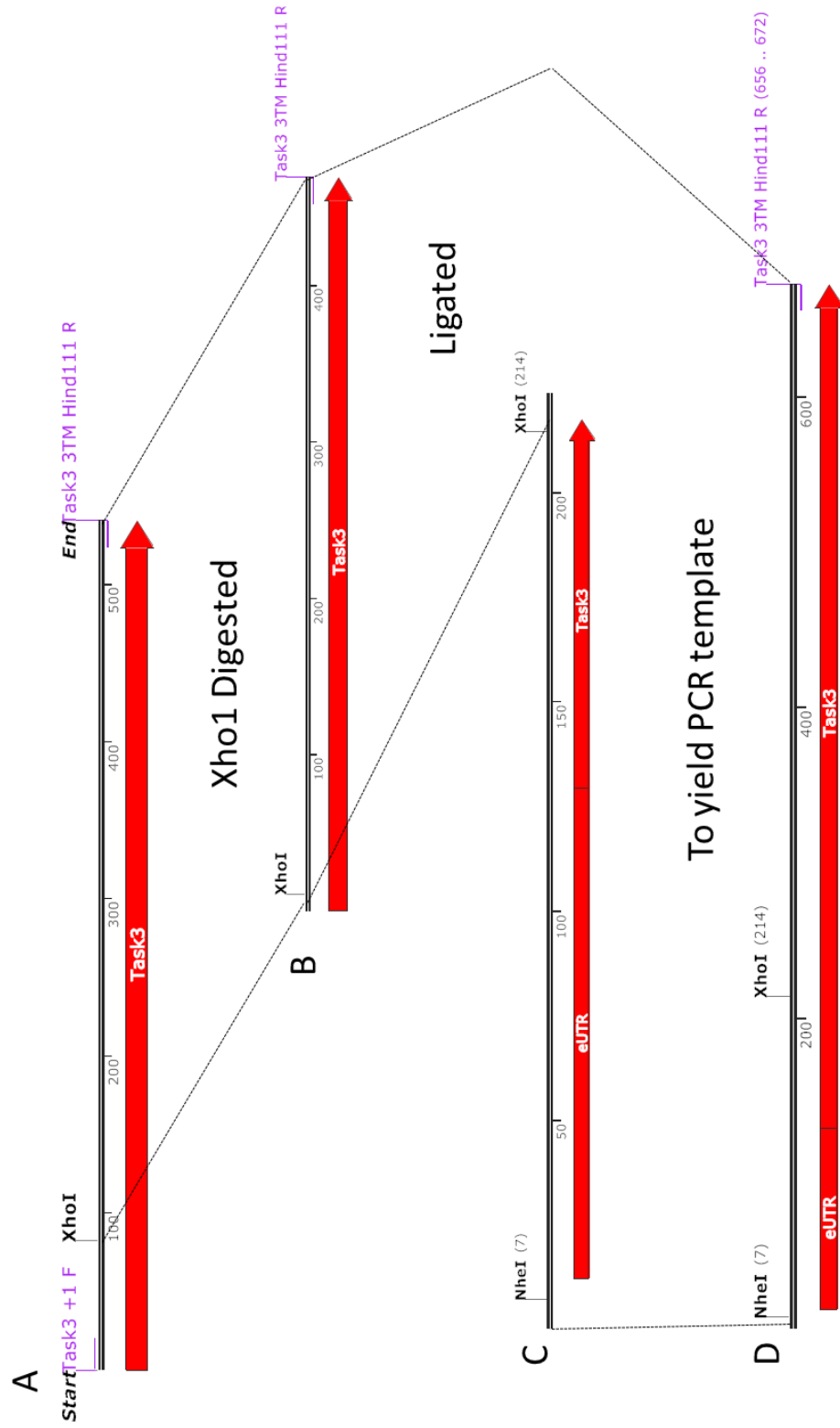


Figure S4 A) The N & C terminal sections of Task3 were digested and ligated to form the template for amplification of the entire sequence to be cloned into GFP expression vector.